

DETERMINATION OF MECHANICAL PROPERTIES USED IN WAY-30 TEST PAVEMENTS

Sang-Soo Kim, Shad Sargand, Teruhisa Masada, and
Jaime Hernandez,



for the
Ohio Department of Transportation
Office of Research and Development

and the
United States Department of Transportation
Federal Highway Administration

State Job Number 437046

May 2010



OHIO
UNIVERSITY

Ohio Research Institute for Transportation and the Environment



1. Report No. FHWA/OH-2010/9	2. Government Accession No.	3. Recipient's Catalog No.	
4. Title and Subtitle Determination of Mechanical Properties of Materials Used in Way-30 Test Pavements		5. Report Date May 2010	
7. Author(s) Sang-Soo Kim, Shad Sargand, Teruhisa Masada, and Jaime Hernandez		6. Performing Organization Code	
9. Performing Organization Name and Address Ohio Research Institute for Transportation and the Environment Ohio University 141 Stocker Center Athens OH 45701		8. Performing Organization Report No.	
12. Sponsoring Agency Name and Address Ohio Department of Transportation 1980 West Broad St. Columbus OH 43223		10. Work Unit No. (TRAIS)	
		11. Contract or Grant No. 437046	
		13. Type of Report and Period Covered Technical Report	
15. Supplementary Notes Prepared in cooperation with the Ohio Department of Transportation (ODOT) and the U.S. Department of Transportation, Federal Highway Administration		14. Sponsoring Agency Code	
16. Abstract The US Route 30 bypass of Wooster, Ohio, in Wayne County, "WAY-30", was constructed to demonstrate two types of extended service pavements, a long-life Portland cement concrete (PCC) pavement on the eastbound lanes and an asphalt concrete (AC) perpetual pavement on the westbound lanes. Both pavements are designed to provide 50 years or more of service with minimal maintenance (e.g. resurfacing). The PCC pavement structure features a thick and extra-wide slab on an asphalt treated base, while the AC pavement structure features a Superpave surface and a Fatigue Resistant Layer (FRL). Report FHWA/OH-2008/7 discusses the instrumentation and studies of the response of the pavement under loads. For this study, samples of all pavement materials, including soils, granular subbase material, PCC mixes, and AC mixes were tested in the laboratory to determine material parameters. Four asphalt mixes were selected to provide a rut and fatigue resistant pavement structure, while two mixes of the PCC were used in different sections of the road. The subgrade material was ODOT type A-4a (AASHTO A-4). The granular subbase material was A-1a with high permeability (1.001 cm/s or 2,838 ft/day). PCC tests included: unit weight, modulus of rupture, static modulus of elasticity, Poisson's ratio, splitting tensile strength, compressive strength, maturity, and thermal coefficient of linear expansion. AC test results indicated that the creation of asphalt-rich bottom by adding additional asphalt binder did work to increase the fatigue resistance by orders of magnitude. At 70 µε, the expected fatigue endurance limit and the designed strain level for the structure, regular 302 mix showed 20,000 cycles to failure while asphalt-rich 302 mix (Fatigue Resistant Layer) is estimated to have 20 million cycles to failure. For average climatic and traffic conditions (25°C or 77°F; 10 Hz or 0.1 sec loading time), the overall dynamic moduli and the resilient moduli of asphalt mixes were higher than the values used in the development of the asphalt perpetual pavement structure. This will reduce the maximum strain at the bottom of FRL significantly than the designed 70 µε. The rutting test results from asphalt pavement analyzer test and flow numbers obtained from the repeated load test indicated that all asphalt mixes were rut-resistant. TSRST cracking temperatures of asphalt mixes were lower than the expected pavement temperatures for the project site determined by LTPPBind software, suggesting the possibility of the low temperature thermal cracking would be very small.			
17. Key Words Long-lived Portland Cement Concrete (PCC) pavement, Asphalt Concrete Perpetual Pavement, mechanical properties.		18. Distribution Statement No Restrictions. This document is available to the public through the National Technical Information Service, Springfield, Virginia 22161	
19. Security Classif. (of this report) Unclassified	20. Security Classif. (of this page) Unclassified	21. No. of Pages 175	22. Price
Form DOT F 1700.7 (8-72) Reproduction of completed pages authorized			

SI* (MODERN METRIC) CONVERSION FACTORS

APPROXIMATE CONVERSIONS TO SI UNITS					APPROXIMATE CONVERSIONS FROM SI UNITS				
Symbol	When You Know	Multiply By	To Find	Symbol	Symbol	When You Know	Multiply By	To Find	Symbol
LENGTH					LENGTH				
in	inches	25.4	millimeters	mm	mm	millimeters	0.039	inches	in
ft	feet	0.305	meters	m	m	meters	3.28	feet	ft
yd	yards	0.914	meters	m	m	meters	1.09	yards	yd
mi	miles	1.61	kilometers	km	km	kilometers	0.621	miles	mi
AREA					AREA				
in ²	square inches	645.2	square millimeters	mm ²	mm ²	square millimeters	0.0016	square inches	in ²
ft ²	square feet	0.093	square meters	m ²	m ²	square meters	10.764	square feet	ft ²
yd ²	square yards	0.836	square meters	m ²	m ²	square meters	1.195	square yards	yd ²
ac	acres	0.405	hectares	ha	ha	hectares	2.47	acres	ac
mi ²	square miles	2.59	square kilometers	km ²	km ²	square kilometers	0.386	square miles	mi ²
VOLUME					VOLUME				
fl oz	fluid ounces	29.57	milliliters	mL	mL	milliliters	0.034	fluid ounces	fl oz
gal	gallons	3.785	liters	L	L	liters	0.264	gallons	gal
ft ³	cubic feet	0.028	cubic meters	m ³	m ³	cubic meters	35.71	cubic feet	ft ³
yd ³	cubic yards	0.765	cubic meters	m ³	m ³	cubic meters	1.307	cubic yards	yd ³
NOTE: Volumes greater than 1000 L shall be shown in m ³ .									
MASS					MASS				
oz	ounces	28.35	grams	g	g	grams	0.035	ounces	oz
lb	pounds	0.454	kilograms	kg	kg	kilograms	2.202	pounds	lb
T	short tons (2000 lb)	0.907	megagrams (or "metric ton")	Mg (or "t")	Mg (or "t")	megagrams (or "metric ton")	1.103	short tons (2000 lb)	T
TEMPERATURE (exact)					TEMPERATURE (exact)				
°F	Fahrenheit temperature	5(°F-32)/9 or (°F-32)/1.8	Celsius temperature	°C	°C	Celsius temperature	1.8°C + 32	Fahrenheit temperature	°F
ILLUMINATION					ILLUMINATION				
fc	foot-candles	10.76	lux	lx	lx	lux	0.0929	foot-candles	fc
fl	foot-Lamberts	3.426	candela/m ²	cd/m ²	cd/m ²	candela/m ²	0.2919	foot-Lamberts	fl
FORCE and PRESSURE or STRESS					FORCE and PRESSURE or STRESS				
lbf	poundforce	4.45	newtons	N	N	newtons	0.225	poundforce	lbf
lbf/in ² or psi	poundforce per square inch	6.89	kilopascals	kPa	kPa	kilopascals	0.145	poundforce per square inch	lbf/in ² or psi

* SI is the symbol for the International Symbol of Units. Appropriate rounding should be made to comply with Section 4 of ASTM E380.

Determination of Mechanical Properties used in Way-30 Test Pavements

Prepared in cooperation with the
Ohio Department of Transportation
and the
U.S. Department of Transportation, Federal Highway Administration

Prepared by

Sang-Soo Kim

Shad Sargand

Teruhisa Masada

Jaime Hernandez

Ohio Research Institute for Transportation and the Environment
Russ College of Engineering and Technology
Ohio University
Athens, Ohio 45701-2979

The contents of this report reflect the views of the authors who are responsible for the facts and the accuracy of the data presented herein. The contents do not necessarily reflect the official views or policies of the Ohio Department of Transportation or the Federal Highway Administration. This report does not constitute a standard, specification or regulation.

Final Report
May 2010

ACKNOWLEDGEMENTS

The authors would like to acknowledge the contributions of the technical liaisons and project panel members to this project, particularly Roger Green, and the ODOT Office of Research and Development. The authors also thank the subcontractors at the University of Minnesota for stepping in at the last minute to complete a set of tests. The authors also acknowledge the contributions of ORITE Research Engineers Issam Khoury and William Edwards, Professor J. Ludwig Figueroa, and graduate students Yun Liao, Andrew Wargo, Abdalla Alrawashdeh, Natalia Quintero, Michael Romanello, David Padilla-Llano, and Jourdan Siemer to various parts of this project.

The authors also would like to acknowledge the assistance from Brian Hickey and Michelle Burchfield, ODOT District 3 engineers and Ed Morrison, Shelly & Sands in collection of field data.

Table of Contents

	Page
1 INTRODUCTION	1
1.1 General Statement	1
1.2 Literature Review	2
1.3 Research Objectives	2
1.4 Outline	2
2 PROJECT BACKGROUND	3
2.1 Site Description	3
2.2 WAY-30 Asphalt Concrete Design	4
2.3 Mechanistic-Based Design Approach	6
2.4 WAY-30 Portland Cement Concrete Design	8
2.5 Construction	9
3 LABORATORY TEST RESULTS ON WAY-30 SUBGRADE SOILS	12
4 LABORATORY TESTING OF SUBBASE MATERIAL (WAY-30)	19
5 MODELING OF RESILIENT BEHAVIOR OF WAY-30 SOILS	29
5.1 Models for Fine-Grained Subgrade Soil	29
5.2 Models for Granular Subbase Materials	32
6 LABORATORY TEST RESULTS ON CONCRETE	37
6.1 Unit Weight (ASTM C138/C 138M-01a)	37
6.2 Modulus of Rupture (ASTM C 78-02)	37
6.3 Static Modulus of Elasticity and Poisson's Ratio (ASTM C 469-02)	40
6.4 Splitting Tensile Strength (ASTM C 496/C 496M-04)	43
6.5 Compressive Strength (ASTM C 39/C39M-03)	44
6.6 Maturity Test	52
6.7 Thermal Coefficient of Linear Expansion	53
7 LABORATORY TEST RESULTS ON ASPHALT CONCRETE	54
7.1 Maximum Specific Gravity	54
7.2 Bulk Specific Gravity Test	54
7.3 Air Void Measurement	55
7.4 Resilient Modulus Test	57
7.5 Rutting Evaluation-Asphalt Pavement Analyzer (APA)	61
7.6 Moisture Susceptibility	64
7.7 Indirect Tensile Creep and Strength at Low Temperature	66
7.8 Beam Fatigue	69
7.9 Thermal Stress Restrained Specimen Test (TSRST)	74
7.10 Dynamic Modulus	82
7.11 Repeated Load Test (Flow Number)	94
7.12 Bulk Modulus	95
7.13 Absorbed Energy Ratio, Indirect Tensile Strength and Unconfined Compressive Strength	97
8 SUMMARY AND CONCLUSIONS	99
9 IMPLEMENTATION	103
REFERENCES	104

Appendices	
Appendix A: As-Designed Job Mix Formulas (JMFs)	107
Appendix B: Quality Control & Quality Assurance Data (Asphalt Pavement)	110
Appendix C: Quality Control & Quality Assurance Data (Portland Cement Concrete Pavement)	124
Appendix D: FHWA Test Results on Void Properties of Hardened Concretes	134
Appendix E: Low Temperature Creep Compliance of Asphalt Mixes	136
Appendix F: Absorbed Energy Ratio of Asphalt Mixes	142
Appendix G: Indirect Tensile Strength of Asphalt Mixes	150
Appendix H: Unconfined Compressive Strength of Asphalt Mixes	155
Appendix I: Implementation Plan	160

List of Figures

	Page
Figure 1. Plan view of the WAY-30 bypass and test section location.	3
Figure 2. AC structure and instrumentation plan for AC Section 664.	7
Figure 3. Required AC thickness for 70 microstrain limit assuming a subgrade CBR in the range 4 – 6. (1 in = 2.54 cm, 41 kip = 182 kN).	8
Figure 4. Pavement structure and instrumentation of the PCC sections of WAY-30.	11
Figure 5. Compaction curves of subgrade soils.(1 pcf = 16.02 kg/m ³)	13
Figure 6. Resilient modulus vs. deviatoric stress for WB STA 876+60 subgrade (Test 1). (1ksi = 6.895 MPa)	16
Figure 7. Resilient modulus vs. deviatoric stress for EB STA 876+60 subgrade (Test 2). (1ksi = 6.895 MPa)	16
Figure 8. Resilient modulus vs. deviatoric stress for WB STA 885+00 subgrade. (1ksi = 6.895 MPa)	17
Figure 9. Resilient modulus vs. deviatoric stress for EB STA 884+00 subgrade. (1ksi = 6.895 MPa)	17
Figure 10. Resilient modulus vs. deviatoric stress for EB STA 884+00 subgrade (Test 2). (1ksi=6.895 MPa)	18
Figure 11. Resilient modulus vs. deviatoric stress for EB STA 663+50 subgrade. (1ksi=6.895 MPa)	18
Figure 12. Grain size distribution curve of subbase material.	19
Figure 13. Preparation of subbase resilient modulus test specimen.	21
Figure 14. Subbase resilient modulus testing: a) close-up of specimen in test chamber, b) test chamber with connections to controller and computer, c) view of computer screen output, d) view of test chamber and workstation.	22
Figure 15. Resilient modulus vs. deviatoric stress of subbase (Trial 1). (1 ksi = 6.89 MPa)	25
Figure 16. Resilient modulus vs. deviatoric stress of subbase (Trial 2). (1 ksi = 6.89 MPa)	25
Figure 17. Resilient modulus vs. bulk stress of subbase (Trial 1).	26
Figure 18. Resilient modulus vs. bulk stress of subbase (Trial 2). (1 ksi = 6.89 MPa)	26
Figure 19. Permeameter with compacted aggregate subbase and vibrating tamper.	27
Figure 20. Specific discharge versus hydraulic gradient of aggregate base. (2.54 cm/sec = 1.0 in./sec)	28
Figure 21. Plot of hyperbolic model constants K and n values vs. (w – OMC).	32
Figure 22. Strength-maturity relationship for fly ash and GGBSF concretes (1 psi = 6.89 kPa, 20°C = 68°F)	53
Figure 23. Resilient modulus versus the temperature for laboratory prepared asphalt specimens. (1 ksi=6.89 MPa)	60

Figure 24. Resilient modulus versus the temperature for cored asphalt specimens. (1 ksi=6.89 MPa)	60
Figure 25. APA rut depth of Mix 301. (25.4 mm=1.00 in.)	61
Figure 26. APA rut depth of Mix 302. (25.4 mm=1.00 in.)	62
Figure 27. APA rut depth of Mix 442. (25.4 mm=1.00 in.)	62
Figure 28. APA rut depth of Mix FRL. (25.4 mm=1.00 in.)	63
Figure 29. APA rut depth of Mix SMA. (25.4 mm=1.00 in.)	63
Figure 30. Average APA rut depth of asphalt mixes. (25.4 mm=1.00 in.)	64
Figure 31. Creep compliance of Mix 301.	67
Figure 32. Creep compliance of Mix 302. (1 ksi = 6.89 MPa)	67
Figure 33. Creep compliance of Mix 442.	68
Figure 34. Creep compliance of Mix FRL. (1 ksi = 6.89 MPa)	68
Figure 35. Creep compliance of Mix SMA. (1 ksi = 6.89 MPa)	69
Figure 36. Flexural stiffness versus number of cycles N for 302 mix. (1 ksi=6.89 MPa)	71
Figure 37. Flexural stiffness versus number of cycles N for 442 mix . (1 ksi=6.89 MPa)	71
Figure 38. Flexural stiffness versus number of cycles N for FRL mix . (1 ksi=6.89 MPa)	72
Figure 39. Flexural stiffness versus number of cycles N for SMA mix. (1 ksi=6.89 MPa)	72
Figure 40. Summary of 4-point beam fatigue test results.	73
Figure 41. Left: TSRST sample after failure; Right: TSRST System.	74
Figure 42. Item 302 mixture TSRST results. (1 MPa = 0.145 ksi)	75
Figure 43. Item 442 mixture TSRST results. (1 MPa = 0.145 ksi)	76
Figure 44. FRL mixture TSRST results. (1 MPa = 0.145 ksi)	76
Figure 45. SMA mixture TSRST results. (1 MPa = 0.145 ksi)	77
Figure 46. Failed 442 mix specimens after TSRST.	78
Figure 47. Failed 302 mix specimens after TSRST.	79
Figure 48. Failed FRL mix specimens after TSRST.	80
Figure 49. Failed SMA mix specimens after TSRST.	81
Figure 50. Dynamic modulus master curve of Mix 301.	89
Figure 51. Shift function $a(T)$ versus temperature of Mix 301.	89
Figure 52. Dynamic modulus master curve of Mix 302.	90
Figure 53. Shift function $a(T)$ versus temperature of Mix 302.	90
Figure 54. Dynamic modulus master curve of Mix FRL.	91
Figure 55. Shift function $a(T)$ versus temperature of Mix FRL.	91
Figure 56. Dynamic modulus master curve of Mix 442.	92
Figure 57. Shift function $a(T)$ versus temperature of Mix 442.	92
Figure 58. Dynamic modulus master curve of Mix SMA.	93
Figure 59. Shift function $a(T)$ versus temperature of Mix SMA.	93

List of Tables

	Page
Table 1. ACC mix design and mix volumetrics.	5
Table 2. Properties of PG binders.	6
Table 3. WAY-30 Asphalt Concrete (AC) Perpetual Pavement Design Properties.	8
Table 4. Percentage by weight of GGBFS and fly ash materials in PCC Mix.	9
Table 5. PCC mix designs and mix properties	10
Table 6. Classification, maximum dry unit weight, and optimum moisture content of soil samples.	13
Table 7. Resilient modulus test results for STA 876+60 and WB STA 885+00 subgrade.	14
Table 8. Resilient modulus for WB STA 884+00 and STA 663+50 subgrade.	15
Table 9. Results of mechanical sieve analysis of subbase.	19
Table 10. Basic characteristics of subbase resilient modulus test specimens.	20
Table 11. Resilient modulus of WAY-30 subbase as a function of deviatoric stress and of bulk stress.	24
Table 12. The results of constant head permeability test for aggregate subbase.	28
Table 13. Regression coefficients of MEPDG universal model for subgrade.	29
Table 14. Evaluation of models for resilient modulus models for A-4 subgrade soil.	31
Table 15. List of subgrade soil specimen properties and hyperbolic model constants.	32
Table 16. Regression coefficients of MEPDG universal model for subbase	33
Table 17. Resilient modulus values predicted for WAY-30 subbase material. (English units at top metric units at bottom)	36
Table 18. Modulus of rupture for Mix A concrete with GGBFS.	38
Table 19. Modulus of rupture for Mix B concrete with fly ash.	39
Table 20. Static modulus of elasticity and Poisson's ratio of GGBFS concrete (Mix A).	41
Table 21. Static modulus of elasticity and Poisson's ratio of fly ash Concrete (Mix B).	42
Table 22. Splitting tensile strength of GGBFS concrete (Mix A).	43
Table 23. Splitting tensile strength for fly ash concrete (Mix B).	44
Table 24. Compressive strength for GGBSF Concrete (Mix A).	45
Table 25. Compressive strength for fly ash concrete (Mix B).	46
Table 26. Compressive strength of fly ash concrete using two curing methods.	47

Table 27. Summary of results for ground granulated blast-furnace slag (GGBSF) concrete (Mix A), English units.	48
Table 28. Summary of results for ground granulated blast-furnace slag (GGBSF) concrete (Mix A), international units.	49
Table 29. Summary of results for fly ash concrete (Mix B), English units.	50
Table 30. Summary of results for fly ash concrete (Mix B), international units.	51
Table 31. Equivalent age and compressive strength of GGBSF concrete.	52
Table 32. Equivalent age and compressive strength of fly ash concrete.	52
Table 33. Maximum specific gravity of AC core specimens.	55
Table 34. Air void content of AC core specimens.	56
Table 35. Summary of total and instantaneous resilient moduli for laboratory prepared asphalt specimens, assuming $\nu = 0.35$.	58
Table 36. Summary of total and instantaneous resilient moduli for asphalt core specimens, assuming $\nu = 0.35$.	59
Table 37. APA rut depth and air void content of asphalt mixes.	64
Table 38. Indirect tensile strength ratio for each asphalt mix.	65
Table 39. Indirect tensile strength of asphalt concretes at three temperatures.	66
Table 40. Average height and width for asphalt beam specimens for fatigue test.	70
Table 41. Fatigue test results summary with number of cycles to failure at each confining stress and fatigue parameters derived from curve fits.	73
Table 42. TSRST fracture temperature and fracture strength of asphalt mixes.	77
Table 43. Dynamic modulus and phase angle of Mix 301 at 5 test temperatures and 6 frequencies.	83
Table 44. Dynamic modulus and phase angle of Mix 302 at 5 test temperatures and 6 frequencies.	84
Table 45. Dynamic modulus and phase angle of Mix FRL at 5 test temperatures and 6 frequencies.	85
Table 46. Dynamic modulus and phase angle of Mix 442 at 5 test temperatures and 6 frequencies.	86
Table 47. Dynamic modulus and phase angle of Mix SMA at 5 test temperatures and 6 frequencies.	87
Table 48. Summary of Sigmoidal function parameters and shift factor equations for dynamic modulus of WAY 30 asphalt mixes.	94
Table 49. Summary of flow numbers at the effective temperature (39°C or 102.2°F).	94
Table 50. Summary of flow numbers at 54.4°C (130°F).	95
Table 51. Estimated bulk modulus at 5, 25, and 40°C (41, 77, and 104°F).	96

Table 52. Average absorbed energy ratio of asphalt mixes.	97
Table 53. Average indirect tensile strength of asphalt mixes.	98
Table 54. Average unconfined compressive strength of asphalt mixes.	98
Table 55. Summary of average WAY-30 concrete material properties at 90 days.	100
Table 56. Summary of properties measured for WAY-30 asphalt mixes.	102

1 INTRODUCTION

1.1 General Statement

Pavement engineers have continuously gained more knowledge in pavement response under loading and the common pavement failure mechanisms. In recent years, innovative idea has been proposed for pavements design which requires only minor changes in the current conventional designs and potentially offers a significant increase in design life. The Ohio Department of Transportation (ODOT), with joint efforts from the rigid and flexible pavement industries, constructed two test projects on WAY-30 bypass of Wooster, Ohio for the evaluation of long life pavement design procedures as alternatives to standard pavement design methods. The eastbound lanes were constructed with a long lasting economical concrete pavement and the westbound lanes were constructed with an asphalt pavement designed following the principles of perpetual pavement, which is rapidly gaining acceptance in the United States. The perpetual asphalt pavement concept uses mechanistic-empirical design procedure that requires accurate input data on mechanical properties of materials, traffic, and environmental conditions to predict pavement responses and distresses. Using input data and pavement response models, the thickness of each pavement layer is determined to keep certain pavement responses at critical locations within limiting values for perpetual performance. The tensile strain at the bottom of the asphalt layers and the compressive strain at the top of the subgrade have long been considered to be the most critical for fatigue cracking and rutting of asphalt pavements, respectively [The Asphalt Institute, 1999]. For example, Monismith, Long, and Harvey [2001] suggested $60 \mu\epsilon$ as the limiting tensile strain at the bottom of the asphalt layers and $200 \mu\epsilon$ as the limiting compressive strain at the top of the subgrade for perpetual asphalt pavement. Design of long-lived concrete pavement also requires accurate material properties. Both WAY-30 pavements are designed to provide 50 years or more of service with minimal maintenance (e.g. resurfacing). The PCC pavement structure features a thick and extra-wide slab on an asphalt treated base, while the AC pavement structure features a Superpave surface and a Fatigue Resistant Layer (FRL).

Two sections of each type of pavement were instrumented with pressure cells to monitor subgrade pressures and deep and shallow LVDTs to record pavement deflections. The AC test sections also had transverse and longitudinal strain gages. A weather station was used to monitor environmental conditions. Nondestructive testing of the subgrade was conducted prior to pavement placement. Controlled vehicle load (CVL) and falling weight deflectometer (FWD) tests were applied to the AC pavement shortly after the road opened to traffic in December 2005 and again under hot weather conditions in July 2006. Similar tests on the PCC pavement were conducted in December 2005 and August 2006. The response on both types of pavement met their respective design criteria. A verification analysis of the AC pavement response using the elastic layer system (ELS) simulation using material properties derived from laboratory and field sample data was also conducted. The results of the nondestructive testing, including CVL, FWD, and ELS analyses, are reported in a previous report [Sargand,

Figueroa, and Romanello, 2008]. This report presents the results of material properties tests on samples collected from the test road.

1.2 Literature Review

The literature on the topics of perpetual AC pavement and long-lived PCC pavement was reviewed in the main project report by Sargand, Figueroa, and Romanello [2008].

1.3 Research Objectives

The objectives of this research are:

- Determine the mechanical properties of the pavement materials used in WAY-30 test pavements during construction and in-service;
- Provide data to calibrate long-life pavement design procedures following the Mechanistic-Empirical Pavement Design Guide (MEPDG).

1.4 Outline

The following outline provides information about the content of each chapter.

- **Chapter 1** is an introduction that includes the research objectives for the project and a summary of related research.
- **Chapter 2** provides the project background.
- **Chapter 3, 4, 5, 6, and 7** presents the mechanical properties for subgrade soil, subbase and base aggregate material, modeling of soils, Portland cement concrete, and asphalt concrete, respectively.
- **Chapter 8** summarizes the results and provides conclusions to the study.
- **Chapter 9** discusses implementation potential of the data.

2 PROJECT BACKGROUND

Long life pavement is an emerging concept based on a set of mechanistic-empirical design procedures where the expected pavement performance is assumed by an empirical relationship with mechanistically determined pavement responses. Without proper validation and calibration of the design model using appropriate inputs for material properties, the resulting design may be inadequate, leading to premature failure, or overly conservative, adding unnecessary cost to construction. In addition, some of the distress modes and properties of new types of material, for example fatigue resistant layer (FRL) in the asphalt concrete (AC) pavement, were not fully considered in the original design of WAY-30 test projects. Low temperature cracking, rutting, and moisture damage resulting from this or other inadequate considerations could result in premature failure of the AC pavement. Similarly, inadequate information on material property inputs for Portland cement concrete (PCC), including changes in properties during curing, may also significantly affect the performance of the PCC test pavement.

2.1 Site Description

In 2002, the Ohio Department of Transportation chose the relocation of the East Lincoln Highway, US Route 30, east of Wooster in Wayne County in northeast Ohio as the location of the perpetual and long lasting pavement demonstration project. The pre-construction ADT on the two-lane road was 17,720. The new test pavement, opened in December 2005, is a rural freeway, a four-lane divided highway section that begins at the interchange with State Route 83 near the east side of Wooster and runs eastward for approximately 8 miles (13 km). The westbound lanes are the perpetual asphalt concrete pavement, while the eastbound lanes are constructed of long lasting Portland cement concrete. Figure 1 shows a close-up map of the bypass and the original Lincoln Highway route.



Figure 1. Plan view of the WAY-30 bypass and test section location.

Two separate locations along the project were chosen for test sections to accommodate two different mix designs in the Portland cement concrete pavement. Test sites are located at Station 664+00 and Station 876+60 on the project mainline, as is also

shown in Figure 1. The perpetual asphalt pavement test sections are located opposite the PCC test sections at both locations. Both sections have a relatively flat topography and lie within straight sections of the project and feature minimal grade cuts. By avoiding deep grade cuts or fill sections complications due to subgrade conditions prior to compaction were avoided. Preliminary test boring results classified the subgrade soils at Station 876+00 as ODOT A-4a and at Station 664+00 as ODOT A-4a and A-6a. The California Bearing Ratio (CBR) for the subgrade soil ranged from 4 to 6 along the project. FWD and DCP tests were conducted on the subgrade to further characterize its strength. FWD testing was also performed on the base materials. The results of these tests are given in Chapter 4 and in Appendix A and Appendix B of the previous report entitled *Instrumentation of WAY-30 Test Pavements* [Sargand, Figueroa, and Romanello, 2008].

2.2 WAY-30 Asphalt Concrete Design

The Ohio asphalt industry, collaborating with ODOT, the Federal Highway Administration (FHWA) and consulting with several national and academic experts, developed the perpetual pavement design and the specifications for the westbound lanes of WAY-30. The mechanistic design approach was used in conjunction with elastic layer analyses to determine the overall design thickness of the pavement. Material specifications were then determined for each pavement layer. To maintain the perpetual lifetime of the pavement, the limiting strain at the bottom of the pavement was set at 70 $\mu\epsilon$, based on the strain caused by a vehicle 20% above the legal load limit. “With these limits, it was determined (using elastic layer analysis) that the asphalt concrete pavement thickness would be 16.25 inches (41 cm) thick on a crushed aggregate base when built on a soil having a CBR range of 4 to 6” [Ursich, 2005].

The dimensions and specifications (from bottom to top) for each layer are shown below, as presented by Ursich [2005].

- 6 in (15 cm) base: ODOT Item 304, densely graded granular base (DGAB), with under drains.
- 4 in (10 cm) fatigue resistant layer (FRL): Modified ODOT Item 302, large stone base mix, made binder rich by designing for 3% air voids; and 94 to 97% constructed density.
- 9 in (23 cm) middle layer: High modulus asphalt treated base (ATB), regular ODOT Item 302, large stone mix, with a PG 64-22 asphalt binder; target density 93% to 96%.
- 3.25 in (8.3 cm) top layer designed as a sacrificial layer to be replaced periodically. It has two sublayers:
 - 1.75 in (4.45 cm) Superpave layer: ODOT Item 442 19 mm (3/4 in.) Superpave, Type A, with PG 76-22M polymer modified binder; target density 93% to 97%.
 - 1.5 in (3.8 cm) surface course: ODOT Item 856 12.5 mm (1/2 in.) stone mastic asphalt with PG 76-22M polymer modified binder; target density 93% to 97%. This asphalt mix is also known as “SMA mix”, for Stone Matrix Asphalt.

Asphalt mix designs used for the actual construction of the test pavements (as-built mix designs) are presented in Table 1 along with their volumetric properties. Properties of

Table 1. ACC mix design and mix volumetrics.

	SMA	442	302	FRL
Mix Design Type	Superpave	Superpave	Marshall	Marshall
Coarse Agg	Limestone	Limestone	Limestone	Limestone
Fine Agg	Limestone	Limestone / N Sand	N Sand	N Sand
Gradation				
2" (50.8 mm)	100	100	100	100
1 1/2" (38 mm)	100	100	100	100
1" (25.4 mm)	100	100	87	87
3/4" (19 mm)	100	99	74	74
1/2" (12.5 mm)	93	88	59	59
3/8" (9.5 mm)	70	81	52	52
#4 (4.75 mm)	23	54	34	34
#8 (2.36 mm)	16	44	26	26
#16 (1.18 mm)	13	29	18	18
#30 (0.600 mm)	11	18	12	12
#50 (0.300 mm)	10	9	6	6
#100 (0.150 mm)	9	5	4	3
#200 (0.075 mm)	8.0	4.0	2.8	2.3
Agg Blend G_{sb}	2.574	2.567	2.572	2.572
G_{mm}	2.395	2.458	2.477	2.455
% Binder Content	6.6	4.8	4.0	4.6
% Virgin Binder	6.6	4.0	3.0	3.4
% G_{mm} @ N_{ini}^a	83.6	88	--	--
% G_{mm} @ N_{des}^a	96.5	96	--	--
% G_{mm} @ N_{max}^a	--	97.7	--	--
Asphalt Binder	PG76-22 SBS	PG76-22 SBS	PG 64-22	PG 64-22
Design Air Void, %	3.5	4.0	4.0	3.0
VMA, %	16.1	12.5	11.6	11.8
F/A ratio	1.2	0.9	--	--
50-30 Ratio	-1	-1	--	--
TSR Ratio (%)	85.7	82.5	--	--
Cellulose Fiber	0.30%	--	--	--
CA Angularity (%)	100	100	--	--
FA Angularity (%)	46.5	45.47	--	--
RAP %	0	10	20	20
RAP %AC		6.01	5.20	6.01

^a N_{ini} , N_{des} , and N_{max} are 7, 65, and 105, respectively.

two PG binders used for this project are given in Table 2. All properties of both PG binders were well within the respective specification limits for their grades. Figure 2, from the previous report [Sargand, Figueroa, and Romanello, 2008] shows the AC layers in Section 664, which are the same throughout the project. The original asphalt mix designs proposed (as-designed JMFs) for the project are very similar to the as-built mix designs and are listed in Appendix A.

2.3 Mechanistic-Based Design Approach

The thickness of the perpetual pavement layers was determined using an elastic layer-based design procedure. This is a mechanistic-based approach that uses the principles of mechanics to compute the pavement structure's reaction to loading and environmental factors [Newcomb, 2002]. Materials are characterized in terms of their elastic modulus and Poisson's ratio, which are functions of temperature and other climatic effects such as moisture. The design values for each layer are shown in Table 3.

Table 2. Properties of PG binders.

Binder Type	PG 76-22 SBS	PG 64-22
Original Binder		
Rotational Rheometer: Viscosity @ 135°C Max 3 Pa·s (0.3 poise)	1.139 Pa·s (0.1139 poise)	0.431 Pa·s (0.0431 poise)
Dynamic Shear Rheometer: G*/sin δ, Min 1.00 kPa (0.145 psi) @ 10 rad/s	1.45 kPa (0.211 psi) @76°C (169°F)	1.38 kPa (0.201 psi) @64°C (147°F)
Rolling Thin-Film Residue		
Mass Loss, Maximum 1.00%	0.291%	0.126%
Dynamic Shear Rheometer: G*/sin δ, Min 2.20 kPa (0.319 psi) @ 10rad/s	2.86 kPa (0.414 psi) @76°C (169°F)	3.24 kPa (0.471 psi) @64°C (147°F)
Pressure-aging Vessel (PAV) Residue		
Dynamic Shear Rheometer: G* sin δ, Max 5000 kPa (726 psi) @ 10rad/s	1198 kPa (173.9 psi) @31°C (88°F)	3129 kPa (454.2 psi) @25°C (77°F)
Bending Beam Rheometer: Creep Stiffness, S, Max 300 MPa (43.54 ksi) @ 60 sec	102 MPa (14.8 ksi) @-12°C (10°F)	209 MPa (30.4 ksi) @-12°C (10°F)
Bending Beam Rheometer: m-value, Min 0.300 @ 60 sec	0.346 @-12°C (10°F)	0.316 @-12°C (10°F)

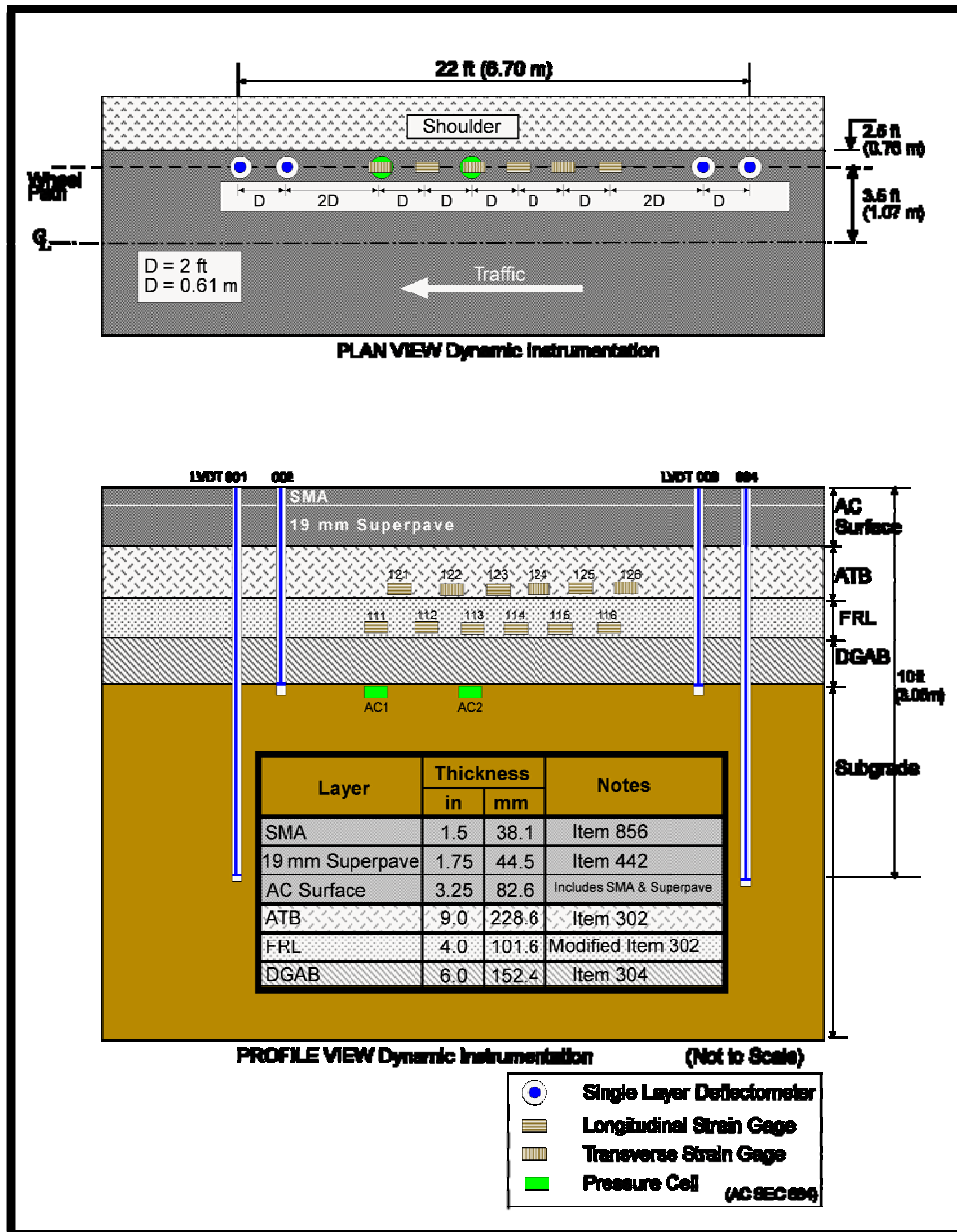


Figure 2. AC structure and instrumentation plan for AC Section 664. [Sargand, Figueroa, and Romanello, 2008]

The initial mechanical properties of materials used in the linear elastic analysis were determined using values from the Ohio database, in particular data from the SHRP Test Road on US Route 23 [Sargand, Masada, and Figueroa, 2003], augmented where appropriate with data from the literature, and laboratory tests on 6 in. (150 mm) core samples. Loading configurations were set for a 20 kip (89 kN) and 24 kip (107 kN) single axle truck and a 41 kip (182 kN) tandem axle truck. The analysis showed that a 9-in. (230 mm) high-modulus layer would be sufficient to limit the tensile strain at the

bottom of the fatigue resistant layer to 70 $\mu\epsilon$. The high-modulus layer in this design consists of Asphalt Treated Base (ATB), ODOT Item 302, as shown in Table 3. Figure 3 shows the predicted relationship between the tensile strain at the bottom of the fatigue layer and the thickness of this ATB layer for a 41 kip (182 kN) tandem axle truck. This load proved to be the most critical in establishing the design parameters.

Table 3. WAY-30 asphalt concrete (AC) perpetual pavement design properties.

Layer (surface to subgrade)	ODOT Item Number	Modulus of Elasticity, E		Poisson's Ratio
		(psi)	(MPa)	
Stone Matrix Asphalt (SMA)	856	1,500,000	10342	0.35
19 mm Superpave	442	1,500,000	10342	0.35
Asphalt Treated Base (ATB) Layer	302	500,000 – 1,500,000	3447 - 10342	0.35
Fatigue Resistance Layer (FRL)	Modified 302	500,000 – 1,500,000	3447 - 10342	0.35
Dense Graded Aggregate Base (DGAB)	304	10,000	69	0.40
Subgrade		5,000	34.5	0.45

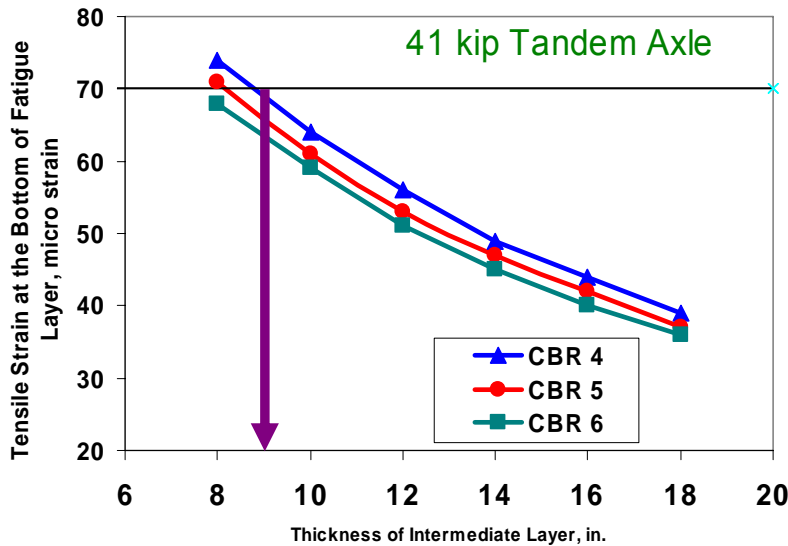


Figure 3. Required AC thickness for 70 microstrain limit assuming a subgrade CBR in the range 4 – 6. (1 in = 2.54 cm, 41 kip = 182 kN).

2.4 WAY-30 Portland Cement Concrete Design

The long-lived PCC pavement in the eastbound lanes of WAY-30 was based on a design provided by the concrete industry. The following design specifications were used:

- 4 in. (10 cm) subbase: ODOT Item 304, a highly crushed densely graded granular base (DGAB), with under drains.
- 3 in. (7.5 cm) AC base: ODOT Item 301 with PG 64-22 asphalt binder.

- 10 in. (25 cm) Portland cement concrete surface layer: jointed plain concrete pavement, Mix A or Mix B, with 15 ft (4.6 m) slab lengths. The joints included 1.5 in. (3.8 cm) diameter dowel bars at 12 in. (30.5 cm) spacing.

Two PCC mixes were used, each with a different partial cement substitutes. Mix Design A featured Ground Granular Blast Furnace Slag (GGBFS) and Mix Design B used Fly Ash. Table 4 shows the percentage of each cement substitute used in the mix designs. Mix A was used on sections 876 and 877, and Mix B was used in Section 664. Both concrete mix designs actually used in the construction of the test pavement (as-built mix designs) are presented in Table 5. The pavement structure is separately illustrated in Figure 4. The original mix designs proposed for this project are almost identical to the as-built designs and are also given in Appendix A.

The slabs were 14 ft (4.27 m) wide, including a standard 12 ft (3.66 m) wide lane plus a 2 ft (0.61 m) strip of PCC pavement on the shoulder. The wider pavement slab is part of the long-life design meant to spread the load over a wider area. The passing lane was 12 ft (3.66 m) wide on a standard 12 ft (3.66 m) wide slab. An 8 ft (2.44 m) tied concrete shoulder was added to the outside of the pavement, and a 4 ft (1.22 m) tied concrete shoulder was added to the inside.

Table 4. Percentage by weight of GGBFS and fly ash materials in PCC mix.

Mix	Section	Substituted Material	Total Cementitious Material	Total Batch Weight SSD
A	876, 877	GGBFS	30%	4.9%
B	664	Fly Ash	20%	3.3%

2.5 Construction

Construction of test pavements was carefully controlled throughout the project and the job mix formulas (JMF) given in Tables 1 and 5 are closely followed. There had not been any change in mix designs during construction for both asphalt concretes and Portland cement concretes other than minor aggregate blending adjustment to correct gradations in asphalt mixes. One example of a JMF change occurred on September 20, 2005 for FRL mix where the proportions of some stock piles of aggregates were changed 1 or 2 % to fine tune the gradation of the blend. Both the contractor and Ohio DOT engineers reported that construction of both asphalt and PCC pavements had proceeded smoothly. In fact, the contractor was awarded by an industry association for its quality paving of the asphalt test pavement. Only interruption due to segregation problem occurred during construction of asphalt base course at the instrumented section. The visually identified segregated section was reported and later confirmed by laboratory tests (resilient modulus and indirect tensile strength). The contractor identified the storage silo as the source of the segregation and fixed the problem immediately. The segregated section was removed and repaved correctly. Quality control and quality assurance data are summarized in Appendices B and C for asphalt ACC and PCC pavements, respectively.

Table 5. PCC mix designs and mix properties.

	Specific Gravity	Absorption %	GGBFS Mix	Fly Ash Mix
Material Batch Weight SSD, lb/yd³ of Fresh Concrete (kg/m³)				
Natural Sand	2.608	1.59	1161 (688.8)	1161 (688.8)
#8 Limestone	2.619	2.29	461 (273.5)	461 (273.5)
#467 Limestone	2.658	1.13	1400 (830.6)	1400 (830.6)
Type I Cement	3.15	X	415 (246.2)	477 (283.0)
GGBFS	2.72	X	178 (105.6)	-
Fly Ash (Type F)	2.70	X	-	119 (70.6)
Water			259 (153.7)	259 (153.7)
Total			3876 (2299.5)	3859 (2289.5)
Admixtures Used, oz/yd³ (ml/m³)				
ASTM C 260 AEA (MBL PAV AIR-90)			31 (1201)	31 (1201)
ASTM C 494 WRR - Type B,D (MBL MSTR PAV RI)			11 (426)	11 (426)
Water/CM Ratio				
			0.44	0.44
Fresh Concrete Properties				
Slump, in. (mm)			1.5 (38)	1.5 (38)
Air Content, %			5.2 – 5.4	5.6 – 6.8
Temperature, °F (°C)			78-88 (25.6-31.1)	81-86 (27.2-30.0)
Unit Weight, lb/ft ³ (kg/m ³)			143.56 (2300)	142.93 (2289)
Hardened Concrete Properties				
Compressive Strength, psi (MPa)				
7-day			5930 (40.9)	4010 (27.6)
14-day			6210 (42.8)	4220 (29.1)
28-day			7880 (54.3)	5290 (36.5)
Specified Design Strength (f _c)			5070 (35.0)	4000 (27.6)
Required Over-Design Value			1400 (9.65)	1200 (8.27)
Modulus of Rupture, psi (MPa)				
14-day Beam			775 (5.34)	775 (5.34)
Permeability (coulombs)				
28-day			1505	1128
Specified Design Permeability			2000	2000

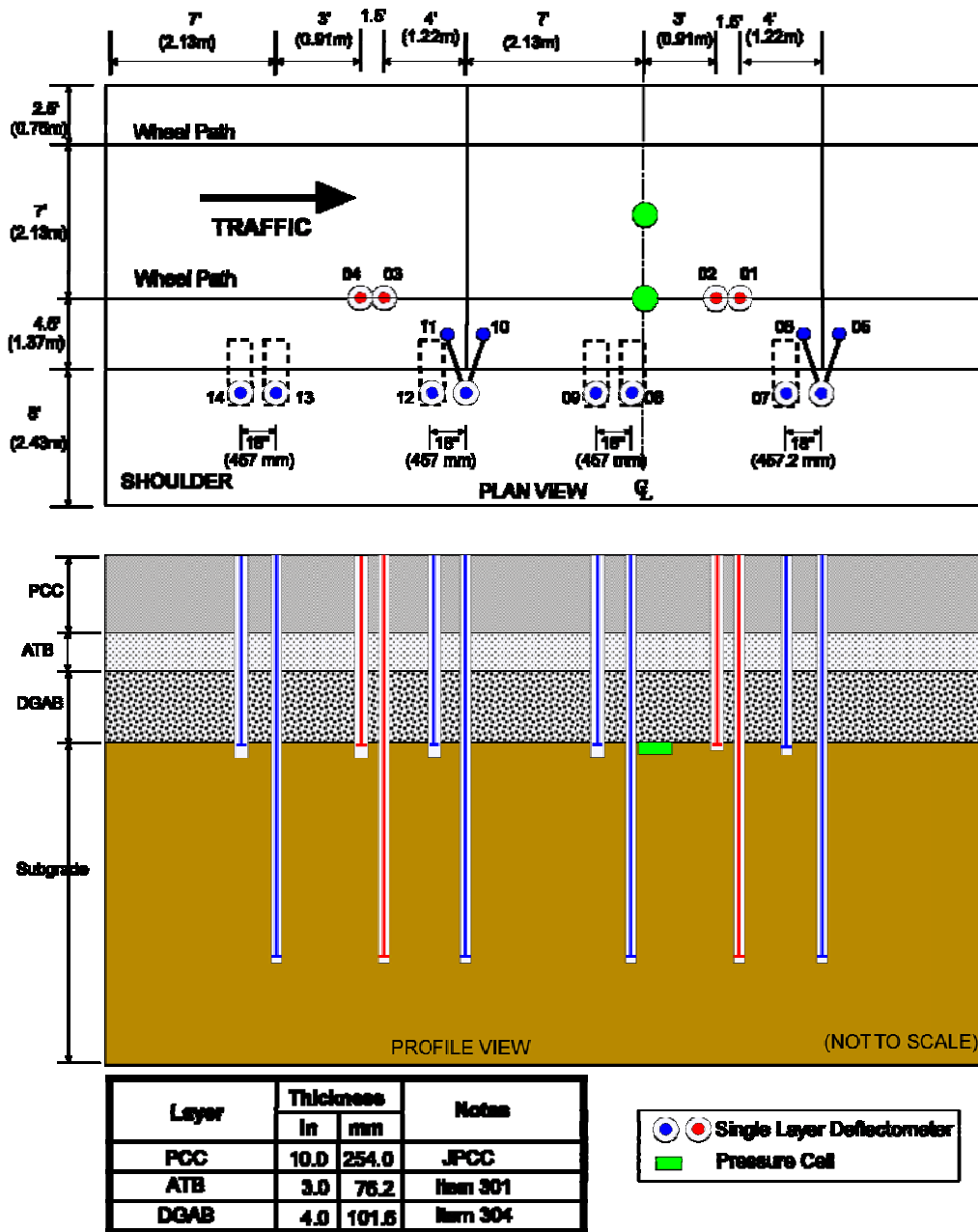


Figure 4. Illustration showing the pavement structure and instrumentation of the PCC sections of WAY-30. [Sargand, Figueroa, and Romanello, 2008]

3 LABORATORY TEST RESULTS ON WAY-30 SUBGRADE SOILS

A total of six samples were taken and identified by their location as: Way Subg WB STA 885+00, Way Subg EB STA 876+60, Way Subg WB STA 876+60, Way Subg EB Right Side STA 884+00, Way Subg EB Left Side STA 884+00, and Way Subg EB STA 663+50, where WB and EB stand for West Bound and East Bound.

Grain size analysis and Atterberg limit tests were performed to classify each sample. Based on the obtained results, all the samples were classified as A-4 (moderately plastic silty soil) according to the ASSHTO Soil Classification System (A-4-a according to the ODOT Soil Classification System). The results are summarized in Table 6.

After being classified, each sample was subjected to the compaction analysis using the Standard Proctor Test in order to obtain the optimum moisture content and maximum dry density. The results and the compaction curves are provided in Figure 5.

Then, the Resilient Modulus was measured for each sample. The equipment used to carry out this test is compatible with the AASHTO T-274 specification and SHRP test protocol P-46. It is composed by an electro-servo-controlled actuator, a large triaxial chamber, and a computerized command generator and data acquisition unit. In each test, load cycles are applied using Haversine-shaped pulse load. This type of pulse load is divided into two parts: the first one is a 0.1-second loading period and the second one is a rest period of 0.9 seconds, for a total of 1.0 second per cycle.

A confining pressure σ_c of 6.0 psi (41 kPa), 4.0 psi, (28 kPa) and 2.0 psi (14 kPa) were used for all samples; except for Way Subg EB STA 663+50 where 6.0 psi (41 kPa), 3.0 psi (21 kPa) and 0.0 psi (0.0 kPa) were used. For each confining pressure, deviatoric stresses σ_d of 2.0 psi (14 kPa), 4.0 psi (28 kPa), 6.0 psi (41 kPa), 8.0 psi (55 kPa), and 10.0 psi (69 kPa) were applied; each of them with 100 repetitions; overall, each sample was subjected to fifteen load sequences. In each load sequence, the data for the last 5 repetitions were recorded and the average recoverable axial strain was used for calculating the Resilient Modulus M_r . The Resilient Modulus M_r for each sequence is shown in Tables 7 and 8. These tables present the actual deviatoric stress σ_d for each chamber pressure, the mean resilient strain ϵ_r , and the corresponding Resilient Modulus M_r .

Figures 6 through 11 illustrate the relationship between the Resilient Modulus M_r (ksi) and deviatoric stress σ_d (psi) for each sample, along with a least-squares exponential fit of the data and the resulting regression relationship. The resilient modulus of the subgrade soil samples ranged mostly between 3 ksi (21 MPa) and 7 ksi (48 MPa) under the laboratory test conditions. This range corresponds particularly well with the values of resilient modulus that Figueroa [1994] backcalculated from his FWD test data for A-4a pavement subgrade soil layers located in Adams County, Ohio. These values were between 2.8 ksi (19 MPa) and 6.1 ksi (42 MPa).

Table 6. Classification, maximum dry unit weight, and optimum moisture content of subgrade soil samples.

Specimen	Liquid Limit (%)	Plastic Limit (%)	Plastic Index (%)	% Passing #200 sieve					Classification		OMC (%)	$\gamma_{d,max}$	
				Total		(-) 200		%	AASHTO	ODOT		(pcf)	(kg/m ³)
				(lb)	(g)	(lb)	(g)						
Way Subg WB STA 885+00	26.94	17.04	9.90	0.527	239.0	0.247	112.0	46.9	A-4	A-4-a	12.1	117.5	1882.2
Way Subg EB STA 876+60	26.66	17.23	9.43	0.459	208.0	0.175	79.5	38.2	A-4	A-4-a	12.8	118.0	1890.2
Way Subg WB STA 876+60	25.90	17.67	8.23	0.474	215.0	0.186	84.5	39.3	A-4	A-4-a	14.4	117.5	1882.2
Way Subg EB Right Side STA 884+00	25.99	18.72	7.27	1.142	518.0	0.476	216.0	41.7	A-4	A-4-a	14.5	116.0	1858.1
Way Subg EB Left Side STA 884+00	24.44	16.49	7.95	0.520	236.0	0.255	115.5	48.9	A-4	A-4-a	13.3	117.5	1882.2
Way Subg EB STA 663+50	23.28	17.20	6.15	0.477	216.4	0.196	88.7	41.0	A-4	A-4-a	11.8	121.0	1938.2

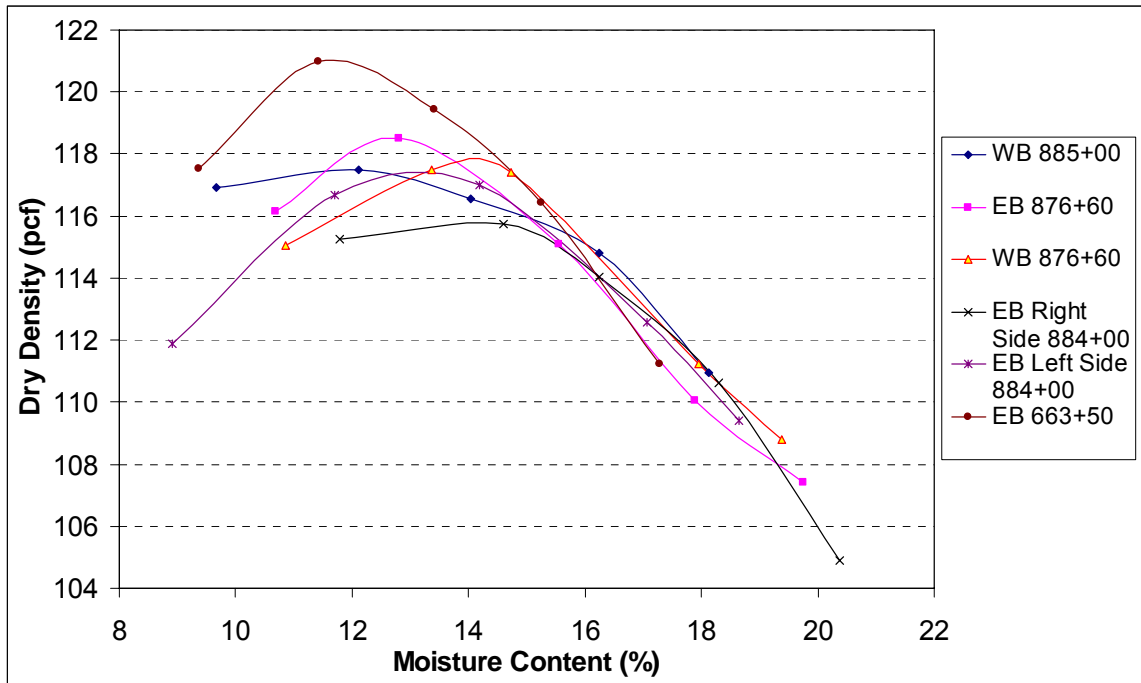


Figure 5. Compaction curves of subgrade soils. (1 pcf = 16.02 kg/m³)

Table 7. Resilient modulus for STA 876+60 and WB STA 885+00 subgrade.

Confining Stress σ_c (psi)	Way Subg WB STA 876+60 (Test 1)			Way Subg EB STA 876+60 (Test 2)			Way Subg WB STA 885+00		
	ENGLISH UNITS								
	w=12.1%; $\gamma_d=113.9$ pcf			w=15.1%; $\gamma_d=119.8$ pcf			w=13.1%; $\gamma_d=115.0$ pcf		
	σ_d (psi)	ϵ_r (%)	M_r (ksi)	σ_d (psi)	ϵ_r (%)	M_r (ksi)	σ_d (psi)	ϵ_r (%)	M_r (ksi)
6.0	2.763	0.028	9.91	1.39	0.029	4.8	0.601	0.017	3.508
6.0	5.799	0.07	8.267	4.012	0.107	3.744	2.543	0.073	3.505
6.0	8.367	0.116	7.229	6.212	0.174	3.574	4.621	0.124	3.714
6.0	10.904	0.169	6.449	8.492	0.253	3.356	6.688	0.178	3.764
6.0	13.526	0.214	6.333	11.078	0.318	3.486	8.532	0.225	3.793
4.0	2.78	0.039	7.083	1.692	0.031	5.41	0.31	0.004	8.294
4.0	5.478	0.075	7.263	3.724	0.104	3.58	2.404	0.06	3.996
4.0	7.961	0.122	6.516	5.881	0.185	3.177	4.137	0.108	3.842
4.0	10.738	0.172	6.248	8.543	0.265	3.22	5.861	0.156	3.748
4.0	13.6	0.221	6.142	11.165	0.333	3.353	7.589	0.199	3.815
2.0	2.559	0.031	8.142	1.689	0.033	5.124	0.258	0.003	7.774
2.0	5.252	0.084	6.281	3.623	0.106	3.404	2.103	0.053	3.989
2.0	7.662	0.134	5.714	5.745	0.191	3.011	3.862	0.101	3.813
2.0	10.474	0.189	5.541	8.377	0.271	3.088	5.448	0.144	3.773
2.0	13.485	0.242	5.566	11.187	0.341	3.284	7.216	0.189	3.821
Confining Stress σ_c (kPa)	INTERNATIONAL UNITS								
	w=12.1%; $\gamma_d=1825$ kg/m ³			w=15.1%; $\gamma_d=1919$ kg/m ³			w=13.1%; $\gamma_d=1842$ kg/m ³		
	σ_d (kPa)	ϵ_r (%)	M_r (MPa)	σ_d (kPa)	ϵ_r (%)	M_r (MPa)	σ_d (kPa)	ϵ_r (%)	M_r (MPa)
41.4	19.05	0.028	68.33	9.58	0.029	33.09	4.14	0.017	24.19
41.4	39.98	0.07	57.00	27.66	0.107	25.81	17.53	0.073	24.17
41.4	57.69	0.116	49.84	42.83	0.174	24.64	31.86	0.124	25.61
41.4	75.18	0.169	44.46	58.55	0.253	23.14	46.11	0.178	25.95
41.4	93.26	0.214	43.66	76.38	0.318	24.04	58.83	0.225	26.15
27.6	19.17	0.039	48.84	11.67	0.031	37.30	2.14	0.004	57.19
27.6	37.77	0.075	50.08	25.68	0.104	24.68	16.57	0.06	27.55
27.6	54.89	0.122	44.93	40.55	0.185	21.90	28.52	0.108	26.49
27.6	74.04	0.172	43.08	58.90	0.265	22.20	40.41	0.156	25.84
27.6	93.77	0.221	42.35	76.98	0.333	23.12	52.32	0.199	26.30
13.8	17.64	0.031	56.14	11.65	0.033	35.33	1.78	0.003	53.60
13.8	36.21	0.084	43.31	24.98	0.106	23.47	14.50	0.053	27.50
13.8	52.83	0.134	39.40	39.61	0.191	20.76	26.63	0.101	26.29
13.8	72.22	0.189	38.20	57.76	0.271	21.29	37.56	0.144	26.01
13.8	92.98	0.242	38.38	77.13	0.341	22.64	49.75	0.189	26.34

Table 8. Resilient modulus for WB STA 884+00 and STA 663+50 subgrade.

Confining Stress σ_c (psi)	Way Subg EB Right Side STA 884+00 (Test 1)			Way Subg EB Left Side STA 884+00 (Test 2)			Way Subg EB STA 663+50		
	ENGLISH UNITS								
	w = 13.2%; γ_d = 116.7 pcf			w = 12.1%; γ_d = 115.4 pcf			w = 12.5%; γ_d = 111.7 pcf		
	σ_d (psi)	ϵ_r (%)	M_r (ksi)	σ_d (psi)	ϵ_r (%)	M_r (ksi)	σ_d (psi)	ϵ_r (%)	M_r (ksi)
6.0	1.597	0.021	7.437	1.496	0.01	15.433	1.697	0.026	6.451
6.0	5.277	0.105	5.045	6.376	0.064	10.033	4.281	0.085	5.055
6.0	8.524	0.164	5.185	9.223	0.101	9.176	6.664	0.145	4.586
6.0	11.32	0.221	5.131	16.73	0.211	7.944	9.349	0.184	5.086
6.0	14.258	0.286	4.987	15.085	0.188	8.029	11.941	0.233	5.123
4.0	1.616	0.026	6.322	3.12	0.026	11.785	1.814	0.026	6.962 ^a
4.0	5.059	0.109	4.657	5.823	0.068	8.509	4.316	0.079	5.472 ^a
4.0	8.146	0.171	4.766	9.06	0.112	8.114	6.691	0.13	5.130 ^a
4.0	10.959	0.226	4.852	11.998	0.151	7.935	9.449	0.184	5.135 ^a
4.0	13.953	0.292	4.774	15.041	0.193	7.781	12.215	0.234	5.222 ^a
2.0	1.561	0.025	6.126	2.946	0.029	10.057	1.741	0.025	7.017 ^b
2.0	4.855	0.107	4.554	5.747	0.076	7.59	4.292	0.08	5.395 ^b
2.0	7.768	0.171	4.536	8.891	0.12	7.432	6.639	0.13	5.095 ^b
2.0	10.562	0.231	4.568	11.813	0.163	7.259	9.386	0.184	5.105 ^b
2.0	13.675	0.298	4.588	14.892	0.208	7.166	12.34	0.235	5.250 ^b
Confining Stress σ_c (kPa)	INTERNATIONAL UNITS								
	w=13.2%; γ_d =1869.3 kg/m ³			w=12.1%; γ_d =1848.5 kg/m ³			w =12.5%; γ_d =1789.3 kg/m ³		
	σ_d (kPa)	ϵ_r (%)	M_r (MPa)	σ_d (kPa)	ϵ_r (%)	M_r (MPa)	σ_d (kPa)	ϵ_r (%)	M_r (MPa)
	41.4	11.01	0.021	51.28	10.31	0.01	106.41	11.70	0.026
41.4	36.38	0.105	34.78	43.96	0.064	69.18	29.52	0.085	34.85
41.4	58.77	0.164	35.75	63.59	0.101	63.27	45.95	0.145	31.62
41.4	78.05	0.221	35.38	115.35	0.211	54.77	64.46	0.184	35.07
41.4	98.31	0.286	34.38	104.01	0.188	55.36	82.33	0.233	35.32
27.6	11.14	0.026	43.59	21.51	0.026	81.25	12.51	0.026	48.00 ^c
27.6	34.88	0.109	32.11	40.15	0.068	58.67	29.76	0.079	37.73 ^c
27.6	56.16	0.171	32.86	62.47	0.112	55.94	46.13	0.13	35.37 ^c
27.6	75.56	0.226	33.45	82.72	0.151	54.71	65.15	0.184	35.40 ^c
27.6	96.20	0.292	32.92	103.70	0.193	53.65	84.22	0.234	36.00 ^c
13.8	10.76	0.025	42.24	20.31	0.029	69.34	12.00	0.025	48.38 ^b
13.8	33.47	0.107	31.40	39.62	0.076	52.33	29.59	0.08	37.20 ^b
13.8	53.56	0.171	31.27	61.30	0.12	51.24	45.77	0.13	35.13 ^b
13.8	72.82	0.231	31.50	81.45	0.163	50.05	64.71	0.184	35.20 ^b
13.8	94.29	0.298	31.63	102.68	0.208	49.41	85.08	0.235	36.20 ^b

^a 3 psi confining stress; ^b no confining stress; ^c 207 kPa confining stress

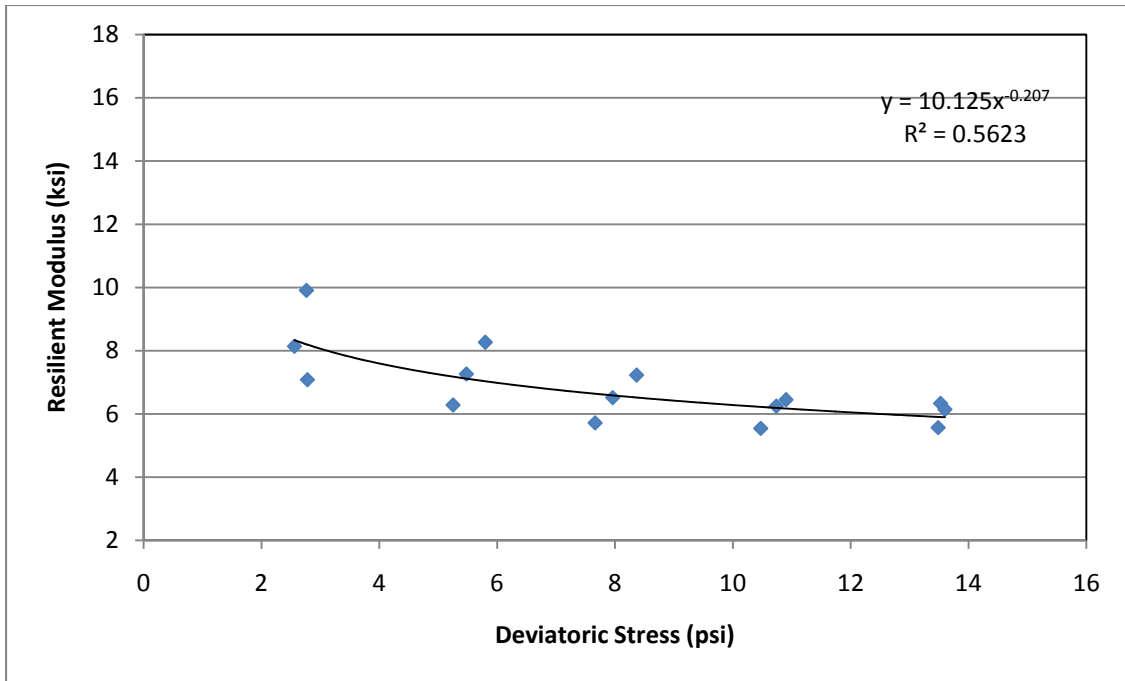


Figure 6. Resilient modulus vs. deviatoric stress for WB STA 876+60 subgrade (Test 1).

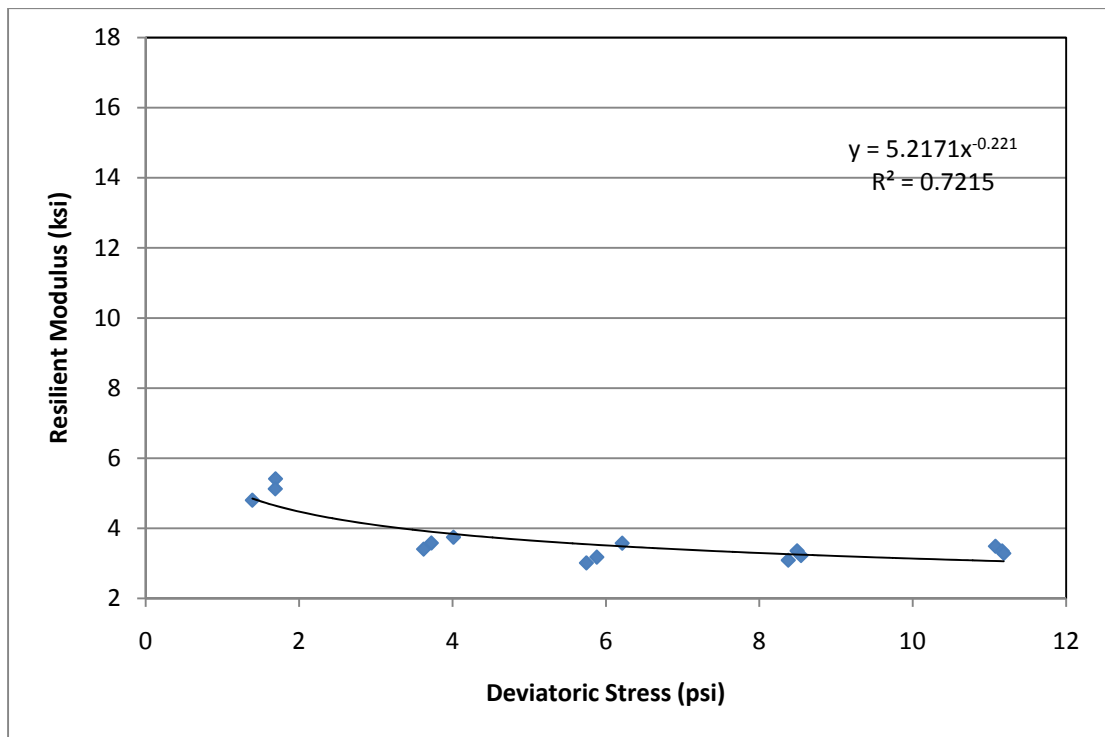


Figure 7. Resilient modulus vs. deviatoric stress for EB STA 876+60 subgrade (Test 2). (1ksi = 6.895 MPa)

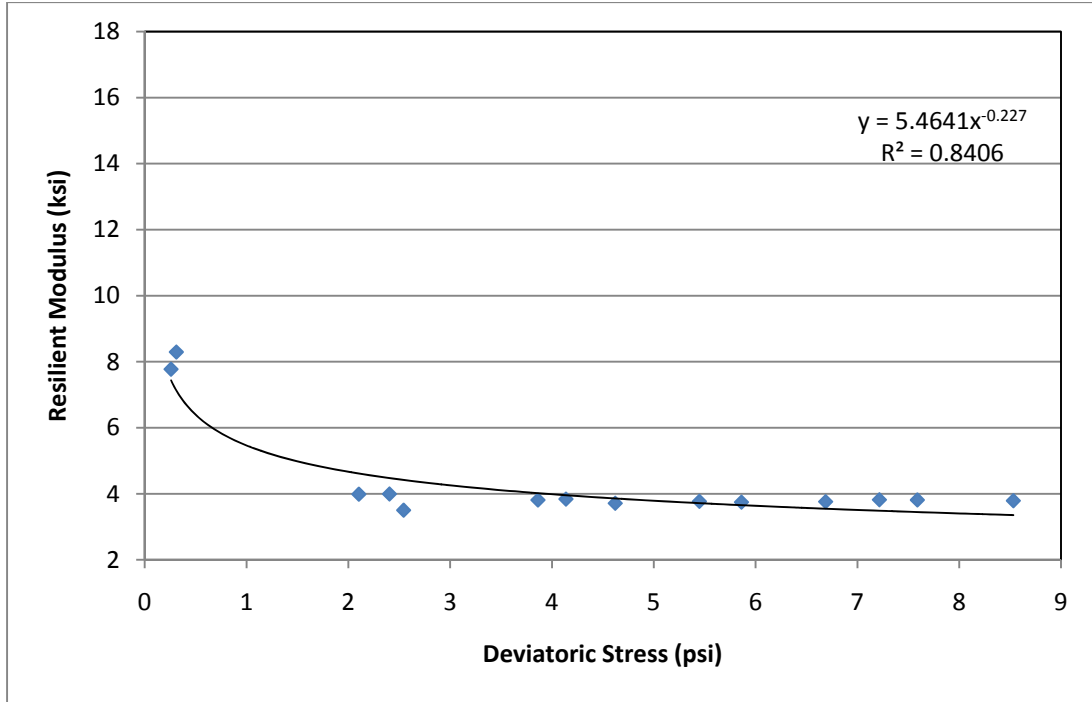


Figure 8. Resilient modulus vs. deviatoric stress for WB STA 885+00 subgrade.

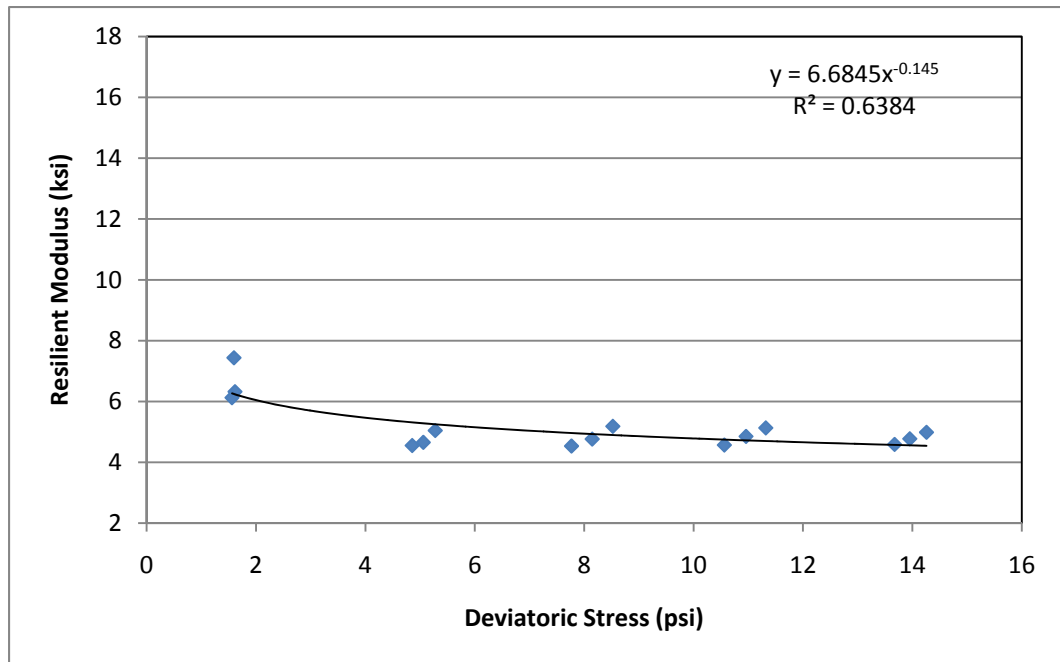


Figure 9. Resilient modulus vs. deviatoric stress for EB STA 884+00 subgrade.
(1 ksi = 6.895 MPa)

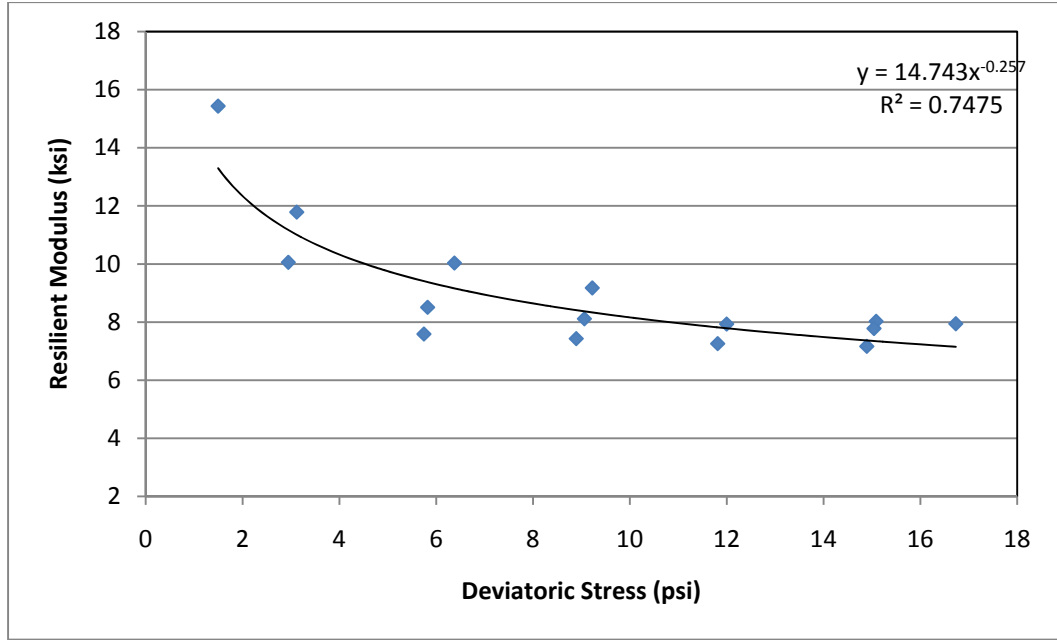


Figure 10. Resilient modulus vs. deviatoric stress for EB STA 884+00 subgrade (Test 2).

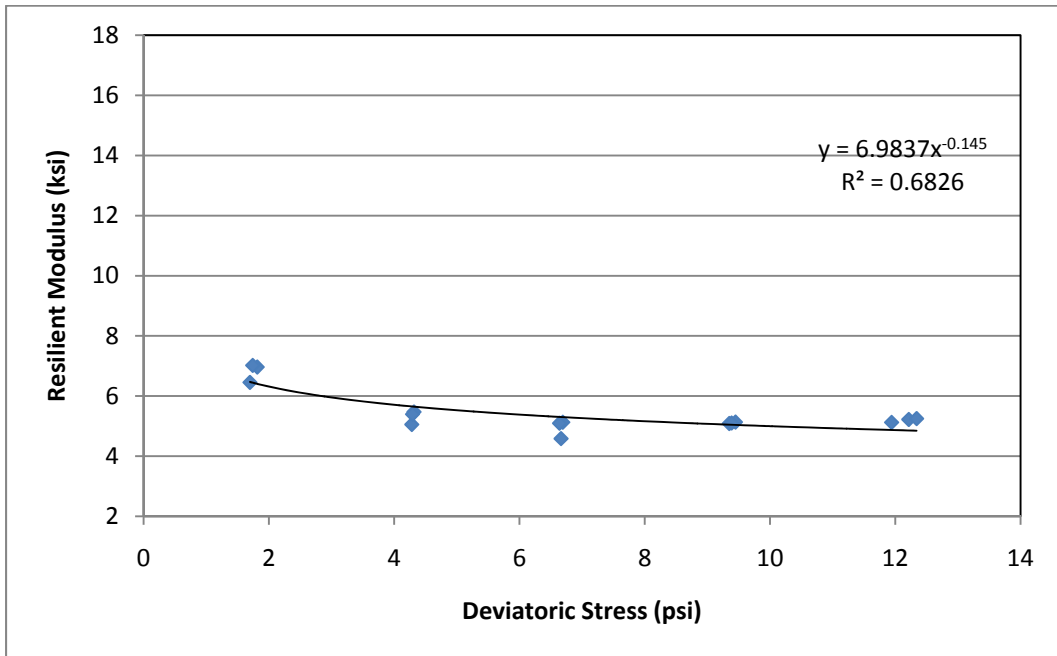


Figure 11. Resilient modulus vs. deviatoric stress for EB STA 663+50 subgrade. (1 ksi = 6.895 MPa)

4 LABORATORY TESTING OF SUBBASE MATERIAL

Subbase material recovered from the project site was subjected to three laboratory test methods: the mechanical sieve analysis and the resilient modulus test. The grain size characteristics of the material were determined according to ASTM D-422 (or AASHTO T-88). A stack of mechanical sieves was prepared with the top sieve opening approximately matching the largest grain size and the bottom sieve being Sieve No. 200. A sizable quantity (12.1 lb or 5.0 kg) of the material was poured into the top sieve. The stack was shaken inside an electric sieve shaker for 15 minutes. After the shaking, the mass of soil retained in each sieve was recorded with a high-precision electronic scale. Results of sieve analysis are summarized in Table 9 and Figure 12 below.

Table 9. Results of mechanical sieve analysis of subbase.

Sieve	Mass Retained		% Passing	Sieve	Mass Retained		% Passing
	(slug)	(g)			(slug)	(g)	
1"	0.0036	52	98.96	#30	0.0111	161.5	17.27
1/2"	0.1401	2044	58.08	#50	0.0155	225.5	12.76
3/8"	0.0354	516	47.76	#100	0.0190	277	7.22
#4	0.0522	762.5	32.51	#200	0.0128	186.5	3.49
#8	0.0264	385.5	24.8	Pan	0.0119	174	--
#16	0.0147	215	20.5	TOTAL	0.3426	4999.5	

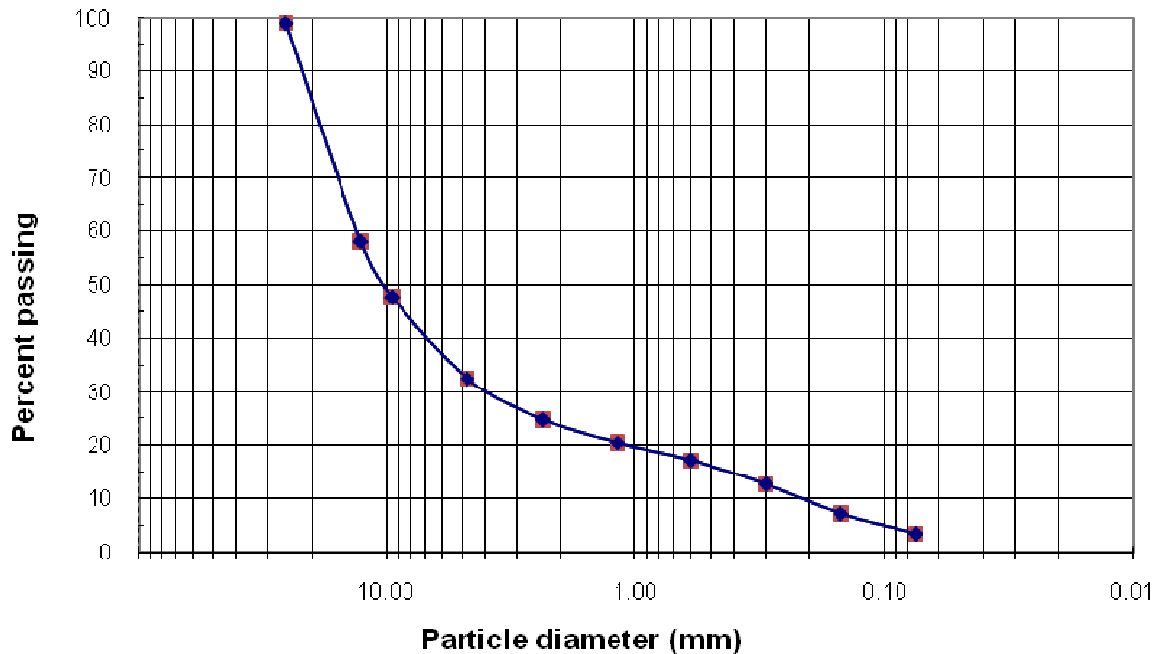


Figure 12. Grain size distribution curve of subbase material. (25.4 mm = 1.00 in.)

According to the sieve analysis data, this soil sample could be categorized as follows:

- Gravel 67.5%
- Coarse Sand 17.5%
- (Medium + Fine) Sand 11.5%
- Fines (Silt + Clay) 3.5%.

This soil sample possessed the following characteristics:

- D_{60} Size = 13.0 mm (0.512 in)
- D_{30} Size = 4.0 mm (0.16 in)
- D_{10} Size = 0.2 mm (0.008 in)
- Uniformity Coefficient (C_u) = 65
- Coefficient of Gradation (C_c) = 6.2

The soil was classified as A-1-*a* (AASHTO) and GW: Well-Graded Gravel w/ Sand (Unified). Thus, based on these test results, it was determined that the material can be treated as Type I (coarse-grained) soil during the subsequent resilient modulus test procedure.

In the resilient modulus test, a sample of the material that was passed through a sieve with a 1-in. (2.54 cm) wire mesh opening, as per requirements of AASHTO T-294, that states that the largest particle size must be less than 1/5 of the mold inside diameter, 6 in (15.2 cm). All particles retained on 1-in. (2.54 cm) opening size sieve were removed from the soil sample, which accounted for only about 1% of the total soil mass.

The resilient modulus test was performed twice using a computerized test system housed in the ORITE Pavement Material Test Laboratory. In each trial, the soil specimen was prepared by compacting six equal thickness layers, using an air-driven vibrating tamper, inside a rubber membrane attached to a split-mold. In each trial, the test specimen was subjected to repeated 1-Hz haversine load sequences under varying levels of chamber confining pressure. Table 10 summarizes basic characteristics of each test specimen. Figure 13 shows pictures taken during the specimen preparation stage, while Figure 14 shows the specimen being tested.

Table 10. Basic characteristics of subbase resilient modulus specimens.

Specimen	Trial 1 Specimen	Trial 2 Specimen
Soil Type	Type I	Type I
Specimen Diameter	6.0 in (15.24 cm)	6.0 in (15.24 cm)
Specimen Height	12.25 in (31.11 cm)	12.75 in (32.38 cm)
Max. Grain Size	1.0 in (2.5 cm)	1.0 in (2.5 cm)
Moisture Content	0% to 1% (dry)	0% to 1 %
No. of Layers	Six (6)	Six (6)
Dry Unit Weight	126.0 pcf (2018 kg/m ³)	121.0 pcf (1938 kg/m ³)
Membrane Thickness	0.025 in. mil (635 μm)	0.025 in. (635 μm)



a)



b)



c)



d)

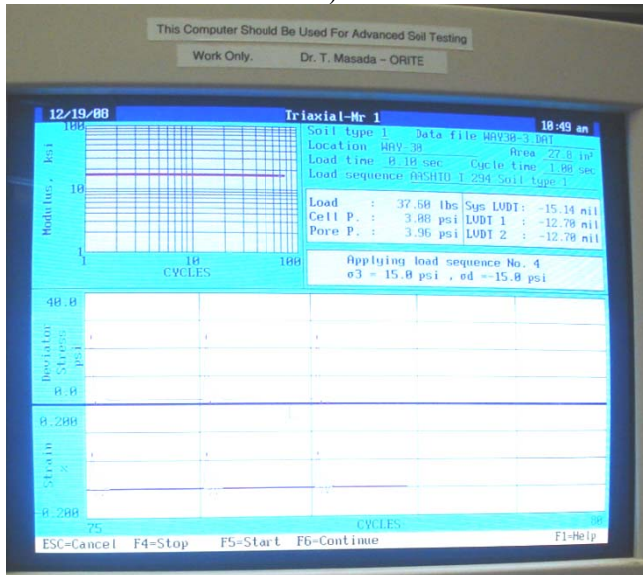
Figure 13. Preparation of subbase resilient modulus test specimen.



a)



b)



c)



d)

Figure 14. Subbase resilient modulus testing: a) close-up of specimen in test chamber, b) test chamber with connections to controller and computer, c) view of computer screen output, and d) view of test chamber and workstation.

Table 11 and Figures 15 through 18 present resilient modulus test results. Figures 15 and 16 provide the test results in terms of measured resilient modulus versus applied deviatoric stress. Resilient modulus (M_R) was defined as deviatoric stress (σ_D) divided by recoverable axial strain (ϵ_R).

In Trial 1, the computerized loading system became somewhat unsteady after loading the specimen under the confining pressure (σ_3) of 15 psi (103 kPa); thus, no test data were available under confining pressure of 20 psi (138 kPa). During Trial 2, the system operated well throughout almost the entire load sequence. The test results are presented in Table 11 and Figures 15 and 16. The resilient modulus (M_R) of the subbase material ranged from about 8 ksi (55 MPa) to 23 ksi (160 MPa) under the deviatoric stress (σ_D) of 3 psi (21 kPa) to 44 psi (303 kPa) and the confining pressure (σ_3) of 3 psi (21 kPa) to 20 psi (138 kPa). The range seen here does not appear to differ greatly from the resilient modulus values other researchers measured on similar unbound granular (ODOT Item 304) material. Abdulshafiq et al. [1994] reported the average resilient modulus of 14 to 15 ksi (97 to 103 MPa) for a DGAB material. Figueroa [2001] reported values between 15 and 26 ksi (97 and 179 MPa) for the ODOT Item 304 DGAB material. Figures 17 and 18 present the power-law correlation observed between the resilient modulus (M_R) and the bulk stress (θ). Here, the bulk stress is defined as a sum of all principal stresses (σ_1 , σ_2 , and σ_3), which reduces to ($\sigma_D + 3\sigma_3$). A strong correlation existed between the resilient modulus and the bulk stress, as evidenced by high coefficient of determination (r^2) values. And, the values of the power law coefficients are fairly consistent between the two trials. The average results can be summarized as:

$$M_R \text{ (ksi)} = 2.64 \theta^{0.46} \quad \text{Eq. 1}$$

where θ = bulk stress (psi).

Table 11. Resilient modulus of WAY-30 subbase as a function of deviatoric stress and of bulk stress.

ENGLISH UNITS						
Confining Pressure (psi)	Trial 1			Trial 2		
	Deviatoric Stress (psi)	Bulk Stress (psi)	Resilient Modulus (ksi)	Deviatoric Stress (psi)	Bulk Stress (psi)	Resilient Modulus (ksi)
3	2.509	11.509	7.522	2.965	11.965	8.823
	6.361	15.361	8.549	7.105	16.105	10.219
	10.933	19.933	9.75	11.957	20.957	11.699
5	5.408	20.408	9.417	5.936	20.936	11.294
	12.79	27.79	11.247	13.953	28.953	13.365
	20.54	35.54	12.534	21.66	36.66	14.137
10	13.942	43.942	13.88	14.47	44.47	15.445
	29.052	59.052	16.17	29.713	59.713	17.688
	43.035	73.035	18.309	43.301	73.301	19.683
15	14.406	59.406	15.389	15.382	60.382	18.072
	22.095	67.095	16.759	23.747	68.747	19.519
	43.211	88.211	19.99	44.181	89.181	22.069
20				23.952	83.952	21.054
				35.169	95.169	22.554
SI UNITS						
Confining Pressure (kPa)	Deviatoric Stress (kPa)	Bulk Stress (kPa)	Resilient Modulus (MPa)	Deviatoric Stress (kPa)	Bulk Stress (kPa)	Resilient Modulus (MPa)
20.7	17.30	79.35	51.86	20.44	82.50	60.83
	43.86	105.91	58.94	48.99	111.04	70.46
	75.38	137.43	67.22	82.44	144.49	80.66
34.5	37.29	140.71	64.93	40.93	144.35	77.87
	88.18	191.61	77.55	96.20	199.62	92.15
	141.62	245.04	86.42	149.34	252.76	97.47
68.9	96.13	302.97	95.70	99.77	306.61	106.49
	200.31	407.15	111.49	204.86	411.71	121.95
	296.72	503.56	126.24	298.55	505.39	135.71
103.4	99.33	409.59	106.10	106.06	416.32	124.60
	152.34	462.60	115.55	163.73	473.99	134.58
	297.93	608.19	137.83	304.62	614.88	152.16
20.7				165.14	578.83	145.16
				242.48	656.17	155.50

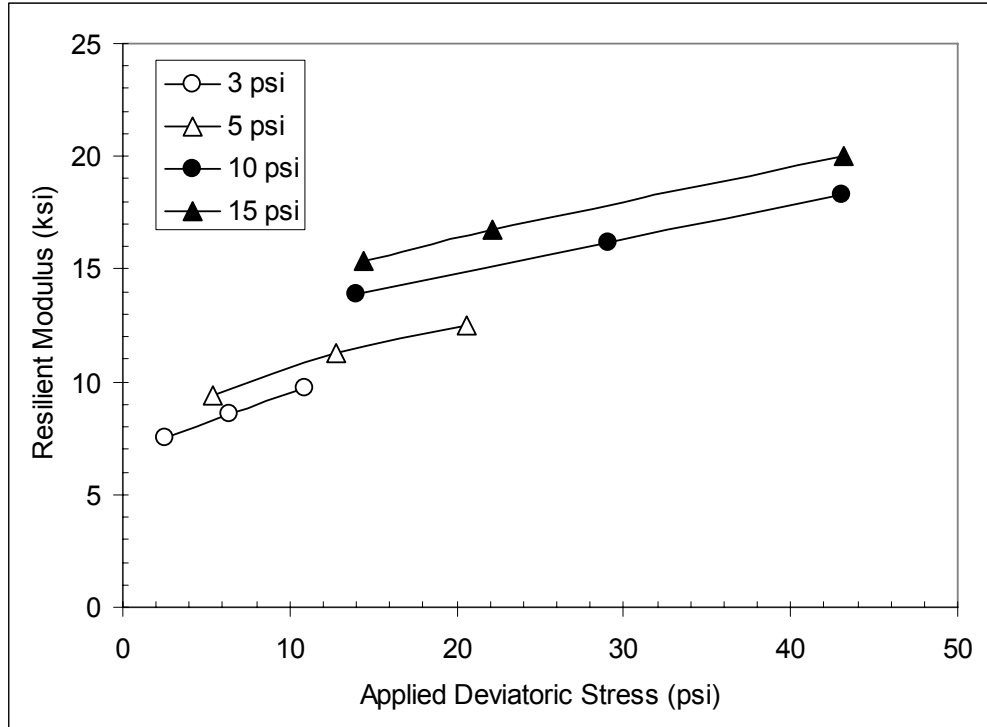


Figure 15. Resilient modulus vs. deviatoric stress of subbase (Trial 1).
 (1 ksi = 6.89 MPa)

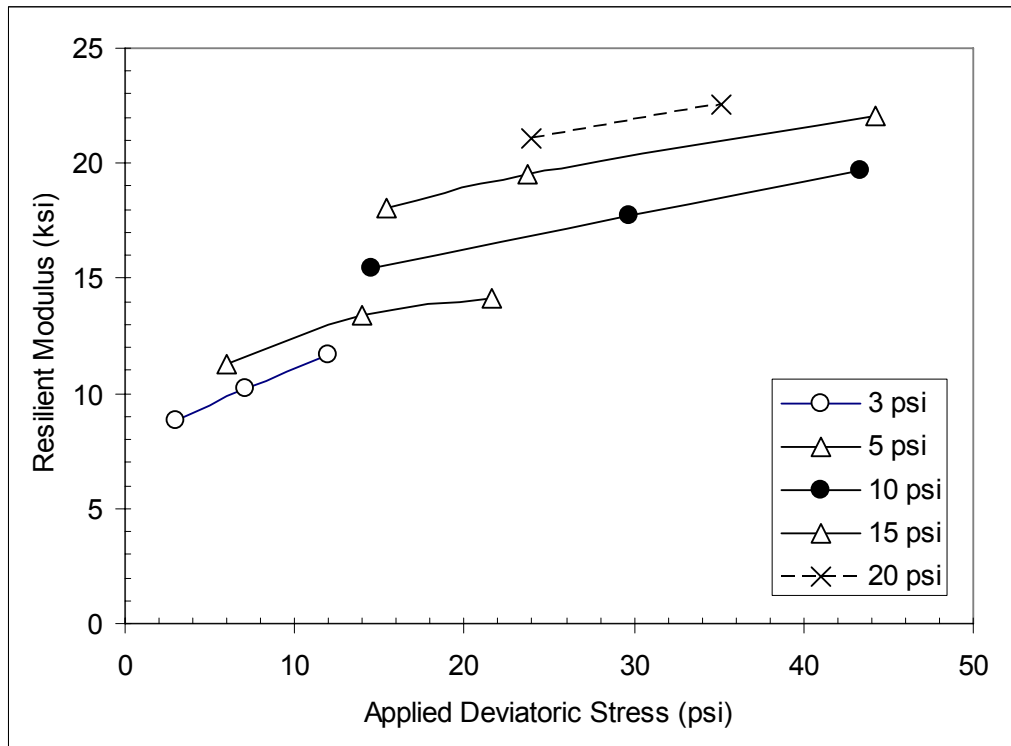


Figure 16. Resilient modulus vs. deviatoric stress of subbase (Trial 2).
 (1 ksi = 6.89 MPa)

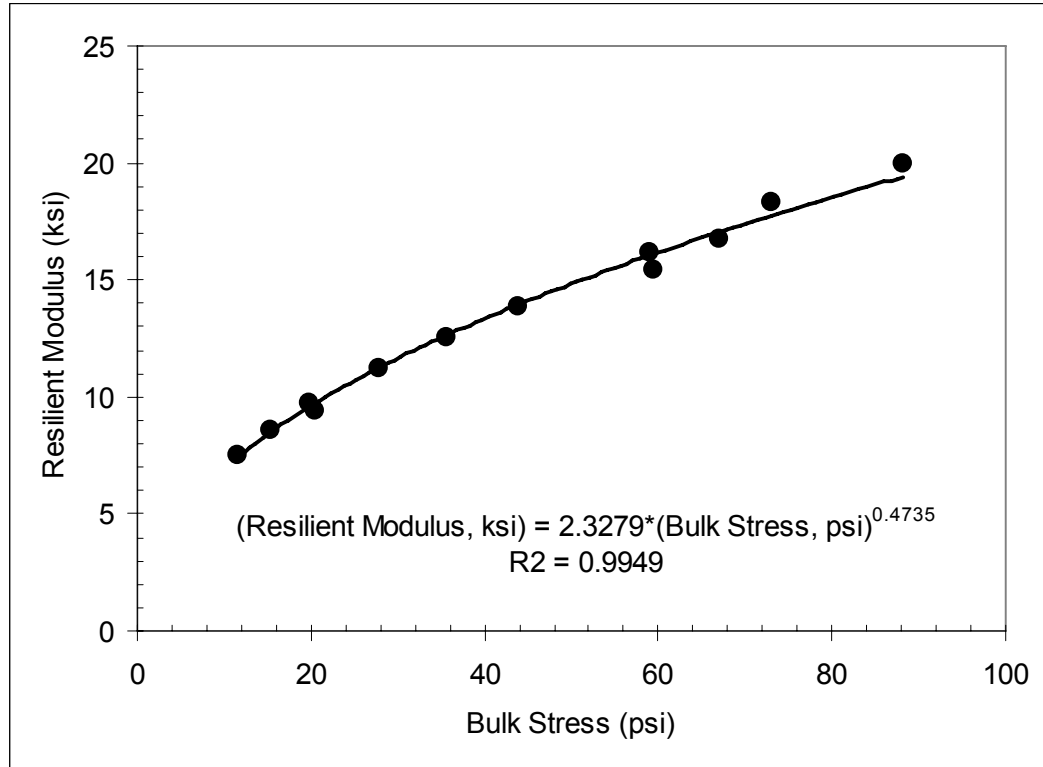


Figure 17. Resilient modulus vs. bulk stress of subbase. (Trial 1)

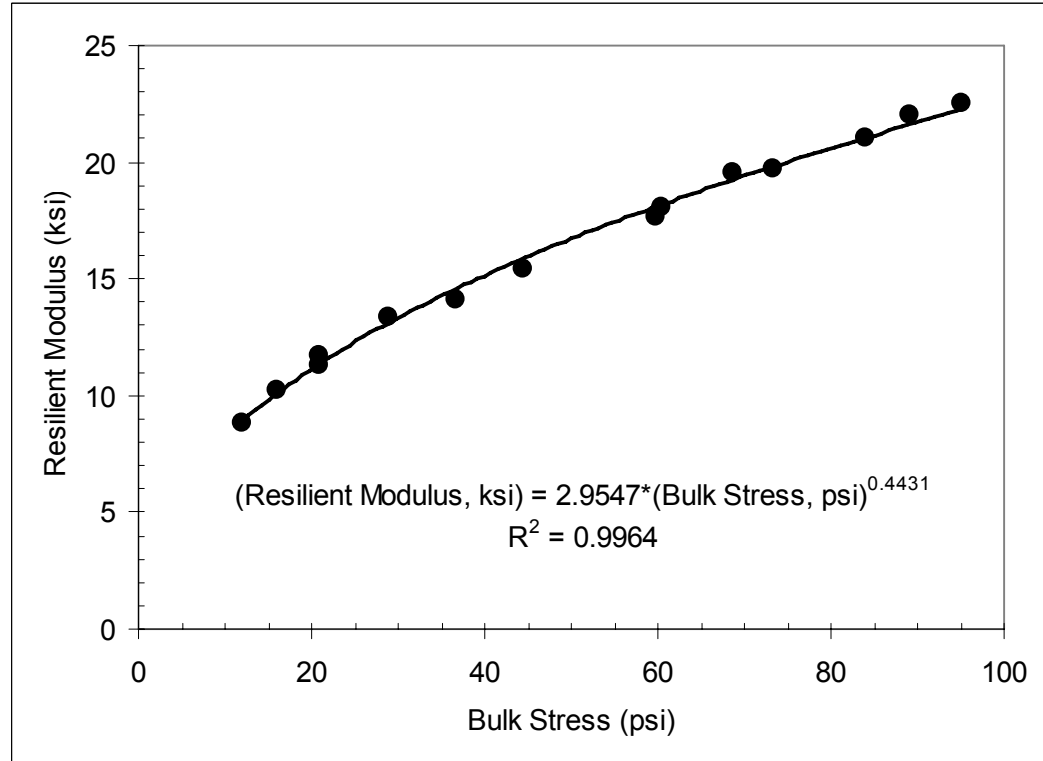


Figure 18. Resilient modulus vs. bulk stress of subbase (Trial 2). (1 ksi = 6.89 MPa)

The permeability of the aggregate base (ODOT item 304) was determined following ASTM D 2434 “Standard Test Method for Permeability of Granular Soils (Constant Head)”. As required in the standard test procedure, all particles larger than 19 mm (3/4 in.) were removed from the test sample. The diameter of the transparent plastic permeameter used for this test was 229 mm (9 in.) as required for the maximum particle size of the prepared aggregate base. The distance between the upper and the lower manometer outlets of the permeameter was 229 mm (9 in.). The test sample was carefully placed inside of the permeameter in multiple layers with caution not to have segregation. Each layer was in the thickness of about 9.5 mm (3/4 in.) and compacted with vibrating tamper as shown in Figure 19. The prepared specimen had $2,065 \text{ kg/m}^3$ (128.9 lb/ft^3) dry unit weight.

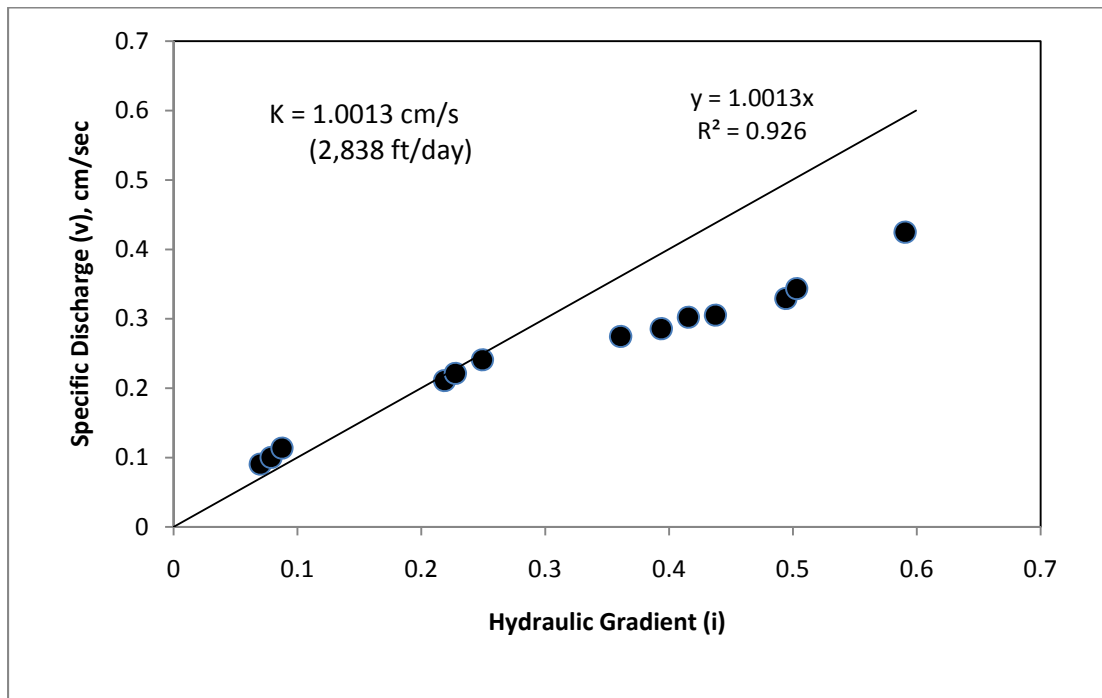
A vacuum pump was used to evacuate the specimen, followed by water saturation. Table 12 summarizes the permeability test results and Figure 20 shows the specific discharge versus hydraulic gradient. The permeability, corrected to 20°C (68°F) temperature, of the aggregate base was 1.001 cm/sec ($2,838 \text{ ft/day}$). This value is consistent with what Randolph et al. [2000] found out for ODOT 304 permeability. They reported the significant effects of passing #200 sieve (and gradation) on the permeability of ODOT item 304. In their experiments, the permeability of the medium gradation 304 aggregate containing 6.5% passing #200 sieve ranged from 0.071 to 0.554 cm/sec (from 201 to 1,570 ft/day). The permeability of the coarse gradation 304 aggregate containing no material passing #200 sieve ranged from 0.416 to 4.513 cm/sec (from 1,179 to 12,793 ft/day). The aggregate base used in WAY-30 project was between the medium and the coarse gradations with 3.5% passing #200 sieve. The permeability determined for this project falls between values reported by Randolph et al. Figure 20 also shows that the deviation from the laminar flow condition occurred at a hydraulic gradient of about 0.25. This compares reasonably well with the observation by Randolph et al. where the deviation occurred a hydraulic gradient of about 0.5 for medium gradation ODOT 304 with much lower permeability of 0.0726 cm/sec (206 ft/day).



Figure 19. Permeameter with compacted aggregate subbase and vibrating tamper.

Table 12. The results of constant head permeability test for aggregate subbase.

Head, h		H. Grad. $i=h/L$	Discharge, Q		time (s)	Specific Discharge, v		Temperature		Permeability $K = v/i$	
(cm)	(in.)		(cm ³)	(in. ³)		(cm/s)	(in./s)	(°C)	(°F)	(cm/s)	(in./s)
1.6	0.63	0.070	2500	152.6	434	0.091	0.0358	22.2	72.0	1.227	0.483
1.8	0.71	0.079	2500	152.6	392	0.100	0.0394	22.2	72.0	1.208	0.476
2.0	0.79	0.087	2500	152.6	346	0.114	0.0449	22.2	72.0	1.232	0.485
5.0	1.97	0.219	4000	244.1	298	0.211	0.0831	27.5	81.5	0.811	0.319
5.2	2.05	0.227	4000	244.1	284	0.221	0.0870	27.5	81.5	0.819	0.322
5.7	2.24	0.249	4000	244.1	261	0.241	0.0949	27.5	81.5	0.813	0.320
8.3	3.27	0.361	4000	244.1	229	0.275	0.1083	27.5	81.5	0.640	0.252
9.0	3.54	0.394	4000	244.1	220	0.286	0.1126	27.5	81.5	0.611	0.241
9.5	3.74	0.416	4000	244.1	208	0.302	0.1189	27.5	81.5	0.612	0.241
10.0	3.94	0.437	4000	244.1	206	0.305	0.1201	24.9	76.8	0.622	0.245
11.3	4.45	0.494	4000	244.1	191	0.329	0.1295	24.9	76.8	0.594	0.234
11.5	4.53	0.503	4000	244.1	183	0.344	0.1354	24.9	76.8	0.609	0.240
13.5	5.31	0.591	2000	122.0	74	0.425	0.1673	27.5	81.5	0.605	0.238



**Figure 20. Specific discharge versus hydraulic gradient of aggregate base.
(2.54 cm/sec = 1.0 in./sec)**

5 MODELING OF RESILIENT BEHAVIOR OF WAY-30 SOILS

5.1 Models for Fine-Grained Subgrade Soil

The resilient modulus is one of the most important properties required for unbound materials in pavement design and analysis. MEPDG use a constitutive model as shown in Eq. 2

$$M_R = k_1 p_a \left(\frac{\theta}{p_a} \right)^{k_2} \left(\frac{\tau_{oct}}{p_a} + 1 \right)^{k_3} \quad \text{Eq. 2}$$

where M_R = resilient modulus (Pa); p_a = atmospheric pressure (14.7 psig); θ = bulk stress; τ_{oct} = Octahedral shear stress; and k_1, k_2, k_3 = regression constants.

The regression results of the resilient moduli of WAY-30 subgrade soils to fit into Eq. 2 are summarized in Table 13. For all tests, the r^2 values are low. When the r^2 value is less than 0.9, MEPDG requires the use a different constitutive model. Evaluation of several other constitutive models for subgrade soils are discussed here.

Table 13. Regression coefficients of MEPDG universal model for subgrade.

	k1	k2	k3	r^2
Way Subg WB STA 876+60 (Test 1)	0.661	0.312	-1.955	0.795
Way Subg EB STA 876+60	0.344	0.048	-1.873	0.587
Way Subg WB STA 885+00	0.379	-0.260	-2.300	0.476
Way Subg EB Right Side STA 884+00 (Test 1)	0.455	0.193	-1.418	0.616
Way Subg EB Left Side STA 884+00 (Test 2)	0.960	0.424	-2.422	0.851
Way Subg EB STA 663+50	0.439	-0.090	-0.790	0.568

At Level 2 or 3 of the M-E design procedure, a prediction model may be used to estimate the resilient modulus of the subgrade soil. Thus, it is important that a reliable model is identified. There have been a number of models proposed by other researchers for estimating the resilient modulus of fine-grained soils. The most basic model used in conjunction with the resilient modulus testing of fine-grained soils is a power model:

$$M_R = K(\sigma_d)^n \quad \text{where } K, n = \text{model constants} \quad \text{Eq. 3}$$

However, the power model cannot represent the bilinear relationship between the resilient modulus and deviatoric stress. The n value of 0 leads to the 0-th order relationship ($M_R = K$). A small negative value for n leads to a slightly nonlinear concave upward curve with no apparent break point.

A bilinear model has been developed by Dingqing and Selig (1994) to embrace the concept of the breakpoint resilient modulus:

$$M_R = K_1 + K_2\sigma_d \quad \text{for } \sigma_d < \sigma_{di} \quad \text{Eq. 4a}$$

$$= K_3 + K_4\sigma_d \quad \text{for } \sigma_d > \sigma_{di} \quad \text{Eq. 4b}$$

where K_1 , K_2 , K_3 , and K_4 are model constants (K_1 and K_3 always positive; K_2 always negative; K_4 occasionally negative); and σ_{di} = breakpoint deviatoric stress.

A hyperbolic model was proposed by Drumm et al. [1991] for estimating the resilient modulus of fine-grained soils found in Tennessee:

$$M_R = \frac{K + n\sigma_d}{\sigma_d} \quad \text{where } K, n = \text{model constants} \quad \text{Eq. 5}$$

A semi-log model was proposed by Fredlund et al. [1977], who examined the resilient responses of a glacial till material:

$$\text{Log}(M_R) = K - n \sigma_d \quad \text{where } K, n = \text{model constants} \quad \text{Eq. 6}$$

A log-log model is presented in the SHRP P-46 test protocol as a means to plot the test data:

$$\text{Log}(M_R) = K + n \text{Log}(\sigma_d) \quad \text{where } K, n = \text{model constants} \quad \text{Eq. 7}$$

An additional model, incorporating the octahedral stresses, may be worthy of evaluation:

$$\text{Log}(M_R) = K + n \cdot \text{Log}\left(\frac{\sigma_{oct}}{\tau_{oct}}\right) \quad \text{where } K, n = \text{model constants} \quad \text{Eq. 8}$$

The advantage of the octahedral model is that it can incorporate the effects of both deviatoric stress and confining stress. When the confining stress is set equal to zero, Eq. 8 cannot express M_R as a function of σ_d . In order to overcome this problem, Eq. 8 may be modified to:

$$\text{Log}(M_R) = K' + n' \cdot \text{Log}\left[\frac{\sigma_{oct}}{(\tau_{oct})^2}\right] \quad \text{where } K', n' = \text{model constants} \quad \text{Eq. 8'}$$

Table 14 summarizes the results of the data analysis performed for each candidate model, which include model constant values and the coefficient of determination (r^2) value. Comparing the overall average r^2 values, the hyperbolic model was considered to be the best model, followed by the octahedral stress model, the bilinear model, and the power model. The power model and the log-log model are equivalent to each other. The semi-log model was the least successful in fitting to the experimental RM test data.

For the bilinear model, the breakpoint resilient modulus (M_{Ri}) was determined to be 3.78 ksi (26.1 MPa, Sample 1), 8.21 ksi (56.6 MPa, Sample 2A), 4.80 ksi (33.1 MPa, Sample 2B), 3.17 ksi (21.9 MPa, Sample 3A), 6.35 ksi (43.8 MPa, Sample 3B), and 4.87 ksi

(33.6 MPa, Sample 5). The breakpoint deviatoric stress (σ_{di}) was 2.39 psi (16.5 kPa, Sample 1), 6.28 psi (43.3 kPa, Sample 2A), 5.00 psi (34.5 kPa, Sample 2B), 4.45 psi (30.7 kPa, Sample 3A), 8.43 psi (58.1 kPa, Sample 3B), and 5.05 psi (34.8 kPa, Sample 5). The axial strain corresponding to the breakpoint (ϵ_i) was 0.06% (Sample 1), 0.07% (Sample 2A), 0.10% (Sample 2B), 0.13% (Samples 3A, 3B), and 0.10% (Sample 5).

Table 14. Evaluation of models for resilient modulus models for A-4 subgrade soil.

	Power Model – Eq. 3:			Bilinear Model – Eq. 4:					
	K	n	r^2	K1	K2	$(r_1)^2$	K3	K4	$(r_2)^2$
Sample 1	5.464	- 0.228	0.840	8.574	- 2.010	0.982	3.775	0.002	0.006
Sample 2(A)	14.748	- 0.257	0.748	15.494	- 1.159	0.685	8.550	- 0.054	0.079
Sample 2(B)	6.686	- 0.146	0.638	7.458	- 0.531	0.800	4.786	0.003	0.001
Sample 3(A)	5.212	- 0.221	0.722	6.129	- 0.664	0.860	3.054	0.027	0.112
Sample 3(B)	10.121	- 0.207	0.561	9.225	- 0.341	0.177	6.920	- 0.068	0.092
Sample 5	6.985	- 0.145	0.685	7.833	- 0.587	0.909	4.629	0.048	0.349
Average	---	---	0.699	---	---	0.736	---	---	0.107
Rank	4 (out of 6)			3 (out of 6)					

	Hyperbolic Model – Eq. 5:			Semi-Log Model - Eq. 6:		
	K	n	r^2	K	n	r^2
Sample 1	0.675	3.676	0.998	3.757	- 0.030	0.441
Sample 2 (A)	11.146	6.961	0.972	4.067	- 0.014	0.536
Sample 2 (B)	1.950	4.641	0.989	3.780	- 0.009	0.411
Sample 3 (A)	2.175	3.075	0.983	3.661	- 0.016	0.492
Sample 3 (B)	8.967	5.356	0.952	3.933	- 0.013	0.513
Sample 5	1.912	4.941	0.993	3.800	- 0.009	0.441
Average	---	---	0.982	---	---	0.472
Rank	1 (out of 6)			6 (out of 6)		

	Log-Log Model – Eq. 7:			Octahedral Model - Eq. 8':		
	K	n	r^2	K'	n'	r^2
Sample 1	3.738	- 0.228	0.840	0.781	0.746	0.781
Sample 2 (A)	4.169	- 0.257	0.748	10.484	1.763	0.953
Sample 2 (B)	3.825	- 0.146	0.638	5.476	0.556	0.787
Sample 3 (A)	3.717	- 0.221	0.722	3.726	0.483	0.739
Sample 3 (B)	4.005	- 0.207	0.561	7.639	1.004	0.745
Sample 5	3.844	- 0.145	0.685	5.460	0.433	0.578
Average	---	---	0.699	---	---	0.764
Rank	4 (out of 6)			2 (out of 6)		

Table 15 lists the basic physical properties and the hyperbolic model constants for the subgrade soil specimens. Statistical analysis using the computer software AXUM indicated that the hyperbolic model constants (K, n) are both correlated strongly to the moisture content relative to the OMC ($= w - OMC$), as seen in Figure 21, and moderately correlated to the percent fines (S200), plasticity index (PI), and relative compaction (R). A multi-variable linear regression analysis produced the following outcome for the A-4

soils. The value of the coefficient of determination (r^2) was very close to 1.00 for each result.

$$K = -391.76 + 5.67(\text{PI}) + 0.68(\text{S200}) - 11.29(w - \text{OMC}) + 3.23(\text{R}) \quad \text{Eq. 9}$$

$$n = -24.01 + 1.20(\text{PI}) - 0.001(\text{S200}) - 2.28(w - \text{OMC}) + 0.19(\text{R}) \quad \text{Eq. 10}$$

$$M_{Ri} = -75.39 + 2.02(\text{PI}) + 0.09(\text{S200}) - 3.65(w - \text{OMC}) + 0.60(\text{R}) \quad \text{Eq. 11}$$

Table 15. List of subgrade soil specimen properties and hyperbolic model constants.

	Test Specimen Property Data:				Hyperbolic Model:	
	PI (%)	S200 (%)	w - OMC (%)	R (%)	K	n
Sample 1	9.9	46.9	+1.0	98	0.675	3.676
Sample 2 (A)	9.4	38.2	- 0.7	98	11.146	6.961
Sample 2 (B)	9.4	38.2	+0.4	99	1.950	4.641
Sample 3 (A)	8.2	39.3	+0.7	102	2.175	3.075
Sample 5	8.0	48.9	- 0.8	95	1.912	4.941

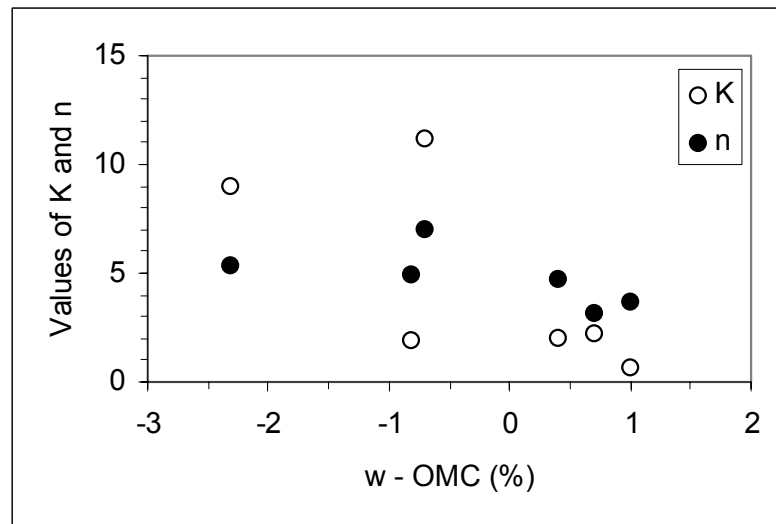


Figure 21. Plot of hyperbolic model constants K and n values vs. (w - OMC).

5.2 Models for Granular Subbase Materials

Non-linear curve fitting was performed to fit the WAY-30 subbase resilient modulus to MEPDG universal model (Eq. 2). The regression coefficients and r^2 values are summarized in Table 16. When Trial 1 and Trial 2 specimens were fitted separately, r^2 values were greater than 0.99. The combined data of both specimens also produced high r^2 value (0.957). The constant k_3 measures softening effect of materials due to shear stress and a negative number is usually expected. However, in both tests, a positive k_3 was obtained. This may be caused by strong aggregate interlock of the crushed aggregate subbase used in WAY-30 project.

Table 16. Regression coefficients of MEPDG universal model for subbase.

	k1	k2	k3	r ²
Trial 1 Specimen	0.551251	0.418695	0.169012	0.999
Trial 2 Specimen	0.654688	0.444031	0.016472	0.996
Combined	0.597608	0.458940	0.056241	0.957

Over the years many prediction models were proposed to estimate the resilient moduli of granular base materials from fundamental index properties. These models can be evaluated in light of the current project's resilient modulus test data. Carmichael and Stuart [1985] developed the following formula for predicting resilient modulus of granular base materials:

$$\text{Log } M_R (\text{ksi}) = 0.523 - 0.0225(\%w) + 0.544(\text{Log } \theta) + 0.173(\text{SM}) + 0.197(\text{GR}) \quad \text{Eq. 12}$$

where %w = moisture content in %; θ = bulk stress; SM = 1 for SM soil, SM = 0 for other soils; and GR = 1 for gravelly (GW, GP, GM, GC) soils, GR = 0 for other soils.

Rahim and George [2004] proposed the following equation for predicting resilient modulus of coarse-grained soils used by Mississippi DOT, based on test data available from 12 soil samples:

$$M_R (MP_a) = 307.4 \left(\frac{\gamma_{dr}}{\%w} \right)^{0.86} \left\{ \frac{P_{200}}{\text{Log}(c_u)} \right\}^{-0.46} \quad \text{Eq. 13}$$

where γ_{dr} = ratio of dry unit weight divided by maximum dry unit weight (= γ_d/γ_{d-max}); and c_u = uniformity coefficient (= D_{60}/D_{10}).

Rahim and George [2005] developed comprehensive resilient modulus models, based on the data they accumulated in two program studies. The model they proposed for coarse granular soils was:

$$M_R = k1 P_a \left(1 + \frac{\theta}{1 + \sigma_d} \right)^{k2} \quad \text{Eq. 14}$$

where M_R = resilient modulus (MPa); k1 and k2 = model coefficients (to be estimated from soil index properties); P_a = atmospheric pressure (14.7 psi or 101.3 kPa); θ = bulk stress (kPa); σ_d = deviatoric stress (kPa); and k1, k2 = model coefficients (defined in Eqs. 15 and 16 below).

$$k1 = 0.12 + 0.90(\gamma_{dr}) - 0.53(w/OMC) - 0.017(P_{200}) + 0.314(\log c_u) \quad \text{Eq. 15}$$

$$k2 = 0.226(\gamma_{dr} \cdot w/OMC)^{1.2385} (P_{200}/\log c_u)^{0.124} \quad \text{Eq. 16}$$

where γ_{dr} = ratio of dry unit weight divided by maximum dry unit weight ($= \gamma_d/\gamma_{d-max}$); w/OMC = ratio of actual moisture content divided by optimum moisture content; and P_{200} = percent passing sieve #200.

One of the latest developments in the modeling of resilient behavior of pavement materials is the universal model. This model is called “universal,” since it is said to be applicable to both granular and fine-grained soils. One of the early universal models had the following nonlinear form:

$$M_R = k_1(\sigma_c)^{k_2}(\sigma_d)^{k_3} \quad \text{Eq. 17}$$

where k_1 , k_2 , and k_3 = model coefficients (to be determined statistically).

Barksdale et al. [1997] examined this model and stated that the term $k_1(\sigma_c)^{k_2}$ reflects the initial tangent modulus. Normally, parameter k_2 is positive and parameter k_3 is negative. Thus, the maximum feasible modulus resulting from Eq. 8 is given by $k_1(\sigma_c)^{k_2}$. If we set $k_1 = K$, $k_2 = 0$, and $k_3 = n$, the above model becomes equal to the two-parameter model for fine-grained soil, Eq. 3.

One of the most recent universal model was proposed by Yau and Quintus [2002]. They developed the following constitutive equation by analyzing a large number of laboratory test data established in the FHWA’s LTPP program:

$$M_R = k_1 p_a \left(\frac{\theta}{p_a} \right)^{k_2} \left(\frac{\tau_{oct}}{p_a} + 1 \right)^{k_3} \quad \text{Eq. 18}$$

where M_R = resilient modulus (Pa); p_a = atmospheric pressure (14.7 psig or 101 kPa); θ = bulk stress; τ_{oct} = Octahedral shear stress (given by Eq. 19); and k_1 , k_2 , k_3 = regression constant. They may be determined from soil’s index properties.

$$\tau_{oct} = \frac{1}{3} \sqrt{(\sigma_1 - \sigma_2)^2 + (\sigma_2 - \sigma_3)^2 + (\sigma_1 - \sigma_3)^2} = \frac{\sqrt{2}}{3} \sigma_d \quad \text{Eq. 19}$$

Equation 18 has been selected for use in MEPDG. The constant k_1 is proportional to Young’s modulus. The constant k_2 reflects the effect of the volumetric stress (θ). The constant k_3 may be negative, for it explains strain softening caused by shear stress. Generally, k_1 and $k_2 > 0$ and $k_3 < 0$.

Yau and Quintus [2002] performed stepwise regression analysis using the Long-Term Pavement Performance (LTPP) Specific Pavement Studies (SPS) data to express the coefficients k_1 through k_3 in terms of soil physical properties. This effort was regarded important since basic physical properties can be easily determined in most laboratories and the incorporation of physical properties into resilient modulus model allows seasonal variations of resilient modulus to be estimated through seasonal changes in the physical state. The expressions for the coefficients changed for each distinct type of material tested. The maximum dry unit weight, optimum moisture content, % passing the 3/8-inch (9.5-mm) sieve, moisture content, and liquid limit were the physical

properties that were often strongly correlated to resilient modulus of coarse granular material. The following provides examples of the regression analysis results reported by Yau and Quintus [2002]:

Crushed Stone Material:

$$k_1 = 0.7632 + 0.0084(P_{3/8}) + 0.0088(LL) - 0.0371(OMC) - 0.0001(\gamma_{d-max}) \quad \text{Eq. 20}$$

$$k_2 = 2.2159 - 0.0016(P_{3/8}) + 0.0008(LL) - 0.038(OMC) - 0.0006(\gamma_{d-max}) + 2.4E(-7)(\gamma_{d-max}^2/P_{40}) \quad \text{Eq. 21}$$

$$k_3 = -1.1720 - 0.0082(LL) - 0.0014(OMC) + 0.0005(\gamma_{d-max}) \quad \text{Eq. 22}$$

Crushed Gravel Material:

$$k_1 = -0.8282 - 0.0065(P_{3/8}) + 0.0114(LL) + 0.0004(PI) - 0.0187(OMC) + 0.0036(\%w) + 0.0013(\gamma_d) - 2.6E(-6)(\gamma_{d-max}^2/P_{40}) \quad \text{Eq. 23}$$

$$k_2 = 4.9555 - 0.0057(LL) - 0.0075(PI) - 0.0470(\%w) - 0.0022(\gamma_{d-max}) + 2.8E(-6)(\gamma_{d-max}^2/P_{40}) \quad \text{Eq. 24}$$

$$k_3 = -3.514 + 0.0016(\gamma_d) \quad \text{Eq. 25}$$

where $P_{3/8}$ = % passing 3/8-inch (9.5 mm) sieve; LL = liquid limit (%); PI = plasticity index (%); OMC = optimum moisture content (%); γ_{d-max} = maximum dry unit weight; P_{40} = % passing sieve #40 (%); w = moisture content (%); γ_d = dry unit weight of test specimen; and P_{200} = % passing sieve #200 (%).

From the mechanical sieve analysis results presented earlier, the following material properties can be enlisted:

$w = 1$; SM = 0; GR = 1; $\gamma_{dr} = 0.98$ (for Trial 1) & 0.94 (for Trial 2); $P_{200} = 3.5$; $c_u = 65$; $P_{3/8} = 47.8$; $P_{40} = 31.0$; LL = 0; $P_1 = 99.0$; $P_{1-1/2} = 100.0$; $P_{10} = 24.0$; and $P_{80} = 9$.

Additional material properties had to be estimated in consultation with a standard geotechnical engineering textbook such as the one by Das [2008] and the ODOT's Construction Inspection Manual of Procedures [ODOT, 2006] as:

Specific Gravity (G_s) = 2.68; Optimum Moisture Content (OMC) = 10%; Maximum Dry Unit Weight (γ_{d-max}) = 130 pcf (20.4 kN/m³)

For the subbase material tested in the current project, Eqs. 12 through 14 and Eq. 18 will reduce to:

$$\text{Log } M_R \text{ (ksi)} = 0.6975 + 0.544(\text{Log } \theta) \quad \text{Eq. 26}$$

$$M_R \text{ (MPa)} = 227.14(\gamma_{dr})^{0.86} \quad \text{Eq. 27}$$

where $\gamma_{dr} = 0.98$ for Trial 1 and 0.94 for Trial 2.

$$M_R = k_1 P_a \left(1 + \frac{\theta}{1 + \sigma_d} \right)^{k_2} \quad \text{Eq. 28}$$

where $k_1 = 0.578 + 0.9(\gamma_{dr})$; $P_a = 101.3$ kPa; and $k_2 = 0.245[0.10(\gamma_{dr})]^{1.2385}$

$$M_R = k_1 p_a \left(\frac{\theta}{p_a} \right)^{k_2} \left(\frac{\tau_{oct}}{p_a} + 1 \right)^{k_3} \quad \text{Eq. 29}$$

where $k_1 = 0.781$; $P_a = 14.7$ psi (101.3 kPa); $k_2 = 1.682$; $k_3 = -1.122$.

Table 17 summarizes resilient moduli predicted for the subbase material by Eqs. 12, 13, 14, and 18. All the predicted values are about two times as large as what were measured in the laboratory. The bottom of the range given by Eq. 18 corresponded to the lower limit of the laboratory test measurements.

**Table 17. Resilient modulus values predicted for WAY-30 subbase material.
(English units at top metric units at bottom)**

	M_R (ksi) for Trial 1 Specimen:	M_R (ksi) for Trial 2 Specimen:
Eq. 12	25 to 54 for θ of 20 to 80 psi	
Eq. 13	32 (average)	31 (average)
Eq. 14	30 to 192 for σ_d of 10 to 50 psi and θ of 20 to 80 psi	29 to 187 for σ_d of 10 to 50 psi and θ of 20 to 80 psi
Eq. 18	6 to 141 for σ_d of 10 to 50 psi and θ of 20 to 80 psi	

	M_R (MPa) for Trial 1 Specimen:	M_R (MPa) for Trial 2 Specimen:
Eq. 12	172 to 372 for θ of 138 to 552 kPa	
Eq. 13	221 (average)	214 (average)
Eq. 14	207 to 1324 for σ_d of 69 to 345 kPa and θ of 138 to 552 kPa	200 to 1289 for σ_d of 69 to 345 kPa and θ of 138 to 552 kPa
Eq. 18	41 to 972 for σ_d of 69 to 345 kPa and θ of 138 to 552 kPa	

6 LABORATORY TEST RESULTS ON CONCRETE

6.1 Unit Weight (ASTM C138/C 138M-01a)

The unit weight was determined for each sample before the execution of any other test. The unit weight γ was obtained dividing the total weight W of the concrete sample by its total volume V :

$$\gamma = W / V \quad \text{Eq. 30}$$

The unit weight of each specimen tested is presented along with other test results discussed below in Tables 18 and 19. The unit weight varied between 136 pcf (2178 kg/m³) and 142 pcf (2275 kg/m³) for fly ash concrete (Mix B), and between 140 pcf (2243 kg/m³) and 145 pcf (2323 kg/m³) for Ground Granulated Blast-Furnace Slag (GGBFS) concrete (Mix A).

6.2 Modulus of Rupture (ASTM C 78-02)

The modulus of rupture or flexural strength was determined using a simple beam with third point loading. The specimens for this test were prismatic beams with square cross section with 6 in. (15 cm) sides and 19 in. (48 cm) span; the mass of this specimen was measured in order to calculate its unit weight. The load was applied at a loading rate of 1700 lbs/min (7.6 kN/min) at the third points of the beam until rupture occurred. The modulus of rupture R was then calculated as follows:

$$R = PL / bd^2 \quad \text{Eq. 31}$$

where P = peak load; L = span length; b = average width of the specimen; and d = average depth of specimen.

The results for the Modulus of Rupture are presented in Tables 18 and 19 for GGBFS (Mix A) and Fly Ash (Mix B) concrete, respectively. At all the ages tested (7, 14, 28 and 90 days) the fly ash concrete presents greater values for the rupture module than the GGBFS concrete. This difference increases with specimen age up to 35% at an age of 90 days.

Table 18. Modulus of rupture for Mix A concrete with GGBFS.

ENGLISH UNITS									
Specimen	Weight (lb)	<i>l</i> (in)	<i>L</i> (in)	<i>b</i> (in)	<i>d</i> (in)	γ (pcf)	<i>P</i> (lb)	<i>R</i> (psi)	
F7-1	63.0	21.19	19.0	6.00	6.00	142.7	6,580	578.8	538.3
F7-2	63.0	21.19	19.0	6.00	6.00	142.7	5,520	485.6	
F7-3	63.0	21.19	19.0	6.00	6.00	142.7	5,660	497.9	
F14-1	62.0	21.13	19.0	5.95	6.00	142.1	4,680	415.1	491.4
F14-2	63.3	21.13	19.0	6.00	6.02	143.2	6,640	580	
F14-3	63.5	21.13	19.0	6.04	6.04	142.3	5,560	479	
F28-1	-	-	-	-	-	145.3	-	585.1	543.3
F28-2	-	-	-	-	-	143.3	-	522.3	
F28-3	-	-	-	-	-	141.5	-	522.4	
F90-1	62.5	21.16	19.0	6.00	6.00	141.8	7,820	687.7	608.7
F90-2	62.5	21.13	19.0	6.02	5.98	142	6,600	582.6	
INTERNATIONAL UNITS									
Specimen	Mass (kg)	<i>l</i> (m)	<i>L</i> (m)	<i>b</i> (m)	<i>d</i> (m)	γ (kg/m ³)	<i>P</i> (kN)	<i>R</i> (kPa)	
F7-1	28.58	0.538	0.483	0.152	0.152	2285.8	29.27	3990.7	3711.4
F7-2	28.58	0.538	0.483	0.152	0.152	2285.8	24.55	3348.1	
F7-3	28.58	0.538	0.483	0.152	0.152	2285.8	25.18	3432.9	
F14-1	28.12	0.537	0.483	0.151	0.152	2276.2	20.82	2862.0	3388.1
F14-2	28.71	0.537	0.483	0.152	0.153	2293.8	29.53	3999.0	
F14-3	28.80	0.537	0.483	0.153	0.153	2279.4	24.73	3302.6	
F28-1	-	-	-	-	-	2327.5	-	4034.1	3745.9
F28-2	-	-	-	-	-	2295.4	-	3601.1	
F28-3	-	-	-	-	-	2266.6	-	3601.8	
F90-1	28.35	0.537	0.483	0.152	0.152	2271.4	34.78	4741.5	4196.8
F90-2	28.35	0.537	0.483	0.153	0.152	2274.6	29.36	4016.9	

[Note] Specimen F7-1=7-day specimen No. 1; *l*=total beam length.

Table 19. Modulus of rupture for Mix B concrete with fly ash.

ENGLISH UNITS									
Specimen	Weight (lb)	<i>l</i> (in)	<i>L</i> (in)	<i>b</i> (in)	<i>d</i> (in)	γ (pcf)	<i>P</i> (lb)	<i>R</i> (psi)	
F7-1(f)	62.5	21.06	19.0	6.02	5.98	142.4	5,840	515.5	554.6
F7-2(f)	62.5	21.25	19.0	6.06	5.98	140.2	4,400	385.7	
F7-3(f)	62.5	21.25	19.0	6.02	6.02	140.2	6,820	593.7	
F14-1(f)	61.5	21.19	19.0	6.02	5.96	139.8	5,980	531.6	566.4
F14-2(f)	63.0	21.13	19.0	6.04	6.04	141.2	7,080	610	
F14-3(f)	62.5	21.19	19.0	6.00	6.00	141.6	6,340	557.7	
F28-1(f)	63.5	21.19	19.0	6.04	6.06	141.4	8,540	730.7	632.6
F28-2(f)	62.5	21.16	19.0	6.00	6.00	141.8	6,180	543.6	
F28-3(f)	62.0	21.19	19.0	6.00	5.94	141.9	6,940	623.4	
F90-1(f)	63.0	21.13	19.0	6.02	6.02	142.2	9,520	828.7	817.7
F90-2(f)	61.5	21.13	19.0	6.02	5.98	139.7	9,400	829.7	
F90-3(f)	61.0	21.13	19.0	6.02	5.96	139.1	8,940	794.7	
INTERNATIONAL UNITS									
Specimen	Mass (kg)	<i>l</i> (m)	<i>L</i> (m)	<i>b</i> (m)	<i>d</i> (m)	γ (kg/m ³)	<i>P</i> (kN)	<i>R</i> (kPa)	
F7-1(f)	28.35	0.5349	0.483	0.153	0.152	2281.0	25.98	3554.2	3823.8
F7-2(f)	28.35	0.5398	0.483	0.154	0.152	2245.8	19.57	2659.3	
F7-3(f)	28.35	0.5398	0.483	0.153	0.153	2245.8	30.34	4093.4	
F14-1(f)	27.90	0.5382	0.483	0.153	0.151	2239.4	26.60	3665.3	3905.2
F14-2(f)	28.58	0.5367	0.483	0.153	0.153	2261.8	31.49	4205.8	
F14-3(f)	28.35	0.5382	0.483	0.152	0.152	2268.2	28.20	3845.2	
F28-1(f)	28.80	0.5382	0.483	0.153	0.154	2265.0	37.99	5038.0	4361.6
F28-2(f)	28.35	0.5375	0.483	0.152	0.152	2271.4	27.49	3748.0	
F28-3(f)	28.12	0.5382	0.483	0.152	0.151	2273.0	30.87	4298.2	
F90-1(f)	28.58	0.5367	0.483	0.153	0.153	2277.8	42.34	5713.7	5637.8
F90-2(f)	27.90	0.5367	0.483	0.153	0.152	2237.8	41.81	5720.6	
F90-3(f)	27.67	0.5367	0.483	0.153	0.151	2228.2	39.77	5479.3	

[Note] Specimen F7-1=7-day specimen No. 1; *l*=total beam length.

6.3 Static Modulus of Elasticity and Poisson's Ratio (ASTM C 469-02)

The modulus of elasticity is the stress to strain ratio, and the Poisson's ratio is the fraction between transverse and longitudinal strain. These mechanical characteristics of concrete were calculated using stresses within 0 and 40% of ultimate strength. Each specimen was loaded three times, but data were not recorded for the first load cycle. The initial load cycle was applied in order to prepare the specimen and verify dial gages. The load was applied continuously and without shock at a rate equal to 55,000 lbs/min (240 kN/min) for the second load cycle and 25,000 lbs/min (110 kN/min) for the third load cycle. The applied load and the longitudinal and circumferential deformations were recorded when the axial strain was equal to 50 and 450 microstrains ($\mu\epsilon$).

Then, the modulus of elasticity E and the Poisson's ratio ν are given by:

$$E = \frac{S_2 - S_1}{\epsilon_2 - 0.000050} \quad \text{and} \quad \nu = \frac{\epsilon_{t2} - \epsilon_{t1}}{\epsilon_2 - 0.000050} \quad \text{Eq. 32}$$

where S_1 = Stress at the first level (equivalent to 50 $\mu\epsilon$); S_2 = stress at the second level; ϵ_2 = longitudinal strain produced by S_2 ; ϵ_{t2} = transverse strain produced by S_2 ; and ϵ_{t1} = transverse strain produced by S_1 .

The results for the modulus of elasticity and the Poisson's ratio are presented in Tables 20 and 21. It is relevant to note that the modulus of elasticity and the Poisson's ratio are always bigger in GGBFS than in fly ash concrete. As expected, the values of Young's Modulus increased with specimen's age, but the Poisson's Ratio decreased with age in both cases, reaching a maximum and a minimum values of 4.07×10^3 ksi (28.1 GPa) and 0.16, respectively in GGBFS concrete and 3.80×10^3 ksi (26.2 GPa) and 0.18 for fly ash concrete.

Table 20. Static modulus of elasticity and Poisson's ratio of GGBFS concrete (Mix A).

ENGLISH UNITS											
Specimen	γ (pcf)	S_2 (psi)	S_1 (psi)	ε_2 ($\times 10^4$)	E ($\times 10^3$ ksi)		ε_{t2} ($\times 10^4$)	ε_{t1} ($\times 10^5$)	ν		
C7-1	141.7	1938.1	378.5	4.375	4.02	3.99	3.85	0.998	1.746	0.21	0.23
		1621.0	337.6	3.750	3.95			0.981	1.663	0.25	
C7-2	142.3	1621.0	304.8	4.000	3.76	3.72	3.85	0.915	1.247	0.23	0.22
		1621.0	334.8	4.000	3.67			0.915	1.497	0.22	
C14-1	141.4	2121.7	371.3	4.750	4.12	4.12	4.01	1.116	0.666	0.25	0.25
		-	-	-	-			-	-	-	
C14-2	142.8	2121.7	334.5	5.063	3.92	3.89	4.01	1.333	1.666	0.26	0.26
		2121.7	381.9	5.000	3.87			1.316	0.833	0.27	
C28-2	140.3	2102.4	316.1	5.125	3.86	3.92	4.03	1.119	0	0.24	0.24
		2102.4	302.7	5.031	3.97			1.078	0.166	0.23	
C28-3	142.3	2102.4	234.1	5.156	4.01	4.15	4.03	0.912	0.083	0.19	0.21
		2102.4	226.4	4.875	4.29			1.003	0.083	0.23	
C90-2	143.3	2370.8	247.7	5.875	3.95	4.04	4.07	0.767	0	0.14	0.14
		2370.8	201.7	5.750	4.13			0.675	0	0.13	
C90-3	141.3	2370.8	221.5	5.813	4.05	4.1	4.07	0.942	0	0.18	0.19
		2370.8	215.9	5.688	4.15			1.033	0	0.2	
INTERNATIONAL UNITS											
Specimen	γ (kg/m^3)	S_2 (kPa)	S_1 (kPa)	ε_2 ($\times 10^4$)	E (GPa)		ε_{t2} ($\times 10^4$)	ε_{t1} ($\times 10^5$)	ν		
C7-1	2269.8	13363	2609.7	4.375	27.72	27.51	26.54	0.998	1.746	0.21	0.23
		11176	2327.7	3.750	27.23			0.981	1.663	0.25	
C7-2	2279.4	11176	2101.5	4.000	25.92	25.65	26.54	0.915	1.247	0.23	0.22
		11176	2308.4	4.000	25.30			0.915	1.497	0.22	
C14-1	2265.0	14629	2560.0	4.750	28.41	28.41	27.65	1.116	0.666	0.25	0.25
		-	-	-	-			-	-	-	
C14-2	2287.4	14629	2306.3	5.063	27.03	26.82	27.65	1.333	1.666	0.26	0.26
		14629	2633.1	5.000	26.68			1.316	0.833	0.27	
C28-2	2247.4	14496	2179.4	5.125	26.61	27.03	27.79	1.119	0	0.24	0.24
		14496	2087.0	5.031	27.37			1.078	0.166	0.23	
C28-3	2279.4	14496	1614.1	5.156	27.65	28.61	27.79	0.912	0.083	0.19	0.21
		14496	1561.0	4.875	29.58			1.003	0.083	0.23	
C90-2	2295.4	16346	1707.8	5.875	27.23	27.85	28.06	0.767	0	0.14	0.14
		16346	1390.7	5.750	28.48			0.675	0	0.13	
C90-3	2263.4	16346	1527.2	5.813	27.92	28.27	28.06	0.942	0	0.18	0.19
		16346	1488.6	5.688	28.61			1.033	0	0.2	

[Note] Specimen C7-1=7-day specimen No. 1

Table 21. Static modulus of elasticity and Poisson's ratio of fly ash concrete (Mix B).

ENGLISH UNITS											
Specimen	γ (pcf)	S_2 (psi)	S_1 (psi)	ϵ_2 ($\times 10^4$)	E ($\times 10^3$ ksi)		ϵ_{t2} ($\times 10^4$)	ϵ_{t1} ($\times 10^5$)	ν		
C7-2(f)	138.4	1395.6	260.3	4.094	3.16	3.21	3.03	0.827	0.662	0.21	0.21
		1395.6	231	4.063	3.27			0.836	0.745	0.21	
C7-3(f)	140.8	1395.6	135.4	4.969	2.82	2.85		0.902	0.662	0.19	0.19
		1395.6	207.2	4.625	2.88			0.836	0.745	0.18	
C14-2(f)	141	1726.2	253.2	5.063	3.23	3.23	2.99	0.882	0.420	0.18	0.18
		1726.2	251.0	4.700	3.51			0.84	0.210	0.20	
C14-3(f)	136.7	1726.2	507.1	5.075	2.66	2.75		1.134	1.470	0.22	0.21
		1726.2	412.8	5.125	2.84			1.113	1.260	0.21	
C28-2(f)	137.2	1893.3	224.4	6.500	2.78	2.85	3.03	1.244	0.912	0.19	0.19
		1893.3	238.4	6.188	2.91			1.253	1.493	0.19	
C28-3(f)	139.4	1893.3	245.4	5.688	3.18	3.21		1.045	0.747	0.19	0.19
		1893.3	270.0	5.500	3.25			1.062	0.747	0.20	
C90-2(f)	138.6	1946.2	350.3	4.238	4.27	4.23	3.8	0.854	0	0.23	0.22
		1946.2	350.3	4.313	4.19			0.813	0	0.21	
C90-3(f)	139.5	1946.2	154.3	5.819	3.37	3.38		0.729	0	0.14	0.13
		1946.2	176.9	5.719	3.39			0.667	0	0.13	
INTERNATIONAL UNITS											
Specimen	γ (kg/m^3)	S_2 (kPa)	S_1 (kPa)	ϵ_2 ($\times 10^4$)	E (GPa)		ϵ_{t2} ($\times 10^4$)	ϵ_{t1} ($\times 10^5$)	ν		
C7-2(f)	2217.0	9622	1794.7	4.094	21.79	22.13	20.89	0.827	0.662	0.21	0.21
		9622	1592.7	4.063	22.55			0.836	0.745	0.21	
C7-3(f)	2255.4	9622	933.6	4.969	19.44	19.65		0.902	0.662	0.19	0.19
		9622	1428.6	4.625	19.86			0.836	0.745	0.18	
C14-2(f)	2258.6	11902	1745.8	5.063	22.27	23.24	21.10	0.882	0.420	0.18	0.18
		11902	1730.6	4.700	24.20			0.84	0.210	0.20	
C14-3(f)	2189.7	11902	3496.3	5.075	18.34	18.96		1.134	1.470	0.22	0.21
		11902	2846.2	5.125	19.58			1.113	1.260	0.21	
C28-2(f)	2197.7	13054	1547.2	6.500	19.17	19.65	20.89	1.244	0.912	0.19	0.19
		13054	1643.7	6.188	20.06			1.253	1.493	0.19	
C28-3(f)	2233.0	13054	1692.0	5.688	21.93	22.13		1.045	0.747	0.19	0.19
		13054	1861.6	5.500	22.41			1.062	0.747	0.20	
C90-2(f)	2220.2	13419	2415.2	4.238	29.44	29.16	26.20	0.854	0	0.23	0.22
		13419	2415.2	4.313	28.89			0.813	0	0.21	
C90-3(f)	2234.6	13419	1063.9	5.819	23.24	23.30		0.729	0	0.14	0.13
		13419	1219.7	5.719	23.37			0.667	0	0.13	

6.4 Splitting Tensile Strength (ASTM C 496/C 496M-04)

At the contact between the specimen and the loading surface, plywood strip are inserted to ensure uniform load. The load was applied continuously and without shock at a rate of 17,000 lbs/min (76 kN/min) until the specimen fails. The splitting tensile strength T of the specimen is calculated as:

$$T = 2P / \pi d \quad \text{Eq. 33}$$

where P = maximum applied load indicated by the testing machine; l = length of the specimen; and d = diameter of the specimen.

The calculation for the splitting tensile strength is shown in Tables 22 and 23 for GGBSF and fly ash concrete, respectively. The splitting strength for GGBFS at 90 days age is 622.4 psi (4291 kPa), 31% greater than the one for fly ash concrete, 472.3 psi (3256 kPa).

Table 22. Splitting tensile strength of GGBFS concrete (Mix A).

ENGLISH UNITS						
Specimen	γ (pcf)	P (lb)	l (in)	d (in)	T (psi)	
S7-1	140.3	54,340	12.08	6.02	475.9	434.7
S7-2	142.8	51,480	12.11	6.00	451.7	
S7-3	142.4	43,080	12.1	6.02	376.6	
S14-1	140.7	48,380	12.19	5.99	422.2	463.6
S14-2	140.6	55,580	12.24	6.01	480.9	
S14-3	142.4	55,480	12.07	6.00	487.7	
S28-1	142.4	-	-	-	454.1	519.4
S28-2	141.9	-	-	-	609.5	
S28-3	141.2	-	-	-	494.7	
S90-2	142.7	67,920	12.08	5.99	598	622.4
S90-3	141.6	73,860	12.09	6.02	646.8	
INTERNATIONAL UNITS						
Specimen	γ (kg/m ³)	P (kN)	l (m)	d (m)	T (kPa)	
S7-1	2247.4	241.7	0.307	0.153	3281.2	2997.2
S7-2	2287.4	229.0	0.308	0.152	3114.4	
S7-3	2281.0	191.6	0.307	0.153	2596.6	
S14-1	2253.8	215.2	0.310	0.152	2911.0	3196.4
S14-2	2252.2	247.2	0.311	0.153	3315.7	
S14-3	2281.0	246.8	0.307	0.152	3362.6	
S28-1	2281.0	-	-	-	3130.9	3581.1
S28-2	2273.0	-	-	-	4202.4	
S28-3	2261.8	-	-	-	3410.8	
S90-2	2285.8	302.1	0.307	0.152	4123.1	4291.3
S90-3	2268.2	328.5	0.307	0.153	4459.5	

Table 23. Splitting tensile strength for fly ash concrete (Mix B).

ENGLISH UNITS						
Specimen	γ (pcf)	P (lb)	l (in)	d (in)	T (psi)	
S7-1(f)	140.2	38,760	12.17	6.02	337.2	437.5
S7-2(f)	138.6	50,960	12.1	6.02	445.3	
S7-3(f)	139.3	48,940	12.08	6.01	429.6	
S14-1(f)	140.5	59,320	12.18	6.02	515.5	475.6
S14-2(f)	139.8	52,580	11.98	6.00	466.1	
S14-3(f)	136.5	51,540	12.19	6.05	445	
S28-1(f)	137.2	54,080	12.12	6.02	472	468.8
S28-2(f)	140.6	57,100	12.17	6.01	497.4	
S28-3(f)	138.2	49,140	11.95	5.99	437	
S90-1(f)	138	55,360	12.03	6.00	488.5	472.3
S90-2(f)	138.8	48,460	11.97	6.00	429.8	
INTERNATIONAL UNITS						
Specimen	γ (kg/m ³)	P (kN)	l (m)	d (m)	T (kPa)	
S7-1	2245.8	172.4	0.309	0.153	2324.9	3016.5
S7-2	2220.2	226.7	0.307	0.153	3070.2	
S7-3	2231.4	217.7	0.307	0.153	2962.0	
S14-1	2250.6	263.9	0.309	0.153	3554.2	3279.1
S14-2	2239.4	233.9	0.304	0.152	3213.6	
S14-3	2186.5	229.2	0.310	0.154	3068.2	
S28-1	2197.7	240.5	0.308	0.153	3254.3	3232.3
S28-2	2252.2	254.0	0.309	0.153	3429.5	
S28-3	2213.8	218.6	0.304	0.152	3013.0	
S90-2	2210.5	246.2	0.306	0.152	3368.1	3256.4
S90-3	2223.4	215.6	0.304	0.152	2963.4	

6.5 Compressive Strength (ASTM C 39/C39M-03)

The load was applied at a loading rate of 55,000 lbs/min (240 kN/min) for the specimens with 6.0 in. (15 cm) diameter continuously and without shock until the specimen fails. The compressive strength C is determined using the following expression:

$$C = 4P / \pi d^2 \quad \text{Eq. 34}$$

where P = maximum load carried by the specimen and d = specimen diameter.

Tables 24 and 25 present the compressive strength for GGBSF and Fly Ash concrete respectively. Table 26 shows the compressive strength for fly ash concrete for

two different curing methods: on-site curing with top surface applied with curing compound, and water bath.

The compressive strength for GGBFS at 90 days age is 6149 psi (42,400 kPa), 20% greater than that for fly ash concrete, 5102 psi (35,200 kPa). Based on the results presented in Table 26, it is evident that on-site curing with curing compound applied to the top surface makes the compressive strength higher than the water bath curing process, but that difference becomes negligible as the age of the specimen increases. That difference changed from 14% at 7 days age to 2% at 28 days age.

Table 24. Compressive strength for GGBSF concrete (Mix A).

ENGLISH UNITS						
Specimen	γ (pcf)	L (in.)	d (in.)	P (in.)	C (psi)	
C7-1	141.9	11.992	6.013	116,500	4105	4260.3
C7-2	142.4	11.974	5.992	130,160	4618	
C7-3	141.1	12.052	6.020	115,420	4058	
C14-1	141.4	12.176	6.002	146,360	5176	5255.9
C14-2	142.8	12.023	5.991	147,400	5232	
C14-3	141.7	12.221	6.005	151,740	5361	
C28-1	141.3	12.156	6.014	150,420	5298	5379.2
C28-2	140.3	12.032	6.030	153,680	5385	
C28-3	142.3	12.241	6.003	154,300	5455	
C90-1	143.7	12.125	6.000	169,700	6005	6148.9
C90-2	143.3	12.094	6.000	183,000	6476	
C90-3	141.3	12.151	6.000	168,600	5966	
INTERNATIONAL UNITS						
Specimen	γ (kg/m ³)	L (m)	d (m)	P (m)	C (kPa)	
C7-1	2273.0	0.305	0.153	2959.1	28305.0	29374
C7-2	2281.0	0.304	0.152	3306.1	31837.9	
C7-3	2260.2	0.306	0.153	2931.7	27977.5	
C14-1	2265.0	0.309	0.152	3717.5	35684.5	36238
C14-2	2287.4	0.305	0.152	3744.0	36069.9	
C14-3	2269.8	0.310	0.153	3854.2	36959.3	
C28-1	2263.4	0.309	0.153	3820.7	36525.0	37088
C28-2	2247.4	0.306	0.153	3903.5	37128.3	
C28-3	2279.4	0.311	0.152	3919.2	37610.9	
C90-1	2301.9	0.308	0.152	4310.4	41403.0	42395
C90-2	2295.4	0.307	0.152	4648.2	44647.7	
C90-3	2263.4	0.309	0.152	4282.4	41134.1	

Table 25. Compressive strength for fly ash concrete (Mix B).

ENGLISH UNITS						
Specimen	γ (pcf)	L (in.)	d (in.)	P (in.)	C (psi)	
C7-1(f)	139.1	12.064	5.993	106,820	3789	3832.4
C7-2(f)	138.4	12.198	6.043	107,640	3756	
C7-3(f)	140.8	12.171	6.012	112,140	3953	
C14-1(f)	140.3	12.019	5.942	120,400	4345	4396.1
C14-2(f)	141	12.053	5.952	122,440	4403	
C14-3(f)	136.7	12.02	6.021	126,380	4441	
C28-1(f)	140	12.173	6.012	135,040	4760	4684.2
C28-2(f)	137.2	12.228	6.028	129,380	4536	
C28-3(f)	139.4	11.944	5.984	105,890	3767	
C90-1(f)	-	12.000	6.000	137,020	4849	5102.4
C90-2 (f)	138.6	11.938	6.000	146,620	5188	
C90-3(f)	139.5	12.063	6.000	148,940	5270	
INTERNATIONAL UNITS						
Specimen	γ (kg/m ³)	L (m)	d (m)	P (m)	C (kPa)	
C7-1(f)	2228.2	0.306	0.152	2713.2	26122.2	26423
C7-2(f)	2217.0	0.310	0.153	2734.1	25893.3	
C7-3(f)	2255.4	0.309	0.153	2848.4	27255.0	
C14-1(f)	2247.4	0.305	0.151	3058.2	29955.7	30310
C14-2(f)	2258.6	0.306	0.151	3110.0	30359.0	
C14-3(f)	2189.7	0.305	0.153	3210.1	30616.2	
C28-1(f)	2242.6	0.309	0.153	3430.0	32820.4	32296
C28-2(f)	2197.7	0.311	0.153	3286.3	31275.3	
C28-3(f)	2233.0	0.303	0.152	2689.6	25973.2	
C90-1(f)	-	0.305	0.152	3480.3	33429.2	35180
C90-2 (f)	2220.2	0.303	0.152	3724.1	35772.1	
C90-3(f)	2234.6	0.306	0.152	3783.1	36337.4	

Table 26. Compressive strength of fly ash concrete using two curing methods.

ENGLISH UNITS							
Specimen	Curing method	γ (pcf)	L (in)	d (in)	P (in)	C (psi)	
S7-1	On-site curing with top surface applied with curing compound	141.4	8.099	4.017	56,740	4479	4410.3
S7-2		141.1	8.018	4.028	54,800	4304	
S7-3		141.3	8.103	4.026	56,580	4448	
W7-1	Water-Bath	144.3	8.056	4.019	46,880	3698	3872.0
W7-2		141.7	8.083	4.016	50,540	3992	
W7-3		143.3	8.117	4.026	49,940	3926	
S28-1	On-site curing with top surface applied with curing compound	141.8	8.147	4.024	76,720	6036	5937.7
S28-2		143.6	8.051	3.996	73,860	5893	
S28-3		147.5	8.054	3.943	71,800	5885	
W28-1	Water-Bath	152	8.006	3.922	70,840	5866	5799.1
W28-2		141.7	8.083	4.016	-	-	
W28-3		146.2	8.089	3.977	71,180	5732	
INTERNATIONAL UNITS							
Specimen	Curing method	γ (kg/m ³)	L (m)	d (m)	P (m)	C (kPa)	
S7-1	On-site curing with top surface applied with curing compound	2265.0	0.206	0.102	1,441	30884	30408
S7-2		2260.2	0.204	0.102	1,392	29673	
S7-3		2263.4	0.206	0.102	1,437	30667	
W7-1	Water-Bath	2311.5	0.205	0.102	1,191	25498	26697
W7-2		2269.8	0.205	0.102	1,284	27523	
W7-3		2295.4	0.206	0.102	1,268	27068	
S28-1	On-site curing with top surface applied with curing compound	2271.4	0.207	0.102	1,949	41614	40939
S28-2		2300.3	0.204	0.101	1,876	40631	
S28-3		2362.7	0.205	0.100	1,824	40572	
W28-1	Water-Bath	2434.8	0.203	0.100	1,799	40444	39983
W28-2		2269.8	0.205	0.102	-	-	
W28-3		2341.9	0.205	0.101	1,808	39522	

Tables 27 through 30 show summaries for the properties described above for each mix in both English and international units. Note that italicized entries in the tables were not included in the averages because, according to the test criteria, they were classed as outliers.

Table 27. Summary of results for ground granulated blast-furnace slag (GGBSF) concrete (Mix A), English units.

	Sample	γ (pcf)	R (psi)	T (psi)	C (psi)	E ($\times 10^3$ ksi)	ν
Day 7	C7-1	141.9				3.99	3.86 0.23 0.22
	C7-2	142.4				3.72	
	S7-1	140.3		475.9	434.7		
	S7-2	142.8		451.7			
	S7-3	142.4		376.6			
	C7-1	141.9			4105.3	4260.3	
	C7-2	142.4			4617.7		
	C7-3	141.1			4057.8		
	F7-1	142.7	578.8	520.8			
	F7-2	142.7	485.6				
	F7-3	142.7	497.9				
	Day 14	C14-1	141.4				4.12
C14-2		142.8				3.89	
S14-1		140.7		422.2	463.6		
S14-2		140.6		480.9			
S14-3		142.4		487.7			
C14-1		141.4			5175.6	5255.9	
C14-2		142.8			5231.5		
C14-3		141.7			5360.5		
F14-1		142.1	415.1	530			
F14-2		143.2	580				
F14-3		142.3	479				
Day 28		C28-2	140.3				3.92
	C28-3	142.3				4.15	
	S28-1	142.4		454.1	519.4		
	S28-2	141.9		609.5			
	S28-3	141.2		494.7			
	C28-1	141.3			5297.5	5379.2	
	C28-2	140.3			5385		
	C28-3	142.3			5455		
	F28-1	145.3	585.1	543.3			
	F28-2	143.3	522.3				
	F28-3	141.5	522.4				
	Day 90	C90-2	143.3				4.04
C90-3		141.3				4.1	
S90-1					622.4		
S90-2		142.7		598			
S28-3		141.6		646.8			
C90-1		143.7			6005	6148.9	
C90-2		143.3			6475.6		
C90-3		141.3			5966		
F90-1		141.8	687.7	608.7			
F90-2		142	582.6				
F90-3		141.5	555.8				

Table 28. Summary of results for ground granulated blast-furnace slag (GGBSF) concrete (Mix A), international units.

	Sample	γ (kg/m ³)	R (kPa)	T (kPa)	C (kPa)	E (GPa)	ν
Day 7	C7-1	2273				27.51	26.61
	C7-2	2281				25.65	
	S7-1	2247		3281			0.22
	S7-2	2287		3114	2997		
	S7-3	2281		2597			
	C7-1	2273			28305		
	C7-2	2281			31838	29374	
	C7-3	2260			27978		
	F7-1	2286	3991				
	F7-2	2286	3348	3591			
	F7-3	2286	3433				
	Day 14	C14-1	2265				28.41
C14-2		2287				26.82	0.25
S14-1		2254		2911			0.26
S14-2		2252		3316	3196		
S14-3		2281		3363			
C14-1		2265			35685		
C14-2		2287			36070	36238	
C14-3		2270			36959		
F14-1		2276	2862				
F14-2		2294	3999	3654			
F14-3		2279	3303				
Day 28		C28-2	2247				27.03
	C28-3	2279				28.61	0.24
	S28-1	2281		3131			0.21
	S28-2	2273		4202	3581		
	S28-3	2262		3411			
	C28-1	2263			36525		
	C28-2	2247			37128	37088	
	C28-3	2279			37611		
	F28-1	2327	4034				
	F28-2	2295	3601	3746			
	F28-3	2267	3602				
	Day 90	C90-2	2295				27.85
C90-3		2263				28.27	0.14
S90-1							0.19
S90-2		142.7		4123	4291		
S28-3		141.6		4460			
C90-1		143.7			41403		
C90-2		143.3			44648	42395	
C90-3		141.3			41134		
F90-1		141.8	4742				
F90-2		142	4017	4197			
F90-3		141.5	3832				

Table 29. Summary of results for fly ash concrete (Mix B), English units.

	Sample	γ (pcf)	R (psi)	T (psi)	C (psi)	E ($\times 10^3$ ksi)	ν
Day 7	C7-2(f)	138.4				3.21	3.03
	C7-3(f)	140.8				2.85	
	S7-1(f)	140.2		337.2	437.5		
	S7-2(f)	138.6		445.3			
	S7-3(f)	139.3		429.6			
	C7-1(f)	139.1			3788.7	3832.4	
	C7-2(f)	138.4			3755.5		
	C7-3(f)	140.8			3953		
	F7-1(f)	142.4	515.5	554.6			
	F7-2(f)	140.2	385.7				
	F7-3(f)	140.2	593.7				
	Day 14	C14-2(f)	141				3.23
C14-3(f)		136.7				2.75	
S14-1(f)		140.5		515.5	475.6		
S14-2(f)		139.8		466.1			
S14-3(f)		136.5		445			
C14-1(f)		140.3			4344.7	4396.1	
C14-2(f)		141			4403.2		
C14-3(f)		136.7			4440.5		
F14-1(f)		139.8	531.6	566.4			
F14-2(f)		141.2	610				
F14-3(f)		141.6	557.7				
Day 28		C28-2(f)	137.2				2.85
	C28-3(f)	139.4				3.21	
	S28-1(f)	137.2		472	468.8		
	S28-2(f)	140.6		497.4			
	S28-3(f)	141.2		437			
	C28-1(f)	140			4760.2	4684.2	
	C28-2(f)	137.2			4536.1		
	C28-3(f)	139.4			3767.1		
	F28-1(f)	141.4	730.7	632.6			
	F28-2(f)	141.8	543.6				
	F28-3(f)	141.9	623.4				
	Day 90	C90-2(f)	138.6				4.23
C90-3(f)		139.5				3.38	
S90-1(f)		138		488.5	472.3		
S90-2(f)		138.8		429.8			
S90-3(f)		137		498.5			
C90-1(f)		N/A			4848.5	5102.4	
C90-2(f)		138.6			5188.3		
C90-3(f)		139.5			5270.3		
F90-1(f)		142.2	828.7	817.7			
F90-2(f)		139.7	829.7				
F90-3(f)		139.1	794.7				

Table 30. Summary of results for fly ash concrete (Mix B), international units.

	Sample	γ (kg/m ³)	R (kPa)	T (kPa)	C (kPa)	E (GPa)	ν		
Day 7	C7-2(f)	2217				22.13	20.89	0.21 0.19	0.20
	C7-3(f)	2255				19.65			
	S7-1(f)	2246		2325	3016				
	S7-2(f)	2220		3070					
	S7-3(f)	2231		2962					
	C7-1(f)	2228				26122	26423		
	C7-2(f)	2217			25893				
	C7-3(f)	2255			27255				
	F7-1(f)	2281	3554	3824					
	F7-2(f)	2246	2659						
	F7-3(f)	2246	4093						
Day 14	C14-2(f)	2259				22.27	20.62	0.18 0.21	0.20
	C14-3(f)	2190				18.96			
	S14-1(f)	2251		3554	3279				
	S14-2(f)	2239		3214					
	S14-3(f)	2187		3068					
	C14-1(f)	2247				29956	30310		
	C14-2(f)	2259			30359				
	C14-3(f)	2190			30616				
	F14-1(f)	2239	3665	3905					
	F14-2(f)	2262	4206						
	F14-3(f)	2268	3845						
Day 28	C28-2(f)	2198				19.65	20.89	0.19 0.19	0.19
	C28-3(f)	2233				22.13			
	S28-1(f)	2198		3254	3232				
	S28-2(f)	2252		3429					
	S28-3(f)	2262		3013					
	C28-1(f)	2243				32820	32296		
	C28-2(f)	2198			31275				
	C28-3(f)	2233			25973				
	F28-1(f)	2265	5038	4362					
	F28-2(f)	2271	3748						
	F28-3(f)	2273	4298						
Day 90	C90-2(f)	2220				29.16	26.20	0.22 0.13	0.18
	C90-3(f)	2235				23.30			
	S90-1(f)			3368	3256				
	S90-2(f)	142.7		2963					
	S90-3(f)	141.6		3437					
	C90-1(f)	143.7				33429	35180		
	C90-2(f)	143.3			35772				
	C90-3(f)	141.3			36337				
	F90-1(f)	141.8	5714	5638					
	F90-2(f)	142	5721						
	F90-3(f)	141.5	5479						

6.6 Maturity Test

The two PCC mixes, fly ash concrete (Mix B) and GGBFS concrete (Mix A), were cured and tested to determine the strength - maturity relationship for each of them. Temperature sensors were embedded in the specimens in order to record the temperature of the concrete. Additionally, compression test were performed at ages of 1, 3, 7, 14, and 28 days. At each test age, the maturity t_e (equivalent age at a specified temperature T_s) is calculated using the following expression:

$$t_e = \sum e^{-Q\left(\frac{1}{T_a} - \frac{1}{T_s}\right)} \Delta t \quad \text{Eq. 35}$$

where Q = activation energy divided by the gas constant; T_a = average temperature of concrete during time interval Δt .

The equivalent age and the strength resulting from the compressive test are presented in Tables 31 and 32, respectively. These data are plotted and a logarithmic regression for each type of concrete is calculated. The plots and the equation of the regression are presented in Figure 22.

Table 31. Equivalent age and compressive strength of GGBSF concrete.

Time (day)	Eq. Age (day)	Strength	
		(psi)	(kN)
1	1.207	910.3	6276.3
3	3.085	2370.8	16346
7	6.742	3056.8	21076
14	12.912	3993.4	27534
28	25.446	4582.4	31595

Table 32. Equivalent age and compressive strength of fly ash concrete.

Time (day)	Eq. Age (day)	Strength	
		(psi)	(kN)
1	1.128	2148.5	14813
3	3.046	3323.8	22917
7	6.812	4120.3	28409
14	13.244	4707.4	32456
28	26.241	5224.0	36018

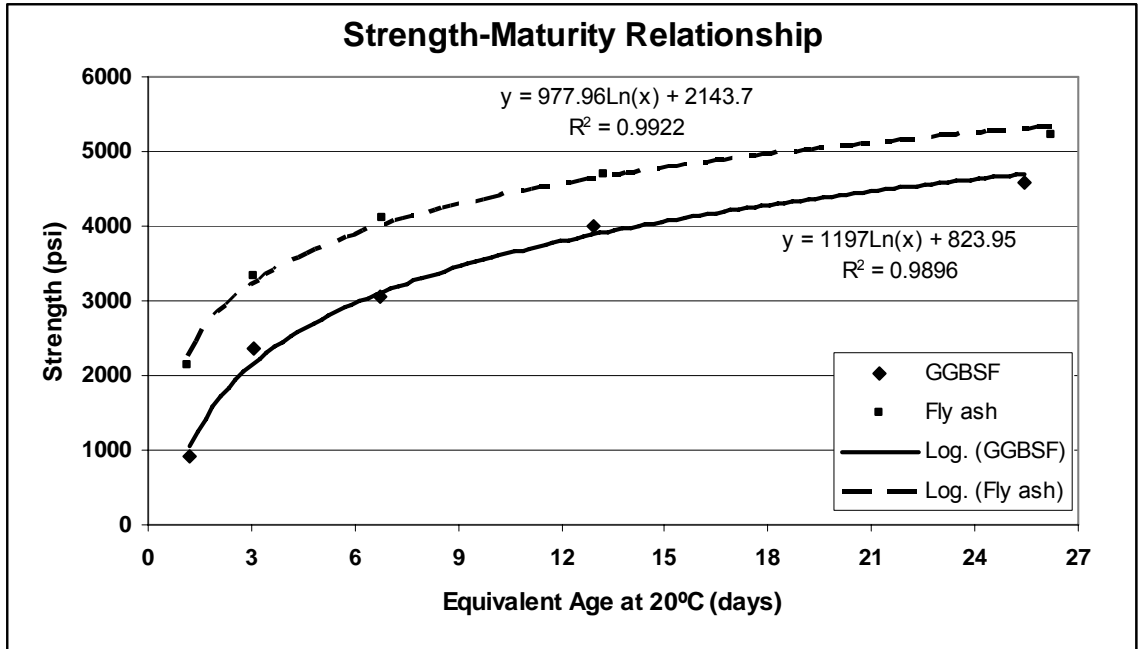


Figure 22. Strength-maturity relationship for fly ash and GGBSF concretes. (1 psi = 6.89 kPa, 20°C = 68°F)

6.7 Thermal Coefficient of Linear Expansion and Void Properties

The value of the linear thermal expansion coefficient for each type of concrete is $5.9 \times 10^{-6} / ^\circ\text{F}$ ($10.6 \times 10^{-6} / ^\circ\text{C}$) for GGBSF concrete and $5.8 \times 10^{-6} / ^\circ\text{F}$ ($10.4 \times 10^{-6} / ^\circ\text{C}$) for fly ash concrete.

The void properties of the hardened concretes were determined by the linear-traverse method (ASTM C457). For GGBSF concrete, total and entrained air voids are 4.8% and 3.1%, respectively. For fly ash concrete, total and entrained air voids are 4.9% and 3.3%, respectively. The details of void properties are summarized at Appendix D.

7 LABORATORY TEST RESULTS ON ASPHALT CONCRETE

Recall from Section 2.2 that for the perpetual pavement structure four asphalt mixes were used: 1. the SMA mix on the surface layer; 2. ODOT Item 442 Superpave, called 442 mix henceforth, below that; 3. ODOT Item 302 asphalt treated base, or 302 mix, below that; and 4. the fatigue resistant layer, or FRL mix, sitting on the dense graded aggregate base. In addition, for some tests a fifth mix was studied: a 301 mix, ODOT Item 301, which was used for the asphalt treated base underneath the PCC lanes.

7.1 Maximum Specific Gravity (AASHTO T 209)

The maximum specific gravity is the specific gravity obtained when there are no air voids in the mixture. In order to calculate the maximum specific gravity, the specimen needs to be covered with water at 77 °F (25 °C) at a vacuum of 27.75 ± 2.25 mm Hg (3.700 ± 0.300 kPa, 0.5366 ± 0.0435 psi) for 15 ± 2 minutes to remove the air from the voids in the mix. Then the sample and the container are weighed in water. The maximum specific gravity (MSG), G_{mm} , is given by:

$$G_{mm} = \frac{C - A}{(C - A) - (D - B)} \quad \text{Eq. 36}$$

where A = Weight of Container in air; B = Weight of Container in water; C = Weight of Container and Sample in air; and D = Weight of Container and Sample in water. Table 33 shows the values of the maximum specific gravity for the specimen. Furthermore, this table presents the comparison with the values provided by contractor.

7.2 Bulk Specific Gravity Test (AASHTO T 166)

In order to determine the bulk specific gravity of a specimen, three measurements need to be taken on each core specimen: the dry mass A , which is the mass of the core sample at standard room temperature of $77 \pm 9^\circ\text{F}$ ($25 \pm 5^\circ\text{C}$); the submerged mass C , which is the mass of the sample after being submerged in water at $77 \pm 1.8^\circ\text{F}$ ($25 \pm 1^\circ\text{C}$) for 4 ± 1 minutes; and the saturated surface-dry (SSD) mass B , which is the mass of the specimen after being removed from water and dried with damp towel. The bulk specific gravity (BSG), G_{mb} , is then computed using this equation:

$$G_{mb} = \frac{A}{B - C} \quad \text{Eq. 37}$$

The BSG values for the AC samples from WAY-30 are presented in Table 34 along with air void data.

Table 33. Maximum specific gravity of AC core specimens.

Spec.	A		B		C		D		MSG (Gmm)		
	lb	g	lb	g	lb	g	lb	g	Calc.	Provided	Δ
301	5.52	2505	3.48	1578.3	10.77	4887.4	6.60	2995.6	2.469	2.480	0.5%
302	0*	0*	3.48	1578.3	5.36	2432.8	6.69	3037	2.497	2.468	1.2%
442	5.52	2505	3.48	1578.3	11.36	5153.9	6.96	3158.5	2.479	2.458	0.8%
FRL	5.52	2505	3.48	1578.3	11.35	5149.1	6.95	3154.2	2.475	2.459	0.7%
SMA	5.52	2505	3.48	1579.5	11.04	5007.6	6.76	3068.5	2.469	2.396	2.8%

* The scale was zeroed with container for measurements A and C with this specimen.

7.3 Air Void Measurement

The air content is the part in the mixture that is not occupied by aggregate or asphalt concrete. The air content gives an indication of how much a mixture can be compacted. The air void content VTM as a percentage of the mass of the sample is calculated as:

$$VTM = 100 \left(1 - \frac{BSG}{MSG} \right) \quad \text{Eq. 38}$$

where BSG = bulk specific gravity; and MSG = maximum specific gravity. Table 34 shows the results of the calculation of the air content for the five mixtures, 7 specimens for each mix.

Table 34. Air void content of AC core specimens.

Mix	Specimen	Dry Mass		Mass in water		SSD Mass		BSG (Gmb)		MSG (Gmm)	VTM	
		(lb)	(g)	(lb)	(g)	(lb)	(g)		Avg.		(%)	Avg. (%)
301	R301-1	6.508	2952	3.715	1685	6.563	2977	2.286	2.290	2.469	7.4	7.26
	R301-2	6.499	2948	3.726	1690	6.561	2976	2.293			7.1	
	R301-3	6.487	2942	3.72	1688	6.548	2970	2.294			7.1	
	R301-4	6.48	2939	3.715	1685	6.548	2970	2.287			7.4	
	R301-5	6.479	2939	3.713	1684	6.549	2971	2.284			7.5	
	R301-6	6.477	2938	3.732	1693	6.551	2972	2.297			7	
	R301-7	6.467	2934	3.713	1684	6.538	2966	2.289			7.3	
302	R302-1	6.485	2942	3.73	1692	6.545	2969	2.304	2.319	2.497	7.7	7.14
	R302-2	6.494	2945	3.736	1695	6.549	2971	2.308			7.6	
	R302-3	6.51	2953	3.761	1706	6.564	2977	2.323			7	
	R302-4	6.502	2949	3.779	1714	6.557	2974	2.34			6.3	
	R302-5	6.498	2947	3.755	1703	6.556	2974	2.32			7.1	
	R302-6	6.502	2949	3.763	1707	6.563	2977	2.322			7	
	R302-7	6.505	2951	3.764	1707	6.575	2983	2.314			7.3	
442	R302-1	6.489	2944	3.72	1687	6.546	2969	2.296	2.300	2.479	7.4	7.24
	R302-2	6.476	2938	3.725	1690	6.547	2970	2.295			7.4	
	R302-3	6.479	2939	3.73	1692	6.546	2969	2.301			7.2	
	R302-4	6.477	2938	3.728	1691	6.555	2973	2.291			7.6	
	R302-5	6.488	2943	3.751	1702	6.561	2976	2.309			6.9	
	R302-6	6.465	2932	3.741	1697	6.553	2972	2.299			7.3	
	R302-7	6.463	2932	3.754	1703	6.554	2973	2.308			6.9	
FRL	R301-1	6.485	2942	3.734	1694	6.55	2971	2.303	2.304	2.475	7	6.92
	R301-2	6.475	2937	3.712	1684	6.527	2961	2.3			7.1	
	R301-3	6.472	2936	3.705	1681	6.528	2961	2.293			7.4	
	R301-4	6.474	2937	3.715	1685	6.528	2961	2.301			7	
	R301-5	6.475	2937	3.728	1691	6.523	2959	2.317			6.4	
	R301-6	6.469	2934	3.731	1692	6.531	2962	2.31			6.6	
SMA	R301-1	6.389	2898	3.672	1666	6.465	2932	2.288	2.296	2.469	7.3	7.00
	R301-2	6.382	2895	3.681	1670	6.46	2930	2.296			7	
	R301-3	6.383	2895	3.67	1665	6.457	2929	2.29			7.2	
	R301-4	6.413	2909	3.689	1674	6.473	2936	2.304			6.7	
	R301-5	6.376	2892	3.671	1665	6.451	2926	2.294			7.1	
	R301-6	6.381	2894	3.683	1670	6.452	2927	2.304			6.7	

7.4 Resilient Modulus Test (SHRP P07)

For this test, a specimen is subjected to a pulse loading in the vertical direction at three different temperatures: 41°F (5°C), 77°F (25°C) and 104°F (40°C), with a tolerance of $\pm 2^\circ\text{F}$ ($\pm 1^\circ\text{C}$). The laboratory test equipment is composed of three main parts: a load frame which includes LVDTs, load cell, and horizontal extensometer; a computer data acquisition unit; and an environmental chamber which has the capability of keeping constant temperature $\pm 2^\circ\text{F}$ ($\pm 1^\circ\text{C}$) in the range from -22°F (-30°C) to 212°F (100°C). The sample is loaded with the same haversine-shape load used in the resilient modulus test in subgrade soil. Each pulse load cycle has two parts: the first one is a 0.1-second loading period and the second one is a rest period of 0.9 seconds, for a total of 1.0 second per cycle. To calculate the resilient modulus and the Poisson's ratio, horizontal and vertical deformations were recorded through the LVDTs.

Two resilient moduli can be computed: the instantaneous resilient modulus and the total resilient modulus. The instantaneous resilient modulus is calculated using the recoverable horizontal deformation that occurs during the unloading portion of the load-unload cycle; this modulus can be viewed as the elastic modulus. The total resilient modulus is computed with the recoverable deformation including both the instantaneous recoverable and the continuing recoverable deformation during the rest period of one cycle; this can be interpreted as a viscoelastic property.

When the test is carried out at 41°F (5°C) and 77°F (25°C), the specimen was kept 24 hours before the test in the environmental chamber. At 104°F (40°C), the sample was kept in the chamber for at least 3 hours but not more than 6 hours, as specified by the test procedure.

The total Poisson's ratio ν_t and instantaneous Poisson's ratio ν_i are respectively given by:

$$\nu_t = 3.59 \frac{\Delta H_t}{\Delta V_t} - 0.27, \quad \text{and} \quad \nu_i = 3.59 \frac{\Delta H_i}{\Delta V_i} - 0.27 \quad \text{Eq. 39}$$

where ΔV_t = total recoverable vertical deformation; ΔV_i = instantaneous recoverable vertical deformation; ΔH_t = total recoverable horizontal deformation; and ΔH_i = instantaneous recoverable horizontal deformation.

The total resilient modulus M_{Rt} and instantaneous resilient modulus M_{Ri} are then calculated using the following formula:

$$M_{Rt} = P \frac{\nu_t + 0.27}{t \Delta H_t}, \quad \text{and} \quad M_{Ri} = P \frac{\nu_i + 0.27}{t \Delta H_i} \quad \text{Eq. 40}$$

where t = thickness and P = repeated load.

The measurements of the vertical deflection proved suspect, and a Poisson's ratio, ν , of 0.35, typical for AC, was assumed to determine the moduli. Table 35 summarizes of the moduli of the laboratory specimens, including averages for each AC mix. Table 36 has the same data as Table 35 for the AC core samples. The moduli for the laboratory specimens are generally higher than those for the core specimens, which is a result laboratory specimens being compacted to about 4% air voids rather than the about 7% air

void for the cores. Figures 23 and 24 show the resilient modulus at three different test temperatures for laboratory prepared and cored specimens, respectively. These values at 25°C (77°F) are similar to the typical resilient moduli of the respective asphalt mixes used in the development of the perpetual pavement structure at the beginning of the project. While the resilient moduli of 302 and FRL mixes at 25°C (77°F) are higher than the typical values (500-1,500 ksi or 3,447-10,342 MPa), the resilient moduli of SMA and 442 mixes are little lower than the typical values used in Table 3 (1,500 ksi or 10,342 MPa).

Table 35. Summary of total and instantaneous resilient moduli for laboratory prepared asphalt specimens, assuming $\nu = 0.35$.

ENGLISH UNITS												
Mixture	41 °F				77 °F				104 °F			
	M_{Ri} (ksi)	Aver.	M_{Rt} (ksi)	Aver.	M_{Ri} (ksi)	Aver.	M_{Rt} (ksi)	Aver.	M_{Ri} (ksi)	Aver.	M_{Rt} (ksi)	Aver.
301-1	3700	3700	3490	3490	1920	1920	1830	1830	826	826	720	720
302-1	4110	3805	3950	3345	1740	1900	1680	1830	747	753.5	644	660.5
302-2	3500		2740		2060		1980		760		677	
442-1	3160	2985	3110	2955	1080	1023	1040	968	438	408	376	349
442-2	2810		2800		966		895		378		322	
FRL-1	4530	4390	4390	4230	2190	2205	2150	2155	916	944	807	789.5
FRL-2	4250		4070		2220		2160		972		772	
SMA-1	3160	3320	3160	3280	1280	1345	1240	1280	511	532	466	485.5
SMA-2	3480		3400		1410		1320		553		505	
INTERNATIONAL UNITS												
Mixture	5 °C				25 °C				40 °C			
	M_{Ri} (MPa)	Aver.	M_{Rt} (MPa)	Aver.	M_{Ri} (MPa)	Aver.	M_{Rt} (MPa)	Aver.	M_{Ri} (MPa)	Aver.	M_{Rt} (MPa)	Aver.
301-1	25511	25511	24063	24063	13238	13238	12617	12617	5695	5695	4964	4964
302-1	28337	26235	27234	23063	11997	13100	11583	12617	5150	5195	4440	4554
302-2	24132		18892		14203		13652		5240		4668	
442-1	21787	20581	21443	20374	7446	7053	7171	6671	3020	2813	2592	2406
442-2	19374		19305		6660		6171		2606		2220	
FRL-1	31233	30268	30268	29165	15100	15203	14824	14858	6316	6509	5564	5443
FRL-2	29303		28062		15306		14893		6702		5323	
SMA-1	21787	22891	21787	22615	8825	9273	8549	8825	3523	3668	3213	3347
SMA-2	23994		23442		9722		9101		3813		3482	

Table 36. Summary of total and instantaneous resilient moduli for asphalt core specimens, assuming $\nu = 0.35$.

ENGLISH UNITS												
Mixture	41 °F				77 °F				104 °F			
	M_{Ri} (ksi)	Aver.	M_{Rt} (ksi)	Aver.	M_{Ri} (ksi)	Aver.	M_{Rt} (ksi)	Aver.	M_{Ri} (ksi)	Aver.	M_{Rt} (ksi)	Aver.
301-1	1625	1625	1600	1600	384	384	332	332	219	219	195	195
302-1	2280	2583.5	2177	2450	805	967	690	812	380	423.5	317	361
302-2	2887		2723		1129		934		467		404	
FRL-1	2093	2370	1983	2502	782	911.5	653	797	326	447.5	277	396
FRL-2	2647		2502		1041		941		569		515	
INTERNATIONAL UNITS												
Mixture	5 °C				25 °C				40 °C			
	M_{Ri} (MPa)	Aver.	M_{Rt} (MPa)	Aver.	M_{Ri} (MPa)	Aver.	M_{Rt} (MPa)	Aver.	M_{Ri} (MPa)	Aver.	M_{Rt} (MPa)	Aver.
301-1	11204	11204	11032	11032	2648	2648	2289	2289	1510	1510	1344	1344
302-1	15720	17812	15010	16892	5550	6667	4757	5599	2620	2920	2186	2489
302-2	19905		18774		7784		6440		3220		2785	
FRL-1	14431	16341	13672	17251	5392	6285	4502	5495	2248	3085	1910	2730
FRL-2	18250		17251		7177		6488		3923		3551	

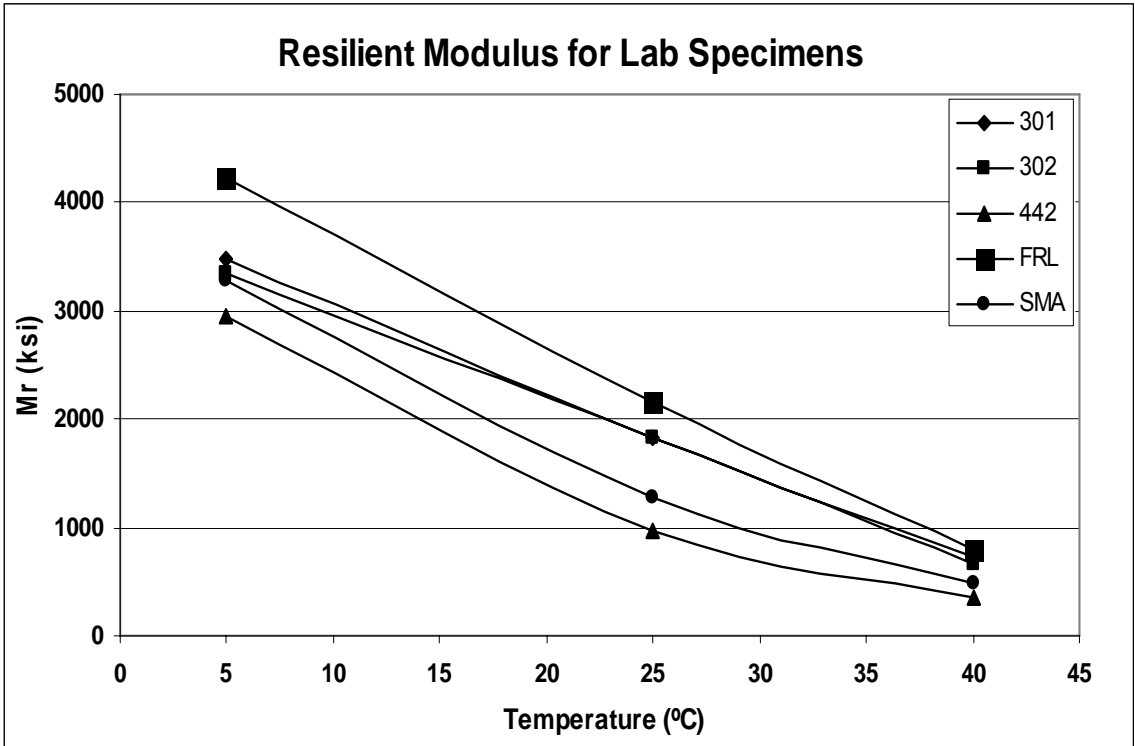


Figure 23. Resilient modulus versus the temperature for laboratory prepared asphalt specimens. (1 ksi=6.89 MPa)

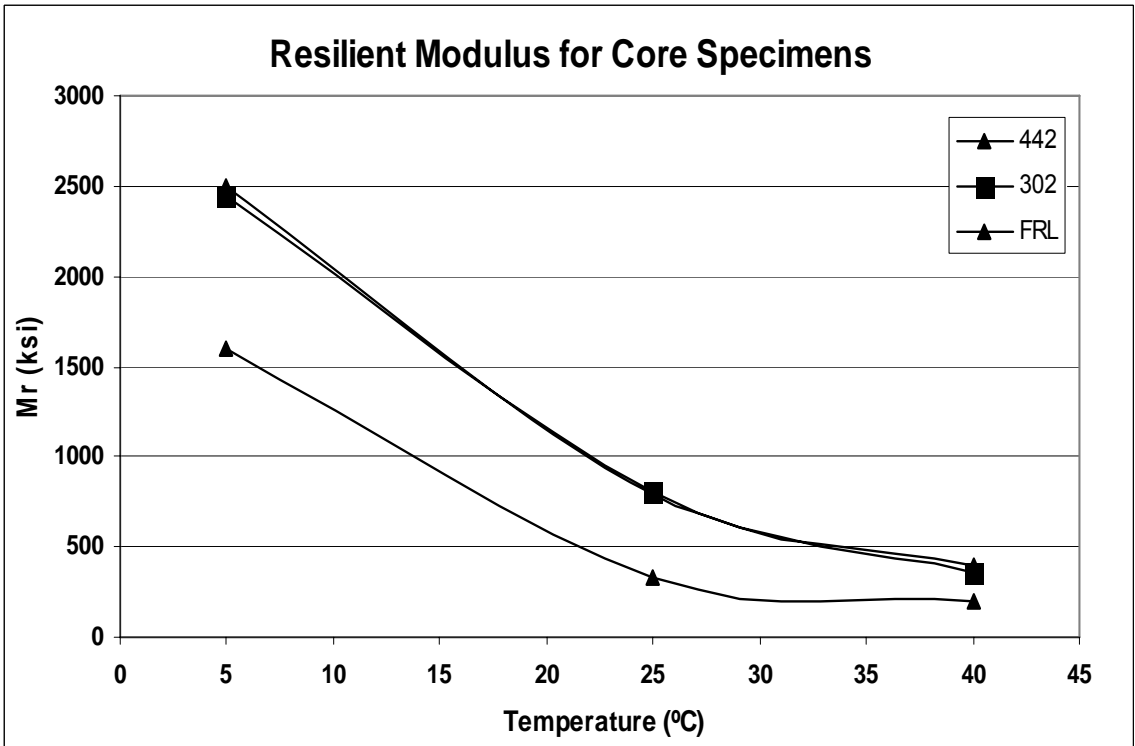


Figure 24. Resilient modulus versus the temperature for cored asphalt specimens. (1 ksi=6.89 MPa)

7.5 Rutting Evaluation-Asphalt Pavement Analyzer (APA)

Rutting is a permanent deformation in an asphalt concrete surface. The Asphalt Pavement Analyzer (APA) is a wheel rut test used to measure asphalt rut resistance. In this test, a concave steel wheel rolls on a pressurized rubber hose. The wheel transmits a load of 115 ± 5 lbs (512 ± 22 N), the pressure in the rubber hose is 100 ± 5 psi (700 ± 35 kPa), and the steel wheel rolls for 8000 cycles. There are two types of samples used in this test; beams and gyratory samples. Both of them can be batched to meet 7% air void requirement at the optimum binder content from the job mix formula (JMF). Deformations are recorded after 5, 500, 1000 and 8000 cycles, with the deformation at 5 cycles used as the zero point. The maximum deformation is 0.20 inches (5.0 mm) for heavy route and other mixes, and 0.12 inches (3.0 mm) for high stress area mixes. In this project, APA tests were performed at 64°C (147°F) using Superpave specimens prepared in a gyratory compactor following Ohio DOT Supplement Specification 1057. The chosen test temperature (64°C or 147°F) was much higher than Ohio DOT specification required (48.9°C [120°F] for non polymer binder mixes and 54.4°C [130°F] for high stress mixes). Figures 25 to 29 present the rut-depth for each mix analyzed. Figure 30 shows the average rut depth for each mix. Table 37 shows the average APA rut depth observed after 8000 cycles for each specimen. While rut resistance of SMA mix is the highest as expected, all mixes are considered rut-resistant.

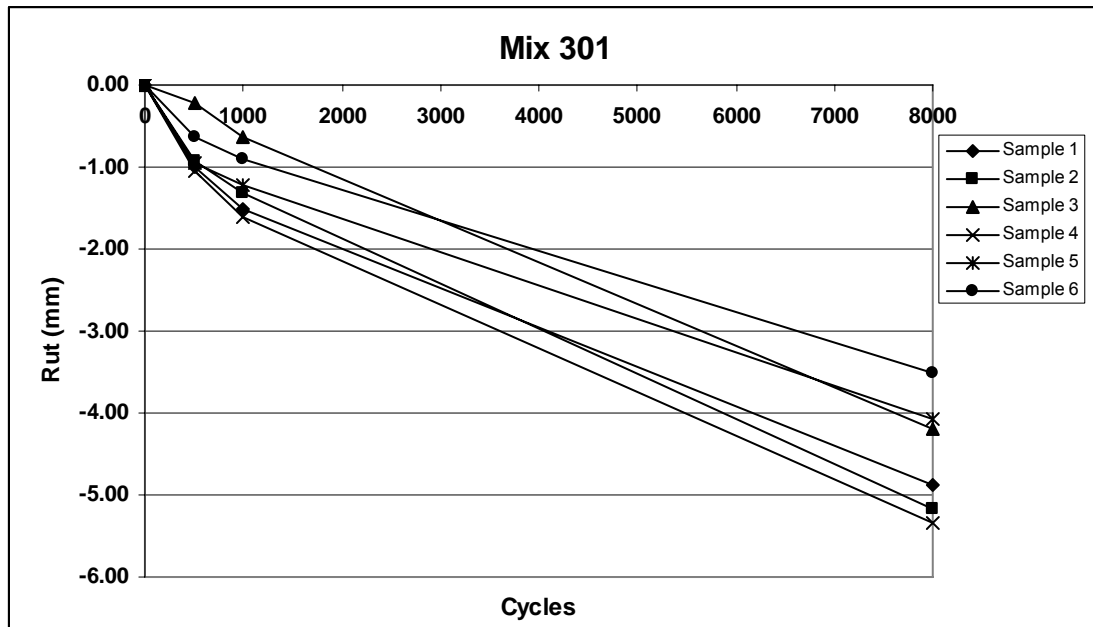


Figure 25. APA rut depth of Mix 301. (25.4 mm=1.00 in.)

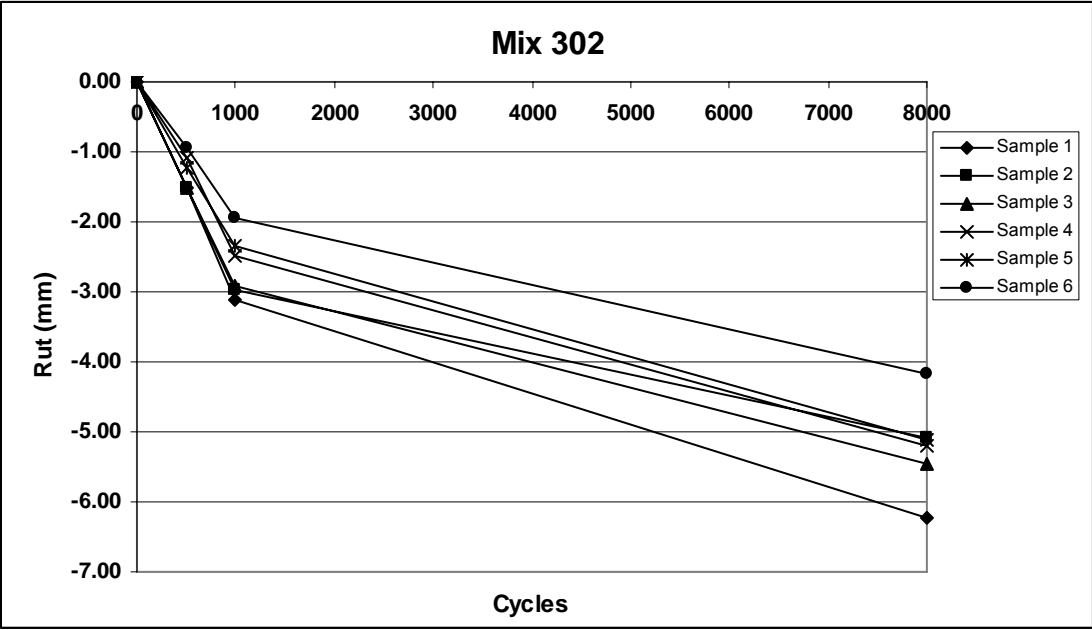


Figure 26. APA rut depth of Mix 302. (25.4 mm=1.00 in.)

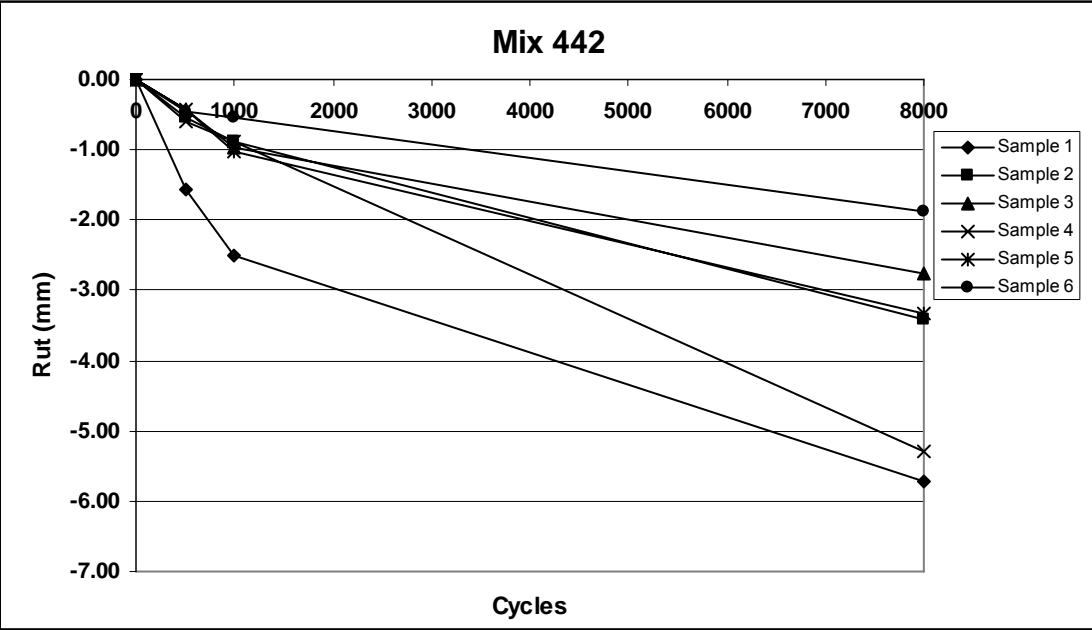


Figure 27. APA rut depth of Mix 442. (25.4 mm=1.00 in.)

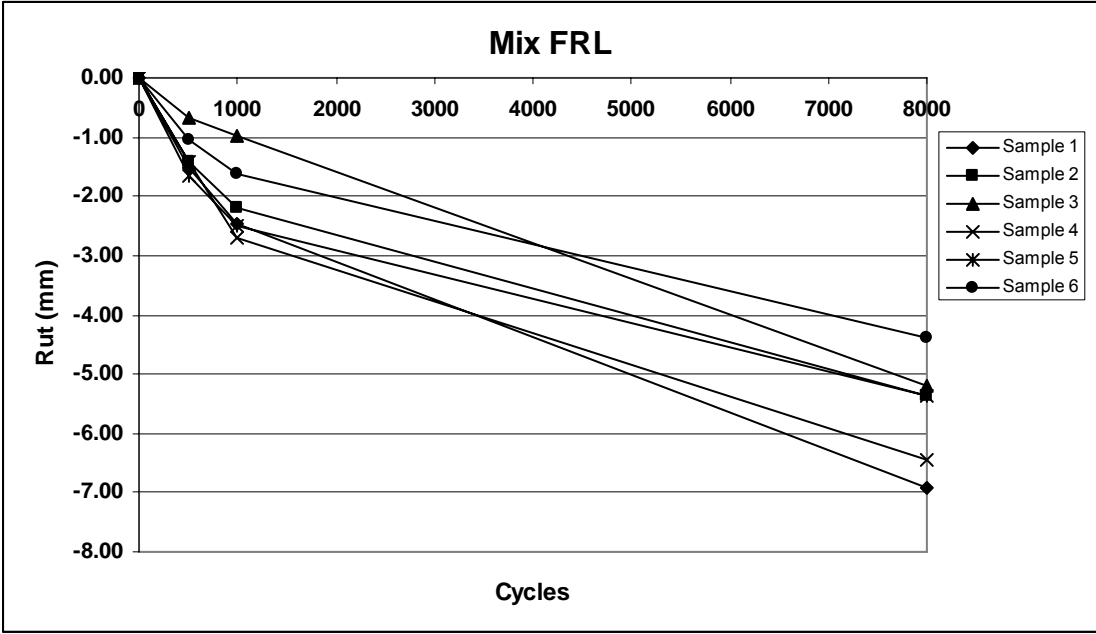


Figure 28. APA rut depth of Mix FRL. (25.4 mm=1.00 in.)

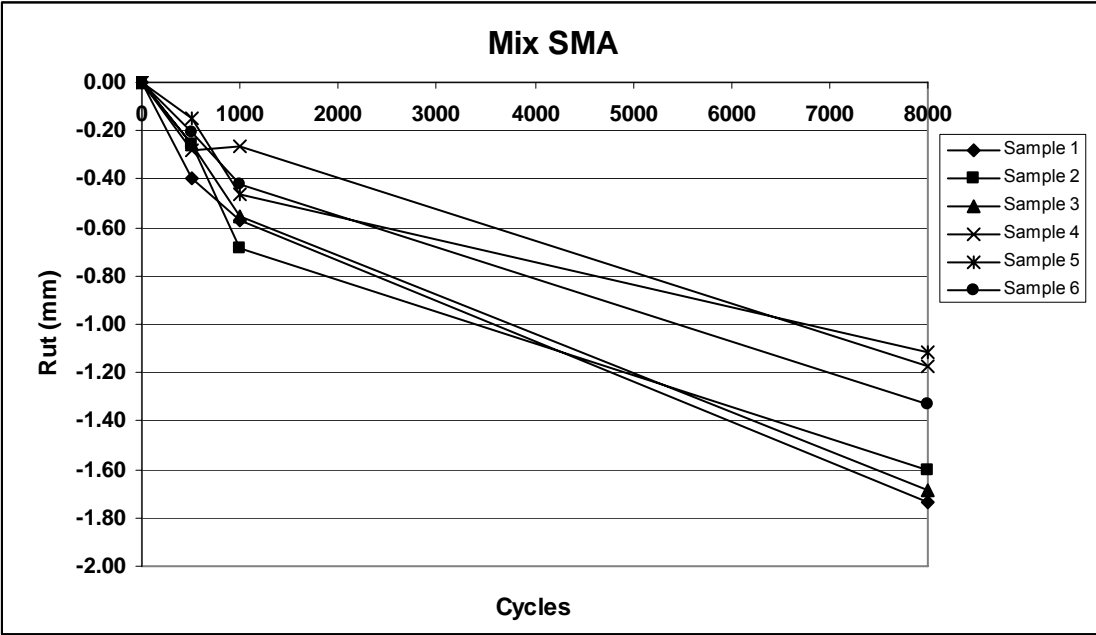


Figure 29. APA rut depth of Mix SMA. (25.4 mm=1.00 in.)

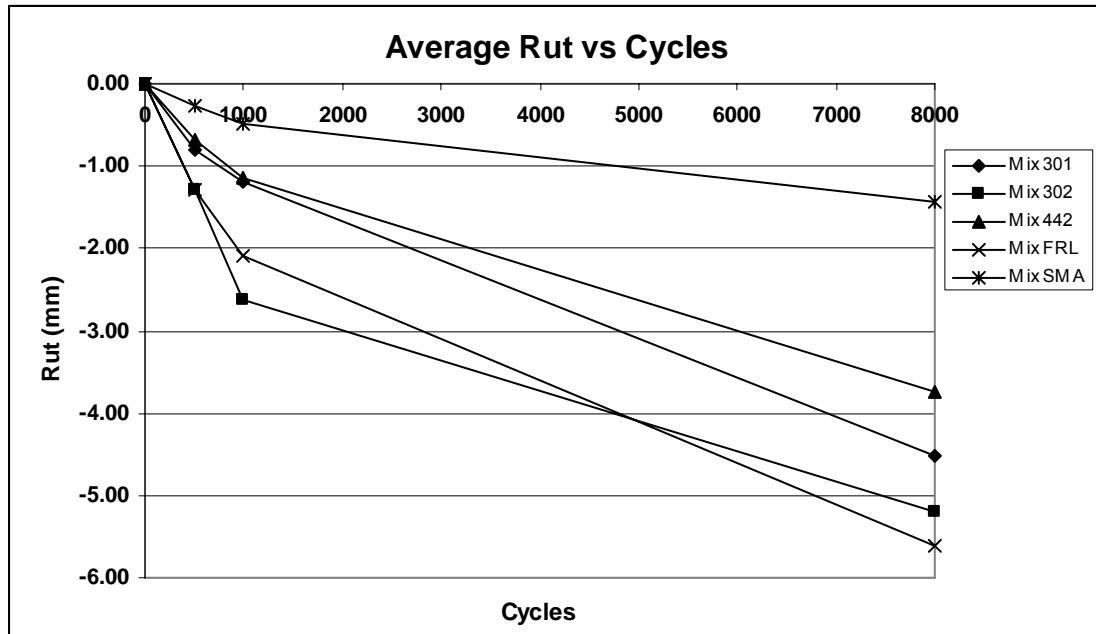


Figure 30. Average APA rut depth of asphalt mixes. (25.4 mm=1.00 in.)

Table 37. APA rut depth and air void content of asphalt mixes.

Mix	301			302			442			FRL			SMA		
	Air (%)	Rut (mil)	Rut (mm)	Air (%)	Rut (mil)	Rut (mm)	Air (%)	Rut (mil)	Rut (mm)	Air (%)	Rut (mil)	Rut (mm)	Air (%)	Rut (mil)	Rut (mm)
Specimen 1	7.4	209	5.3	7.6	205	5.2	7.4	209	5.3	7.0	252	6.4	6.7	47	1.2
Specimen 2	7.1	193	4.9	7.0	244	6.2	7.4	224	5.7	6.6	272	6.9	7.1	67	1.7
Specimen 3	7.1	161	4.1	7.1	201	5.1	7.2	130	3.3	7.1	213	5.4	7.3	43	1.1
Specimen 4	7.4	205	5.2	6.3	201	5.1	6.9	134	3.4	7.4	213	5.4	7.2	63	1.6
Specimen 5	7.0	138	3.5	7.3	165	4.2	6.9	75	1.9	6.4	173	4.4	6.7	51	1.3
Specimen 6	7.3	165	4.2	7.0	217	5.5	7.3	110	2.8	7.0	205	5.2	7.0	67	1.7
Average	7.2	177	4.5	7.1	205	5.2	7.2	146	3.7	6.9	220	5.6	7.0	55	1.4

7.6 Moisture Susceptibility

The moisture susceptibility was measured following AASHTO T283; which compares the indirect tensile strength of dry samples with that of a samples exposed to water saturation and a freezing cycle. Six cylindrical specimens for each mixture were used, each with 6.00 in (150 mm) diameter and 3.75 in (68 mm) height. Three specimens were saturated with water to between 70% and 80% (the test specifies between 55% and 80% saturation), then conditioned at 0 °F (-18 °C) for 15 hours followed by thawing for 24 hours in a water bath at 140 °F (60 °C). After the freeze-thaw conditioning cycle was complete, all specimens, including dry and conditioned, were placed in a water bath for 2 hours at 77 °F (25 °C). Finally, the indirect tensile strength was measured for all the specimens. The moisture susceptibility is given by the tensile strength ratio *TSR*:

$$TSR = \frac{S_2}{S_1}$$

Eq. 41

where S_1 = average dry sample tensile strength; and S_2 = average conditioned (frozen) sample tensile strength. TSR of 0.8 or larger is considered to be satisfactory. Table 38 presents the moisture susceptibility results as tensile strength ratios. Except SMA mix, TSR of all other asphalt mixes resulted in less than 0.80, indicating possible moisture damage potential. The high permeability of aggregate base would help to minimize the moisture damage potential.

Table 38. Indirect tensile strength ratio for each asphalt mix.

Specimen	Condition	Tensile Strength		Average		TSR	Air Void (%)	Degree of Sat. (%)
		psi	kPa	psi	kPa			
301-1	Dry	212.6	1465.9	214.3	1477.3	0.72	7.6	
301-2	Dry	211.9	1461.3				7.8	
301-3	Dry	218.3	1504.8				7.8	
301-4	Freeze	142.7	983.8	154.7	1066.9		7.9	75.6
301-5	Freeze	164.6	1134.8				7.6	74.0
301-6	Freeze	156.9	1082.0				7.6	70.6
302-1	Dry	167.2	1152.9	185.4	1278.5	0.68	8.9	
302-2	Dry	180.8	1246.4				8.8	
302-6	Dry	208.3	1436.3				8.5	
302-3	Freeze	136.8	943.4	125.8	867		8.8	73.6
302-4	Freeze	126.8	874.1				8.9	73.1
302-5	Freeze	113.7	783.6				8.5	71.1
442-1	Dry	135.3	933.0	97.4	671.9	0.77	6.6	
442-2	Dry	66.8	460.8				6.3	
442-4	Dry	90.2	621.8				6.6	
442-3	Freeze	38.6	266.0	74.6	514.5		6.5	70.6
442-5	Freeze	85.4	588.7				6.2	70.9
442-6	Freeze	99.9	688.8				6.3	72.2
FRL-1	Dry	240.2	1655.8	239.5	1650.9	0.73	6.9	
FRL-4	Dry	235.7	1625.0				6.9	
FRL-6	Dry	242.5	1672.0				6.9	
FRL-2	Freeze	172.3	1187.9	175.7	1211.3		7.3	70.2
FRL-3	Freeze	188.1	1296.9				6.4	78.5
FRL-5	Freeze	166.6	1149.0				6.6	71.6
SMA-1	Dry	190.4	1312.7	180.4	1243.6	0.80	7.6	
SMA-2	Dry	174.6	1203.7				8.5	
SMA-4	Dry	176.1	1214.5				7.8	
SMA-3	Freeze	158.9	1095.5	143.9	992.4		7.6	71.1
SMA-5	Freeze	133.0	917.2				8.0	72.6
SMA-6	Freeze	139.9	964.6				8.3	70.7

7.7 Indirect Tensile Creep and Strength at Low Temperature

To measure creep properties at low temperatures, a static load was applied to the diametral direction of the cylindrical specimen for 1000 seconds and the deformation was measured as a function of time. The indirect tensile creep test was performed at -4, 14, and 32°F (-20, -10, and 0 °C) following AASHTO T322. After the creep test, the indirect tensile strength (ITS) of each sample was determined at the respective test temperature by applying load to fracture. Table 39 presents the indirect tensile strength at three different temperatures for three specimens of each mixture. Figure 31 through Figure 35 show the creep compliance for each mixture and the data are tabulated in Appendix E.

Table 39. Indirect tensile strength of asphalt concretes at three temperatures.

ENGLISH UNITS								
Specimen	ITS (psi)		Specimen	ITS (psi)		Specimen	ITS (psi)	
-4 °F			14 °F			32 °F		
301-1	932.9	903.1	301-4	911.2	892.8	301-7	818.7	783.9
301-2	887.4		301-5	853.5		301-8	728.8	
301-3	889.0		301-6	913.7		301-9	804.3	
302-1	637.5	677.7	302-4	656.5	599.8	302-7	600.6	583.2
302-2	584.6		302-5	573.0		302-8	557.5	
302-3	811.0		302-6	569.8		302-9	591.5	
442-1	712.3	781.1	442-4	665.7	581.2	442-7	476.1	394.6
442-2	904.7		442-5	505.1		442-8	341.1	
442-3	726.4		442-6	572.7		442-9	366.7	
FRL-1	861.8	831.2	FRL-4	674.0	745.8	FRL-7	776.1	802.8
FRL-2	841.6		FRL-5	805.5		FRL-8	809.7	
FRL-3	790.1		FRL-6	757.9		FRL-9	822.4	
SMA-1	723.7	787.9	SMA-4	750.3	755.1	SMA-7	637.3	585.9
SMA-2	760.9		SMA-5	761.3		SMA-8	500.5	
SMA-3	879.1		SMA-6	753.8		SMA-9	620.1	
INTERNATIONAL UNITS								
Specimen	ITS (kPa)		Specimen	ITS (kPa)		Specimen	ITS (kPa)	
-20 °C			-10 °C			0 °C		
301-1	6432.1	6226.6	301-4	6282.7	6155.7	301-7	5644.7	5405.0
301-2	6118.4		301-5	5884.5		301-8	5025	
301-3	6129.4		301-6	6299.8		301-9	5545.3	
302-1	4395.2	4672.5	302-4	4526.4	4135.4	302-7	4141.2	4021.1
302-2	4030.6		302-5	3950.9		302-8	3844	
302-3	5591.8		302-6	3928.8		302-9	4078	
442-1	4911.2	5385.8	442-4	4589.9	4006.9	442-7	3282.5	2721.0
442-2	6237.5		442-5	3482.2		442-8	2352	
442-3	5008.6		442-6	3948.6		442-9	2528.4	
FRL-1	5942.2	5730.8	FRL-4	4646.9	5141.9	FRL-7	5351.3	5534.9
FRL-2	5802.7		FRL-5	5553.6		FRL-8	5582.9	
FRL-3	5447.4		FRL-6	5225.2		FRL-9	5670.5	
SMA-1	4989.7	5432.3	SMA-4	5172.9	5206.5	SMA-7	4393.7	4039.9
SMA-2	5246.2		SMA-5	5248.9		SMA-8	3450.9	
SMA-3	6061		SMA-6	5197.6		SMA-9	4275.2	

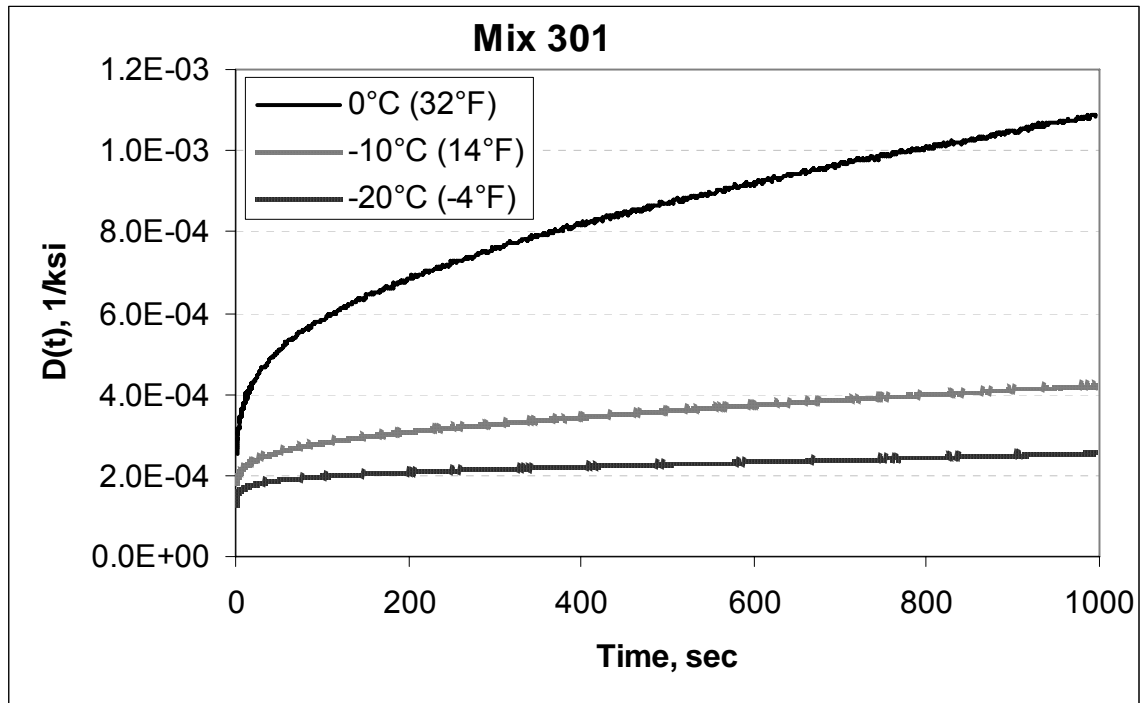


Figure 31. Creep compliance of Mix 301.

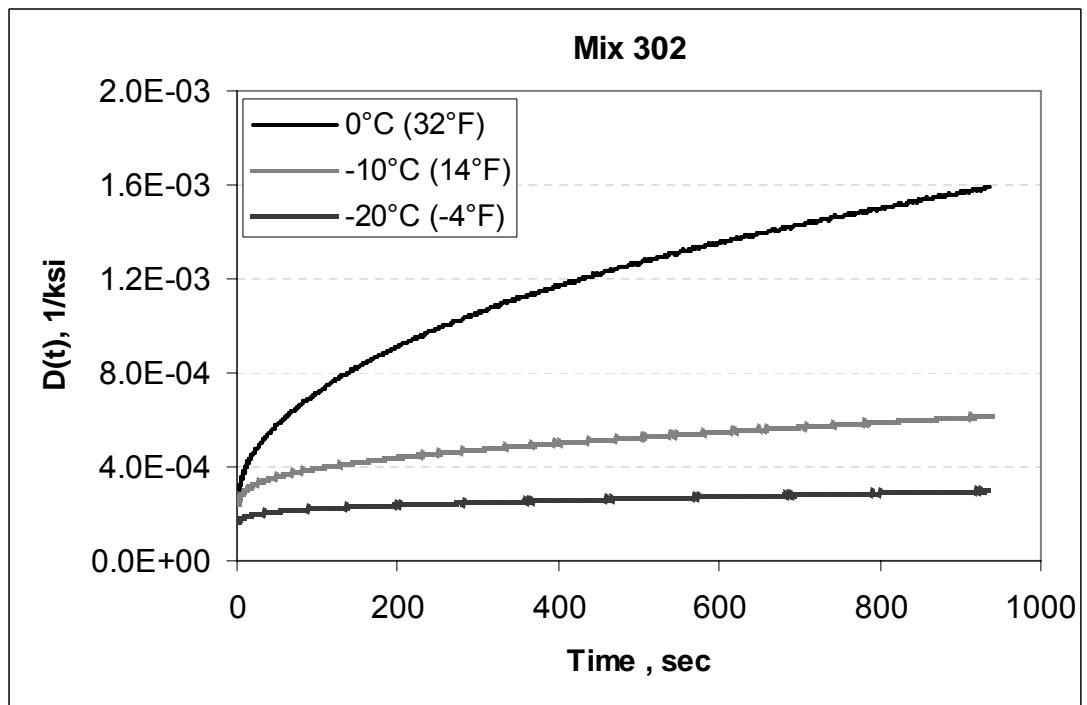


Figure 32. Creep compliance of Mix 302. (1 ksi = 6.89 MPa)

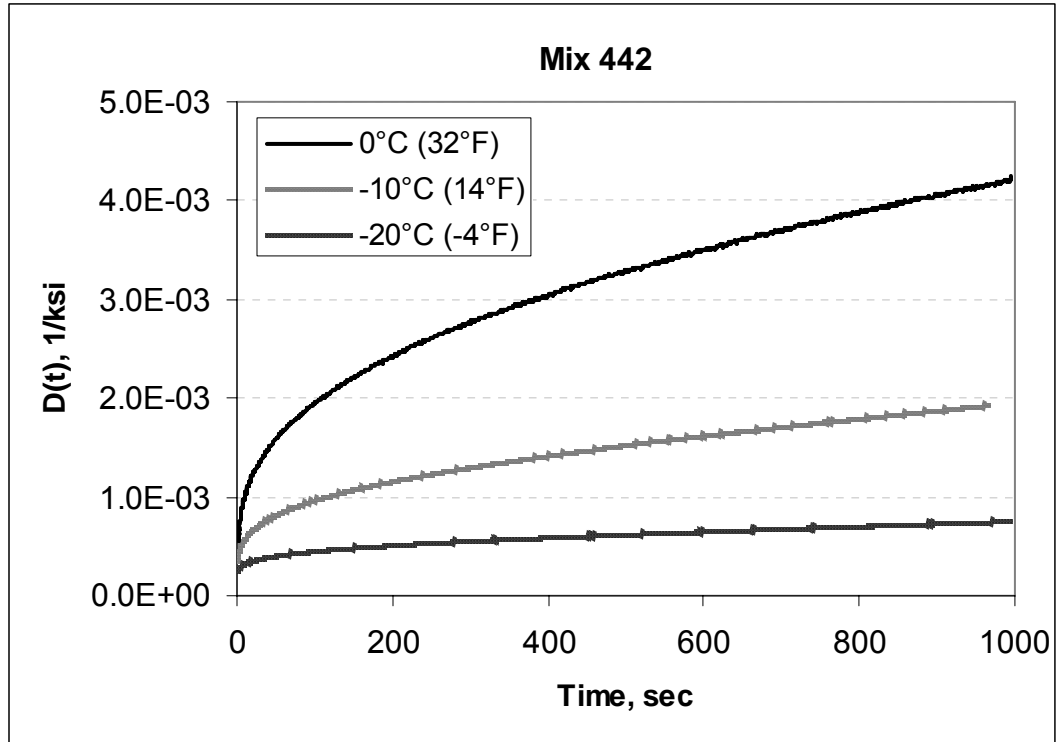


Figure 33. Creep compliance of Mix 442.

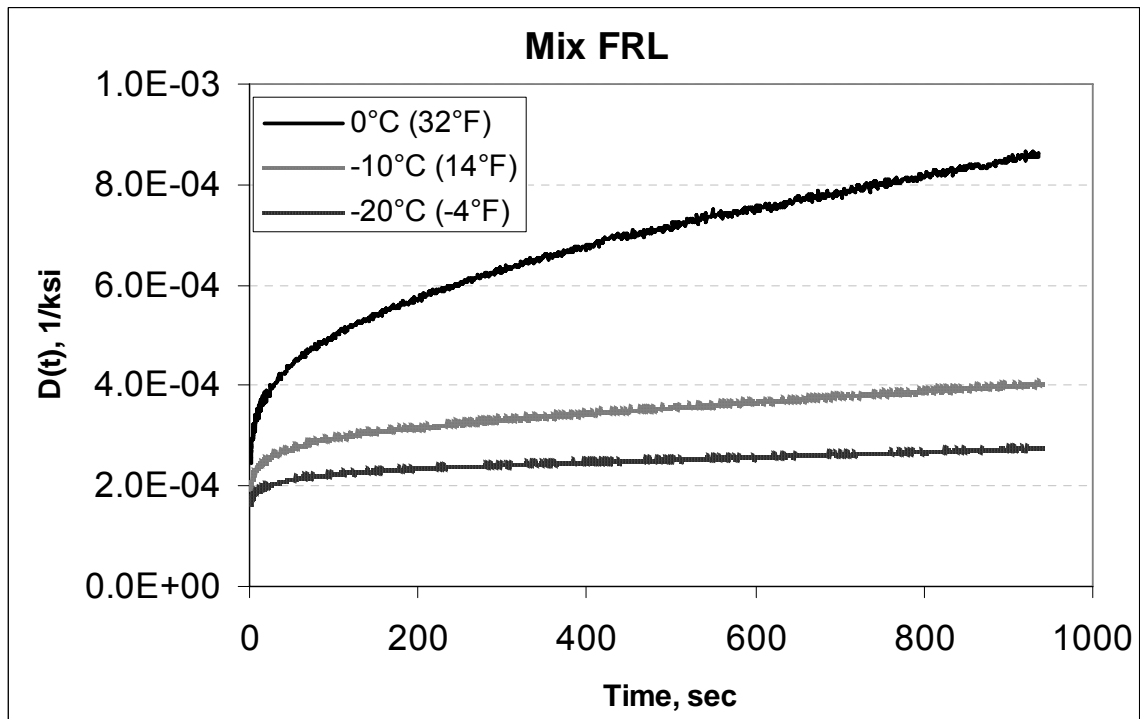


Figure 34. Creep compliance of Mix FRL. (1 ksi = 6.89 MPa)

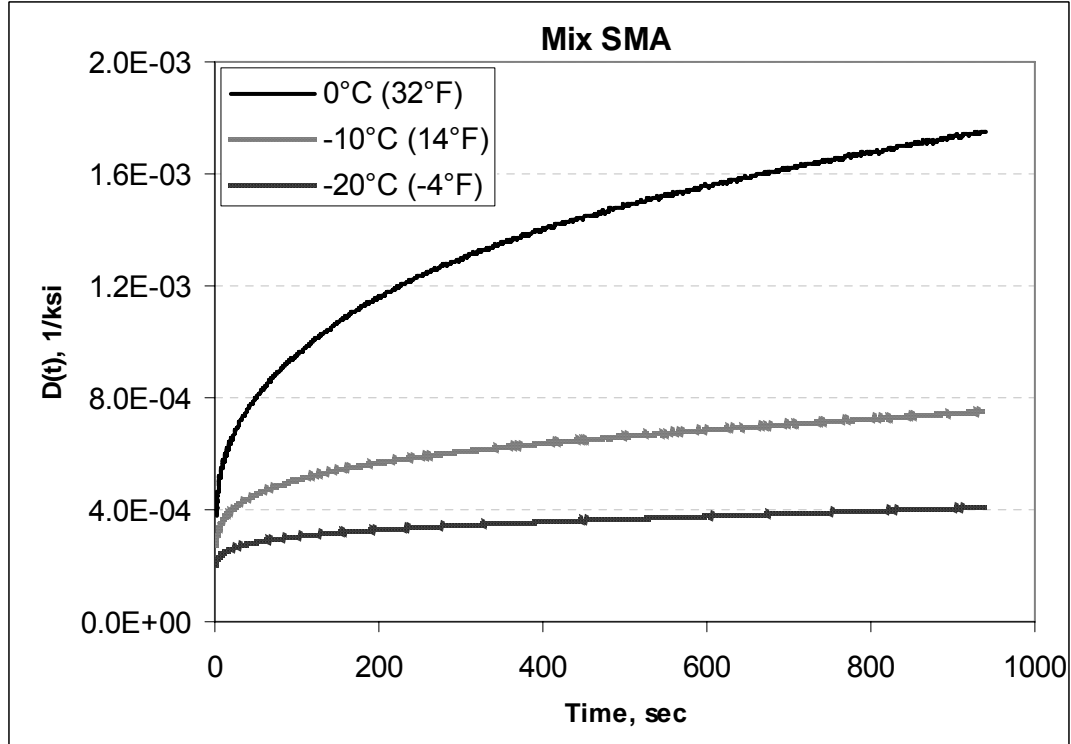


Figure 35. Creep compliance of Mix SMA. (1 ksi = 6.89 MPa)

7.8 Beam Fatigue

In the fatigue test, rectangular-shaped asphalt beams were subjected to third-point, controlled-strain flexure at 20°C (68°F) until failure occurred, following AASHTO T321. Failure is defined as the point when the flexural stiffness S reaches half of its initial value, and the output datum is the number of load cycles N to reach failure. If failure is not achieved after one million load cycles, the curve of S versus $\log N$ is extrapolated to estimate the number of cycles to failure, N_f . The peak-to-peak stress σ , peak-to-peak strain ε and flexural stiffness S are calculated as:

$$\sigma = \frac{3aP}{wh^2}, \quad \varepsilon = \frac{12h\delta}{3L^2 - 4a^2}, \quad \text{and} \quad S = \frac{\sigma}{\varepsilon} \quad \text{Eq. 42}$$

where P = applied peak-to-peak load, L = beam span length, w = beam width, h = beam height, δ = beam deflection at neutral axis, and $a = L/3$, the position of the third point. For each mix, four beam specimens were prepared from a roller-compacted slab. Table 40 presents the beam cross section dimensions for each specimen. The fatigue tests were performed in strain-controlled mode with the maximum flexural strain, ε , at the surface of the specimen to be 100 $\mu\varepsilon$, 200 $\mu\varepsilon$, 300 $\mu\varepsilon$, or 400 $\mu\varepsilon$ for each specimen. Figures 36 through 39 show the flexural stiffness as a function of the number of load cycles for the specimens of each mix.

The fatigue properties of asphalt materials are commonly characterized by the relationship between the number of cycles to failure, N_f , and the applied strain, ε , in the form of

$$N_f = k_1 \cdot (1/\epsilon)^{k_2}$$

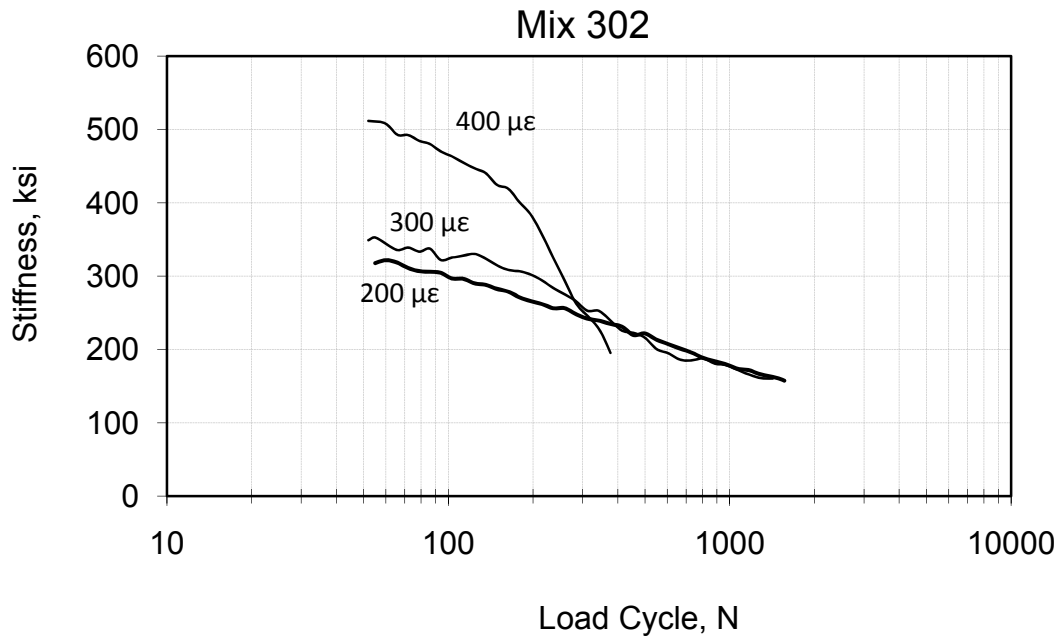
Eq. 43

where k_1 and k_2 = material constants.

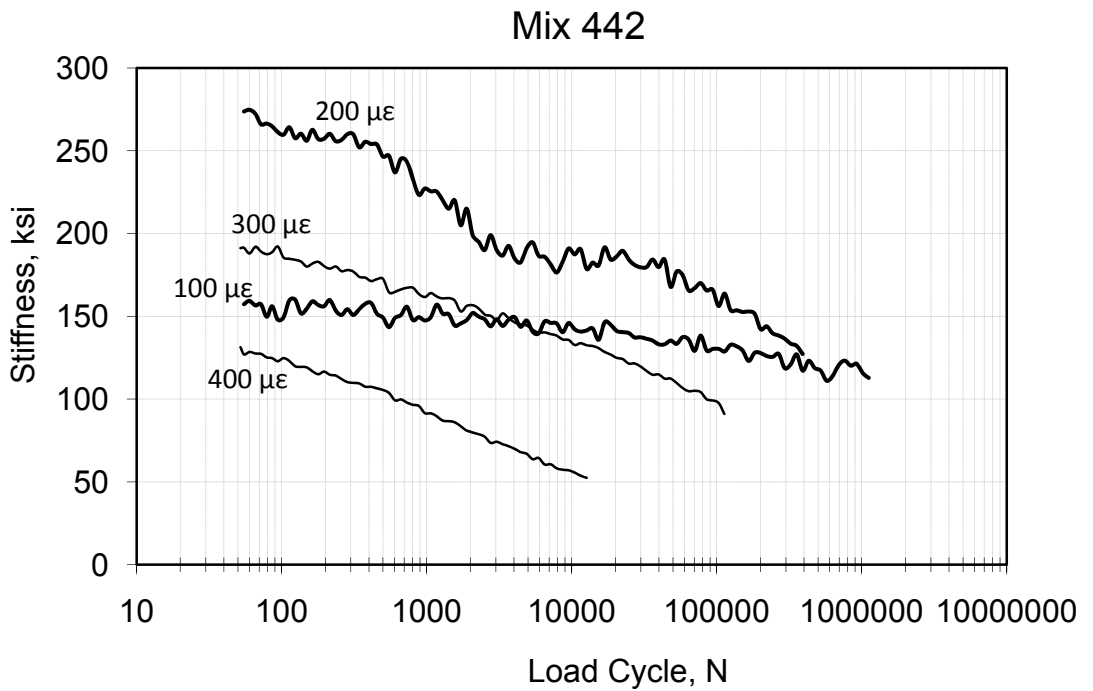
The flexural beam fatigue test results are summarized in Table 41 and Figure 40. During the fatigue test, it was observed that the number of cycles to failure (N_f) for FRL mix at 100 $\mu\epsilon$ was questionable. As reducing the level of flexural strain from 200 or 300 $\mu\epsilon$ to 100 $\mu\epsilon$, the number of cycles to failure would increase in orders of magnitude. However, for FRL mix at 100 $\mu\epsilon$ fatigue test, the number of cycles to failure was lower than those of both 200 $\mu\epsilon$ or 300 $\mu\epsilon$ tests. This data point was considered as an outlier and was not used in the further analysis of fatigue behavior. From the fatigue test results, material properties for fatigue model (Eq. 43), k_1 and k_2 , were determined and also presented in Table 41. For the 302 and FRL mixes, R^2 values are low because the maximum size of aggregate was too large relative to the dimensions of the sample used in the fatigue test, resulting in more scattering of data.

Table 40. Average height and width for asphalt beam specimens for fatigue test.

Specimen	Average height		Average width	
	in	mm	in	mm
F302-1	1.98	50.2	2.27	57.7
F302-2	1.91	48.6	2.33	59.3
F302-3	1.88	47.8	2.39	60.6
F442-1	1.89	48.0	2.30	58.5
F442-2	1.95	49.5	2.43	61.6
F442-3	1.87	47.6	2.25	57.2
F442-4	1.98	50.2	2.38	60.5
FFRL-1	1.93	49.0	2.31	58.8
FFRL-2	1.89	48.1	2.34	59.5
FFRL-3	1.96	49.8	2.42	61.5
FFRL-4	1.88	47.8	2.27	57.7
FSMA-1	2.06	52.4	2.47	62.7
FSMA-2	2.03	51.6	2.38	60.5
FSMA-3	1.92	48.8	2.29	58.1
FSMA-4	2.05	52.0	2.29	58.1



**Figure 36. Flexural stiffness versus number of cycles N for 302 mix.
(1 ksi=6.89 MPa)**



**Figure 37. Flexural stiffness versus number of cycles N for 442 Mix.
(1 ksi=6.89 MPa)**

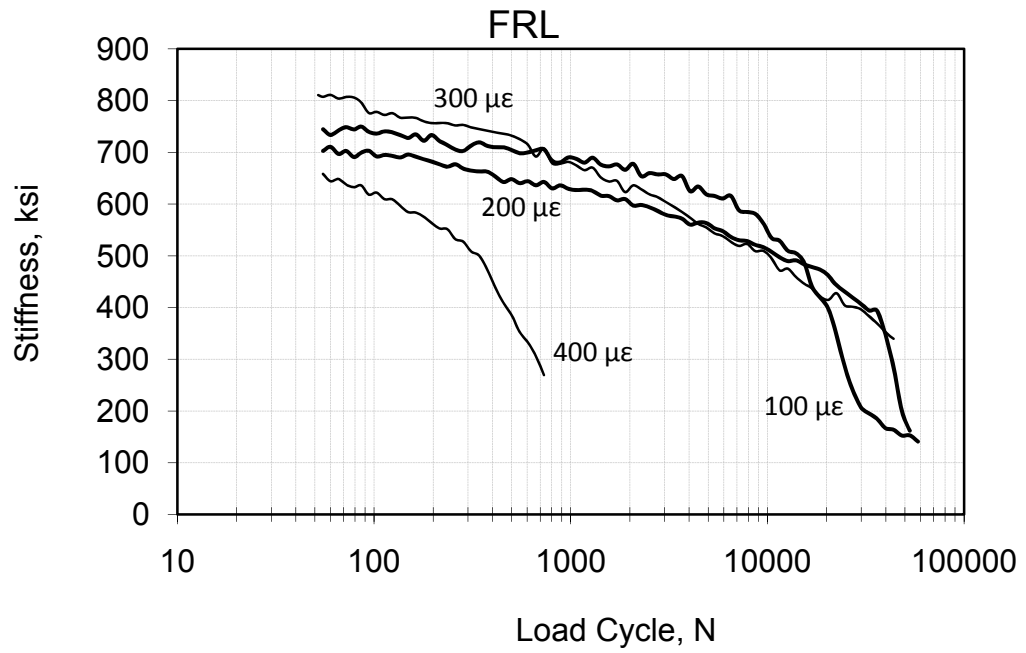


Figure 38. Flexural stiffness versus number of cycles N for FRL mix. (1 ksi=6.89 MPa)

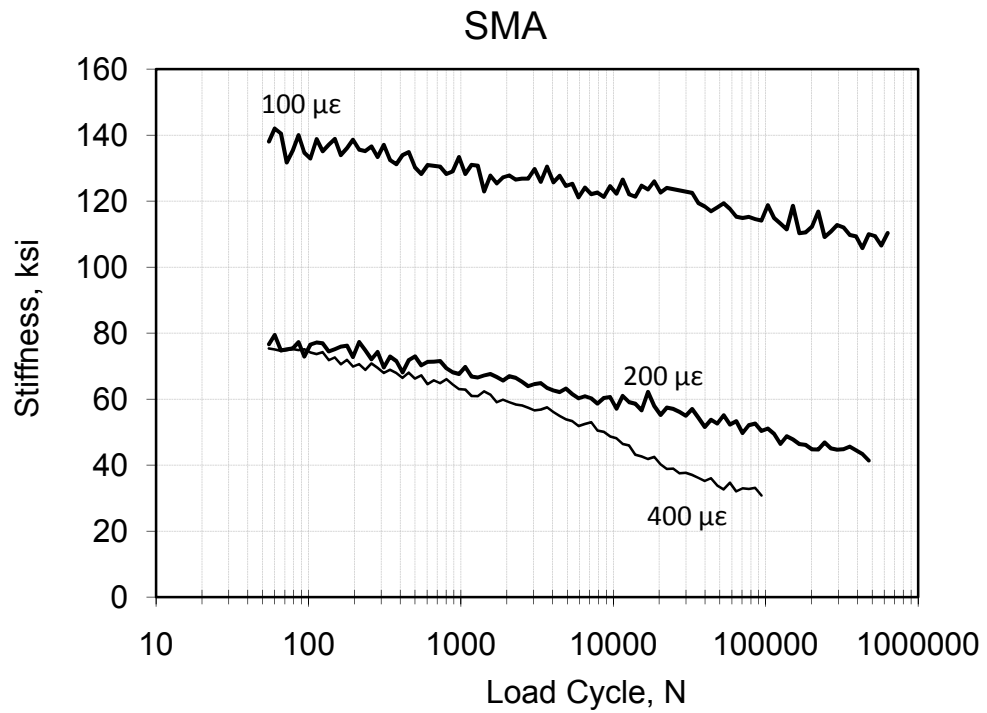


Figure 39. Flexural stiffness versus number of cycles N for SMA mix. (1 ksi = 6.89 MPa)

Table 41. Fatigue test results summary with number of cycles to failure at each strain level and fatigue parameters derived from curve fits.

Applied strain (ϵ)	($\mu\epsilon$)	Number of Cycles to failure (N_f)				Fatigue Parameters		
		400	300	200	100	k_1	k_2	R^2
Mix	SMA	31,000	- ^a	1,470,000	2.39×10^9	$2.28E+25$	8.117	0.968
	442	5,140	102,800	294,000	57.6×10^6	$2.67E+20$	6.371	0.971
	302	295	1,000	1,500	- ^a	$2.73E+08$	2.258	0.863
	FRL	650	24,000	38,000	$22,000^b$	$3.97 E+17$	5.559	0.755

^a Specimen was broken during handling. No data were recovered.

^b Considered as outlier. Not included in analysis.

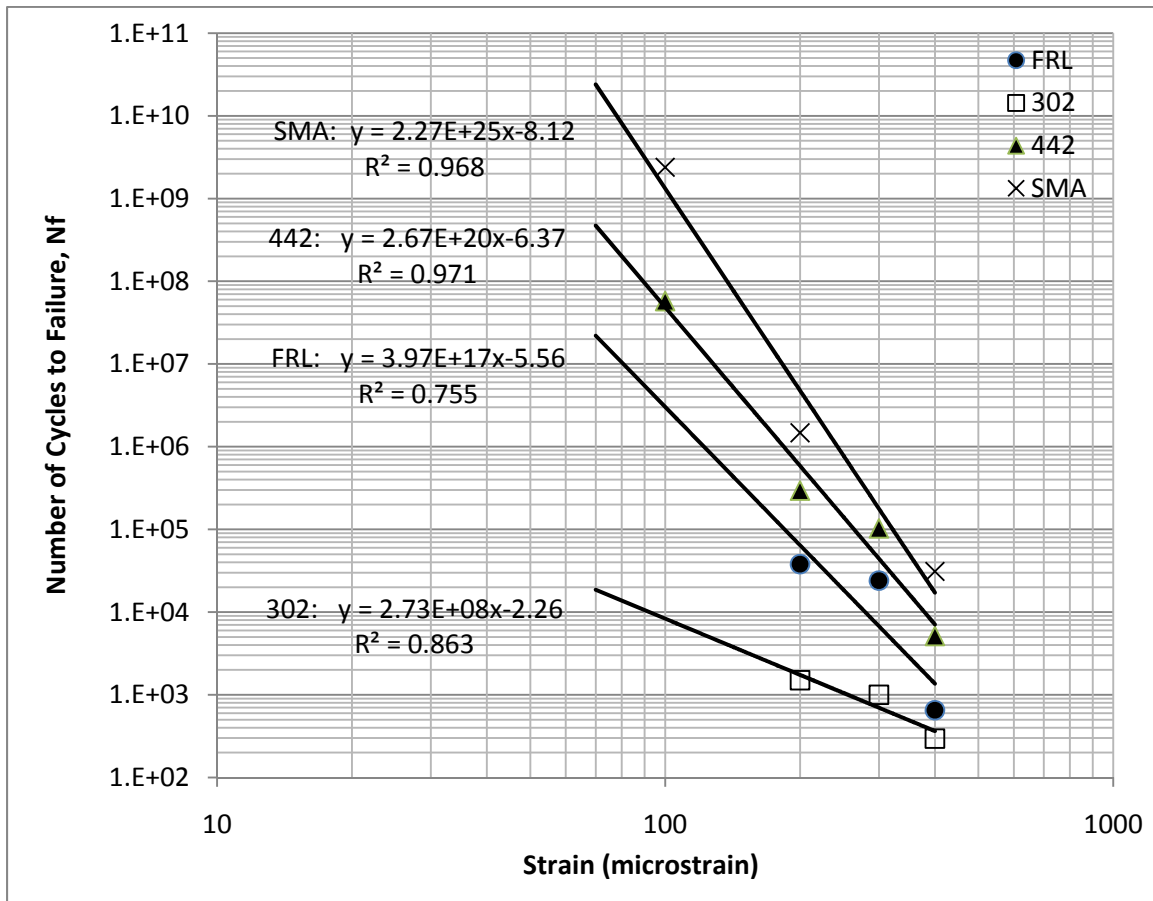


Figure 40. Summary of 4-point beam fatigue test results.

As shown in Table 41 and Figure 40, SMA mix and 442 mix showed the best fatigue performance, probably due to the polymer modification. Mix 302 showed the worst fatigue cracking resistance, showing the estimated number of cycles to failure at 70 $\mu\epsilon$ about 20,000 cycles. However, the additional asphalt binder content introduced into the 302 mix to make the asphalt-rich FRL mix improved the fatigue cracking resistance significantly. For FRL mix at 70 $\mu\epsilon$ fatigue strain, the estimated number of cycles to failure is over 20×10^6 cycles and the initiation of the bottom-up fatigue crack at the FRL seems very unlikely.

7.9 Thermal Stress Restrained Specimen Test (TSRST)

The TSRST system developed by Jung and Vinson in SHRP Report A-400 [Jung and Vinson, 1994] is an automated closed loop system which measures the thermal tensile stress in an asphalt mixture specimen as it is cooled at constant rate. As the temperature drops, the specimen is restrained from contracting thus inducing tensile stresses. The load and temperature are monitored and collected during the test using a load cell and four thermistors, respectively. The TSRST system consists of a chamber, load frame, computer, data acquisition system, temperature controller, two LVDT's, four thermistors, load cell and nitrogen cylinder. Figure 41 shows TSRST system and typical specimen after failure. The cooling rate used for all tests was 18°F/hr (10C°/hr). This test was performed at the University of Minnesota following AASHTO TP10-93.



Figure 41. Left: TSRST sample after failure; Right: TSRST System

The test procedure according to Jung and Vinson [1994] is as follows:

- Clean the platens with degreasing agent to remove previous material and use sand paper to make sure the surface is rough and clean to glue specimens.
- Attach the end platens to the specimen alignment stand and place the specimen between the platens with epoxy making sure the specimen is well aligned. Misalignment of the specimen will produce bending stresses during testing.
- Leave the specimen in the stand until the epoxy is cured.
- Remove the specimen with the end platens from the stand and store it at 5°C (41°F) for one hour for precooling if air is circulated or for 6 hours if no air circulation is used.
- Connect the specimen-platen system to the TSRST machine. Attach the two LVDTs.
- Attach the four thermistors using modeling clay in different locations of the specimen. Close the chamber.
- Set the cooling rate (e.g. 10C°/hr (18°F/hr)) with the temperature controller and apply an initial tension load before starting the test.
- Initialize the computer program with the correct position of the specimen. Start program to run test sequence and record the surface temperature and load until the specimen fails.

Figures 42 through 45 show the results from TSRST testing of the four replicates of the four asphalt mixes. For the 442 and FRL mixes in Figure 43 and Figure 44, it was

observed that as the temperature inside the chamber was dropped at a constant rate, the thermally induced tensile stresses increased until fracture occurred. On the other hand, for the 302 and SMA mixes in Figure 42 and Figure 45 a more ductile behavior was observed, where a constant low thermal stress was reached and maintained until specimen failed. Table 42 summarizes the fracture strength and fracture temperature for all TSRST specimens tested. Photographs of the specimens after TSRST testing are presented in Figures 46 through 49.

For WAY-30 project site, the expected low pavement surface temperature is 3.7°F (-15.7°C) based on LTPPBind version 2.1 (Wooster weather station). This temperature is much warmer than the TSRST low temperature cracking temperatures of the top three layers (SMA, 442 and 302 mix), indicating no possibility of the low temperature thermal cracking problem. The average TSRST cracking temperature of FRL mixes is warmer than the expected surface pavement temperature. However, the fatigue resistant layer was placed more than 12 in. (305 mm) below the surface. The expected pavement temperature at FRL would be significantly warmer (16.3°F (-8.7°C) based on LTPPBind) and the low temperature thermal cracking would not occur.

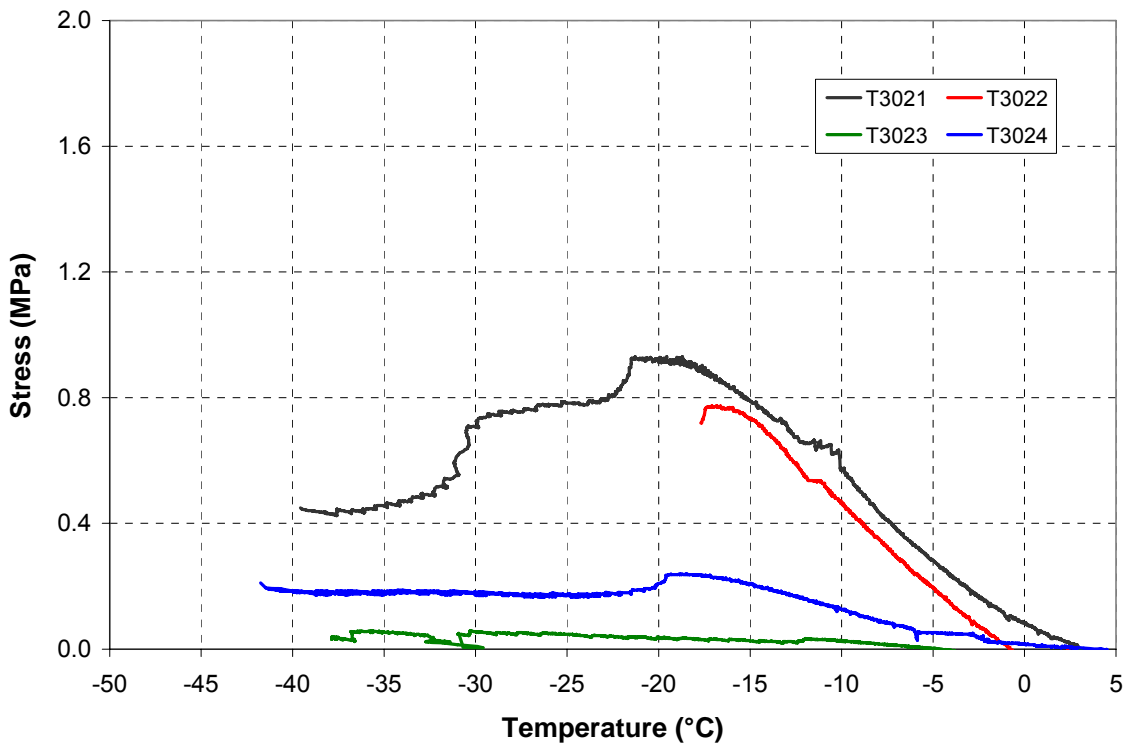


Figure 42. Item 302 mixture TSRST results. (1 MPa = 0.145 ksi)

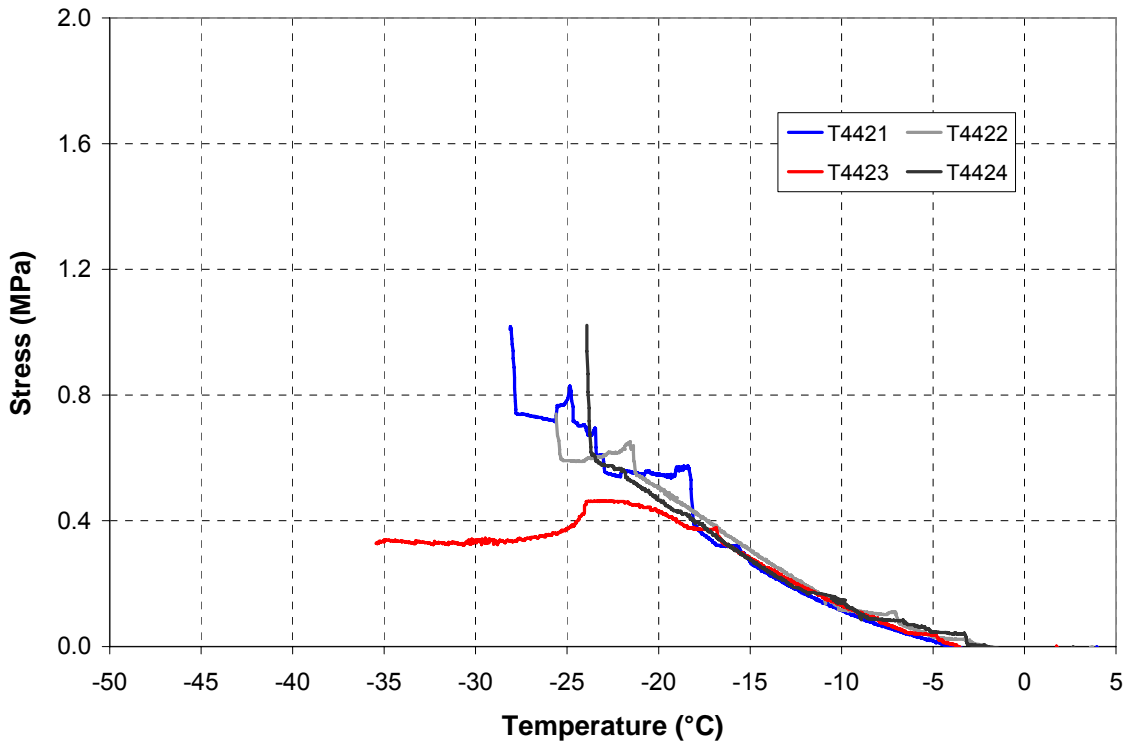


Figure 43. Item 442 mixture TSRST results.

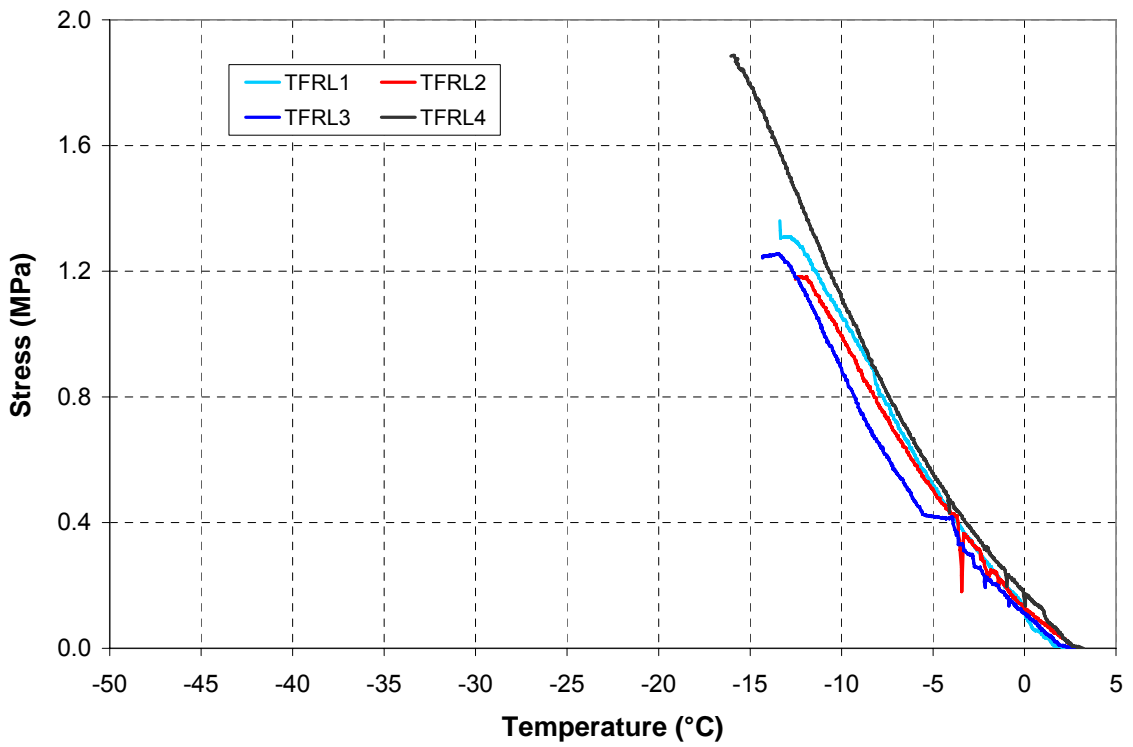


Figure 44. FRL mixture TSRST results. (1 MPa = 0.145 ksi)

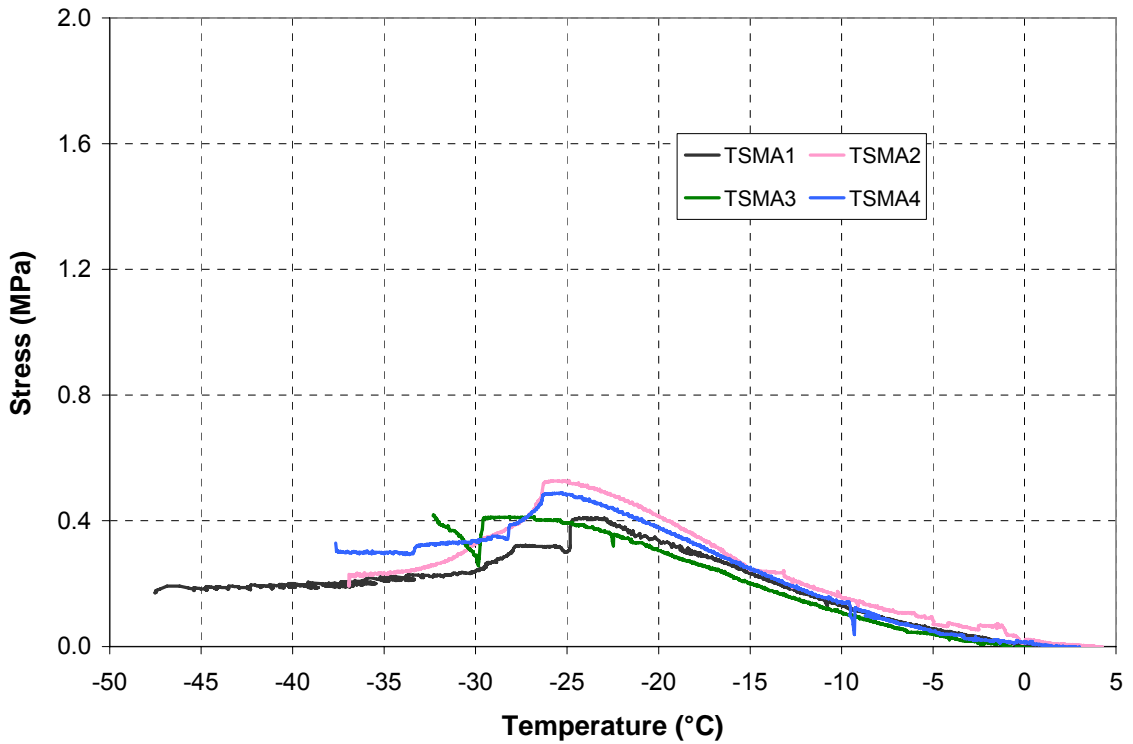
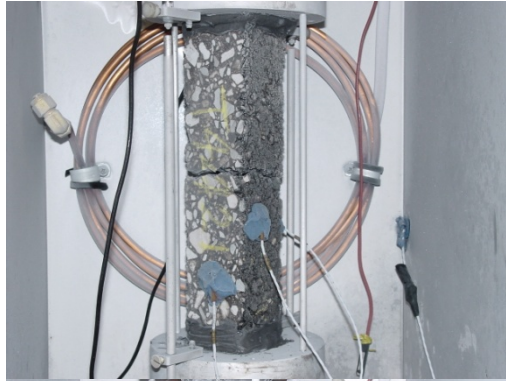


Figure 45. SMA mixture TSRST results (1 MPa = 0.145 ksi)

Table 42. TSRST fracture temperature and fracture strength of asphalt mixes.

Mix	Specimen ID	Fracture Temperature		Average Fracture Temperature		Fracture Strength		Average Fracture Strength	
		(°F)	(°C)	(°F)	(°C)	(ksi)	(MPa)	(ksi)	(MPa)
302	T3021	-39.2	-39.6	-29.6	-34.2	0.135	0.93	0.072	0.50
	T3022	0.1	-17.7			0.112	0.77		
	T3023	-36.2	-37.9			0.008	0.06		
	T3024	-43.2	-41.8			0.035	0.24		
442	T4421	-18.6	-28.1	-18.9	-28.3	0.148	1.02	0.118	0.81
	T4422	-14.1	-25.6			0.107	0.74		
	T4423	-31.8	-35.5			0.067	0.46		
	T4424	-11.1	-23.9			0.148	1.02		
FRL	TFRL1	7.9	-13.4	6.7	-14.1	0.197	1.36	0.206	1.42
	TFRL2	9.7	-12.5			0.171	1.18		
	TFRL3	6.2	-14.3			0.182	1.26		
	TFRL4	3.1	-16.1			0.274	1.89		
SMA	TSMA1	-53.6	-47.5	-37.5	-38.6	0.059	0.41	0.067	0.46
	TSMA2	-34.5	-36.9			0.076	0.53		
	TSMA3	-26.2	-32.3			0.061	0.42		
	TSMA4	-35.8	-37.6			0.071	0.49		

T4421



T4422



T4423



T4424



Figure 46. Failed 442 mix specimens after TSRST.

T3021



T3022



T3024



Figure 47. Failed 302 mix specimens after TSRST.

TFRL1



TFRL2



TFRL3



TFRL4



Figure 48. Failed FRL mix specimens after TSRST.

TSMA1



TSMA2



TSMA3



TSMA4



Figure 49. Failed SMA mix specimens after TSRST.

7.10 Dynamic Modulus

Asphalt mixture is a viscoelastic material and its mechanical properties including dynamic modulus (E^*) are time-dependent and temperature-dependent. The dynamic modulus master curve describes the time (or frequency) dependence of the asphalt concrete over wide range of time (or frequency), and the shift factor obtained in the process of the master curve determination describes the temperature dependency of asphalt concrete.

Dynamic modulus tests were performed following procedure developed in NCHRP Project 9-29 [Bonaquist et al., 2003]. Specimens were prepared as follows: the loose plant mixes were compacted to 150 mm (5.91 in.) diameter and 165 mm (6.5 in.) height using a gyratory compactor. From these specimens, 100 mm (3.94 in.) diameter test specimens were cored and about 6.35 mm (0.25 in.) of both ends were cut off using a diamond saw, yielding a thickness of 150mm (5.91 in.). Four replicate tests were performed for each asphalt mix. Each test specimen was tested at -10°C (14°F), 4.4°C (40°F), 21.1°C (70°F), 37.8°C (100°F) and 54.4°C (130°F), in that order. At each test temperature, dynamic modulus was determined at 25Hz, 10Hz, 5Hz, 1Hz, 0.5Hz, and 0.1Hz, in that order. For each test temperature and each frequency, dynamic modulus was determined as follows;

$$|E^*(T,f)| = \sigma_o / \varepsilon_o \quad \text{Eq. 44}$$

σ_o = maximum stress

ε_o = maximum strain

Phase angle was also determined from the difference between times when the maximum stress and strain occurred.

$$\varphi = 360 * (t_{\sigma_o} - t_{\varepsilon_o}) / \text{period} \quad \text{Eq. 45}$$

φ = phase angle in degree

t_{σ_o} = time the maximum stress occurred

t_{ε_o} = time the maximum strain occurred

Tables 43-47 show dynamic moduli and phase angles of 5 compacted asphalt mixes at 5 temperatures and 6 frequencies.

Dynamic moduli determined at various temperatures were then plotted against frequency using a log-log scale. Data for each temperature were parallel-shifted to a reference temperature (21.1°C (70°F) in this study) to form a single continuous curve (master curve) in the plot using following equation

$$f_r = f/a(T) \quad \text{Eq. 46}$$

f_r = reduced frequency at the reference temperature

f = actual frequency at the test temperature

$a(T)$ = shift factor

Table 43. Dynamic modulus and phase angle of Mix 301 at 5 test temperatures and 6 frequencies.

Temp	Freq (Hz)	Dynamic Modulus				Phase Angle	
		SI Unit		English Unit		Avg (degree)	StDev (degree)
		Avg (MPa)	StDev (MPa)	Avg (ksi)	StDev (ksi)		
-10 °C (14°F)	25.0	28987	4294	4204	623	4.6	3.9
	10.0	28623	3436	4151	498	2.8	4.3
	5.0	28057	3335	4069	484	3.4	0.6
	1.0	26563	3128	3853	454	3.6	1.0
	0.5	25826	3094	3746	449	3.9	1.3
	0.1	24155	2801	3503	406	3.9	0.9
4.4°C (40°F)	25.0	20820	3804	3020	552	4.6	3.4
	10.0	21320	2521	3092	366	6.4	1.4
	5.0	20486	2498	2971	362	5.4	0.9
	1.0	18491	2191	2682	318	6.2	0.6
	0.5	17614	2081	2555	302	6.6	0.7
	0.1	15504	2004	2249	291	9.6	0.8
21.1°C (70°F)	25.0	14207	2486	2061	361	11.1	8.9
	10.0	12907	1865	1872	270	9.3	3.4
	5.0	12061	1585	1749	230	11.9	1.0
	1.0	9582	1633	1390	237	14.6	1.8
	0.5	8675	1360	1258	197	17.6	3.2
	0.1	6491	1196	941	173	22.7	3.7
37.8°C (100°F)	25.0	8391	918	1217	133	15	8.4
	10.0	6484	948	940	137	20.8	6.5
	5.0	5515	834	800	121	21.8	3.6
	1.0	3581	680	519	99	26.7	2.5
	0.5	2899	615	420	89	30.8	2.8
	0.1	1796	445	260	65	30.8	2.3
54.4°C (130°F)	25.0	3367	835	488	121	19.5	5.8
	10.0	2358	594	342	86	27.2	3.3
	5.0	1717	497	249	72	30.7	2.3
	1.0	848	315	123	46	35.6	4.2
	0.5	616	253	89	37	40.3	4.7
	0.1	323	151	47	22	40.7	2.3

Table 44. Dynamic modulus and phase angle of Mix 302 at 5 test temperatures and 6 frequencies.

Temp	Freq (Hz)	Dynamic Modulus				Phase Angle	
		SI Unit		English Unit		Avg (degree)	StDev (degree)
		Avg (MPa)	StDev (MPa)	Avg (ksi)	StDev (ksi)		
-10 °C (14°F)	25.0	25377	2748	3681	399	2.3	3.9
	10.0	27284	3208	3957	465	2.7	0.8
	5.0	26817	3149	3889	457	3.0	0.3
	1.0	25050	3182	3633	462	3.8	0.5
	0.5	24353	3186	3532	462	4.4	0.9
	0.1	22599	3408	3278	494	5.3	1.6
4.4°C (40°F)	25.0	23070	3684	3346	534	4.0	2.3
	10.0	22121	3426	3208	497	5.5	1.4
	5.0	22258	3789	3228	550	6.7	1.1
	1.0	19847	3519	2879	510	6.8	1.3
	0.5	18953	3563	2749	517	7.4	1.4
	0.1	16390	3194	2377	463	10.3	2.8
21.1°C (70°F)	25.0	15087	2390	2188	347	13.1	1.8
	10.0	13629	2051	1977	297	12.1	2.5
	5.0	12485	1906	1811	276	13.9	3.3
	1.0	9645	2008	1399	291	16.6	3.1
	0.5	8506	1867	1234	271	20.1	3.9
	0.1	6219	1700	902	247	27.8	5.0
37.8°C (100°F)	25.0	7019	4090	1018	593	13.9	5.1
	10.0	6763	1893	981	275	24.3	3.9
	5.0	5610	1600	814	232	21.5	2.7
	1.0	3430	1267	497	184	27.8	2.9
	0.5	2680	1127	389	163	32.0	4.6
	0.1	1578	772	229	112	31.5	2.3
54.4°C (130°F)	25.0	2982	993	433	144	17.7	6.8
	10.0	1907	706	277	102	29.2	3.4
	5.0	1329	542	193	79	31.8	1.5
	1.0	623	302	90	44	37.2	3.5
	0.5	443	242	64	35	40.2	4.2
	0.1	221	139	32	20	35.3	5.6

Table 45. Dynamic modulus and phase angle of Mix FRL at 5 test temperatures and 6 frequencies.

Temp	Freq (Hz)	Dynamic Modulus				Phase Angle	
		SI Unit		English Unit		Avg (degree)	StDev (degree)
		Avg (MPa)	StDev (MPa)	Avg (ksi)	StDev (ksi)		
-10 °C (14°F)	25.0	32487	4459	4712	647	1.4	3.7
	10.0	33489	3130	4857	454	1.9	0.6
	5.0	32986	3119	4784	452	3.1	0.4
	1.0	31472	2905	4565	421	3.4	1.4
	0.5	30761	2978	4462	432	4.0	0.6
	0.1	28870	2622	4187	380	4.1	1.3
4.4°C (40°F)	25.0	27608	1883	4004	273	3.1	2.2
	10.0	26556	1750	3852	254	4.4	1.2
	5.0	25711	1611	3729	234	5.2	0.9
	1.0	23324	1479	3383	215	6.3	1.4
	0.5	22223	1356	3223	197	6.8	1.2
	0.1	19340	1113	2805	161	9.3	0.8
21.1°C (70°F)	25.0	19228	1466	2789	213	13.0	5.4
	10.0	17206	1090	2496	158	6.3	9.8
	5.0	15792	937	2290	136	12.7	1.2
	1.0	12515	727	1815	105	16.0	0.8
	0.5	11148	673	1617	98	19.0	0.7
	0.1	8046	505	1167	73	25.7	1.9
37.8°C (100°F)	25.0	9535	324	1383	47	15.7	3.3
	10.0	7550	149	1095	22	21.4	2.9
	5.0	6304	131	914	19	21.9	0.9
	1.0	3775	113	548	16	29.4	1.4
	0.5	2899	124	420	18	33.6	2.0
	0.1	1589	122	230	18	32.3	0.9
54.4°C (130°F)	25.0	3480	305	505	44	19.0	1.8
	10.0	2112	194	306	28	28.4	1.7
	5.0	1422	155	206	22	33.9	1.2
	1.0	576	59	84	9	45.2	2.1
	0.5	365	35	53	5	47.3	4.8
	0.1	156	16	23	2	39.4	3.6

Table 46. Dynamic modulus and phase angle of Mix 442 at 5 test temperatures and 6 frequencies.

Temp	Freq (Hz)	Dynamic Modulus				Phase Angle	
		SI Unit		English Unit		Avg (degree)	StDev (degree)
		Avg (MPa)	StDev (MPa)	Avg (ksi)	StDev (ksi)		
-10 °C (14°F)	25.0	17561	5882	2547	853	7.1	1.1
	10.0	17829	6737	2586	977	6.4	3.6
	5.0	17089	6752	2479	979	8.4	4.3
	1.0	15156	6610	2198	959	9.0	5.4
	0.5	14379	6487	2085	941	10.0	5.3
	0.1	12472	6013	1809	872	12.9	6.6
4.4°C (40°F)	25.0	12112	4825	1757	700	7.4	2.5
	10.0	11453	5097	1661	739	9.5	3.1
	5.0	10717	4925	1554	714	12.6	3.7
	1.0	8750	4316	1269	626	14.2	3.9
	0.5	7960	3992	1155	579	16.2	3.1
	0.1	6229	3093	903	449	20.5	3.1
21.1°C (70°F)	25.0	6862	3089	995	448	15.0	1.6
	10.0	5786	2402	839	348	16.0	1.4
	5.0	5085	2189	738	317	16.6	1.3
	1.0	3431	1690	498	245	20.5	1.6
	0.5	2920	1502	424	218	22.8	1.9
	0.1	1958	1037	284	150	23.5	3.0
37.8°C (100°F)	25.0	3298	1480	478	215	15.7	2.6
	10.0	2537	978	368	142	18.7	3.6
	5.0	2068	763	300	111	20.0	3.4
	1.0	1139	536	165	78	24.2	3.0
	0.5	878	439	127	64	26.7	3.4
	0.1	543	306	79	44	26.2	2.8
54.4°C (130°F)	25.0	1171	427	170	62	17.4	4.3
	10.0	797	263	116	38	21.9	3.2
	5.0	529	198	77	29	26.6	2.0
	1.0	222	101	32	15	27.6	0.9
	0.5	162	72	23	10	30.2	1.6
	0.1	97	44	14	6	31.6	2.5

Table 47. Dynamic modulus and phase angle of Mix SMA at 5 test temperatures and 6 frequencies.

Temp	Freq (Hz)	Dynamic Modulus				Phase Angle	
		SI Unit		English Unit		Avg (degree)	StDev (degree)
		Avg (MPa)	StDev (MPa)	Avg (ksi)	StDev (ksi)		
-10 °C (14°F)	25.0	21371	3792	3100	550	3.0	1.1
	10.0	21764	3469	3157	503	4.0	0.6
	5.0	21261	3267	3084	474	4.2	0.5
	1.0	19768	3092	2867	448	4.7	0.7
	0.5	19080	2983	2767	433	5.7	0.6
	0.1	17484	2685	2536	389	6.5	1.4
4.4°C (40°F)	25.0	16973	2853	2462	414	4.2	1.3
	10.0	15922	2806	2309	407	6.0	0.7
	5.0	15268	2738	2214	397	7.5	0.4
	1.0	13356	2371	1937	344	8.1	0.3
	0.5	12547	2263	1820	328	8.2	0.7
	0.1	10595	1847	1537	268	12.4	0.6
21.1°C (70°F)	25.0	9482	2148	1375	312	9.7	0.8
	10.0	8462	2050	1227	297	13.3	4.2
	5.0	7451	1714	1081	249	13.4	1.3
	1.0	5676	1480	823	215	17.1	0.8
	0.5	4998	1285	725	186	18.7	1.9
	0.1	3636	1003	527	145	21.8	1.4
37.8°C (100°F)	25.0	5053	786	733	114	17.3	4.5
	10.0	4237	832	615	121	19.3	2.4
	5.0	3506	758	509	110	20.2	2.5
	1.0	2103	496	305	72	24.0	1.0
	0.5	1662	395	241	57	27.6	1.3
	0.1	1078	248	156	36	26.9	0.9
54.4°C (130°F)	25.0	2050	403	297	58	19.5	2.8
	10.0	1492	275	216	40	21.9	1.7
	5.0	1043	217	151	31	27.4	1.9
	1.0	520	129	75	19	29.0	2.1
	0.5	397	104	58	15	30.6	2.1
	0.1	248	68	36	10	32.5	1.6

By plotting $\log a(T)$ versus temperature and finding a best fit 2nd order polynomial, the shift factor function for each asphalt concrete was determined.

The recently proposed AASHTO Mechanistic Empirical Pavement Design Guide [ARA, 2004] uses the Sigmoidal model for dynamic modulus of asphalt concrete as shown below.

$$\log(E^*) = \delta + \frac{\alpha}{1 + e^{\beta + \gamma(\log t_r)}} \quad \text{Eq. 47}$$

where

E^* = dynamic modulus

t_r = reduced time of loading at the reference temperature

$\alpha, \delta, \beta, \gamma$ = fitting parameters; δ represents the minimum value of E^* and $\delta + \alpha$ represents the maximum value of E^* ; β and γ describes the shape of the Sigmoidal function

Using an Excel-based non-linear optimization program, the temperature shift factors and Sigmoidal parameters were determined. Figures 50 through 59 show the master curves shift factor versus temperature for each compacted asphalt mix. For all mixes, the predicted moduli using the Sigmoidal model fit very well with the measured moduli. Table 48 summarized the Sigmoidal model parameters and the temperature shift function for each asphalt mix.

The range of the dynamic moduli for asphalt mixes are within the typical values for the respective mixes. The dynamic moduli of asphalt mixes at 21.1°C (70°F) and 10 Hz are similar to the resilient moduli at 25°C (77°F) in Table 35 and the typical values assumed at the beginning of the project for the design of the perpetual asphalt pavement structure in Table 3.

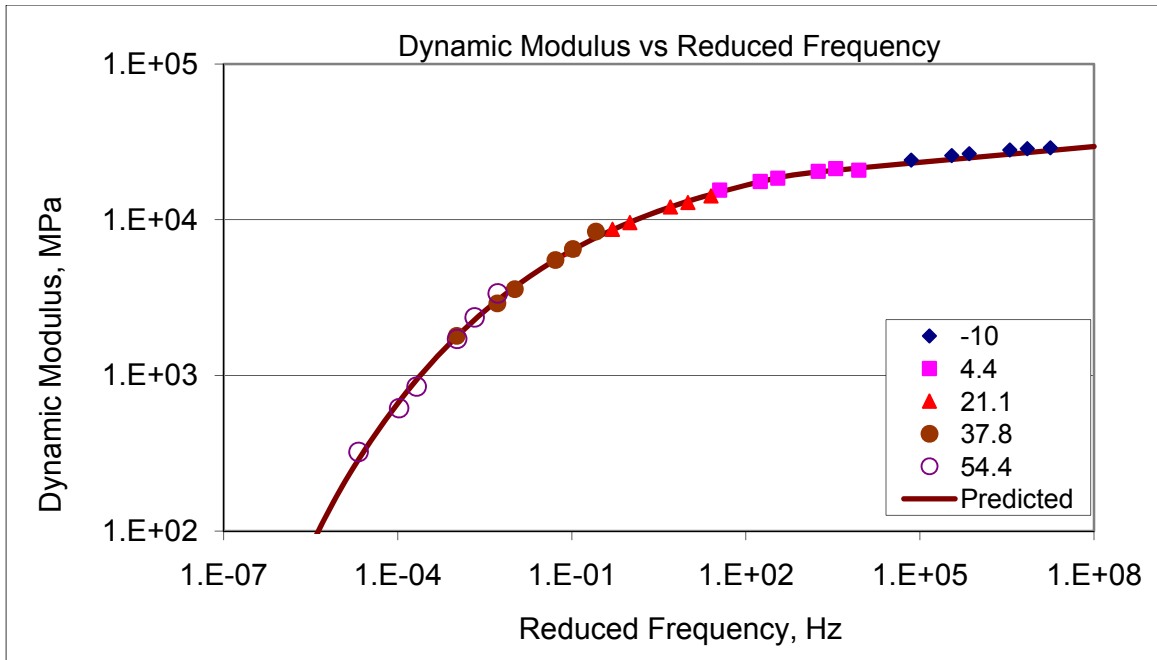


Figure 50. Dynamic modulus master curve of Mix 301 (reference temperature is 21.1°C or 70.0°F; Sigmoidal model parameters are $\alpha = -110.97$; $\beta = 5.3201$; $\delta = 4.5238$; $\gamma = 0.2897$). [1 MPa = 0.145 ksi]

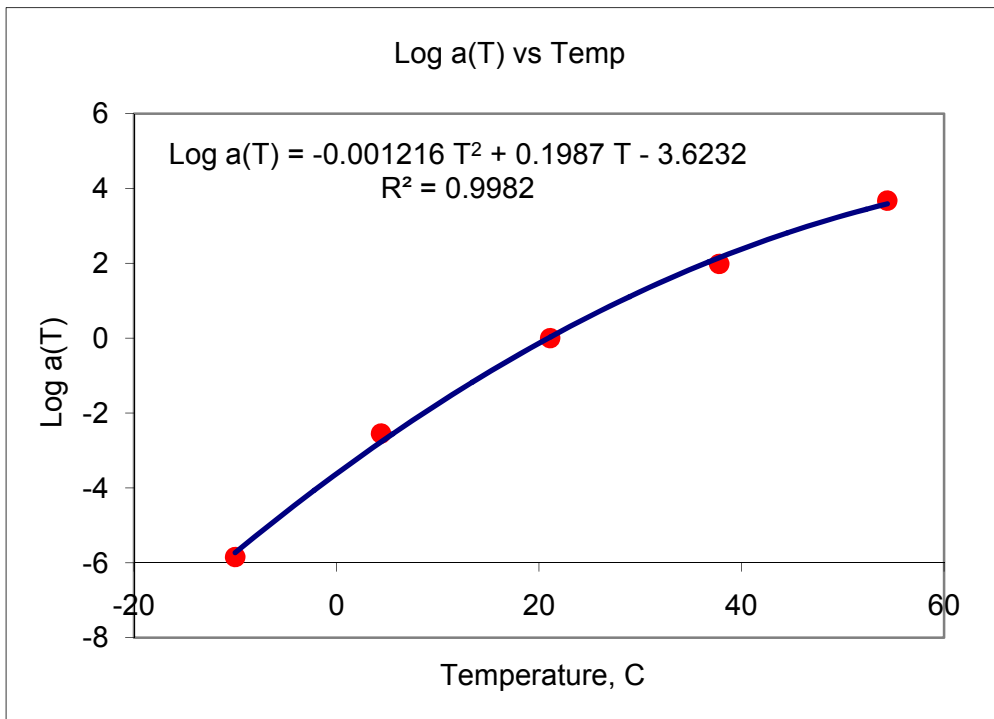


Figure 51. Shift function $a(T)$ versus temperature of Mix 301.

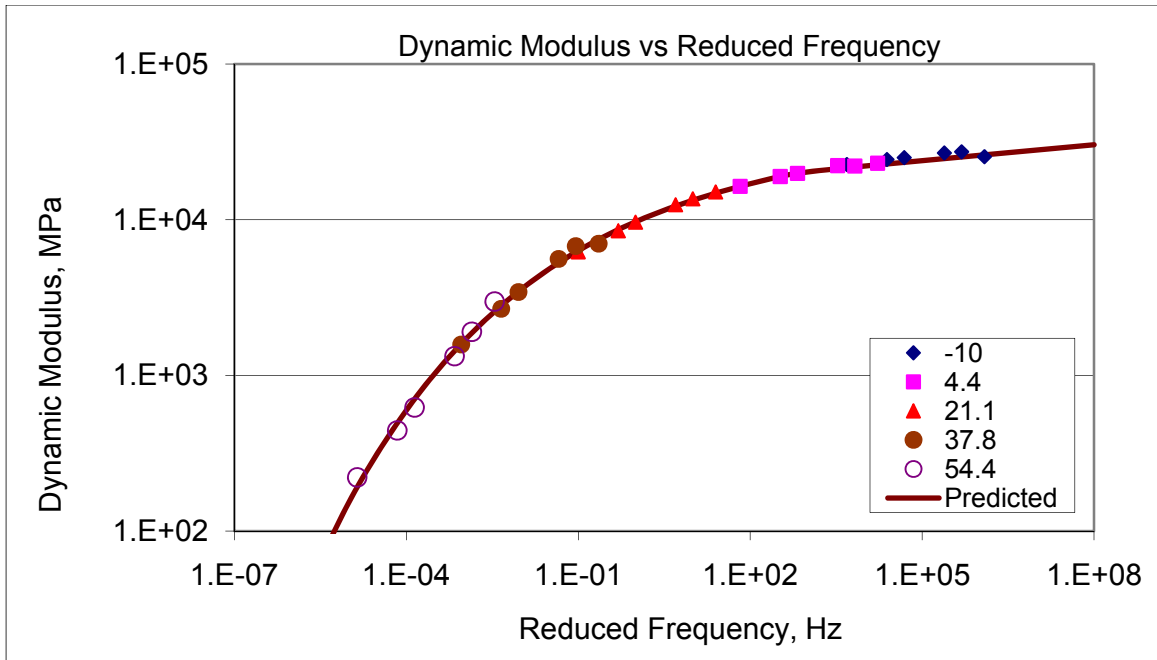


Figure 52. Dynamic modulus master curve of Mix 302 (reference temperature is 21.1°C or 70.0°F; Sigmoidal model parameters are $\alpha = -110.96$; $\beta = 5.3081$; $\delta = 4.5333$; $\gamma = 0.2947$). [1 MPa = 0.145 ksi]

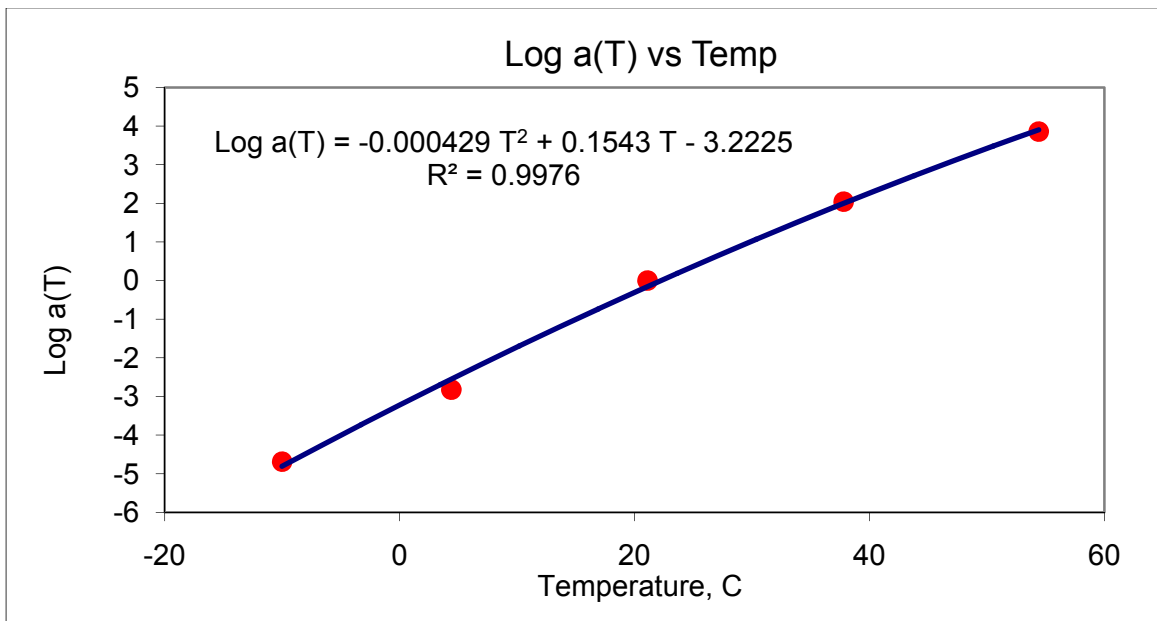


Figure 53. Shift function $a(T)$ versus temperature of Mix 302.

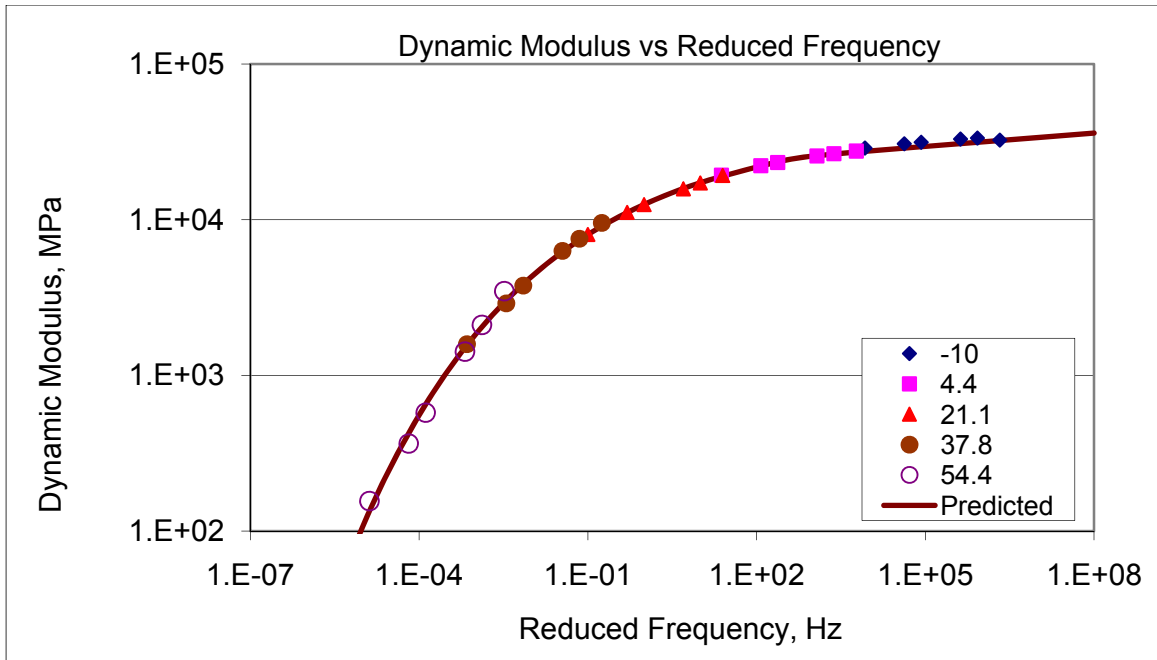


Figure 54. Dynamic modulus master curve of Mix FRL (reference temperature is 21.1°C or 70.0°F; Sigmoidal model parameters are $\alpha = -110.96$; $\beta = 5.4114$; $\delta = 4.5916$; $\gamma = 0.3331$). [1 MPa = 0.145 ksi]

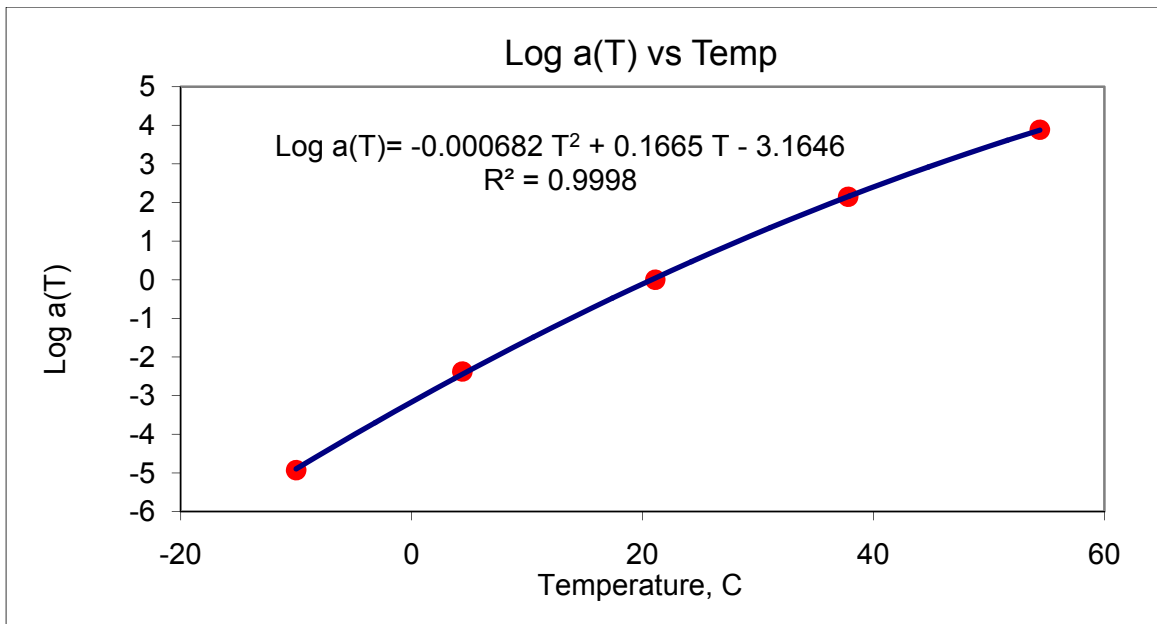


Figure 55. Shift function $a(T)$ versus temperature of Mix FRL.

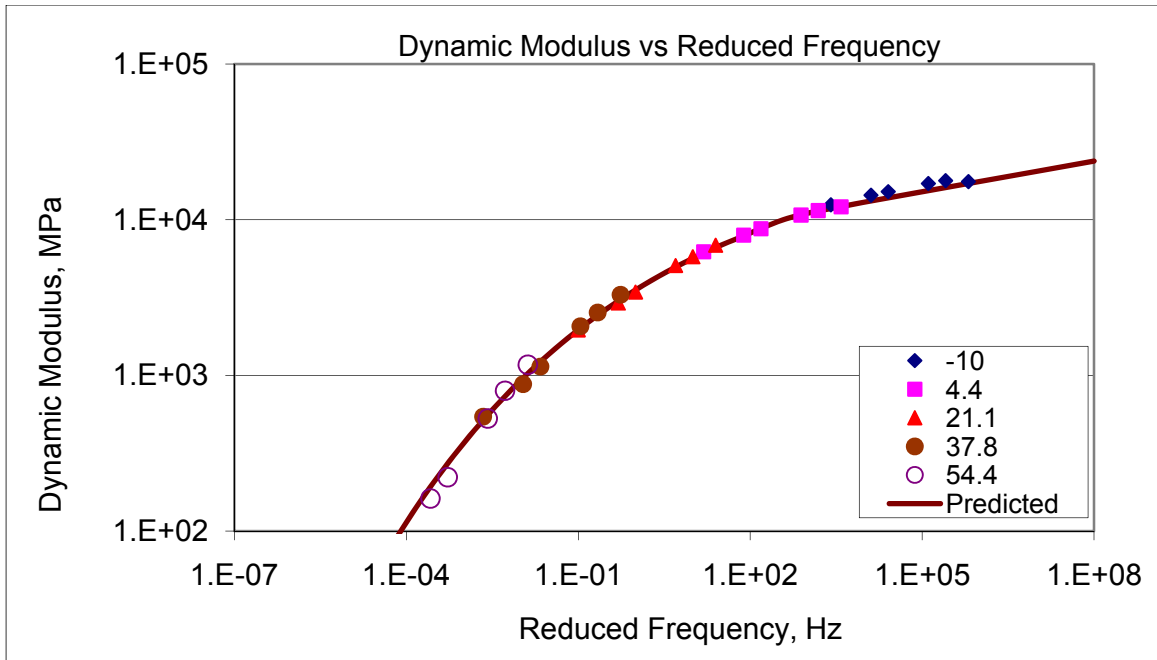


Figure 56. Dynamic modulus master curve of Mix 442 (reference temperature is 21.1°C or 70.0°F; Sigmoidal model parameters are $\alpha = -110.92$; $\beta = 4.7225$; $\delta = 4.5267$; $\gamma = 0.2352$). [1 MPa = 0.145 ksi]

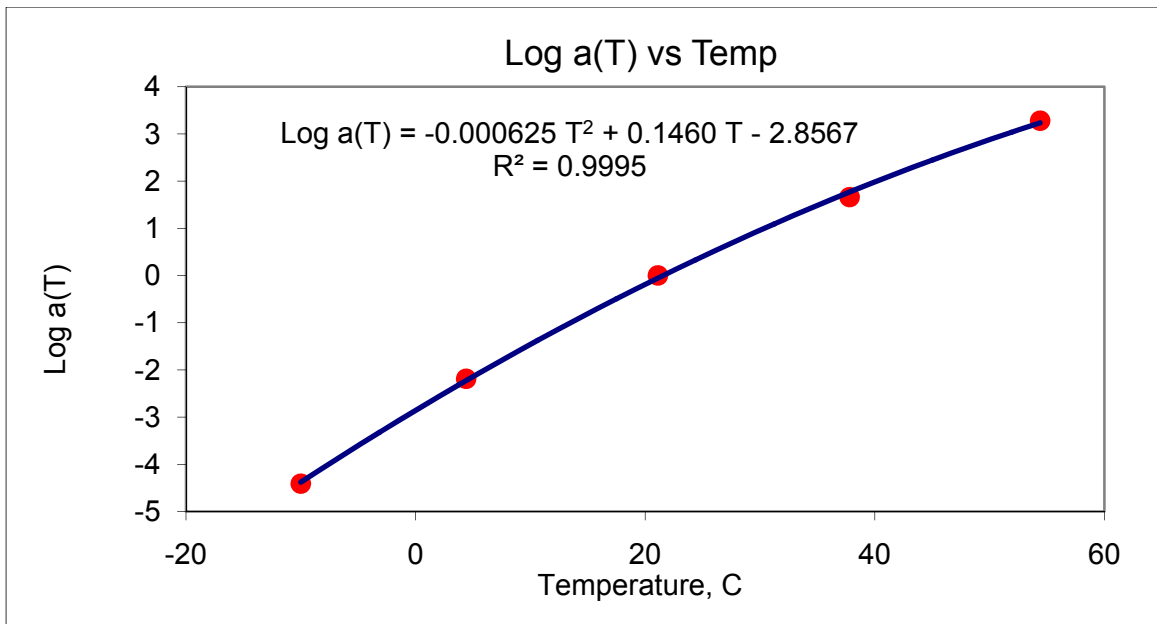


Figure 57. Shift function $a(T)$ versus temperature of Mix 442.

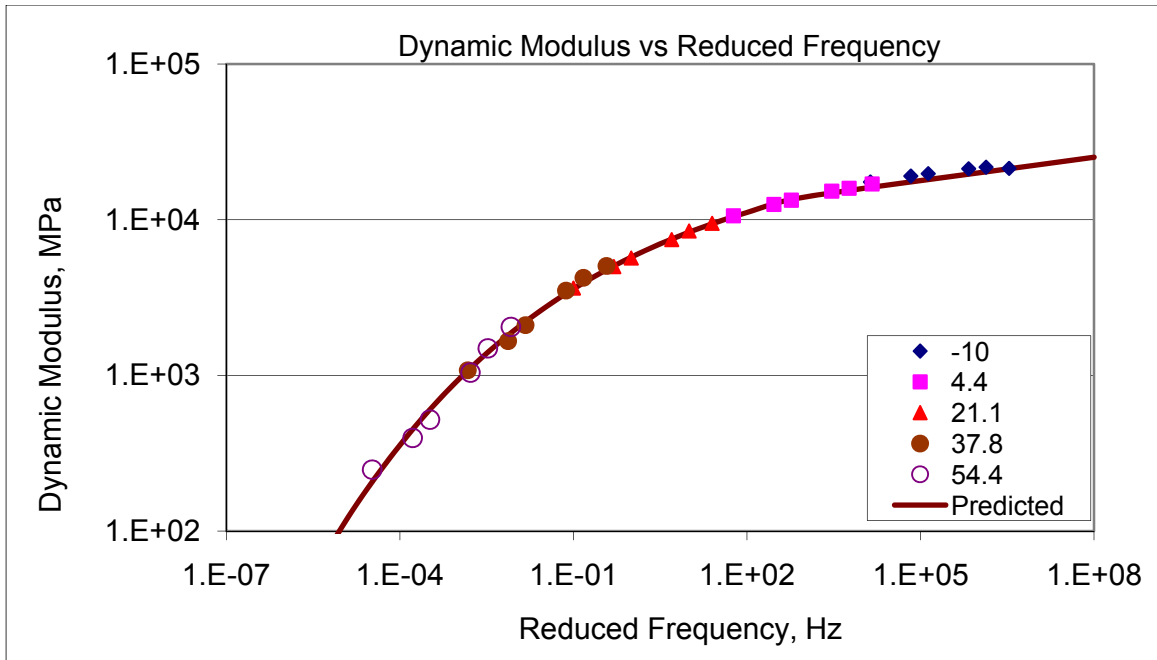


Figure 58. Dynamic modulus master curve of Mix SMA (reference temperature is 21.1°C or 70.0°F; Sigmoidal model parameters are $\alpha = -110.96$; $\beta = 4.9894$; $\delta = 4.5102$; $\gamma = 0.2424$). [1 MPa = 0.145 ksi]

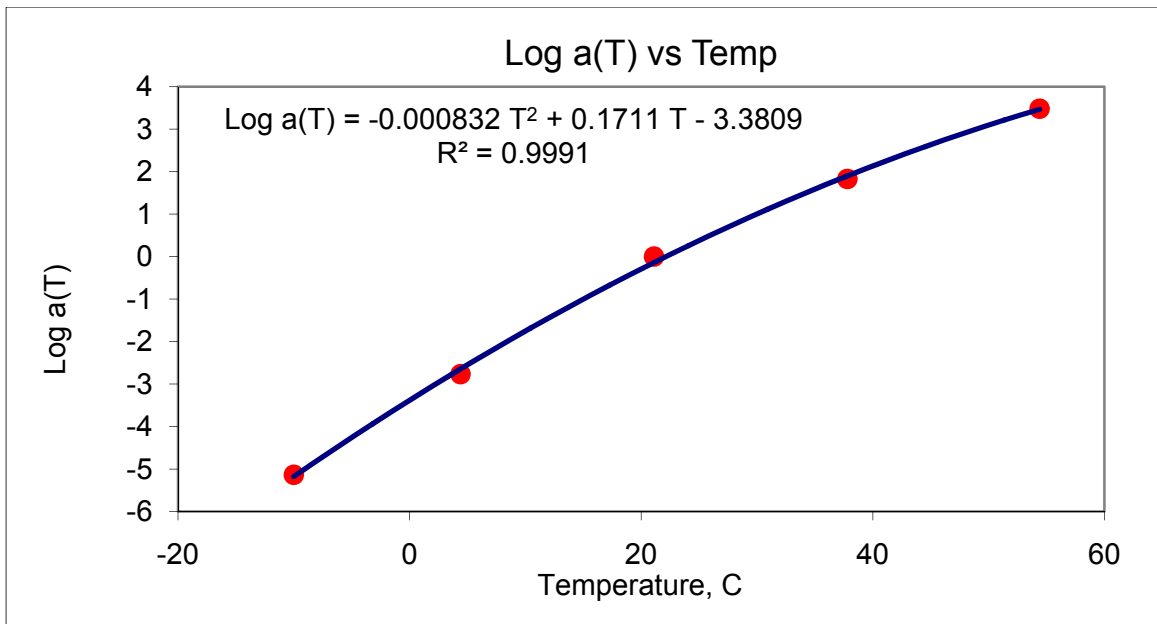


Figure 59. Shift function $a(T)$ versus temperature of Mix SMA.

Table 48. Summary of Sigmoidal function parameters and shift factor equations for dynamic modulus of WAY 30 asphalt mixes.

Mix Type	Sigmoidal Function Parameters				Temperature Shift Function	
	α	β	δ	γ	Log a(T)	R ²
301	-110.966	5.32009	4.52384	0.28965	= -0.001216 T ² + 0.1987 T - 3.623	0.9982
302	-110.962	5.30814	4.53334	0.29468	= -0.000429 T ² + 0.1543 T - 3.222	0.9976
FRL	-110.957	5.41136	4.59155	0.33314	= -0.000682 T ² + 0.1665 T - 3.164	0.9998
442	-110.923	4.72248	4.52665	0.23520	= -0.000625 T ² + 0.1460 T - 2.856	0.9995
SMA	-110.961	4.98943	4.51016	0.24243	= -0.000832 T ² + 0.1711 T - 3.380	0.9991

reference temperature = 21.1°C (70.0°F); Temperature is in degree Celsius.

7.11 Repeated Load Test (Flow Number)

After completion of dynamic modulus tests, tested samples were further subjected to a repeated load to determine the rutting potential of asphalt mixes. In the Simple Performance Test (SPT) procedure, the number of load cycles corresponding to the onset of a tertiary creep (or flow) is defined as a flow number. In this study, two tested samples of each mix were tested for flow number at the effective temperature (39°C (102.2°F) for the WAY-30 project site) with the maximum stress level recommended for unconfined test (30 psi or 207 kPa) [Bonaquist, 2003]. The results are summarized in Table 49. None of the mixes showed tertiary creep or minimum strain per load cycle at this effective temperature, indicating all mixes were highly rut-resistant. Two more samples per each mix were tested at 54.4°C (130°F), the highest temperature used in the development of simple performance test procedure. As shown in Table 50, when $\Delta(\epsilon)/\Delta(N)$ was used for flow number determination as recommended in the SPT procedure, all mixes did not show the minimum value within 10,000 cycle loading. When plotted on log-log scale, all mixes except SMA showed minimums in strain rate per cycle, $\Delta\log(\epsilon)/\Delta\log(N)$ as presented in Table 49.

Flow number is a newly introduced property measuring rutting potential of an asphalt mix. Its implication to actual rutting performance is still under development. Based on the limited understanding of flow number, it can be concluded that the flow number results agree well APA test results; the SMA mix showing the highest rut resistant and all other mixes also showing good rut resistant.

Table 49. Summary of flow numbers at the effective temperature (39°C or 102.2°F).

Sample	Flow Number			
	Read from $\Delta\log(\epsilon)/\Delta\log(N)$ plot		Read from $\Delta(\epsilon)/\Delta(N)$ plot	
		Average		Average
301C	>10000	>10000	>10000	>10000
301D	>10000		>10000	
302C	>10000	>10000	>10000	>10000
302D	>10000		>10000	
442C	>10000	>10000	>10000	>10000
442D	>10000		>10000	
FRLC	>10000	>10000	>10000	>10000
FRLD	>10000		>10000	
SMAC	>10000	>10000	>10000	>10000
SMAD	>10000		>10000	

Table 50. Summary of flow numbers at 54.4°C (130°F).

Sample	Flow Number			
	Read from $\Delta\log(\epsilon)/\Delta\log(N)$ plot		Read from $\Delta(\epsilon)/\Delta(N)$ plot	
		Average		Average
301A	272	227	>10000	>10000
301B	182		>10000	
302A	362	362	>10000	>10000
302B	NM		>10000	
442A	402	240	>10000	>10000
442B	78		>10000	
FRLA	77	67	>10000	>10000
FRLB	92		>10000	
FRLC2	33		>10000	
SMAA	>10000	>10000	>10000	>10000
SMAB	>10000		>10000	

NM = not measured

7.12 Bulk Modulus

Bulk modulus is defined as

$$K(T, t) = \frac{P}{\epsilon_v(T, t)} \quad \text{Eq. 48}$$

where, K = bulk modulus, P = hydrostatic stress, $\epsilon_v(T, t)$ = time and temperature dependent volumetric strain ($\Delta V/V$). It was attempted to utilize the pressurized triaxial cell to apply a hydrostatic stress to a cylindrical specimen and to measure volume change by means of measuring two axial and one diametral deformation. However, it was observed that the pressurizing of the triaxial cell was a very slow process, taking several minutes to achieve a significant level of hydrostatic stress. Furthermore, the possible error in volume measurement in the proposed test system would result in inaccurate bulk modulus. Literature search revealed that the bulk modulus is rarely measured in the laboratory. The most common method determining bulk modulus in practice is estimating it from other materials properties [Wang et al., 2006, and Kim et al., 2008]. When a constant Poisson's ratio is assumed for asphalt materials, the bulk modulus can be estimated as

$$K(T, t) = E(T, t)/3(1 - 2\nu) \quad \text{Eq. 49}$$

Where, $E(T, t)$ = relaxation modulus, ν = Poisson's ratio

The relaxation modulus was approximated from the dynamic modulus by converting the frequency into loading time using loading time (t) and frequency (f) relationship, $t = 1/(2\pi f)$. Poisson's ratio is assumed to be 0.35. Then, the bulk moduli at 5, 25, and 40°C (41, 77, and 104°F) at 0.1, 1, 10, 100, and 1000 seconds can be estimated as shown in Table 51.

Table 51. Estimated bulk modulus at 5, 25, and 40°C (41, 77, and 104°F).

Mix Type	(SI Units)				
	Bulk modulus at various loading time, MPa				
	0.1 sec	1 sec	10 sec	100 sec	1,000 sec
5°C					
302	21,331	17,521	13,460	9,455	5,893
FRL	26,660	22,003	16,841	11,607	6,918
442	10,159	7,209	4,676	2,711	1,364
SMA	14,759	11,572	8,493	5,732	3,479
25°C					
302	10,121	6,455	3,538	1,585	544
FRL	12,011	7,254	3,602	1,365	357
442	3,529	1,901	873	329	96
SMA	5,929	3,632	1,950	887	327
40°C					
302	3,798	1,742	617	154.9	24.8
FRL	4,117	1,642	461	79.8	7.2
442	1,237	509	167	41.3	7.2
SMA	2,303	1,094	427	129.9	29.0
Mix Type	(English Units)				
	Bulk modulus at various loading time, ksi				
	0.1 sec	1 sec	10 sec	100 sec	1,000 sec
41°F					
302	3,094	2,541	1,952	1,371	855
FRL	3,867	3,191	2,443	1,683	1,003
442	1,473	1,046	678	393	198
SMA	2,141	1,678	1,232	831	505
77°F					
302	1,468	936	513	230	79
FRL	1,742	1,052	522	198	52
442	512	276	127	48	14
SMA	860	527	283	129	47
104°F					
302	551	253	89.4	22.5	3.6
FRL	597	238	66.8	11.6	1.0
442	179	74	24.2	6.0	1.0
SMA	334	159	61.9	18.8	4.2

7.13 Absorbed Energy Ratio, Indirect Tensile Strength and Unconfined Compressive Strength

During construction, the contractor determined the absorbed energy ratio, indirect tensile strength and unconfined compressive strength for each asphalt mix. The ratio of absorbed energy between dry and moisture conditioned asphalt concretes is believed to be related with the performance of asphalt pavement. For the determination of absorbed energy, six Superpave gyratory specimens were compacted to 7% air void after aging loose mix for 7 hours at 135°C (275°F). Three compacted specimens were moisture-conditioned following AASHTO T283 procedures; vacuum saturation, one freeze-thaw cycle, 24 hours soaking at 60°C (140°F), and 2 hours soaking at 25°C (77°F). Three moisture-conditioned and three dry specimens were tested for indirect tensile strength following AASHTO T283 procedure. The absorbed energy is calculated as:

$$E = 1/2 P\delta/t \quad \text{Eq. 50}$$

where, E = absorbed energy;
 P = peak load
 δ = load line displacement
 t = specimen thickness

Average absorbed energy and the absorbed energy ratio ($E_{\text{soaked}}/E_{\text{dry}}$) for four asphalt mixes are summarized in Table 52. Individual test results are presented in Appendix F. As shown in Table 52, the SMA mix and 442 mix show high absorbed energy ratio probably due to the use of polymer modification which would make these asphalt mixes more durable.

For indirect tensile strength measurement, each 150 mm (6 in.) test specimen was compacted with Superpave gyratory compactor to its design air void. Test was performed at 25°C (77°F) following AASHTO T283 without conditioning steps. Compressive load was applied in diametral direction at a rate of 50 mm/min. (2 in./min.) until failure. Test results are presented at Appendix G and are summarized in Table 53.

Table 52. Average absorbed energy ratio of asphalt mixes.

Mix	Air Void	Absorbed Energy, E				Absorbed Energy Ratio ($E_{\text{soaked}}/E_{\text{dry}}$)	Std Dev
		Dry		Soaked			
		lb·in./in.	(kN·m/m)	lb·in./in.	(kN·m/m)		
302	6.92	5805	(25.8)	3929	(17.5)	0.70	0.20
FRL	7.05	5111	(22.7)	5001	(22.2)	0.76	0.15
SMA	6.94	6304	(28.0)	5319	(23.7)	0.84	0.06
442	6.86	8402	(37.4)	7183	(32.0)	0.85	0.005

Table 53. Average indirect tensile strength of asphalt mixes.

Mix	AV	ITS		Standard Deviation	
	(%)	(psi)	(MPa)	(psi)	(MPa)
302	4.01	175.84	1.212	33.3	0.230
FRL	3.35	166.46	1.148	25.3	0.174
SMA	3.51	132.15	0.911	10.7	0.074
442	3.75	179.55	1.238	8.3	0.057

For unconfined compressive strength measurement, 150 mm (6 in.) test specimens were compacted to their respective design air void using Superpave gyratory compactor. Axial load was applied at 23°C (73.4°F) at a rate of 20 to 50 psi (138 to 345 kPa) per second until failure. The results of unconfined compressive strength tests are presented in Appendix H and are summarized in Table 54.

Table 54. Average unconfined compressive strength of asphalt mixes.

Mix	AV	Unconfined Compressive Strength		Standard Deviation	
	(%)	(psi)	(MPa)	(psi)	(MPa)
302	4.01	977.0	6.74	218.5	1.506
FRL	3.26	987.42	6.81	197.7	1.363
SMA	3.48	721.3	4.97	102.3	0.705
442	3.83	941.5	6.49	186.9	1.289

8 SUMMARY AND CONCLUSIONS

The US Route 30 bypass of Wooster, Ohio, in Wayne County, “WAY-30”, was constructed to demonstrate two types of extended service pavements, a long-life Portland cement concrete (PCC) pavement on the eastbound lanes and an asphalt concrete (AC) perpetual pavement on the westbound lanes. Both pavements are designed to provide 50 years or more of service with only minimal maintenance (e.g. resurfacing). The PCC pavement structure features a thick and extra-wide slab on an asphalt treated base, while the AC pavement structure features a SMA surface, a Superpave layer and a Fatigue Resistant Layer (FRL). Report FHWA/OH-2008/7 [Sargand, Figueroa, and Romanello, 2008] discusses the instrumentation and response of the pavement under loads. For this study, samples of all pavement materials, including soils, granular subbase material, PCC mixes, and AC mixes were tested in the laboratory to determine material parameters. The AC materials included mixes used in different layers of the perpetual pavement structure. Two mixes of the PCC were used in different sections of the road.

The subgrade material was subjected to grain size, Atterberg limit, Standard Proctor, maximum dry density, and resilient modulus measurements. The subgrade was ODOT type A-4a (AASHTO A-4). The granular subbase material was subjected to a sieve analysis, a resilient modulus test and a permeability test. It was classified as type A-1a.

PCC tests included: unit weight, modulus of rupture, static modulus of elasticity, Poisson’s ratio, splitting tensile strength, compressive strength, maturity, and thermal coefficient of linear expansion. AC tests included: resilient modulus, rutting evaluation using an asphalt pavement analyzer, moisture susceptibility, indirect tensile creep and strength, beam fatigue, thermal stress restrained specimen test, dynamic modulus, and dynamic creep (flow number) test.

From these tests, the following general conclusions can be reached:

- The subgrade soil samples were classified as a moderately plastic silty soil, ODOT classification A-4-a (AASHTO A-4). All samples had similar compaction curves.
- The resilient modulus of the subgrade at 12%-15% water content ranged from about 3 ksi (20 MPa) to 10 ksi (69 MPa).
- The subgrade resilient modulus M_R could be fitted with a power law of the form $M_R \propto \sigma_d^{-\alpha}$, where σ_d is the deviatoric stress and α is a least-squares fit parameter.
- The granular subbase material was classified as AASHTO type A-1-a, well-graded gravel with sand. The composition was 67.5% gravel, 17.5% coarse sand, 11.5% medium and fine sand, and 3.5% fines.
- The resilient modulus of the granular subbase ranged from 8 ksi (55 MPa) to 23 ksi (160 MPa) under deviatoric stresses in the range of 3 psi (21 kPa) to 20 psi (138 kPa).
- The resilient modulus M_R of the subbase was fitted well with the universal model with model parameters $k_1 = 0.597608$, $k_2 = 0.458940$, and $k_3 = 0.056241$ and $r^2 = 0.957$.
- The permeability of the subbase was 1.0013 cm/s (2,838 ft/day), much higher than recommended 0.353 cm/s (1,000 ft/day) for pavement.

- The average values measured for each concrete property for both concrete mixes, as well as the differences between the mixes are given in Table 55. All properties were measured after 90 days of curing. With the exception of modulus of rupture, the various strength parameters for Mix A were greater than those for Mix B.

Table 55. Summary of average WAY-30 concrete material properties at 90 days

Property	Variable	English	Mix A	Mix B	Diff	% Diff
		unit	GGBFS	Fly ash	Δ	Δ/GGBFS
unit weight	γ	pcf	141.9	139.4	-2.5	-1.76%
Modulus of rupture	R	psi	608.7	817.7	209	34.34%
Modulus of elasticity	E	10^3 ksi	4.07	3.8	-0.27	-6.63%
Poisson's Ratio	ν	-	0.16	0.18	0.02	12.50%
Splitting Tensile Strength	T	psi	622.4	472.3	-150.1	-24.12%
Compressive strength	C	psi	6149	5102	-1047	-17.03%
Coefficient of linear expansion	α	$^{\circ}\text{F}^{-1}$	5.9×10^{-6}	5.8×10^{-6}	0.1×10^{-6}	1.69%

Property	Variable	International	Mix A	Mix B	Diff	% Diff
		unit	GGBFS	Fly ash	Δ	Δ/GGBFS
unit weight	γ	kg/m^3	2273	2233	-40	-1.76%
Modulus of rupture	R	kPa	4197	5638	1441	34.33%
Modulus of elasticity	E	GPa	28.1	26.2	-1.9	-6.76%
Poisson's Ratio	ν	-	0.16	0.18	0.02	12.50%
Splitting Tensile Strength	T	kPa	4291	3256	-1035	-24.12%
Compressive strength	C	MPa	42.4	35.2	-7.2	-16.98%
Coefficient of linear expansion	α	C^{-1}	10.6×10^{-6}	10.4×10^{-6}	0.2×10^{-6}	1.69%

- The fly ash concrete (Mix B) was cured for 28 days using two different methods, one using a curing compound applied to the top surface and the other involving a water bath. The compressive strength was 14% higher using the curing compound, but that difference declined to 2% at the end of 28 days.
- Strength-maturity relationships were established for both PCC mixes.
- Properties for each asphalt mix are summarized in Table 56.
- As expected, the SBS modified mixes (SMA and 442 mixes) showed much higher fatigue resistance than the unmodified mixes.
- The creation of asphalt-rich bottom by adding additional asphalt binder did work to increase the fatigue resistance by orders of magnitude. At $70 \mu\epsilon$, the expected fatigue endurance limit and the designed strain level for the structure, regular 302 mix showed 20,000 cycles to failure while asphalt-rich 302 mix (FRL) is estimated to have 20 million cycles to failure.
- Dynamic modulus master curves were fitted well with the Sigmoidal model.
- For average climatic and traffic conditions (25°C or 77°F ; 10 Hz or 0.1 sec loading time), the dynamic moduli and the resilient moduli of asphalt mixes were

similar to the values used in the development of the asphalt perpetual pavement structure. For SMA and 442 mixes, the measured moduli were slightly lower than the values used in the design, while for 302 and FRL mixes, the moduli were significantly higher than the design value. Since the thickness of 302 and FRL layers consists of 80% of the total pavement thickness, the maximum strain at the bottom of FRL would be significantly smaller than the designed 70 $\mu\epsilon$.

- The rutting test results from asphalt pavement analyzer test and flow numbers obtained from the repeated load test indicate that all asphalt mixes are rut-resistant.
- TSRST cracking temperatures of asphalt mixes were lower than the expected pavement temperatures for the project site determined by LTPPBind software, meaning the possibility of the low temperature thermal cracking is very unlikely.

Table 56. Summary of properties measured for WAY-30 AC mixes.

Property	Variable	English unit	Mix				
			301	302	442	FRL	SMA
Maximum specific gravity	<i>MSG</i>	-	2.469	2.497	2.479	2.475	2.469
Instantaneous resilient modulus at 41°F	<i>M_{Ri}</i>	ksi	3700	3805	2985	4390	3320
Total resilient modulus at 41°F	<i>M_{Rt}</i>	ksi	3490	3345	2955	4230	3280
Instantaneous resilient modulus at 77°F	<i>M_{Ri}</i>	ksi	1920	1900	1023	2205	1345
Total resilient modulus at 77°F	<i>M_{Rt}</i>	ksi	1830	1830	967.5	2155	1280
Instantaneous resilient modulus at 104°F	<i>M_{Ri}</i>	ksi	826	753.5	408	944	532
Total resilient modulus at 104°F	<i>M_{Rt}</i>	ksi	720	660.5	349	789.5	485.5
Poisson's ratio (assumed)	<i>v</i>	-	0.35	0.35	0.35	0.35	0.35
Average rutting after 8000 cycles	-	mil	177	205	146	220	55
Tensile strength ratio	<i>TSR</i>	-	0.72	0.68	0.77	0.73	0.80
Tensile strength at -4°F	<i>T</i>	psi	903.1	677.7	781.1	831.2	787.9
Tensile strength at 14°F	<i>T</i>	psi	892.8	599.8	581.2	745.8	755.1
Tensile strength at 32°F	<i>T</i>	psi	783.9	583.2	394.6	802.8	585.9
Cycles to failure at 100 $\mu\epsilon$	<i>N_f</i>	-	-	-	57.6 $\times 10^6$	22000	2.39 $\times 10^9$
Cycles to failure at 200 $\mu\epsilon$	<i>N_f</i>	-	-	1500	294000	38000	1.47 $\times 10^6$
Cycles to failure at 300 $\mu\epsilon$	<i>N_f</i>	-	-	1000	102800	24000	-
Cycles to failure at 400 $\mu\epsilon$	<i>N_f</i>	-	-	295.0	5140.0	650.0	31000.0
TSRST fracture temperature	-	°F	-	-29.6	-18.9	6.68	-37.5
TSRST fracture strength	-	ksi	-	0.072	0.118	0.206	0.067
Dynamic Modulus (Sigmoidal α)			-110.96	-110.96	-110.92	-110.95	-110.96
Dynamic Modulus (Sigmoidal β)			5.32009	5.30814	4.72248	5.41136	4.98943
Dynamic Modulus (Sigmoidal δ)			4.52384	4.53334	4.52665	4.59155	4.51016
Dynamic Modulus (Sigmoidal γ)			0.28965	0.29468	0.2352	0.33314	0.24243
Temperature Shift Function $a(T) = a T^2 + b T + c$							
Temperature Shift Function (a)			-0.001216	-0.00043	-0.00063	-0.00068	-0.00083
Temperature Shift Function (b)			0.1987	0.1543	0.146	0.1665	0.1711
Temperature Shift Function (c)			-3.623	-3.222	-2.856	-3.164	-3.38
Flow Number at 54.4°C			227	362	240	67	>10000
Absorbed Energy Ratio			-	1.58	1.17	1.44	1.19
Property	Variable	SI unit	Mix				
			301	302	442	FRL	SMA
Maximum specific gravity	<i>MSG</i>	-	2.469	2.497	2.479	2.475	2.469
Instantaneous resilient modulus at 5°C	<i>M_{Ri}</i>	GPa	25.51	26.23	20.58	30.27	22.89
Total resilient modulus at 5°C	<i>M_{Rt}</i>	GPa	24.06	23.06	20.37	29.16	22.61
Instantaneous resilient modulus at 25°C	<i>M_{Ri}</i>	GPa	13.24	13.10	7.05	15.20	9.27
Total resilient modulus at 25°C	<i>M_{Rt}</i>	GPa	12.62	12.62	6.67	14.86	8.83
Instantaneous resilient modulus at 40°C	<i>M_{Ri}</i>	GPa	5.70	5.20	2.81	6.51	3.67
Total resilient modulus at 40°C	<i>M_{Rt}</i>	GPa	4.96	4.55	2.41	5.44	3.35
Poisson's ratio (assumed)	<i>v</i>	-	0.35	0.35	0.35	0.35	0.35
Average rutting after 8000 cycles	-	mm	4.5	5.2	3.7	5.6	1.4
Tensile strength ratio	<i>TSR</i>	-	0.72	0.68	0.77	0.73	0.80
Tensile strength at -20°C	<i>T</i>	MPa	6227	4673	5385	5731	5432
Tensile strength at -10°C	<i>T</i>	MPa	6156	4135	4007	5142	5206
Tensile strength at 0°C	<i>T</i>	MPa	5405	4021	2721	5535	4040
Cycles to failure at 100 $\mu\epsilon$	<i>N_f</i>	-	-	-	57.6 $\times 10^6$	22000	2.39 $\times 10^9$
Cycles to failure at 200 $\mu\epsilon$	<i>N_f</i>	-	-	1500	294000	38000	1.47 $\times 10^6$
Cycles to failure at 300 $\mu\epsilon$	<i>N_f</i>	-	-	1000	102800	24000	-
Cycles to failure at 400 $\mu\epsilon$	<i>N_f</i>	-	-	295.0	5140.0	650.0	31000.0
TSRST fracture temperature	-	°C	-	-34.2	-28.3	-14.1	-38.6
TSRST fracture strength	-	MPa	-	0.50	0.81	1.42	0.46

9 IMPLEMENTATION

The results and data from this study can be directly implemented by researchers validating or calibrating the long life pavement design procedures. In fact, some of the data have already been used in the ELS analysis in the previous report on WAY-30. [Sargand, Figueroa, and Romanello, 2008] Data obtained from this research project will be used as inputs for the elastic or viscoelastic models used in design of pavements to predict pavement responses. The predicted pavement responses may then be compared with the actual observed pavement response to validate the design. The ultimate result of this process will be revisions in specifications, standard drawings, and the Pavement Design and Rehabilitation Manual to incorporate the new materials and design procedures. There are no immediate impediments to implementation. A more detailed implementation plan is provided in Appendix I.

REFERENCES

- Abdulshafi, O., Mukhtar, H., and Kedzierski, B. (1994). "Reliability of AASHTO Design Equation for Predicting Pavement Performance of Flexible and Rigid Pavements in Ohio." Report No. FHWA/OH/95/006, Final Report to Ohio Dept. of Transportation & Federal Highway Administration, CTL Engineering Inc., Columbus, Ohio, 167 pp.
- American Society of Testing and Materials (ASTM) (2004), "Standard Test Method for Compressive Strength of Cylindrical Concrete Specimens" Standard No. C 39/C 39M - 03, Philadelphia, Pennsylvania.
- American Society of Testing and Materials (ASTM) (2004), "Standard Test Method for Flexural Strength of Concrete (Using Simple Beam with Third-Point Loading)" Standard No. C 78 - 02, Philadelphia, Pennsylvania.
- American Society of Testing and Materials (ASTM), (2004), "Standard Test Method for Density (Unit Weight), Yield, and Air Content (Gravimetric) of Concrete" Standard No. C138/C 138M – 01a, Philadelphia, Pennsylvania.
- American Society of Testing and Materials (ASTM), (2004), "Standard Test Method for Static Modulus of Elasticity and Poisson's Ratio of Concrete in Compression" Standard No. C 469 - 02, Philadelphia, Pennsylvania.
- American Society of Testing and Materials (ASTM), (2004), "Standard Test Method for Splitting Tensile Strength of Cylindrical Concrete Specimens" Standard No. C 496/C 496M - 04, Philadelphia, Pennsylvania.
- American Society of Testing and Materials (ASTM), (2004), "Standard Practice for Estimating Concrete Strength by the Maturity Method" Standard No. C 1074 Philadelphia, Pennsylvania.
- ARA (2004). Guide for Mechanistic-Empirical Design of New and Rehabilitated Pavement Structures. Final Report. NCHRP 1-37A.
- The Asphalt Concrete Institute (1999). *Thickness Design-Highways & Streets*, MS-1, 9th edition.
- Barksdale, R. D., Alba, J., Khosla, P. N., Kim, R., Lambe, P. C., and Rahman, M. S. (1997). "Laboratory Determination of Resilient Modulus for Flexible Pavement Design." NCHRP Web Document 14, Federal Highway Administration, Washington, D.C., 486 pp.
- Bonaquist, R.F., Christensen, D.W., Stump, III, W. "Simple Performance Tester for Superpave Mix Design: First-Article Development and Evaluation." NCHRP Report 513, Transportation Research Board, Washington, D.C. (2003)

- Carmichael, R. F. and Stuart, E. (1985). "Predicting Resilient Modulus: a Study to Determine Mechanical Properties of Subgrade Soils." Transportation Research Record No. 1043, Transportation Research Board, National Research Council, Washington, D.C.
- Dingqing, L., and Selig, E. T. (1994). "Resilient Modulus for Fine-Grained Subgrade Soils." Journal of Geotechnical Engineering, Vol. 120, No. 6, American Society of Civil Engineers (ASCE), pp. 939-957.
- Drumm, E. C., Boateng-Poku, Y., and Pierce, T. J. (1991). "Estimation of Subgrade Resilient Modulus from Standard Tests." Journal of Geotechnical Engineering, Vol. 116, No. 5, American Society of Civil Engineers (ASCE), pp. 774-789.
- Figueroa, J. L. (1994). "Characterization of Ohio Subgrade Types." Report No. FHWA/OH-94/006, Final Report to Ohio Dept. of Transportation & Federal Highway Administration, Civil Eng. Dept., Case Western Reserve University, Cleveland, Ohio.
- Figueroa, J. L. (2001). "Extended Monitoring and Analysis of Moisture-Temperature Data." Short Report, Presented to Ohio Dept. of Transportation, Civil Engineering Dept., Case Western Reserve University, Cleveland, Ohio, 40 pp.
- Fredlund, D. G., Bergan, A. T., and Sauer, E. K. (1977). "Relation Between Resilient Modulus and Stress Conditions for Cohesive Subgrade Soils." Transportation Research Record (TRR), No. 642, pp 73-81.
- George, K. P. (2004). "Prediction of Resilient Modulus from Soil Index Properties." Report No. FHWA/MS-DOT-RD-04-172, Final Report to Mississippi Dept. of Transportation and Federal Highway Administration, Research Division of Mississippi DOT, Jackson, MS, 72 pp.
- Jung, D. H., and T.S. Vinson, (1994), *Low Temperature Cracking: Test Selection*, Report No. SHRP-A-400, Strategic Highway Research Program, National Research Council, Washington DC.
- Kim, J, Byron, T, Sholar, G., and Kim, S. (2008). "Comparison of a three-dimensional viscoelastic pavement model with full-scale field tests," Presented at 87th Annual Meeting of the Transportation Research Board, Washington, D.C.
- Monismith, C.L., F. Long, and J.T. Harvey, (2001), "California's Interstate-710 Rehabilitation: Mix and Structural Section Designs, Construction Specifications", Journal of the Association of Asphalt Paving Technologists, 70: 762-799.
- Newcomb, D., (2002), "Perpetual Pavement: A Synthesis", APA 101, Asphalt Pavement Alliance, Lanham, MD.

- Rahim, A M and K. P. George, (2004), “Subgrade soil Index properties to Estimate Resilient Modulus”, Paper Presented at 83rd Annual Meeting of Transportation Research Board, Washington, D. C.
- Rahim, A. M., and George, K. P. (2005). “Models to Estimate Subgrade Resilient Modulus for Pavement Design.” Paper presented at the 84th Annual Meeting of Transportation Research Board (TRB), Washington, D.C., 21 pp.
- Randolph, B.W., Heydinger, A.G., and Gupta , J.D. (2000). “Permeability and Stability of Base and Subbase Materials”, Ohio DOT Final Report FHWA/OH 2000-017
- Sargand, S. M., Masada, T., and Figueroa, J. L., (2003), *Material Properties for Implementation of Mechanistic/Empirical (M-E) Pavement Design Procedures*, Report No. FHWA/OH-2003-021 to Ohio Department of Transportation & Federal Highway Administration (w/ CD-ROM Disk), 209 pp., Ohio Research Institute for Transportation and the Environment, Athens, OH, December 2003.
- Sargand, Shad, J. Ludwig Figueroa, and Michael Romanello, (2008), *Instrumentation of the WAY-30 Test Pavements*, Federal Highway Administration Report No. FHWA/OH-2008/7, Ohio Research Institute for Transportation and the Environment, Athens, OH, June 2008.
- Ursich, C., (2005), “Ohio Takes Perpetual Pavement Another Step Forward”, *Better Roads Magazine*, November 2005.
- Wang, J., Birgisson, B., and Roque, R. (2006). “Effect of viscoelastic stress redistribution on the cracking performance of asphalt pavements.” *Journal of the Association of Asphalt Paving Technologists*, 75, 637-675.
- Yau, A., and Quintus, H. L. V. (2002). “Study of LTPP Laboratory Resilient Modulus Test Data and Response Characteristics: Final Report.” Report No. FHWA-RD-02-051, Office of Infrastructure Research and Development, Federal Highway Administration, McLean, VA.

Appendix A: As-Designed Job Mix Formulas (JMFs)

Table A1. As-Designed Job Mix Formulas for PCC pavement.

	Specific Gravity	Absorption %	GGBFS Mix	Fly Ash Mix
Material Batch Weight SSD, lb/yd³ of Fresh Concrete (kg/m³)				
Natural Sand	2.608	1.59	1161 (688.8)	1161 (688.8)
#8 Limestone	2.619	2.29	461 (273.5)	461 (273.5)
#467 Limestone	2.658	1.13	1400 (830.6)	1400 (830.6)
Type I Cement	3.15	X	415 (246.2)	477 (283.0)
GGBFS	2.72	X	178 (105.6)	-
Fly Ash (Type F)	2.70	X	-	119 (70.6)
Water			259 (153.7)	259 (153.7)
Total			3876 (2299.5)	3859 (2289.5)
Admixtures Used, oz/yd³ (ml/m³)				
ASTM C 260 AEA			31 (1199)	63.8 (2468)
ASTM C 494 WRR - Type B,D			24 (928)	23.8 (921)
Water/CM Ratio				
			0.44	0.44
Fresh Concrete Properties				
Slump, in. (mm)			1.5 (38)	1.5 (38)
Air Content, %			5.5	5.8
Temperature, °F (°C)			70 (21.1)	78 (25.6)
Unit Weight, lb/ft ³ (kg/m ³)			144.9 (2321)	141.3 (2263)
Hardened Concrete Properties				
Compressive Strength, psi (MPa)				
7-day			5930 (40.9)	4010 (27.6)
14-day			6210 (42.8)	4220 (29.1)
28-day			7880 (54.3)	5290 (36.5)
Specified Design Strength (f _c)			5070 (35.0)	4000 (27.6)
Required Over-Design Value			1400 (9.65)	1200 (8.27)
Modulus of Rupture, psi (MPa)				
14-day Beam			775 (5.34)	775 (5.34)
Permeability (coulombs)				
28-day			1505	1128
Specified Design Permeability			2000	2000

Table A2. As-Designed Job Mix Formulas for asphalt pavement.

	SMA (As-Built)	442 (As-Built)	302	FRL
Mix Design Type	Superpave	Superpave	Marshall	Marshall
Coarse Agg	Limestone	Limestone	Limestone	Limestone
Fine Agg	Limestone	Limestone / N Sand	N Sand	N Sand
Gradation				
2" (50.8 mm)	100	100	100	100
1 1/2" (38 mm)	100	100	100	100
1" (25.4 mm)	100	100	81	81
3/4" (19 mm)	100	99	66	66
1/2" (12.5 mm)	93	88	55	55
3/8" (9.5 mm)	70	81	48	48
#4 (4.75 mm)	23	54	33	33
#8 (2.36 mm)	16	44	26	26
#16 (1.18 mm)	13	29	20	20
#30 (0.600 mm)	11	18	14	14
#50 (0.300 mm)	10	9	8	8
#100 (0.150 mm)	9	5	4	4
#200 (0.075 mm)	8.0	4.0	3.3	3.3
Agg Blend G_{sb}	2.574	2.567	2.595	2.595
G_{mm}	2.395	2.458	2.491	2.473
% Binder Content				
% Binder Content	6.6	4.8	4.1	4.6
% Virgin Binder	6.6	4.0	2.7	3.2
% G_{mm} @ N_{ini}^a	83.6	88	--	--
% G_{mm} @ N_{des}^a	96.5	96	--	--
% G_{mm} @ N_{max}^a	--	97.7	--	--
Asphalt Binder	PG76-22 SBS	PG76-22 SBS	PG 64-22	PG 64-22
Design Air Void, %	3.5	4.0	4.0	3.0
VMA, %	16.1	12.5	12.1	11.8
F/A ratio	1.2	0.9	--	--
50-30 Ratio	-1	-1	--	--
TSR Ratio (%)	85.7	82.5	--	--
Cellulose Fiber	0.30%	--	--	--
CA Angularity (%)	100	100	--	--
FA Angularity (%)	46.5	45.47	--	--
RAP %				
RAP %	0	10	27	27
RAP %AC				
RAP %AC		6.01	5.20	5.20

^a N_{ini} , N_{des} , and N_{max} are 7, 65, and 105, respectively.

For SMA and 442 mixes, as-designed JMF were not available.

**Appendix B: Quality Control & Quality Assurance Data
(Asphalt Pavement)**

SMA Mix QA Data

Table B1. ODOT SMA mix field density and pay factor.

Lot/Day	Date	Density	Pay Factor	Represented Quantity (TONS)
1	03-10-05	94.9	1.04	1,047
2	03-10-05	94.7	1.04	1,423
3	05-10-05	92.5	0.98	913
4	07-10-05	94.4	1.04	1,258
5	13-10-05	95.5	1.04	1,760
6	15-10-05	94.6	1.04	1,543
7	17-10-05	94.2	1.04	1,005
8	30-10-05	94.2	1.04	1,817
9	03-10-05	94.8	1.04	1,254
10	04-11-05	94.8	1.04	986
11	04-11-05	92.7	0.98	1,189
Total				14,199

Table B2. ODOT SMA mix bulk specific gravity (Gmb) and percent air void (Marshall Pill Test).

Sample Date	Test Date	VMA (%)	Gmm	Gmb		% Void	
				Contractor	ODOT	Contractor	ODOT
10-31-05	11-02-05	15.5	2.420	2.328	2.331	3.8	3.7
10-15-05	10-19-05	-	2.420	2.320	2.336	4.1	3.5
10-14-05	10-17-05	-	2.425	2.330	2.354	3.9	2.9
10-13-05	10-13-05	14.8	2.429	2.348	2.354	3.3	3.1
10-05-05	10-06-05	15.7	2.427	2.324	2.326	4.2	4.2
10-03-05	10-04-05	15.3	2.417	2.335	2.334	3.4	3.4
10-03-05	10-03-05	15.1	2.422	2.340	2.338	3.4	3.5

Table B3. ODOT SMA mix maximum specific gravity (Gmm)

Date	Gmm	
	Contractor	ODOT
10-31-05	2.42	2.427
10-19-05	2.428	2.441
10-14-05	2.425	2.449
10-13-05	2.429	2.425
10-03-05	2.417	2.418
10-03-05	2.422	2.419

ODOT 442 Mix QA data

Table B4. ODOT 442 mix field density and pay factor.

Lot/Day	Date	Density	Pay Factor	Represented Quantity (TONS)
1	09-20-05	95.1	1.04	1,908
2	09-21-05	94.0	1.04	1,665
3	09-22-05	93.5	1.00	1,782
4	09-23-05	93.5	1.00	1,188
5	10-12-05	94.4	1.04	3,771
6	10-13-05	96.5	1.00	2,399
7	10-29-05	95.3	1.04	1,031
8	10-29-05	94.9	1.04	1,446
9	10-30-05	94.1	1.04	1,247
10	11-08-05	94.1	1.04	418
			Total	16,858

Table B5. ODOT 442 mix bulk specific gravity (Gmb) and percent air void.

Sample Date	Test Date	VMA (%)	Gmm	Gmb		Percent Void	
				Contractor	ODOT	Contractor	ODOT
10-29-05	11-02-05	12.3	2.441	2.364	2.376	3.2	2.7
10-11-05	10-12-05	12.5	2.435	2.359	2.366	3.1	2.8
09-19-05	09-21-05	12.3	2.449	2.367	2.369	3.3	3.3
09-19-05	09-21-05	12.3	2.449	2.391	2.394	2.4*	2.2*

* Percent air void at N_{max}

Table B6. ODOT 442 mix maximum specific gravity (Gmm)

Date	Contractor	ODOT
10-29-05	2.441	2.453
10-11-05	2.435	2.441
09-19-05	2.449	2.453

Table B7. ODOT 302 mix QA Data: Gradation and Extraction for Binder Content

Date	Ohio DOT Test Results, Percent Passing														Contractor QC Data	
	1.5 in. (38 mm)	1 in. (25 mm)	3/4 in. (19 mm)	1/2 in. (12.5 mm)	3/8 in. (9.5 mm)	#4 (4.75 mm)	#8 (2.36 mm)	#16 (1.18 mm)	#30 (0.600 mm)	#50 (0.300 mm)	#100 (0.150 mm)	#200 (0.075 mm)	AC%	AC% (Nuc Gauge)	#4	AC
JMF	100	87	74	59	52	34	26	18	12	6	4	2.8	4.00		34	4.0
7-13-05	100	88	82	72	64	39	27	20	14	9	5	3	5.44	4.6	30	4.8
7-26-05	100	91	74	56	47	31	23	18	13	8	5	2.8	4.04	3.6		
8-12-05	98	90	81	69	60	39	29	22	16	9	5	2.8	4.72	3.7	35	4.0
8-15-05	100	93	79	60	51	32	25	20	15	9	5	2.6	3.99	3.3	32	3.8
8-16-05	100	90	80	66	57	39	29	22	15	9	5	2.6	4.82	3.7	35	4.4
8-16-05	100	85	78	67	59	39	29	22	16	9	5	2.7	4.61	3.7	33	4.1
8-22-05	100	89	79	67	57	35	27	21	15	9	5	2.8	4.94	4.0	35	4.3
8-26-05	100	93	80	64	54	34	26	20	15	9	5	2.7	4.57	4.0	35	3.8
8-28-05	100	94	86	71	61	42	33	25	18	11	6	3.3	5.14	4.4	36	4.3
8-31-05	99	92	81	70	62	41	30	23	16	10	5	2.7	4.69	3.9	35	4.2
9-06-05	100	89	80	68	60	40	29	22	15	8	4	2.1	4.67	3.9	34	3.9
9-08-05	100	91	85	66	59	44	33	23	16	11	7	3.7	3.66	4.5	36	4.5
9-10-05	100	95	87	75	65	43	31	23	16	10	6	3.1	5.44	4.5	36	4.2
9-13-05	100	94	84	68	58	40	31	23	16	10	6	3.1	4.89	4.0	37	3.8
9-16-05	100	86	75	58	44	30	24	19	14	9	5	3	4.32	3.4	35	4.2
9-19-05	99	87	78	61	53	39	30	23	16	10	6	3.3	4.85	4.2	29	3.6
9-22-09	99	90	81	68	58	36	27	21	15	9	5	3.1	5.37	4.2	37	3.8
9-26-05	97	86	74	62	53	39	30	23	16	10	6	3.3	4.82	4.0	36	3.7
9-27-05	100	86	78	66	56	41	31	23	17	11	7	4	5.06	4.5	36	4.1
9-28-05	100	94	86	73	62	46	34	25	17	10	6	3.6	5.56	4.5	34	3.8
9-30-05	100	89	68	47	37	26	21	16	12	8	5	2.2	3.87	3.3	29	3.6

Table B8. ODOT FRL mix QA Data: Gradation and Extraction for Binder Content

Date	Ohio DOT Test Results, Percent Passing														Contractor QC Data		
	1.5 in. (38 mm)	1 in. (25 mm)	3/4 in. (19 mm)	1/2 in. (12.5 mm)	3/8 in. (9.5 mm)	#4 (4.75 mm)	#8 (2.36 mm)	#16 (1.18 mm)	#30 (0.600 mm)	#50 (0.300 mm)	#100 (0.150 mm)	#200 (0.075 mm)	AC%	AC% (Nuc Gauge)	#4	AC	
B322229																	
JMF	100	87	74	59	52	34	26	18	12	6	3	2.3	4.60		34	4.60	
7-07-05	100	94	84	71	62	38	26	20	14	9	5	2.9	5.41	4.6	40	4.7	
7-09-05	100	86	77	66	59	38	27	20	14	9	5	2.8	5.92	5.2	35	4.7	
7-26-05	100	82	73	63	55	36	27	20	14	9	5	3.0	5.19	4.2			
8-04-05	100	93	85	71	63	43	32	24	16	9	4	2.1	5.68	4.7	37	4.7	
8-04-05	100	91	85	70	63	43	32	24	17	10	5	2.8	5.71	4.7	37	4.7	
8-08-05	100	95	87	75	67	45	33	24	17	10	5	2.8	5.79	4.8	34	4.6	
8-11-05	100	90	81	69	61	41	30	22	16	10	6	3.1	5.69	4.8	34	4.7	
8-11-05	100	90	81	69	61	41	30	22	16	10	6	3.1	5.69	4.8	34	4.7	
8-15-05	100	93	83	71	61	40	30	23	16	10	5	2.7	5.27	4.4	33	4.5	
8-21-05	100	92	81	69	58	36	28	22	16	10	5	2.8	5.77	4.7	36	4.8	
8-22-05	100	92	84	74	59	38	29	22	16	10	6	3.0	5.67	4.8	35	4.6	
9-11-05	100	90	85	69	58	38	29	22	16	10	6	3.4	5.68	4.6	35	4.7	
9-14-05	100	92	83	68	55	38	29	22	16	10	6	3.2	5.55	4.8	36	4.9	
9-20-05	100	89	82	71	61	42	32	24	17	11	6	3.4	5.94	5.3	39	4.6	
B322254																	
JMF	100	87	74	60	52	34	26	19	13	7	4	2.7	4.60		34	4.60	
10-05-05	100	89	80	64	52	34	26	20	14	9	6	3.2	5.27	4.8	34	4.7	
10-07-05	100	93	83	59	50	34	26	20	15	10	6	3.4	5.33	4.7	36	4.7	
10-13-05	99	91	85	74	61	38	30	22	17	10	6	3.4	5.33	5.0	32	4.7	
10-13-05	100	84	76	65	59	41	31	23	16	10	6	3.3	5.80	5.1	39	4.9	
10-18-05	100	85	76	64	56	40	30	21	15	10	6	3.0	6.06	5.3	39	4.7	

*JMF change from B322229 to B322254 was for minor gradation adjustment.

Table B9. ODOT PG binder test results.

Date	Temp (°C)	Dynamic Shear Rheometer			Spec $G^*/\sin\delta$ Minimum 1.00 kPa
		G^* (kPa)	Phase Angle, δ (degree)	$G^*/\sin\delta$ (kPa)	
PG 76-22 SBS (for SMA and 442 Mixes)					
9/19/2005	76	1.88	73.5	1.96	OK
10/6/2005	76	1.42	73.2	1.48	OK
11/2/2005	76	1.42	67.6	1.54	OK
PG 64-22 (for FRL and 302 Mixes)					
4/10/2006	64	1.15	86.9	1.15	OK
6/17/2005	64	1.53	88.0	1.53	OK
11/15/2004	64	2.16	71.1	2.28	OK

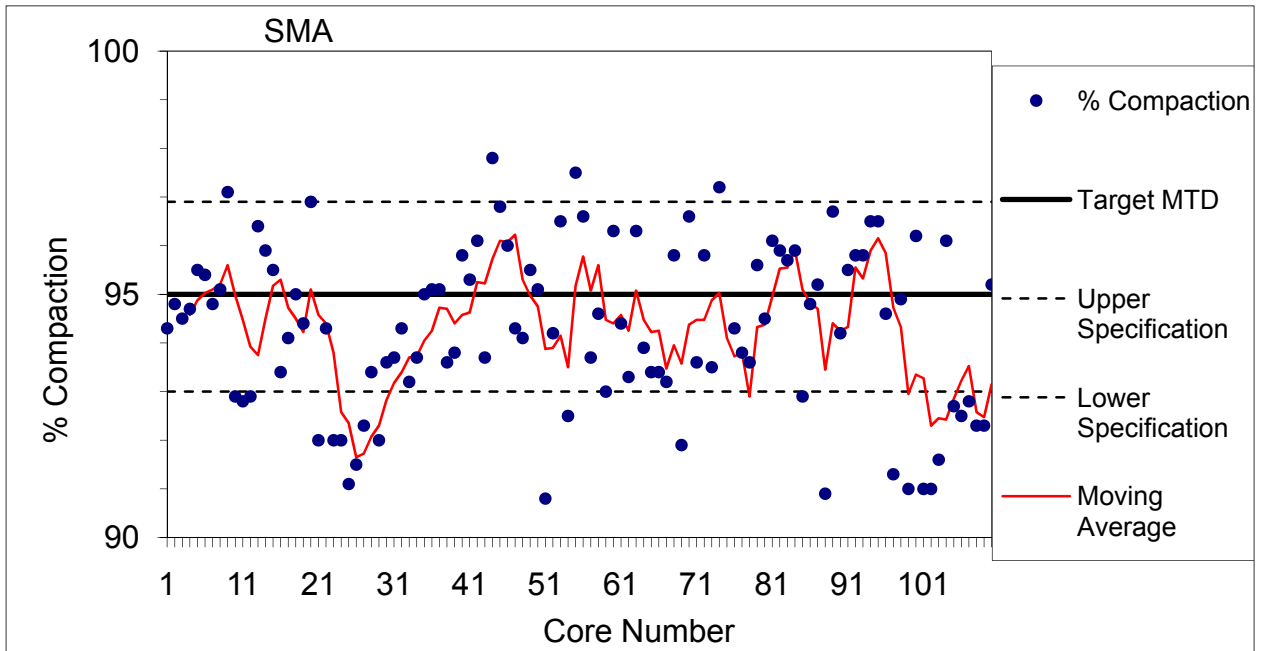


Figure B1. SMA mix density QC data.

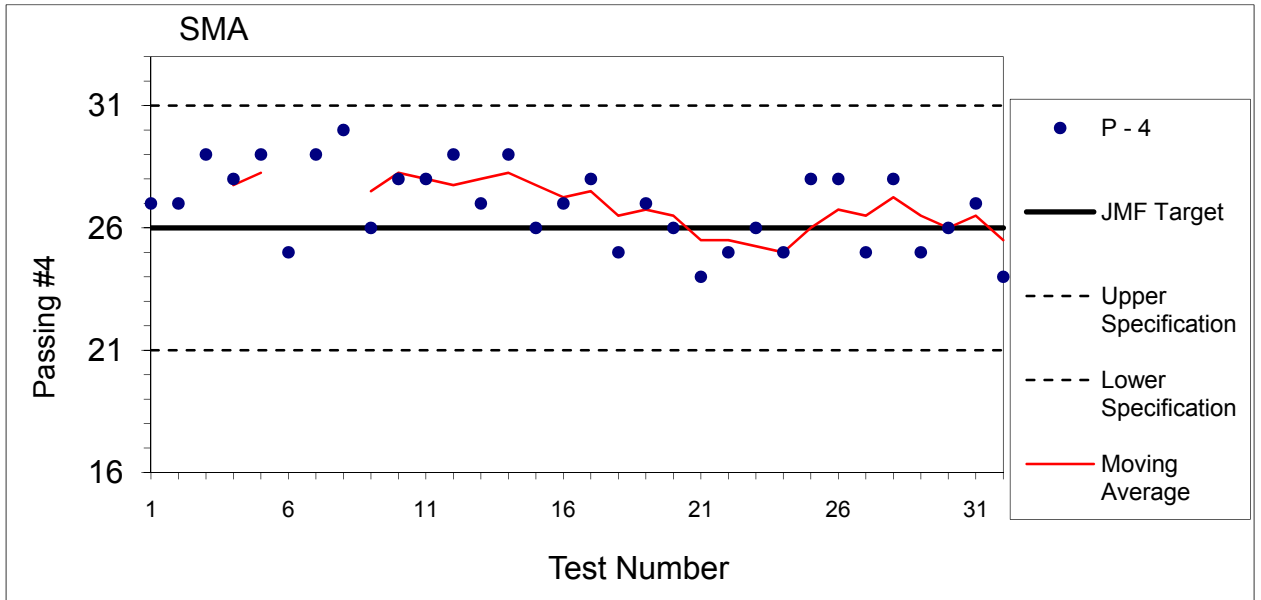


Figure B2. SMA mix #4 sieve gradation QC data.

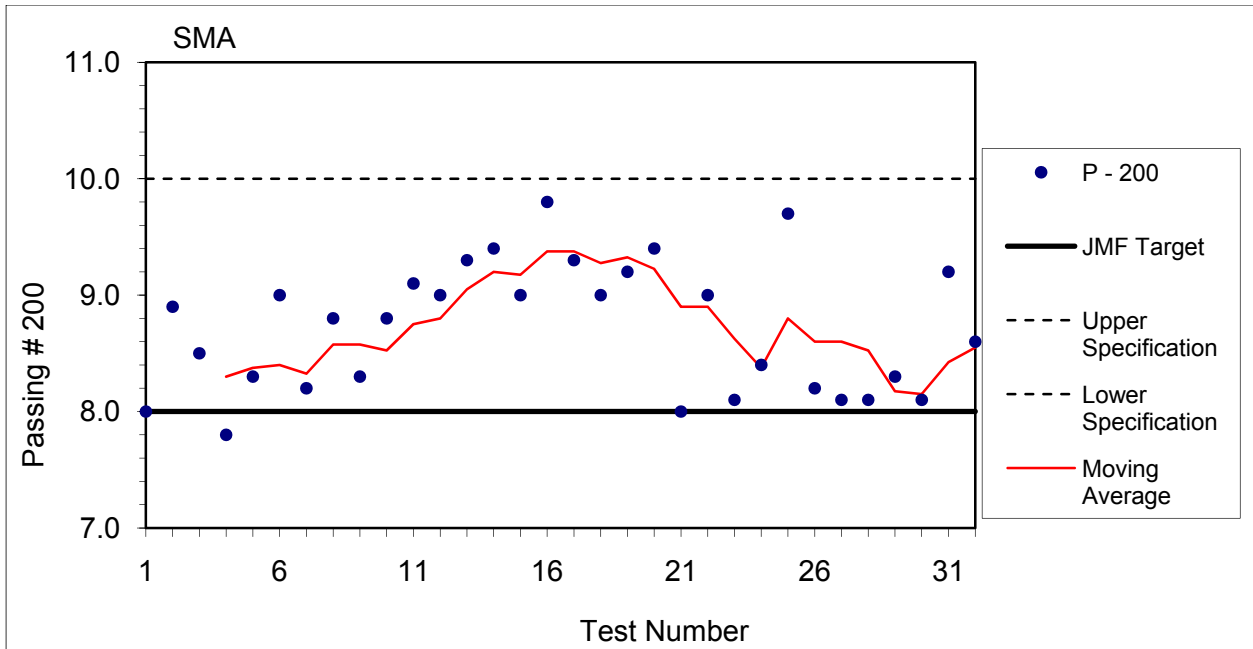


Figure B3. SMA mix #200 sieve gradation QC data.

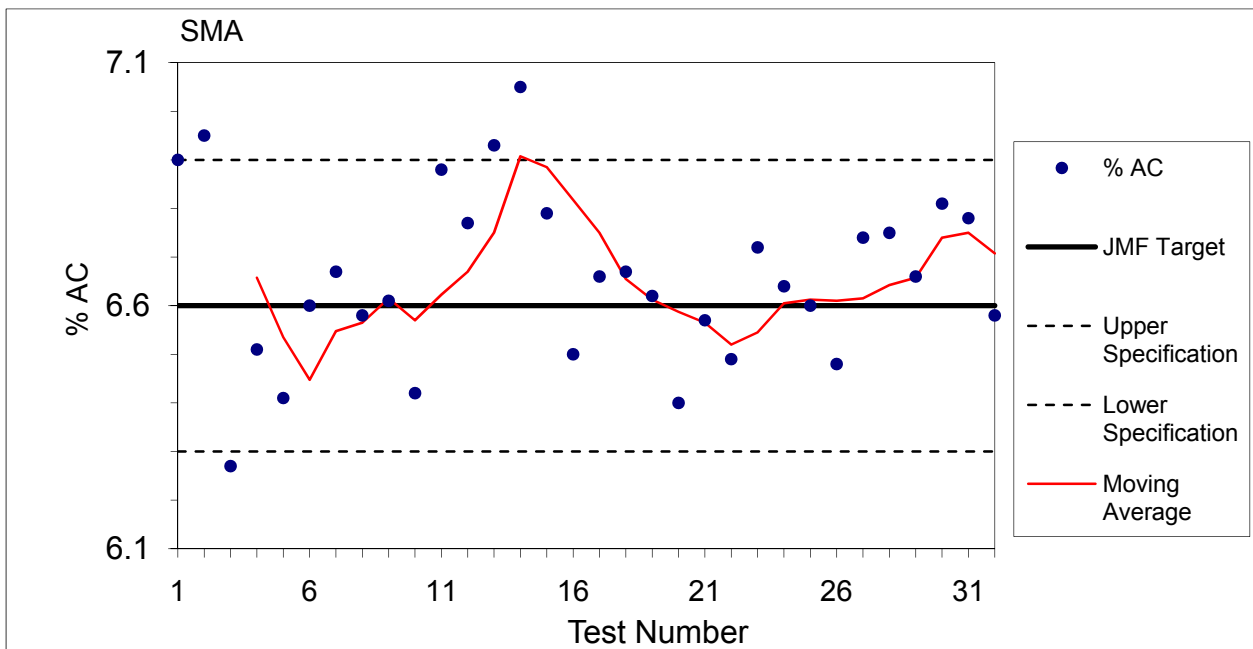


Figure B4. SMA mix binder content QC data.

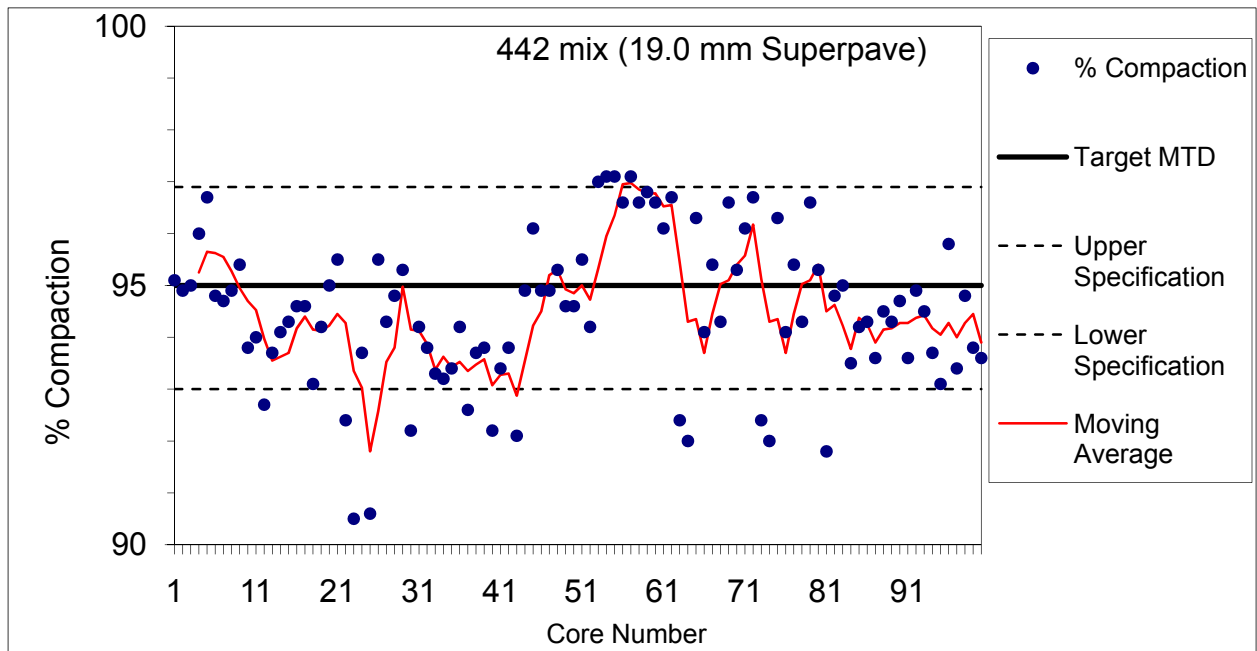


Figure B5. ODOT 442 mix density QC data.

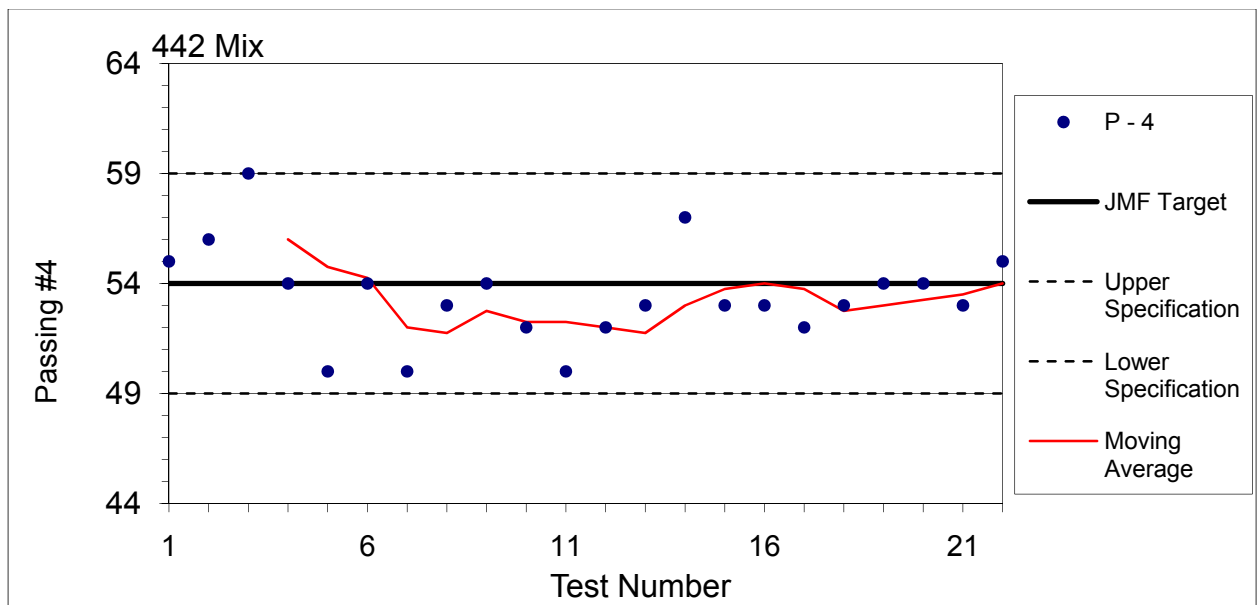


Figure B6. ODOT 442 mix #4 sieve gradation QC data.

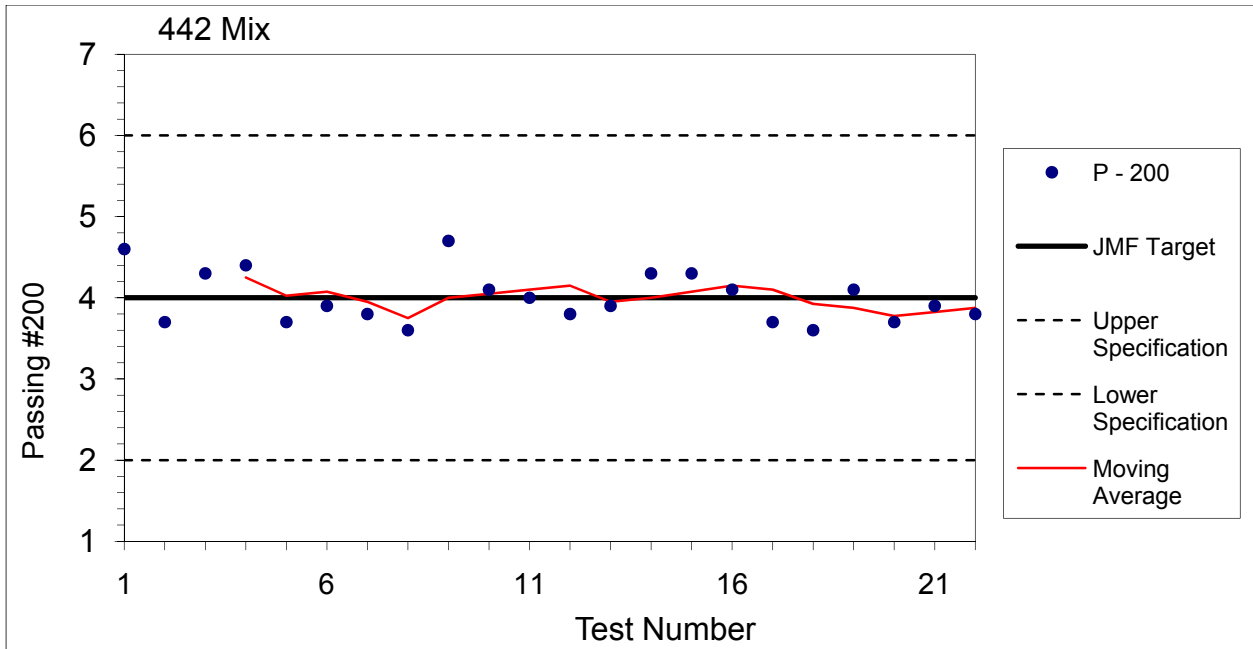


Figure B7. ODOT 442 mix #200 sieve gradation QC data.

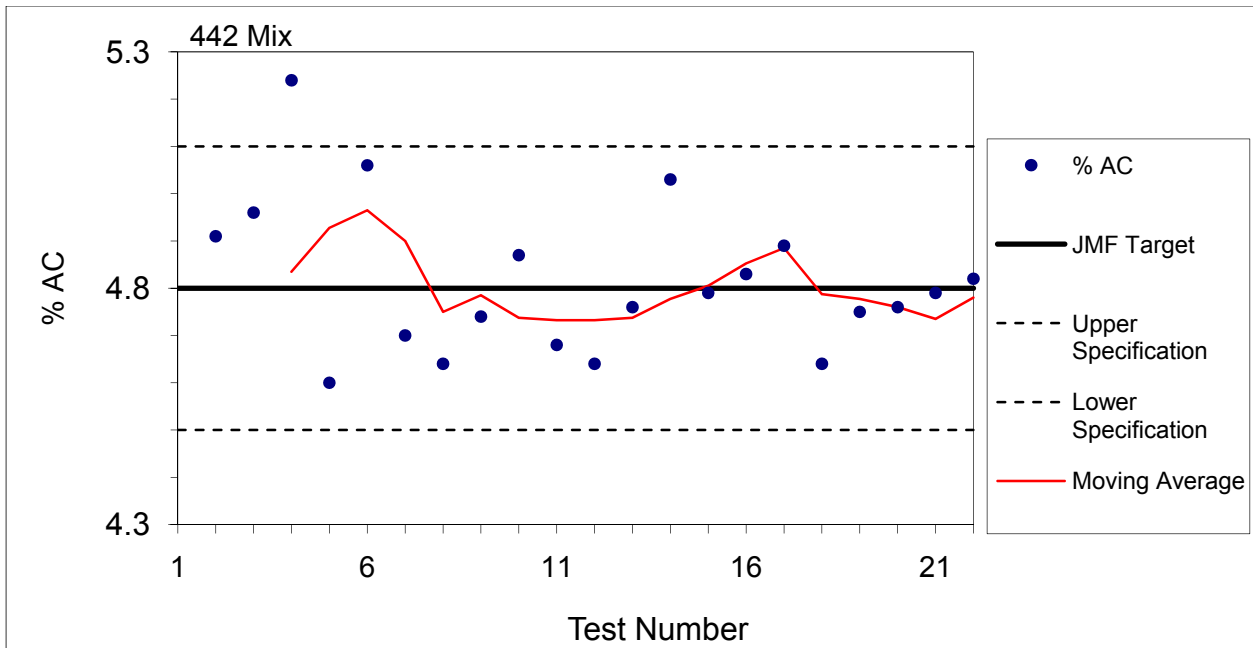


Figure B8. ODOT 442 mix binder content QC data.

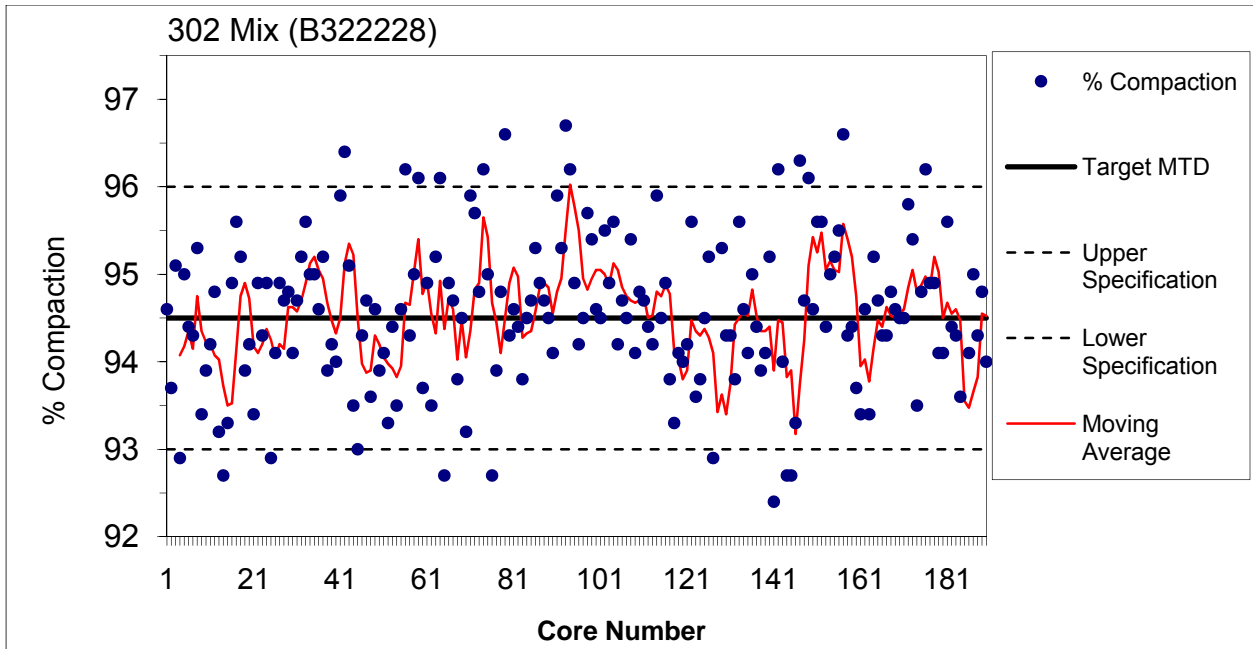


Figure B9. ODOT 302 mix density QC data.

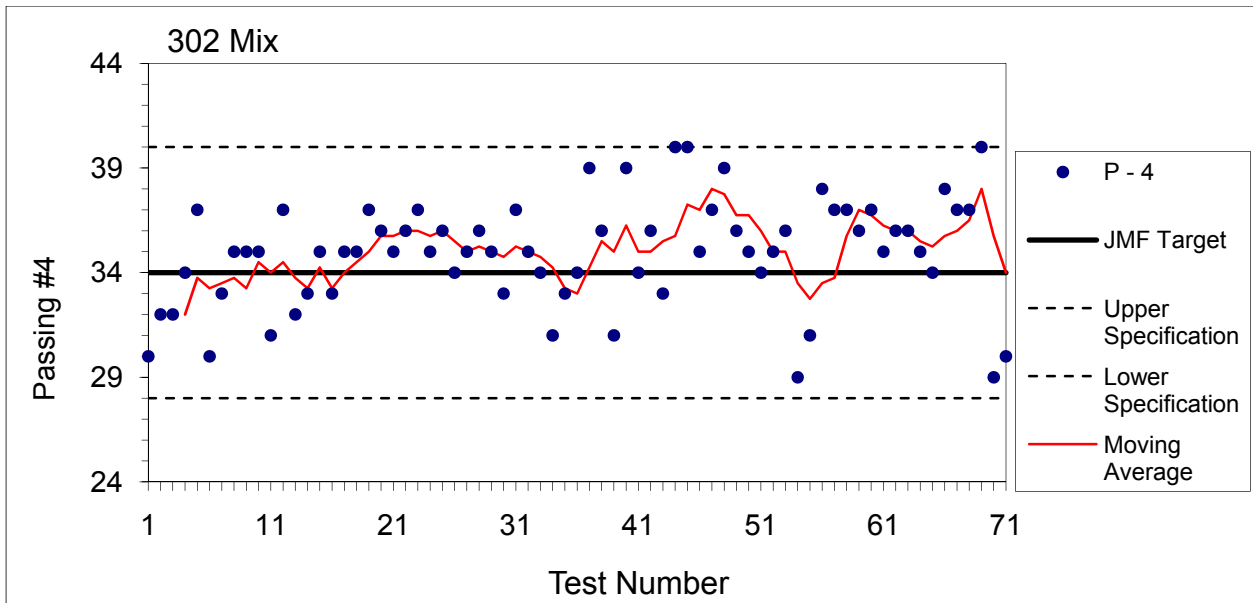


Figure B10. ODOT 302 mix #4 sieve gradation QC data.

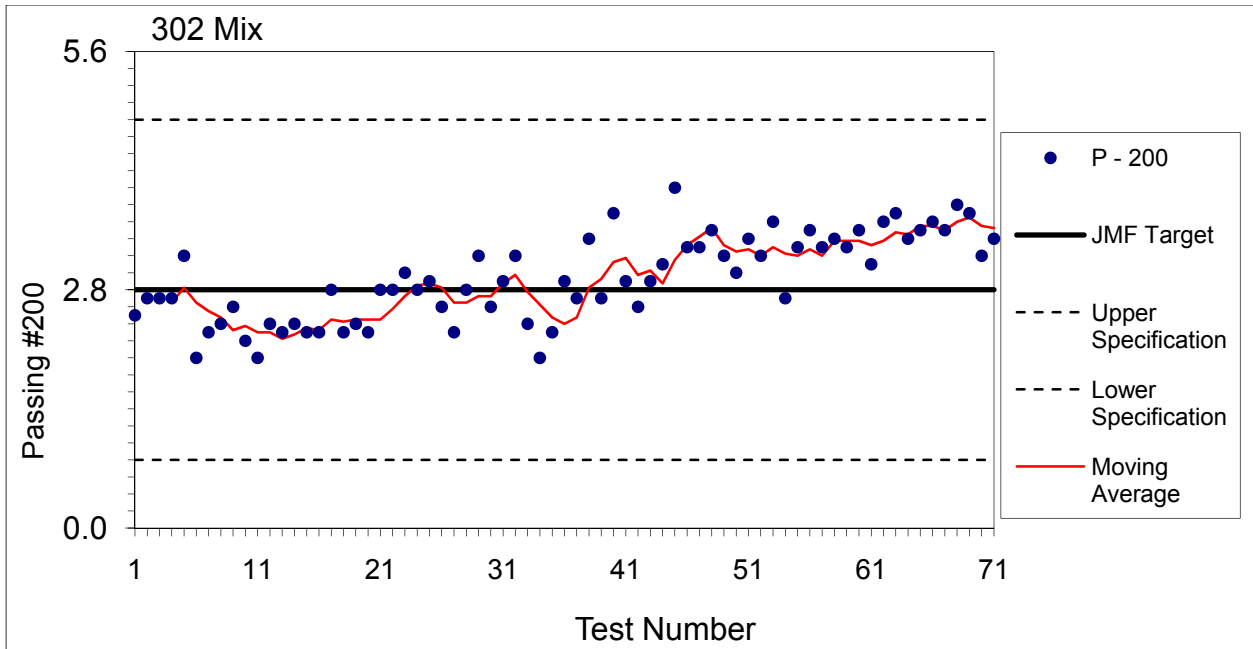


Figure B11. ODOT 302 mix #200 sieve gradation QC data.

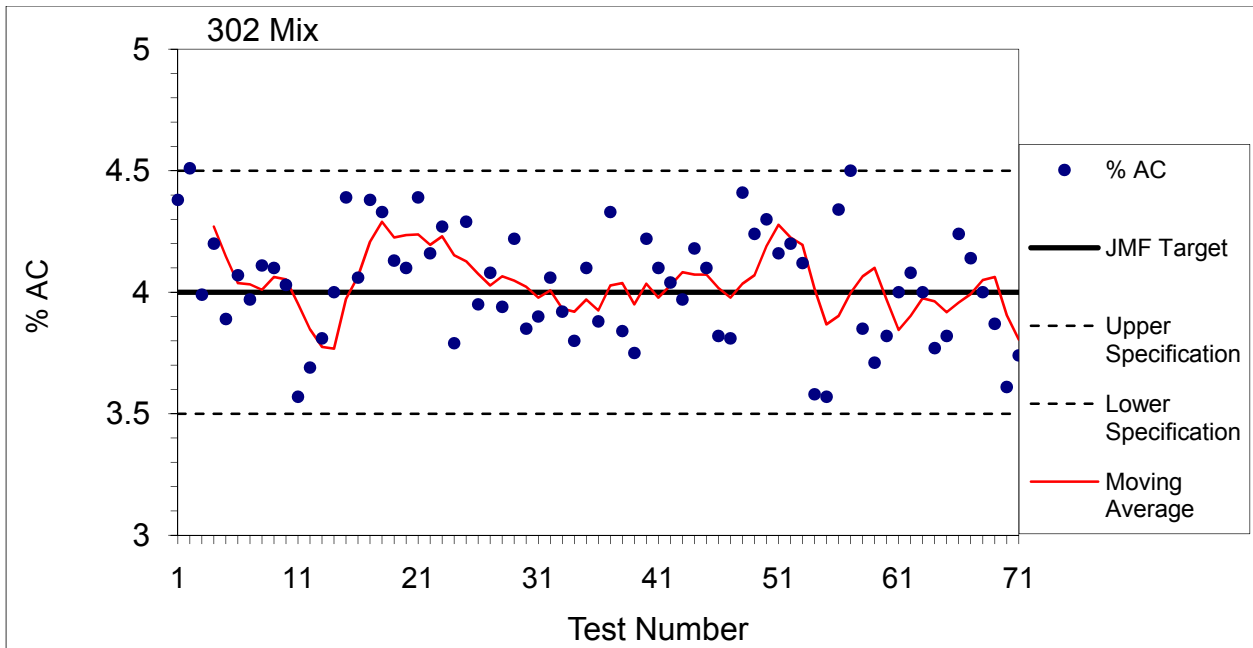


Figure B12. ODOT 302 mix binder content QC data.

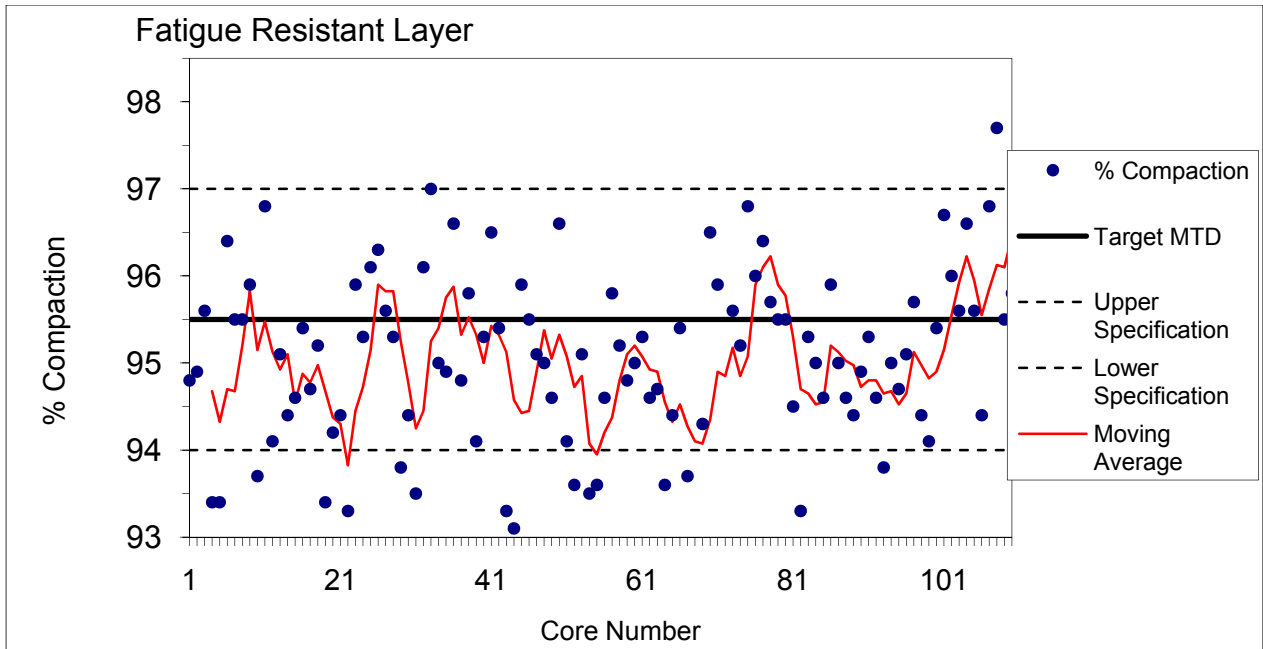


Figure B13. FRL mix density QC data.

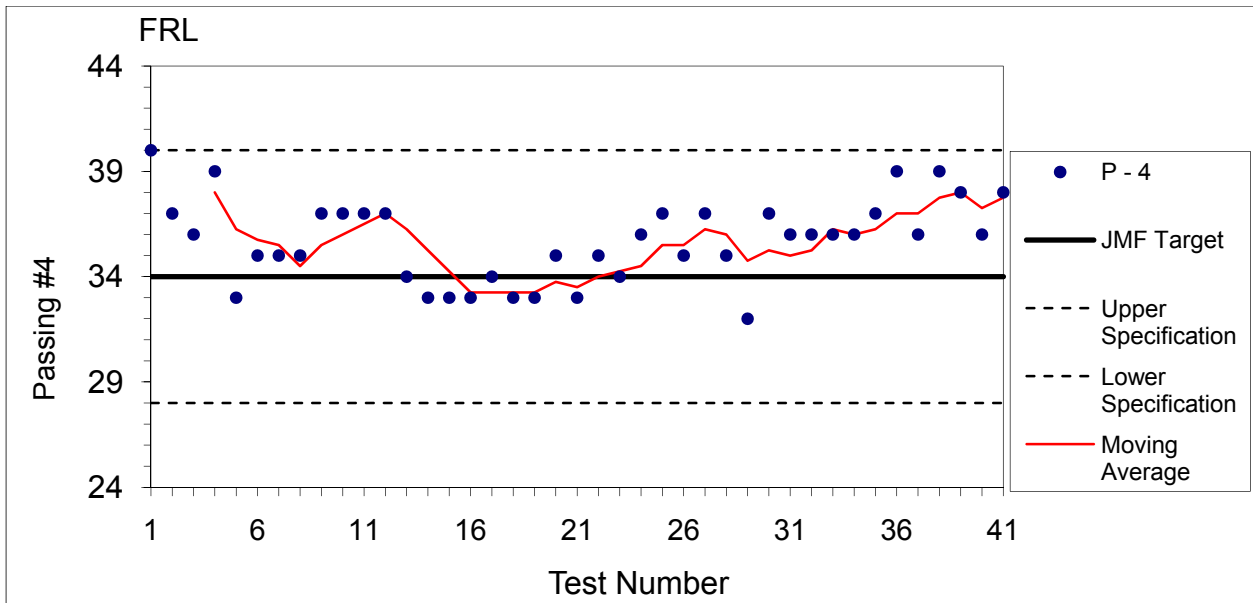


Figure B14. FRL mix #4 sieve gradation QC data.

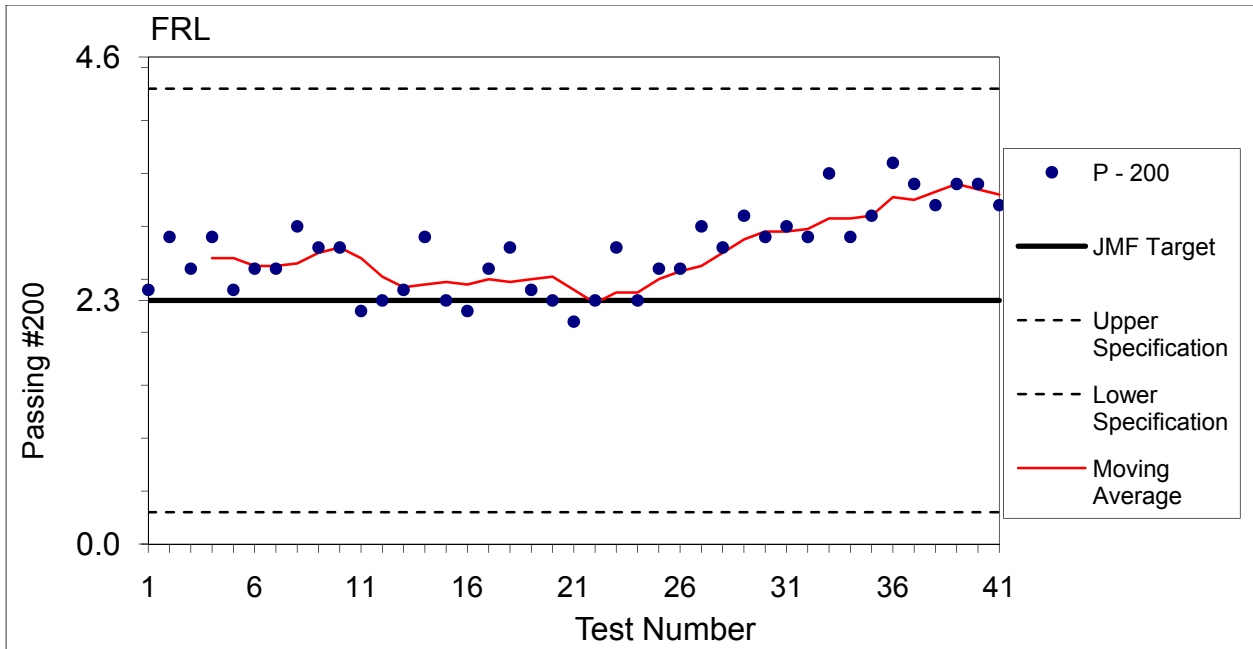


Figure B15. FRL mix #200 sieve gradation QC data.

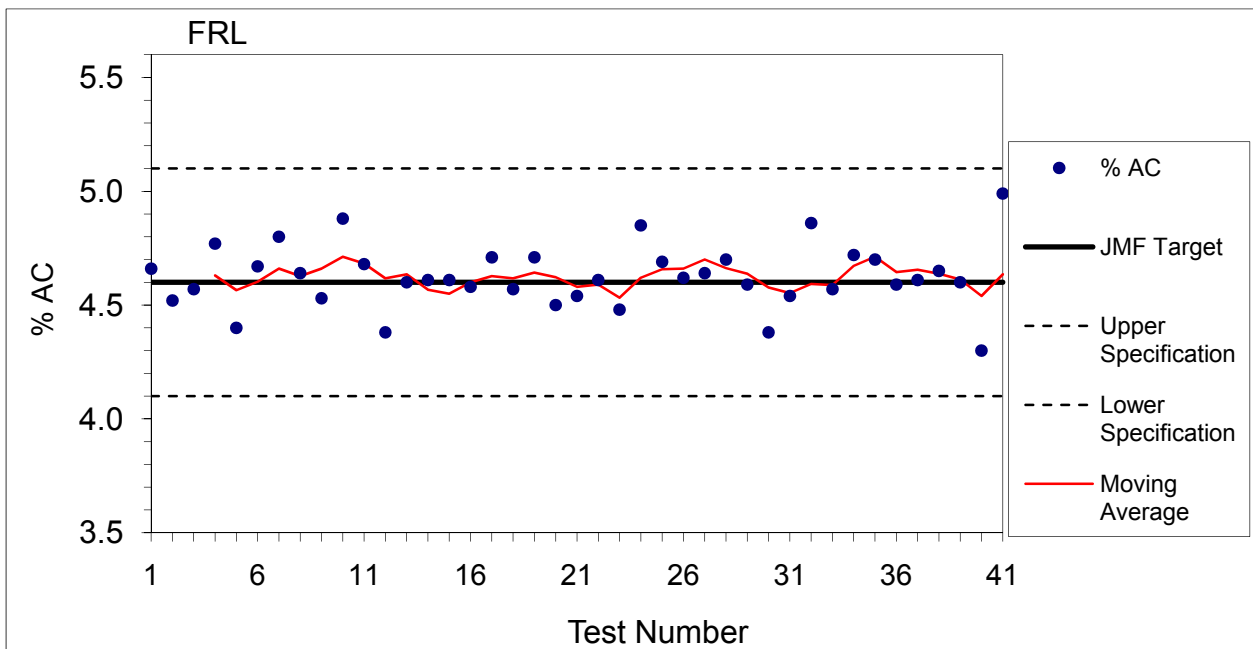


Figure B16. FRL mix binder content QC data.

**Appendix C: Quality Control & Quality Assurance Data
(Portland Cement Concrete Pavement)**

**Table C1. Compressive strength of cylinders, 28 day curing.
(English Unit)**

Date	%Air	Slump	Compressive Strength, psi		
			1	2	Average
Mix A, GGBFS					
4/18/2006	6.5	2	4860	5200	5030
4/17/2006	6.5	2	4900	4910	4905
7/21/2005	5.5	1.5	6770	6320	6545
7/21/2005	6.1	1.5	5080	6160	5620
Average					5525
Mix B, Fly ash					
7/27/2005	5.5	1.5	6730	5870	6300

**Table C2. Compressive strength of cylinders, 28 day curing.
(SI Unit)**

Date	%Air	Slump	Compressive Strength, MPa		
			1	2	Average
Mix A, GGBFS					
4/18/2006	6.5	50.8	33.51	35.85	34.68
4/17/2006	6.5	50.8	33.78	33.85	33.82
7/21/2005	5.5	38.1	46.68	43.57	45.13
7/21/2005	6.1	38.1	35.03	42.47	38.75
Average					38.09
Mix B, Fly ash					
7/27/2005	5.5	38.1	46.40	40.47	43.44

**Table C3. PCC Inspectors report; Batch weight of Mix A (GGBFS) for 1.00 yd³.
(English Unit)**

Date	Location	Time	Cementitious Material	FA (Natural Sand)	Moist	FA Batch Weight	CA1 (#8 LS)	Moist	CA1 Batch Weight	CA2 (#467 LS)	Moist	CA2 Batch Weight	Water
			lb	lb	%	lb	lb	%	lb	lb	%	lb	lb
06/30/05	MAINLINE	7:45	590	1191	5.0	1232	459	2.5	465	1402	3.3	1432	173
		9:30	589	1190	5.0	1231	459	2.5	465	1403	3.3	1433	168
		12:30	588	1189	5.0	1230	459	2.5	465	1406	3.3	1436	168
07/05/05	HAUL ROAD	8:30	590	1186	4.5	1221	458	2.5	464	1410	3.0	1436	182
07/11/05	MAINLINE	8:15	590	1178	5.3	1222	470	1.7	472	1404	2.0	1416	195
		14:15	591	1185	5.3	1229	463	1.7	465	1406	2.0	1418	190
07/12/05	MAINLINE	10:00	589	1189	5.3	1233	471	1.7	473	1413	2.5	1432	172
		14:00	591	1189	5.3	1233	472	1.7	474	1406	2.5	1425	186
07/13/05	MAINLINE	8:00	590	1187	5.3	1231	470	1.7	472	1405	2.5	1424	182
		13:30	606	1167	5.3	1211	456	1.7	458	1402	2.5	1402	202
07/14/05	MAINLINE	9:00	606	1184	5.0	1225	457	1.4	458	1407	2.1	1421	189
		11:00	588	1181	5.0	1222	464	1.4	462	1408	2.1	1422	193
07/18/05	MAINLINE	8:00	588	1185	5.3	1230	464	1.4	465	1405	2.7	1427	179
		14:00	589	1183	5.3	1228	469	1.4	470	1409	2.7	1431	177
07/19/05	MAINLINE	9:45	590	1191	5.5	1238	471	1.7	473	1406	2.7	1429	177
07/20/05	MAINLINE	7:45	588	1185	5.5	1232	462	1.5	463	1416	3.1	1443	169
07/25/05	4" SHOULDER	8:45	606	1188	5.2	1232	468	1.2	468	1404	2.4	1421	188
		13:00	589	1188	5.2	1232	467	1.2	467	1399	2.4	1416	183
08/08/05	901+00 – 854+00 sh ¹	8:40	588	1184	5.5	1231	468	1.9	471	1404	2.3	1420	175
		16:15	590	1181	5.5	1229	464	1.9	464	1402	2.3	1418	190
08/09/05	1018+00 – 982+00 sh	8:40	588	1196	5.1	1239	467	1.9	470	1411	2.2	1427	185
		15:30	589	1196	5.1	1239	460	1.9	463	1415	2.2	1430	179
08/10/05	864+00 – 926+65	8:00	608	1198	5.1	1242	458	1.9	474	1411	2.2	1420	177
		15:30	589	1195	5.1	1239	471	1.9	474	1411	2.2	1426	170
08/17/05	1025+00 – 1028+00	8:00	595	1178	5.2	1222	463	1.9	466	1408	2.0	1420	177
08/25/05	RAMP D	13:00	588	1185	5.1	1227	459	1.9	462	1410	2.0	1422	192
10/19/05	1014+35 – 1011+75	15:15	588	1191	4.7	1229	462	2.0	466	1404	2.8	1427	181
11/02/05	WIM ²	14:15	588	1192	5.7	1242	469	2.0	473	1406	4.0	1446	147
04/24/06	CARR-C,D	8:30	588	1202	4.9	1242	472	1.5	473	1428	2.4	1446	191

¹ sh=shoulder; ² WIM=Weigh-In-Motion

**Table C4. PCC Inspectors report; Batch weight of Mix A (GGBFS) for 1.00 m³.
(SI Unit)**

Date	Location	Time	Cementitious Material	FA (Natural Sand)	Moist	FA Batch Weight	CA1 (#8 LS)	Moist	CA1 Batch Weight	CA2 (#467 LS)	Moist	CA2 Batch Weight	Water
			kg	kg	%	kg	kg	%	kg	kg	%	kg	kg
06/30/05	MAINLINE	7:45	350	706.6	5.0	730.9	272.3	2.5	275.9	831.8	3.3	849.6	102.6
		9:30	349	706.0	5.0	730.3	272.3	2.5	275.9	832.4	3.3	850.2	99.7
		12:30	349	705.4	5.0	729.7	272.3	2.5	275.9	834.1	3.3	851.9	99.7
07/05/05	HAUL ROAD	8:30	350	703.6	4.5	724.4	271.7	2.5	275.3	836.5	3.0	851.9	108.0
07/11/05	MAINLINE	8:15	350	698.9	5.3	725.0	278.8	1.7	280.0	833.0	2.0	840.1	115.7
		14:15	351	703.0	5.3	729.1	274.7	1.7	275.9	834.1	2.0	841.3	112.7
07/12/05	MAINLINE	10:00	349	705.4	5.3	731.5	279.4	1.7	280.6	838.3	2.5	849.6	102.0
		14:00	351	705.4	5.3	731.5	280.0	1.7	281.2	834.1	2.5	845.4	110.3
07/13/05	MAINLINE	8:00	350	704.2	5.3	730.3	278.8	1.7	280.0	833.5	2.5	844.8	108.0
		13:30	360	692.4	5.3	718.5	270.5	1.7	271.7	831.8	2.5	831.8	119.8
07/14/05	MAINLINE	9:00	360	702.4	5.0	726.8	271.1	1.4	271.7	834.7	2.1	843.0	112.1
		11:00	349	700.7	5.0	725.0	275.3	1.4	274.1	835.3	2.1	843.6	114.5
07/18/05	MAINLINE	8:00	349	703.0	5.3	729.7	275.3	1.4	275.9	833.5	2.7	846.6	106.2
		14:00	349	701.8	5.3	728.5	278.2	1.4	278.8	835.9	2.7	849.0	105.0
07/19/05	MAINLINE	9:45	350	706.6	5.5	734.5	279.4	1.7	280.6	834.1	2.7	847.8	105.0
07/20/05	MAINLINE	7:45	349	703.0	5.5	730.9	274.1	1.5	274.7	840.1	3.1	856.1	100.3
07/25/05	10CM SHOULDER	8:45	360	704.8	5.2	730.9	277.7	1.2	277.7	833.0	2.4	843.0	111.5
		13:00	349	704.8	5.2	730.9	277.1	1.2	277.1	830.0	2.4	840.1	108.6
08/08/05	901+00 – 854+00 sh ¹	8:40	349	702.4	5.5	730.3	277.7	1.9	279.4	833.0	2.3	842.4	103.8
		16:15	350	700.7	5.5	729.1	275.3	1.9	275.3	831.8	2.3	841.3	112.7
08/09/05	1018+00 – 982+00 sh	8:40	349	709.6	5.1	735.1	277.1	1.9	278.8	837.1	2.2	846.6	109.8
		15:30	349	709.6	5.1	735.1	272.9	1.9	274.7	839.5	2.2	848.4	106.2
08/10/05	864+00 – 926+65	8:00	361	710.7	5.1	736.8	271.7	1.9	281.2	837.1	2.2	842.4	105.0
		15:30	349	709.0	5.1	735.1	279.4	1.9	281.2	837.1	2.2	846.0	100.9
08/17/05	1025+00 – 1028+00	8:00	353	698.9	5.2	725.0	274.7	1.9	276.5	835.3	2.0	842.4	105.0
08/25/05	RAMP D	13:00	349	703.0	5.1	727.9	272.3	1.9	274.1	836.5	2.0	843.6	113.9
10/19/05	1014+35 – 1011+75	15:15	349	706.6	4.7	729.1	274.1	2.0	276.5	833.0	2.8	846.6	107.4
11/02/05	WIM ²	14:15	349	707.2	5.7	736.8	278.2	2.0	280.6	834.1	4.0	857.9	87.2
04/24/06	CARR-C,D	8:30	349	713.1	4.9	736.8	280.0	1.5	280.6	847.2	2.4	857.9	113.3

¹ sh=shoulder; ² WIM=Weigh-In-Motion

Table C5. PCC Inspectors report; Batch weight of Mix B (Fly ash) for 1.00 yd³. (English Unit)

Date	Location	Time	Cementitious Material	FA (Natural Sand)	Moist	FA Batch Weight	CA1 (#8 LS)	Moist	CA1 Batch Weight	CA2 (#467 LS)	Moist	CA2 Batch Weight	Water
			lb	lb	%	lb	lb	%	lb	lb	%	lb	lb
07/28/05	839+00 – 819+00	8:45	595	1197	5.3	1241	493	1.4	489	1429	2.4	1447	142
		14:30	596	1171	5.3	1214	490	1.4	486	1426	2.4	1460	177
		17:15	596	1168	5.3	1211	489	1.4	485	1438	2.4	1473	168
08/01/05	796+90 - 777+55	7:50	591	1175	4.9	1214	487	1.4	483	1409	2.8	1432	180
08/02/05	769+30 – 742+20	6:45	770	1181	5.0	1221	491	1.4	487	1408	2.0	1420	185
		13:30	596	1181	5.0	1221	491	1.4	487	1421	2.0	1433	162
08/03/05	742+20 – 717+10	6:30	597	1180	6.0	1232	492	1.4	488	1410	3.0	1436	159
		10:45	591	1178	6.0	1230	492	1.4	488	1410	3.0	1436	172
08/04/05	717+10 – 693+00	4:15	593	1180	5.7	1228	495	1.9	493	1422	2.9	1447	152
		9:00	602	1176	5.7	1224	493	1.9	492	1408	2.9	1433	167
08/11/05	835+85 – 799+10	9:00	593	1179	6.5	1237	499	1.9	497	1411	3.3	1441	147
08/16/05	750+40 – 693+35 sh ¹	8:15	595	1177	5.3	1222	491	1.9	489	1420	2.3	1436	164
		14:00	593	1165	5.3	1209	595	1.9	593	1411	2.3	1427	180
08/17/05	693+67 – 761+15	12:25	595	1179	5.2	1222	491	1.9	489	1441	2.0	1423	186
08/18/05	778+00 – 822+80	7:30	591	1168	5.7	1216	491	1.9	489	1412	2.2	1427	182
		13:00	594	1178	5.7	1226	498	1.9	497	1415	2.2	1430	168
08/22/05	841+10 – 851+90 sh	8:15	595	1174	5.5	1220	498	1.9	496	1408	2.5	1427	171
08/23/05	689+65 – 669+25	8:00	592	1177	5.2	1219	500	1.9	498	1411	2.4	1428	175
		15:30	593	1172	5.2	1215	489	1.9	488	1410	2.4	1427	169
08/24/05	APLCRK, RAMPS A,B,C	5:15	596	1176	5.1	1217	493	1.9	492	1411	2.0	1423	187
08/25/05	APLCRK, RAMP C	8:15	597	1177	5.1	1218	495	1.9	494	1407	2.0	1419	187
09/15/05	669+25 – 641+75	8:00	594	1175	5.3	1219	489	1.9	487	1413	2.0	1425	184
		4:20	594	1183	5.3	1227	491	1.9	490	1423	2.0	1435	163
09/19/05	846+00	9:20	594	1170	5.6	1217	490	2.0	489	1411	2.3	1427	168
09/21/05	690+15 – 650+95	10:45	595	1178	5.7	1227	491	1.7	489	1415	1.9	1426	182
		14:25	594	1170	5.7	1218	499	1.7	496	1406	1.9	1417	190
10/13/05	RAMP F	10:30	594	1175	5.4	1220	491	2.0	490	1411	4.0	1452	154
10/17/05	8" SHLDR	11:15	591	1181	5.2	1223	495	2.0	494	1410	3.6	1444	163



¹ sh=shoulder

Table C6. PCC Inspectors report; Batch weight of Mix B (Fly ash) for 1.00 m³. (SI Unit)

Date	Location	Time	Cementitious Material	FA (Natural Sand)	Moist	FA Batch Weight	CA1 (#8 LS)	Moist	CA1 Batch Weight	CA2 (#467 LS)	Moist	CA2 Batch Weight	Water
			kg	kg	%	kg	kg	%	kg	kg	%	kg	kg
07/28/05	839+00 – 819+00	8:45	353	710.1	5.3	736.3	292.5	1.4	289.9	847.8	2.4	858.6	84.2
		14:30	354	694.7	5.3	720.2	290.7	1.4	288.1	846.0	2.4	866.2	105.0
		17:15	354	692.9	5.3	718.5	290.1	1.4	287.5	853.1	2.4	873.6	99.7
08/01/05	796+90 - 777+55	7:50	351	697.1	4.9	720.2	288.9	1.4	286.6	835.9	2.8	849.6	106.8
08/02/05	769+30 – 742+20	6:45	457	700.7	5.0	724.4	291.3	1.4	288.9	835.3	2.0	842.4	109.8
		13:30	354	700.7	5.0	724.4	291.3	1.4	288.9	843.0	2.0	850.2	96.1
08/03/05	742+20 – 717+10	6:30	354	700.1	6.0	730.9	291.9	1.4	289.5	836.5	3.0	851.9	94.3
		10:45	351	698.9	6.0	729.7	291.9	1.4	289.5	836.5	3.0	851.9	102.0
08/04/05	717+10 – 693+00	4:15	352	700.1	5.7	728.5	293.7	1.9	292.5	843.6	2.9	858.5	90.2
		9:00	357	697.7	5.7	726.2	292.5	1.9	291.9	835.3	2.9	850.2	99.1
08/11/05	835+85 – 799+10	9:00	352	699.5	6.5	733.9	296.0	1.9	294.9	837.1	3.3	854.9	87.2
08/16/05	750+40 – 693+35 sh ¹	8:15	353	698.3	5.3	725.0	291.3	1.9	290.1	842.4	2.3	851.9	97.3
		14:00	352	691.2	5.3	717.3	353.0	1.9	351.8	837.1	2.3	846.6	106.8
08/17/05	693+67 – 761+15	12:25	353	699.5	5.2	725.0	291.3	1.9	290.1	854.9	2.0	844.2	110.3
08/18/05	778+00 – 822+80	7:30	351	692.9	5.7	721.4	291.3	1.9	290.1	837.7	2.2	846.6	108.0
		13:00	352	698.9	5.7	727.4	295.5	1.9	294.9	839.5	2.2	848.4	99.7
08/22/05	841+10 – 851+90 sh	8:15	353	696.5	5.5	723.8	295.5	1.9	294.3	835.3	2.5	846.6	101.4
08/23/05	689+65 – 669+25	8:00	351	698.3	5.2	723.2	296.6	1.9	295.5	837.1	2.4	847.2	103.8
		15:30	352	695.3	5.2	720.8	290.1	1.9	289.5	836.5	2.4	846.6	100.3
08/24/05	APLCRK, RAMPS A,B,C	5:15	354	697.7	5.1	722.0	292.5	1.9	291.9	837.1	2.0	844.2	110.9
08/25/05	APLCRK, RAMP C	8:15	354	698.3	5.1	722.6	293.7	1.9	293.1	834.7	2.0	841.9	110.9
09/15/05	669+25 – 641+75	8:00	352	697.1	5.3	723.2	290.1	1.9	288.9	838.3	2.0	845.4	109.2
		4:20	352	701.8	5.3	727.9	291.3	1.9	290.7	844.2	2.0	851.3	96.7
09/19/05	846+00	9:20	352	694.1	5.6	722.0	290.7	2.0	290.1	837.1	2.3	846.6	99.7
09/21/05	690+15 – 650+95	10:45	353	698.9	5.7	727.9	291.3	1.7	290.1	839.5	1.9	846.0	108.0
		14:25	352	694.1	5.7	722.6	296.0	1.7	294.3	834.1	1.9	840.7	112.7
10/13/05	RAMP F	10:30	352	697.1	5.4	723.8	291.3	2.0	290.7	837.1	4.0	861.4	91.4
10/17/05	20cm SHLDR	11:15	351	700.7	5.2	725.6	293.7	2.0	293.1	836.5	3.6	856.7	96.7

¹ sh=shoulder

**Table C7. PCC air, slump, yield, and strength test results (Mix A GGBFS).
(English Unit)**

Date	Location	Temperature	Unit Weight	Batch Weight	Yield	Slump	%Air	MOR	Age for MOR	Represented Quantity
		°F	lb/ft ³	lb	ft ³	in.	%	psi	day	yd ³
06/30/05	MAINLINE	80	143.35	3892	27.150	1.5	5.7	525	5	900
	MAINLINE	80	142.67	3885	27.231	1.5	6.0	575	5	
07/05/05	HAUL ROAD	81	143.43	3892	27.135	1.5	5.4	675	6	970
07/11/05	975+00	73	144.40	3895	26.974	1.5	5.4	650	7	1000
	980+00	80	145.20	3892	26.804	1.5	4.2	650	7	
07/12/05	948+25	79	145.28	3898	26.831	1.5	5.0	650	7	1310
	940+00	84	144.16	3907	27.102	1.5	5.4	650	7	
07/13/05	933+00	79	142.95	3899	27.275	1.5	6.0	600	5	990
	1008+00	88	145.36	3898	26.816	1.5	5.0	650	5	
07/14/05	924+75	79	143.84	3899	27.107	1.5	5.8	575	5	1140
	916+50	84	142.71	3886	27.230	1.5	6.2	625	5	
07/18/05	907+00	79	144.76	3888	26.858	1.5	5.3	650	7	2066
	898+00	86	143.76	3894	27.087	1.5	5.8	650	7	
07/19/05	881+00	81	144.56	3906	27.020	1.5	5.7	650	6	1652
07/20/05		78	143.92	3895	27.064	1.5	5.4	600	5	1508
07/25/05	969+00 sh ¹	83	144.96	3914	27.001	1.5	5.6	650	7	830
08/08/05	901+00 sh	82	145.20	3884	26.749	1.5	5.4	650	7	1382
08/09/05	1018+00 sh	76	144.24	3908	27.094	1.5	5.3	620	3	975
08/10/05	864+00	78	144.32	3908	27.079	1.5	5.2	650	5	883
08/17/05	1027+00	77	145.28	3880	26.707	1.5	5.4	625	5	144
08/25/05	1024+80 sh	80	144.64	3891	26.901	1.5	5.4	650	7	376
10/19/05	1013+45	66	142.95	3890	27.212	1.5	6.4	650	6	225
11/02/05	872+00	49	141.18	3895	27.589	1.5	7.9	425	5	491
04/24/06	CARR-D	70	144.43	3889	26.927	1.5	5.5	600	7	540
Average		78.0	144.1	3895	27.039	1.5	5.60	621	5.9	996
Std Dev		7.8	1.04	9	0.20	0.0	0.7	54	1.1	503

¹ sh=shoulder

**Table C8. PCC air, slump, yield, and strength test results (Mix A GGBFS).
(SI Unit)**

Date	Location	Temperature	Unit Weight	Batch Weight	Yield	Slump	%Air	MOR	Age for MOR	Represented Quantity
		°C	kg/m ³	kg	m ³	mm	%	MPa	day	m ³
06/30/05	MAINLINE	26.7	2296.2	1765	0.769	38.1	5.7	3.62	5	688.1
	MAINLINE	26.7	2285.3	1762	0.771	38.1	6.0	3.96	5	
07/05/05	HAUL ROAD	27.2	2297.5	1765	0.768	38.1	5.4	4.65	6	741.6
07/11/05	975+00	22.8	2313.1	1767	0.764	38.1	5.4	4.48	7	764.6
	980+00	26.7	2325.9	1765	0.759	38.1	4.2	4.48	7	
07/12/05	948+25	26.1	2327.2	1768	0.760	38.1	5.0	4.48	7	1002
	940+00	28.9	2309.2	1772	0.767	38.1	5.4	4.48	7	
07/13/05	933+00	26.1	2289.8	1769	0.772	38.1	6.0	4.14	5	756.9
	1008+00	31.1	2328.4	1768	0.759	38.1	5.0	4.48	5	
07/14/05	924+75	26.1	2304.1	1769	0.768	38.1	5.8	3.96	5	871.6
	916+50	28.9	2286.0	1763	0.771	38.1	6.2	4.31	5	
07/18/05	907+00	26.1	2318.8	1764	0.761	38.1	5.3	4.48	7	1580
	898+00	30.0	2302.8	1766	0.767	38.1	5.8	4.48	7	
07/19/05	881+00	27.2	2315.6	1772	0.765	38.1	5.7	4.48	6	1263
07/20/05		25.6	2305.4	1767	0.766	38.1	5.4	4.14	5	1153
07/25/05	969+00 sh ¹	28.3	2322.0	1775	0.765	38.1	5.6	4.48	7	634.6
08/08/05	901+00 sh	27.8	2325.9	1762	0.757	38.1	5.4	4.48	7	1057
08/09/05	1018+00 sh	24.4	2310.5	1773	0.767	38.1	5.3	4.27	3	745.4
08/10/05	864+00	25.6	2311.8	1773	0.767	38.1	5.2	4.48	5	675.1
08/17/05	1027+00	25.0	2327.2	1760	0.756	38.1	5.4	4.31	5	110.1
08/25/05	1024+80 sh	26.7	2316.9	1765	0.762	38.1	5.4	4.48	7	287.5
10/19/05	1013+45	18.9	2289.8	1764	0.771	38.1	6.4	4.48	6	172
11/02/05	872+00	9.4	2261.5	1767	0.781	38.1	7.9	2.93	5	375.4
04/24/06	CARR-D	21.1	2313.5	1764	0.762	38.1	5.5	4.14	7	412.9
Average										
		25.6	2307.7	1767	0.766	38.1	5.60	4.28	5.9	738
St Dev										
		4.3	16.7	3.9	0.0	0.0	0.7	0.4	1.1	385

¹ sh=shoulder

**Table C9. PCC air, slump, yield, and strength test results (Mix B Fly ash).
(English Unit)**

Date	Location	Temperature	Unit Weight	Batch Weight	Yield	Slump	%Air	MOR	Age for MOR	Represented Quantity
		°F	lb/ft ³	lb	ft ³	in.	%	psi	day	yd ³
07/28/05	839+00	76	145.52	3913	26.890	1.5	5.4	650	4	2290
	825+00	86	144.16	3897	27.032	1.5	5.4	625	4	
08/01/05	794+00	75	143.67	3899	27.139	1.5	6.0	650	7	1670
08/02/05	762+50	77	144.88	4082	28.175	1.5	5.4	633	6	2250
08/03/05	736+00	77	143.51	3911	27.252	1.5	6.4	650	5	2130
08/04/05	700+00	81	144.24	3917	27.156	1.5	5.6	650	6	1970
08/11/05	823+25 sh ¹	77	144.24	3915	27.142	1.5	5.6	650	5	1270
08/16/05	746+00	75	144.48	3906	27.035	1.5	5.4	650	6	1942
08/17/05	713+00 sh	80	145.28	3902	26.858	1.5	5.6	625	5	900
08/18/05	790+75	74	144.08	3904	27.096	1.5	5.6	625	5	828
	829+00	89	144.96	3914	27.001	1.5	5.0	525	5	
08/22/05	851+00 sh	75	143.27	3908	27.277	1.5	6.4	625	7	450
08/23/05	687+00	69	143.27	3911	27.298	1.5	6.6	650	6	1720
	670+50	75	145.68	3891	26.709	1.5	5.4	650	6	
08/24/05	827+60	69	144.80	3914	27.030	1.5	5.8	650	5	460
08/25/05	795+00	72	144.08	3914	27.165	1.5	6.4	650	7	270
09/15/05	667+00	75	144.72	3908	27.004	1.5	5.4	600	5	2310
	647+75	79	144.00	3908	27.139	1.5	5.8	650	5	
09/19/05	846+00	75	143.11	3895	27.217	1.5	6.0	650	8	570
09/21/05	650+50	81	142.55	3918	27.485	1.5	6.8	650	4	1050
10/13/05	817+00	69	144.48	3909	27.056	1.5	5.4	625	5	460
10/17/05	641+00	61	141.66	3914	27.630	1.5	6.9	650	7	310
Average		75.8	144.12	3916	27.172	1.5	5.8	636	5.6	1269
St Dev		6.0	1.0	37.8	0.3	0.0	0.53	28.4	1.1	763

¹ sh=shoulder

**Table C10. PCC air, slump, yield, and strength test results (Mix B Fly ash).
(SI Unit)**

Date	Location	Temperature	Unit Weight	Batch Weight	Yield	Slump	%Air	MOR	Age for MOR	Represented Quantity
		°C	kg/m ³	kg	m ³	mm	%	MPa	day	m ³
07/28/05	839+00	24.4	2331.0	1775	0.761	38.1	5.4	4.48	4	1751
	825+00	30.0	2309.2	1768	0.765	38.1	5.4	4.31	4	
08/01/05	794+00	23.9	2301.4	1769	0.768	38.1	6.0	4.48	7	1277
08/02/05	762+50	25.0	2320.7	1852	0.798	38.1	5.4	4.36	6	1720
08/03/05	736+00	25.0	2298.8	1774	0.772	38.1	6.4	4.48	5	1629
08/04/05	700+00	27.2	2310.5	1777	0.769	38.1	5.6	4.48	6	1506
08/11/05	823+25 sh ¹	25.0	2310.5	1776	0.769	38.1	5.6	4.48	5	971
08/16/05	746+00	23.9	2314.3	1772	0.766	38.1	5.4	4.48	6	1485
08/17/05	713+00 sh	26.7	2327.2	1770	0.761	38.1	5.6	4.31	5	688
08/18/05	790+75	23.3	2307.9	1771	0.767	38.1	5.6	4.31	5	633
	829+00	31.7	2322.0	1775	0.765	38.1	5.0	3.62	5	
08/22/05	851+00 sh	23.9	2295.0	1773	0.772	38.1	6.4	4.31	7	344
08/23/05	687+00	20.6	2295.0	1774	0.773	38.1	6.6	4.48	6	1315
	670+50	23.9	2333.6	1765	0.756	38.1	5.4	4.48	6	
08/24/05	827+60	20.6	2319.5	1775	0.765	38.1	5.8	4.48	5	352
08/25/05	795+00	22.2	2307.9	1775	0.769	38.1	6.4	4.48	7	206
09/15/05	667+00	23.9	2318.2	1773	0.765	38.1	5.4	4.14	5	1766
	647+75	26.1	2306.6	1773	0.768	38.1	5.8	4.48	5	
09/19/05	846+00	23.9	2292.4	1767	0.771	38.1	6.0	4.48	8	436
09/21/05	650+50	27.2	2283.4	1777	0.778	38.1	6.8	4.48	4	803
10/13/05	817+00	20.6	2314.3	1773	0.766	38.1	5.4	4.31	5	352
10/17/05	641+00	16.1	2269.2	1775	0.782	38.1	6.9	4.48	7	237
Average		24.3	2308.6	1776	0.769	38.1	5.8	4	5.6	971
St Dev		3.3	15.5	17.2	0.0	0.0	0.53	0.2	1.1	584

¹ sh=shoulder

Appendix D: FHWA Test Results on Void Properties of Hardened Concretes

Table D1. Analysis of air void system in hardened concrete measured by ASTM C 457 linear traverse method.

	Mix B (Fly ash)					Mix A (GGBFS)				
Sample ID	WAY03D 671+00 #1					WAY03D 875+00 #1				
Number of Traverse Lines	19					19				
Actual Area, in ²	18.75					18.75				
Nom. Max. Size Agg., in.	1					1				
Length of Traverse, in.	95					95				
Replicates	1	2	3	4	Avg	1	2	3	4	Avg
Sum of Chord Lengths, in. (Total)	4.74	3.73	5.91	4.31	4.67	3.67	5.84	5.72	2.96	4.55
Sum of Chord Lengths, in. (Entrapped)	1.98	0.89	1.83	1.35	1.51	1.62	2.75	1.81	0.43	1.65
Air Content, % (Total)	5.0	3.9	6.2	4.5	4.90	3.9	6.2	6.0	3.1	4.80
Air Content, % (Entrapped)	2.1	0.9	1.9	1.4	1.58	1.7	2.9	1.9	0.4	1.73
Air Content, % (Entrained)	2.9	3.0	4.3	3.1	3.33	2.2	3.3	4.1	2.7	3.08
Voids Intersected (Total Number)	799	681	989	782	813	499	680	860	537	644
Mean Chord Length, x10 ⁻³ in.	5.9	5.5	6.0	5.5	5.73	7.4	8.6	6.6	5.5	7.03
Voids per inch	8.4	7.2	10.4	8.2	8.55	5.3	7.2	9.1	5.7	6.83
Specific Surface, in ² /in ³	674	730	669	726	700	543	466	602	725	584
Spacing Factor, x10 ⁻³ in.	7.5	7.7	6.8	7.3	7.3	10.4	9.8	7.7	8.6	9.1
Cord Length Distribution										
Chord (µm)	#1	#2	#3	#4	Avg	#1	#2	#3	#4	Avg
0-25	49	14	28	59	38	25	17	20	9	18
25-50	322	165	270	253	253	153	128	221	88	148
50-75	177	194	257	181	202	99	181	217	145	161
75-100	77	96	136	89	100	72	105	135	104	104
100-125	41	65	92	46	61	31	62	62	57	53
125-150	23	26	46	31	32	25	35	40	24	31
150-175	13	20	23	16	18	17	23	25	20	21
175-200	12	8	24	12	14	7	17	16	12	13
200-225	7	10	13	12	11	7	9	15	13	11
225-250	7	12	7	6	8	3	5	8	8	6
250-300	6	13	19	12	13	7	15	17	12	13
300-350	5	9	8	7	7	10	17	15	7	12
350-400	5	9	8	11	8	5	7	10	8	8
400-500	10	13	16	7	12	7	9	11	12	10
500-750	12	8	16	15	13	10	15	22	7	14
750-1000	9	4	9	7	7	5	7	11	5	7
1000-3000	18	15	13	16	16	11	22	11	5	12
> 3000	6	0	4	2	3	5	6	4	1	4
Total	799	681	989	782	813	499	680	860	537	644

Note: Air voids with cord length more than 1mm are considered as entrapped air.

Analysis performed 5/30/2006 at Turner Fairbank Highway Research Center, McLean, Virginia

Appendix E: Low Temperature Creep Compliance of Asphalt Mixes

Table E1. Creep compliance of Mix 301.

Time second	ENGLISH UNITS $\times 10^{-4}$ (1/ksi)			INTERNATIONAL UNITS 1/GPa		
	Test Temperature			Test Temperature		
	-4°F	14°F	32°C	-20°C	-10°C	0°C
2	1.51	1.82	2.69	0.0218	0.0264	0.0391
3	1.56	1.96	3.05	0.0227	0.0285	0.0443
4	1.60	2.02	3.21	0.0232	0.0292	0.0466
5	1.62	2.05	3.31	0.0235	0.0298	0.0479
6	1.64	2.09	3.43	0.0238	0.0303	0.0497
7	1.65	2.12	3.54	0.0240	0.0307	0.0513
8	1.67	2.14	3.59	0.0242	0.0311	0.0520
9	1.68	2.15	3.66	0.0243	0.0312	0.0531
10	1.69	2.16	3.78	0.0245	0.0313	0.0549
12	1.71	2.20	3.90	0.0248	0.0319	0.0566
14	1.72	2.26	4.05	0.0249	0.0328	0.0588
16	1.73	2.31	4.14	0.0251	0.0335	0.0601
18	1.74	2.34	4.18	0.0252	0.0340	0.0607
20	1.75	2.32	4.30	0.0254	0.0336	0.0624
25	1.78	2.40	4.42	0.0258	0.0349	0.0641
30	1.80	2.44	4.62	0.0262	0.0353	0.0670
35	1.82	2.49	4.74	0.0264	0.0361	0.0688
40	1.83	2.53	4.88	0.0266	0.0366	0.0707
45	1.85	2.55	4.99	0.0268	0.0370	0.0724
50	1.87	2.59	5.06	0.0271	0.0375	0.0734
60	1.89	2.63	5.25	0.0274	0.0381	0.0762
70	1.91	2.67	5.39	0.0277	0.0388	0.0782
80	1.93	2.72	5.59	0.0279	0.0395	0.0811
90	1.94	2.76	5.75	0.0282	0.0401	0.0834
100	1.96	2.81	5.84	0.0285	0.0408	0.0847
150	2.02	2.96	6.37	0.0294	0.0429	0.0925
200	2.06	3.06	6.84	0.0299	0.0444	0.0992
250	2.11	3.18	7.27	0.0306	0.0461	0.1054
300	2.14	3.25	7.59	0.0310	0.0471	0.1101
350	2.17	3.35	7.90	0.0315	0.0487	0.1145
400	2.21	3.42	8.15	0.0320	0.0496	0.1182
450	2.23	3.50	8.50	0.0323	0.0508	0.1232
500	2.26	3.58	8.69	0.0328	0.0519	0.1260
550	2.29	3.65	8.93	0.0332	0.0529	0.1296
600	2.32	3.72	9.20	0.0336	0.0539	0.1334
650	2.34	3.77	9.44	0.0339	0.0547	0.1369
700	2.37	3.85	9.66	0.0343	0.0558	0.1401
750	2.40	3.92	9.90	0.0348	0.0568	0.1436
800	2.43	3.98	10.10	0.0353	0.0577	0.1465
850	2.47	4.03	10.26	0.0358	0.0585	0.1488
900	2.49	4.10	10.49	0.0361	0.0595	0.1522
950	2.53	4.16	10.70	0.0367	0.0604	0.1552

Table E2. Creep compliance of Mix 302.

Time second	ENGLISH UNITS $\times 10^{-4}$ (1/ksi)			INTERNATIONAL UNITS 1/GPa		
	Test Temperature			Test Temperature		
	-4°F	14°F	32°C	-20°C	-10°C	0°C
2	1.62	2.38	2.71	0.0235	0.0346	0.0392
3	1.70	2.56	3.05	0.0246	0.0372	0.0442
4	1.73	2.66	3.23	0.0251	0.0386	0.0468
5	1.75	2.73	3.35	0.0254	0.0396	0.0485
6	1.78	2.79	3.47	0.0258	0.0404	0.0504
7	1.79	2.84	3.59	0.0260	0.0412	0.0521
8	1.81	2.89	3.67	0.0263	0.0419	0.0533
9	1.83	2.94	3.76	0.0265	0.0426	0.0546
10	1.84	2.98	3.91	0.0267	0.0432	0.0567
12	1.85	3.03	4.06	0.0269	0.0439	0.0589
14	1.88	3.07	4.20	0.0273	0.0446	0.0610
16	1.90	3.11	4.37	0.0276	0.0452	0.0633
18	1.92	3.13	4.45	0.0278	0.0455	0.0646
20	1.93	3.20	4.57	0.0280	0.0464	0.0663
25	1.95	3.25	4.77	0.0283	0.0472	0.0692
30	1.99	3.33	5.03	0.0289	0.0483	0.0729
35	2.01	3.39	5.23	0.0291	0.0492	0.0759
40	2.03	3.45	5.43	0.0295	0.0501	0.0788
45	2.05	3.51	5.61	0.0298	0.0508	0.0814
50	2.07	3.56	5.82	0.0300	0.0516	0.0844
60	2.11	3.63	6.10	0.0305	0.0527	0.0885
70	2.12	3.71	6.38	0.0308	0.0538	0.0926
80	2.15	3.78	6.68	0.0312	0.0548	0.0969
90	2.18	3.85	6.92	0.0316	0.0558	0.1004
100	2.20	3.90	7.15	0.0319	0.0566	0.1037
150	2.27	4.17	8.26	0.0330	0.0605	0.1198
200	2.34	4.38	9.09	0.0339	0.0635	0.1318
250	2.40	4.55	9.91	0.0348	0.0660	0.1438
300	2.45	4.70	10.59	0.0355	0.0681	0.1536
350	2.49	4.85	11.20	0.0362	0.0703	0.1624
400	2.54	4.97	11.70	0.0368	0.0721	0.1697
450	2.57	5.10	12.20	0.0373	0.0740	0.1770
500	2.62	5.21	12.64	0.0380	0.0756	0.1833
550	2.66	5.34	13.10	0.0387	0.0775	0.1899
600	2.70	5.44	13.57	0.0391	0.0789	0.1968
650	2.73	5.58	13.96	0.0397	0.0809	0.2024
700	2.77	5.67	14.33	0.0402	0.0822	0.2078
750	2.81	5.76	14.66	0.0407	0.0835	0.2126
800	2.85	5.86	14.99	0.0413	0.0849	0.2174
850	2.89	5.96	15.33	0.0419	0.0865	0.2223
900	2.92	6.04	15.67	0.0424	0.0876	0.2273
950	2.96	6.13	16.04	0.0429	0.0889	0.2327

Table E3. Creep compliance of Mix 442.

Time second	ENGLISH UNITS $\times 10^{-4}$ (1/ksi)			INTERNATIONAL UNITS 1/GPa		
	Test Temperature			Test Temperature		
	-4°F	14°F	32°C	-20°C	-10°C	0°C
2	2.37	3.58	5.63	0.0343	0.0519	0.0816
3	2.62	4.13	6.94	0.0380	0.0600	0.1006
4	2.75	4.47	7.72	0.0399	0.0648	0.1120
5	2.84	4.71	8.35	0.0412	0.0683	0.1211
6	2.93	4.91	8.81	0.0425	0.0713	0.1277
7	3.00	5.11	9.20	0.0434	0.0741	0.1335
8	3.04	5.28	9.57	0.0441	0.0766	0.1388
9	3.09	5.43	9.77	0.0448	0.0787	0.1418
10	3.11	5.56	10.01	0.0451	0.0807	0.1451
12	3.18	5.83	10.57	0.0462	0.0845	0.1533
14	3.25	5.99	10.99	0.0471	0.0869	0.1595
16	3.32	6.18	11.36	0.0482	0.0896	0.1647
18	3.36	6.34	11.76	0.0488	0.0920	0.1706
20	3.42	6.49	12.18	0.0497	0.0941	0.1767
25	3.52	6.80	12.96	0.0511	0.0987	0.1880
30	3.64	7.10	13.68	0.0529	0.1030	0.1984
35	3.72	7.37	14.23	0.0540	0.1069	0.2063
40	3.80	7.59	14.84	0.0551	0.1101	0.2152
45	3.88	7.82	15.34	0.0562	0.1134	0.2225
50	3.94	8.03	15.83	0.0572	0.1164	0.2295
60	4.05	8.40	16.69	0.0587	0.1218	0.2420
70	4.16	8.74	17.44	0.0603	0.1268	0.2530
80	4.27	9.02	18.30	0.0619	0.1309	0.2654
90	4.35	9.29	18.86	0.0630	0.1347	0.2736
100	4.42	9.56	19.47	0.0641	0.1387	0.2823
150	4.75	10.66	22.16	0.0690	0.1545	0.3214
200	5.04	11.49	24.19	0.0730	0.1666	0.3509
250	5.26	12.24	26.11	0.0763	0.1775	0.3786
300	5.46	12.89	27.66	0.0791	0.1870	0.4011
350	5.64	13.49	29.13	0.0817	0.1956	0.4225
400	5.80	14.06	30.39	0.0841	0.2039	0.4408
450	5.97	14.60	31.74	0.0866	0.2118	0.4604
500	6.12	15.16	33.00	0.0887	0.2199	0.4787
550	6.26	15.65	33.82	0.0908	0.2270	0.4906
600	6.40	16.11	34.96	0.0929	0.2337	0.5070
650	6.53	16.55	36.22	0.0946	0.2401	0.5253
700	6.67	16.97	36.97	0.0967	0.2461	0.5363
750	6.81	17.42	37.89	0.0987	0.2527	0.5495
800	6.95	17.85	38.90	0.1007	0.2589	0.5642
850	7.08	18.24	39.77	0.1027	0.2646	0.5768
900	7.21	18.65	40.63	0.1045	0.2705	0.5893
950	7.33	19.07	41.37	0.1063	0.2766	0.6000

Table E4. Creep compliance of Mix FRL.

Time second	ENGLISH UNITS $\times 10^{-4}$ (1/ksi)			INTERNATIONAL UNITS 1/GPa		
	Test Temperature			Test Temperature		
	-4°F	14°F	32°C	-20°C	-10°C	0°C
2	1.69	1.94	2.57	0.0245	0.0281	0.0373
3	1.78	2.07	2.82	0.0258	0.0300	0.0409
4	1.81	2.12	2.96	0.0262	0.0308	0.0429
5	1.84	2.20	3.06	0.0267	0.0319	0.0443
6	1.86	2.26	3.10	0.0270	0.0327	0.0449
7	1.87	2.28	3.20	0.0271	0.0331	0.0464
8	1.88	2.30	3.32	0.0273	0.0333	0.0481
9	1.89	2.32	3.37	0.0275	0.0336	0.0488
10	1.90	2.36	3.48	0.0275	0.0343	0.0505
12	1.90	2.40	3.57	0.0275	0.0348	0.0519
14	1.93	2.43	3.68	0.0280	0.0353	0.0534
16	1.94	2.46	3.73	0.0281	0.0356	0.0541
18	1.97	2.49	3.83	0.0286	0.0361	0.0556
20	1.99	2.52	3.90	0.0288	0.0365	0.0566
25	2.01	2.55	3.94	0.0292	0.0370	0.0571
30	2.05	2.60	4.04	0.0297	0.0377	0.0585
35	2.06	2.64	4.14	0.0299	0.0383	0.0600
40	2.09	2.67	4.25	0.0302	0.0387	0.0617
45	2.10	2.68	4.31	0.0305	0.0389	0.0624
50	2.12	2.71	4.40	0.0308	0.0394	0.0639
60	2.15	2.78	4.53	0.0312	0.0403	0.0657
70	2.17	2.82	4.65	0.0314	0.0409	0.0675
80	2.19	2.88	4.74	0.0318	0.0418	0.0687
90	2.21	2.94	4.89	0.0321	0.0426	0.0709
100	2.24	2.95	5.03	0.0325	0.0428	0.0729
150	2.28	3.07	5.42	0.0331	0.0445	0.0786
200	2.34	3.14	5.73	0.0339	0.0455	0.0831
250	2.38	3.24	6.06	0.0344	0.0470	0.0878
300	2.41	3.31	6.26	0.0349	0.0480	0.0908
350	2.45	3.40	6.53	0.0355	0.0493	0.0947
400	2.47	3.43	6.79	0.0359	0.0498	0.0985
450	2.48	3.51	6.95	0.0360	0.0509	0.1008
500	2.50	3.56	7.11	0.0363	0.0517	0.1031
550	2.55	3.57	7.49	0.0370	0.0518	0.1087
600	2.56	3.66	7.45	0.0371	0.0531	0.1081
650	2.59	3.70	7.71	0.0376	0.0537	0.1118
700	2.62	3.78	7.82	0.0380	0.0548	0.1133
750	2.64	3.82	8.04	0.0383	0.0555	0.1166
800	2.67	3.89	8.15	0.0387	0.0564	0.1182
850	2.69	3.94	8.38	0.0390	0.0571	0.1215
900	2.74	3.99	8.49	0.0397	0.0578	0.1231
950	2.75	4.04	8.57	0.0399	0.0586	0.1243

Table E5. Creep compliance of Mix SMA.

Time second	ENGLISH UNITS $\times 10^{-4}$ (1/ksi)			INTERNATIONAL UNITS 1/GPa		
	Test Temperature			Test Temperature		
	-4°F	14°F	32°C	-20°C	-10°C	0°C
2	2.02	2.78	3.88	0.0293	0.0403	0.0563
3	2.15	3.04	4.41	0.0312	0.0441	0.0639
4	2.22	3.20	4.67	0.0322	0.0464	0.0678
5	2.27	3.29	4.89	0.0329	0.0478	0.0709
6	2.31	3.35	5.13	0.0335	0.0486	0.0744
7	2.34	3.41	5.30	0.0339	0.0494	0.0768
8	2.37	3.47	5.43	0.0344	0.0503	0.0788
9	2.40	3.52	5.58	0.0348	0.0511	0.0809
10	2.42	3.57	5.70	0.0351	0.0517	0.0826
12	2.47	3.63	5.92	0.0359	0.0527	0.0859
14	2.50	3.73	6.00	0.0362	0.0541	0.0870
16	2.52	3.82	6.17	0.0365	0.0553	0.0895
18	2.55	3.91	6.35	0.0370	0.0567	0.0921
20	2.58	3.94	6.49	0.0375	0.0572	0.0941
25	2.63	4.07	6.81	0.0381	0.0591	0.0988
30	2.68	4.18	7.10	0.0388	0.0606	0.1029
35	2.71	4.28	7.36	0.0394	0.0621	0.1067
40	2.75	4.36	7.60	0.0399	0.0632	0.1103
45	2.78	4.46	7.80	0.0404	0.0647	0.1131
50	2.82	4.53	8.00	0.0408	0.0657	0.1160
60	2.87	4.66	8.38	0.0416	0.0675	0.1215
70	2.91	4.76	8.71	0.0422	0.0690	0.1264
80	2.95	4.86	9.00	0.0427	0.0705	0.1305
90	2.99	4.94	9.27	0.0433	0.0717	0.1344
100	3.02	5.04	9.53	0.0438	0.0731	0.1383
150	3.17	5.41	10.73	0.0459	0.0784	0.1556
200	3.27	5.65	11.63	0.0474	0.0819	0.1687
250	3.35	5.87	12.36	0.0486	0.0851	0.1793
300	3.43	6.06	12.96	0.0497	0.0878	0.1879
350	3.49	6.24	13.54	0.0507	0.0905	0.1964
400	3.55	6.33	13.98	0.0514	0.0918	0.2027
450	3.60	6.47	14.43	0.0522	0.0938	0.2093
500	3.65	6.60	14.89	0.0530	0.0957	0.2159
550	3.71	6.73	15.27	0.0538	0.0976	0.2215
600	3.76	6.85	15.57	0.0545	0.0993	0.2258
650	3.80	6.93	15.86	0.0551	0.1005	0.2300
700	3.84	7.01	16.21	0.0557	0.1017	0.2351
750	3.89	7.13	16.47	0.0564	0.1035	0.2388
800	3.93	7.23	16.76	0.0571	0.1049	0.2431
850	3.98	7.32	17.04	0.0578	0.1062	0.2471
900	4.03	7.43	17.31	0.0584	0.1078	0.2511
950	4.07	7.51	17.52	0.0590	0.1089	0.2542

Appendix F: Absorbed Energy Ratio of Asphalt Mixes

Table F1. Absorbed energy ratio of MIX 302.

Date		AV (%)	E (lb-in/in)		E (lb-in/in)		$E_{\text{soaked}}/E_{\text{dry}}$
7/25/05	Dry	7.32	7548.4	7053.0	33.6	31.4	0.954
		6.87	6675.0		29.7		
		7.19	6935.5		30.9		
	Soaked	6.69	7525.0	6730.7	33.5	29.9	
		7.35	6583.3		29.3		
		7.22	6083.9		27.1		
7/28/05	Dry	7.77	5638.7	5828.0	25.1	25.9	0.514
		7.53	5806.5		25.8		
		7.65	6038.7		26.9		
	Soaked	7.28	3561.3	2993.5	15.8	13.3	
		8.01	2967.7		13.2		
		7.49	2451.6		10.9		
8/12/05	Dry	6.56	3740.6	4101.0	16.6	18.2	0.820
		6.03	4575.0		20.4		
		7.01	3987.5		17.7		
	Soaked	6.40	3162.5	3364.6	14.1	15.0	
		6.28	3025.0		13.5		
		6.49	3906.3		17.4		
8/16/05	Dry	7.78	5687.5	5418.8	25.3	24.1	0.954
		7.03	5550.0		24.7		
		8.14	5018.8		22.3		
	Soaked	8.38	5618.8	5168.8	25.0	23.0	
		6.87	3987.5		17.7		
		7.53	5900.0		26.2		
8/23/05	Dry	6.96	4451.6	5453.8	19.8	24.3	0.709
		7.05	5922.6		26.3		
		7.38	5987.1		26.6		
	Soaked	7.34	2890.3	3866.7	12.9	17.2	
		7.13	4167.7		18.5		
		7.13	4541.9		20.2		
8/28/05	Dry	6.77	4125.0	4276.0	18.3	19.0	0.672
		7.22	4250.0		18.9		
		6.77	4453.1		19.8		
	Soaked	6.85	2700.0	2875.0	12.0	12.8	
		7.05	2887.5		12.8		
		6.68	3037.5		13.5		

Table F1 Continues

Date	Condition	AV (%)	E (lb-in/in)		E (lb-in/in)		$E_{\text{soaked}}/E_{\text{dry}}$
9/2/05	Dry	6.33	5419.4	5263.0	24.1	23.4	0.695
		7.40	5037.5		22.4		
		6.33	5332.3		23.7		
	Soaked	6.13	3853.3	3657.4	17.1	16.3	
		7.03	3612.5		16.1		
		7.24	3506.3		15.6		
9/8/05	Dry	6.71	6813.3	6439.4	30.3	28.6	0.666
		6.71	6160.0		27.4		
		6.18	6344.8		28.2		
	Soaked	6.99	3677.4	4288.0	16.4	19.1	
		6.42	3853.3		17.1		
		6.34	5333.3		23.7		
9/12/05	Dry	7.21	6562.5	6021.7	29.2	26.8	0.653
		7.09	5622.6		25.0		
		6.87	5880.0		26.2		
	Soaked	7.11	3750.0	3935.0	16.7	17.5	
		6.99	4480.0		19.9		
		7.02	3575.0		15.9		
9/15/05	Dry	7.54	6969.7	4607.7	31.0	20.5	1.068
		7.13	6062.5		27.0		
		7.62	790.9		3.5		
	Soaked	7.70	6136.4	4921.2	27.3	21.9	
		7.21	5000.0		22.2		
		7.34	3627.3		16.1		
9/19/05	Dry	6.76	6593.3	5861.6	29.3	26.1	0.804
		6.60	5025.8		22.4		
		7.33	5965.6		26.5		
	Soaked	7.17	3712.5	4710.4	16.5	21.0	
		6.35	4700.0		20.9		
		7.05	5718.8		25.4		
9/27/05	Dry	6.97	4600.0	5055.1	20.5	22.5	0.823
		7.38	6109.1		27.2		
		6.97	4456.3		19.8		
	Soaked	7.17	2687.5	4160.4	12.0	18.5	
		6.35	5200.0		23.1		
		7.05	4593.8		20.4		

Table F1 Continues

Date	Condition	AV (%)	E (lb-in/in)		E (kN-m/m)		$E_{\text{soaked}}/E_{\text{dry}}$
9/28/05	Dry	7.39	4727.3	6082.5	21.0	27.1	0.419
		7.27	7484.8		33.3		
		7.55	6035.3		26.8		
	Soaked	7.14	2875.0	2547.5	12.8	11.3	
		7.27	2230.3		9.9		
		7.67	2537.1		11.3		
9/30/05	Dry	6.84	3767.7	4445.9	16.8	19.8	0.897
		7.05	4250.0		18.9		
		6.66	5320.0		23.7		
	Soaked	6.66	3826.7	3990.1	17.0	17.7	
		6.93	3750.0		16.7		
		6.99	4393.8		19.5		
10/9/05	Dry	7.81	4941.2	4921.2	22.0	21.9	0.806
		7.40	5066.7		22.5		
		7.81	4755.9		21.2		
	Soaked	7.77	3241.2	3965.7	14.4	17.6	
		7.56	4520.6		20.1		
		7.77	4135.3		18.4		
10/16/05	Dry	6.95	5843.8	6561.3	26.0	29.2	0.600
		6.59	7590.0		33.8		
		7.11	6250.0		27.8		
	Soaked	7.02	3918.8	3939.6	17.4	17.5	
		6.87	3206.7		14.3		
		6.81	4693.3		20.9		
10/18/05	Dry	7.00	7800.0	7800.0	34.7	34.7	0.389
		6.35	8400.0		37.4		
		6.82	7200.0		32.0		
	Soaked	6.76	3251.6	3035.1	14.5	13.5	
		6.95	2681.3		11.9		
		6.54	3172.4		14.1		
10/19/05	Dry	6.08	8965.5	7101.5	39.9	31.6	0.310
		6.08	7310.3		32.5		
		5.43	5028.6		22.4		
	Soaked	5.88	2813.8	2202.7	12.5	9.8	
		6.12	1466.7		6.5		
		5.72	2327.6		10.4		

Table F1 Continues

Date	Condition	AV (%)	E (lb-in/in)		E (kN-m/m)		E _{soaked} /E _{dry}
10/26/05	Dry	6.08	5546.7	5951.6	24.7	26.5	0.671
		5.75	7543.8		33.6		
		6.57	4764.3		21.2		
	Soaked	6.20	5041.4	3996.1	22.4	17.8	
		5.79	2785.7		12.4		
		6.32	4161.3		18.5		
10/27/05	Dry	6.23	8620.7	7852.1	38.3	34.9	0.539
		7.01	7000.0		31.1		
		5.82	7935.7		35.3		
	Soaked	6.11	4703.4	4233.5	20.9	18.8	
		5.95	4435.7		19.7		
		6.72	3561.3		15.8		

Table F2. Absorbed energy ratio of Mix 442.

	Date	AV (%)	Absorbed Energy				E _{soaked} /E _{dry}
			(lb-in/in)		(kN·m/m)		
Dry	9/20/05	6.94	7994.7	8102.6	35.6	36.0	0.858
		6.21	7368.4		32.8		
		6.5	8944.7		39.8		
Soaked		6.58	6444.7	6953.5	28.7	30.9	
		6.66	7121.1		31.7		
		6.33	7294.7		32.4		
Dry	10/11/05	7.42	8266.7	8702.0	36.8	38.7	0.852
		6.93	8547.4		38.0		
		7.25	9292.1		41.3		
Soaked		7.58	6517.9	7412.1	29.0	33.0	
		6.64	8510.5		37.9		
		7.3	7207.9		32.1		

Table F3. Absorbed energy ratio of Mix FRL.

	Date	AV (%)	Absorbed Energy				E _{soaked} /E _{dry}
			(lb·in/in)		(kN·m/m)		
Dry	7/13/05	7.72	6924.5	7504.7	30.8	33.4	0.683
		7.92	7127.3		31.7		
		7.44	8462.4		37.6		
Soaked		8.00	4134.4	5127.9	18.4	22.8	
		7.56	5156.3		22.9		
		7.40	6093.1		27.1		
Dry	8/10/05	7.38	6877.4	7068.8	30.6	31.4	0.917
		6.48	6096.8		27.1		
		7.09	8232.3		36.6		
Soaked		7.21	7354.8	6481.7	32.7	28.8	
		6.84	5703.2		25.4		
		7.17	6387.1		28.4		
Dry	8/15/05	6.48	7425.0	5695.8	33.0	25.3	0.735
		7.34	5625.0		25.0		
		6.82	4037.5		18.0		
Soaked		7.40	4359.4	4186.5	19.4	18.6	
		7.38	3075.0		13.7		
		7.62	5125.0		22.8		
Dry	8/21/05	6.47	6141.9	5514.0	27.3	24.5	0.829
		6.51	5200.0		23.1		
		6.68	5200.0		23.1		
Soaked		6.80	5519.4	4571.9	24.6	20.3	
		6.80	4712.5		21.0		
		5.98	3483.9		15.5		
Dry	9/11/05	7.13	4609.4	4997.8	20.5	22.2	0.848
		6.56	5462.1		24.3		
		7.13	4921.9		21.9		
Soaked		6.97	4800.0	4238.6	21.4	18.9	
		7.05	4062.5		18.1		
		6.97	3853.3		17.1		
Dry	9/15/05	6.96	5045.2	4788.2	22.4	21.3	0.666
		7.05	5225.8		23.2		
		6.96	4093.5		18.2		
Soaked		6.60	3848.3	3189.0	17.1	14.2	
		7.21	2906.3		12.9		
		7.42	2812.5		12.5		

Table F3 Continues

Date	Condition	AV (%)	E (lb-in/in)		E (kN-m/m)		E _{soaked} /E _{dry}
9/22/05	Dry	7.11	5950.0	7252.2	26.5	32.3	0.443
		6.86	7135.5		31.7		
		6.79	8671.0		38.6		
	Soaked	7.02	3353.1	3211.0	14.9	14.3	
		6.90	2800.0		12.5		
		6.82	3480.0		15.5		
10/6/05	Dry	7.02	4700.0	5511.8	20.9	24.5	0.712
		6.59	8400.0		37.4		
		6.82	3435.5		15.3		
	Soaked	7.10	2812.5	3921.7	12.5	17.4	
		7.00	4125.0		18.3		
		6.28	4827.6		21.5		
10/13/05	Dry	7.13	4837.5	4985.1	21.5	22.2	0.926
		6.57	5655.2		25.2		
		6.95	4462.5		19.9		
	Soaked	7.31	3900.0	4618.6	17.3	20.5	
		7.04	5359.4		23.8		
		6.33	4596.6		20.4		
10/18/05	Dry	7.00	3487.5	4465.6	15.5	19.9	0.848
		6.92	4621.9		20.6		
		6.90	5287.5		23.5		
	Soaked	6.94	3437.5	3786.5	15.3	16.8	
		7.03	4143.8		18.4		
		6.88	3778.1		16.8		

Table F4. Absorbed energy ratio of Mix SMA.

Day	Condition	AV (%)	E (lb-in/in)		E (kN-m/m)		$E_{\text{soaked}}/E_{\text{dry}}$
2	Dry	6.72	6750.0	6523.7	30.0	29.0	0.929
		7.43	6484.2		28.8		
		7.14	6336.8		28.2		
	Soaked	7.01	5336.8	6059.6	23.7	27.0	
		7.26	6000.0	26.7			
		6.97	6842.1	30.4			
5	Dry	6.23	6021.1	6500.9	26.8	28.9	0.786
		6.77	7157.9		31.8		
		6.64	6323.7		28.1		
	Soaked	6.19	4863.2	5107.0	21.6	22.7	
		7.10	5300.0	23.6			
		6.56	5157.9	22.9			
8	Dry	6.97	6552.6	6375.4	29.1	28.4	0.822
		7.10	6257.9		27.8		
		7.22	6315.8		28.1		
	Soaked	7.26	4236.8	5240.4	18.8	23.3	
		6.85	5084.2	22.6			
		7.18	6400.0	28.5			
11	Dry	7.14	5647.4	5814.9	25.1	25.9	0.838
		7.26	5955.3		26.5		
		6.52	5842.1		26.0		
	Soaked	7.10	4421.1	4870.2	19.7	21.7	
		7.51	5210.5	23.2			
		6.39	4978.9	22.1			

Appendix G: Indirect Tensile Strength of Asphalt Mixes

Table G1. Indirect tensile strength of Mix 302.

Date	AV (%)	Indirect Tensile Strength (ITS)		ITS Average	
		(psi)	(MPa)	(psi)	(MPa)
7/25/05	4.03	210.0	1.448	207.5	1.431
	4.65	201.9	1.392		
	4.41	210.7	1.453		
7/28/05	4.40	222.4	1.534	206.8	1.426
	4.08	250.2	1.725		
	3.97	147.8	1.019		
8/12/05	3.95	248.8	1.715	207.4	1.430
	3.98	187.3	1.291		
	3.98	186.2	1.284		
8/16/05	3.68	216.6	1.493	223.7	1.542
	4.54	212.2	1.463		
	3.35	242.3	1.671		
8/23/05	4.55	134.4	0.927	166.4	1.148
	2.62	181.1	1.248		
	3.24	183.9	1.268		
8/28/05	3.69	147.8	1.019	149.2	1.029
	4.43	156.1	1.076		
	4.06	143.7	0.991		
9/2/05	4.77	108.6	0.749	136.0	0.938
	3.74	160.2	1.104		
	4.00	139.2	0.960		
9/8/05	3.84	230.1	1.587	221.8	1.529
	3.60	237.6	1.638		
	3.23	197.5	1.362		
9/12/05	4.24	179.0	1.234	186.7	1.287
	4.06	183.0	1.262		
	3.89	198.0	1.365		
9/15/05	3.77	200.1	1.379	172.1	1.187
	5.74	149.2	1.028		
	6.07	167.2	1.153		
9/19/05	4.22	115.4	0.795	113.6	0.783
	4.10	124.7	0.859		
	4.10	100.8	0.695		
9/27/05	4.49	167.1	1.152	161.3	1.112
	4.16	198.9	1.371		
	4.44	118.0	0.814		

Table G1 Continues.

Date	AV (%)	Indirect Tensile Strength (ITS)		ITS Average	
		(psi)	(MPa)	(psi)	(MPa)
9/28/05	3.88	185.7	1.280	169.8	1.171
	4.29	177.7	1.225		
	4.78	146.0	1.007		
9/30/05	4.22	143.2	0.987	134.4	0.927
	3.79	120.7	0.832		
	3.86	139.2	0.960		
10/9/05	3.42	169.7	1.170	161.6	1.114
	4.03	159.1	1.097		
	3.74	156.1	1.076		
10/16/05	3.91	195.2	1.346	161.7	1.115
	4.06	155.6	1.073		
	3.81	134.4	0.927		
10/18/05	4.02	176.4	1.216	165.8	1.143
	4.30	156.5	1.079		
	3.88	164.4	1.134		
10/19/05	3.80	241.4	1.664	239.1	1.649
	3.23	253.2	1.745		
	4.04	222.8	1.536		
10/26/05	3.71	130.1	0.897	147.3	1.015
	4.12	120.7	0.832		
	3.22	191.0	1.317		
10/27/05	3.50	199.4	1.375	180.7	1.246
	3.01	178.2	1.229		
	4.20	164.4	1.134		

Table G2. Indirect tensile strength of Mix 442.

Date	AV (%)	Indirect Tensile Strength (ITS)		ITS Average	
		(psi)	(MPa)	(psi)	(MPa)
9/20/05	3.55	179.2	1.235	173.7	1.197
	3.59	168.6	1.162		
	3.51	173.3	1.195		
10/11/05	3.95	203.0	1.400	185.4	1.278
	3.86	172.0	1.186		
	4.01	181.2	1.249		

Table G3. Indirect tensile strength of Mix FRL.

Date	AV (%)	Indirect Tensile Strength (ITS)		ITS Average	
		(psi)	(MPa)	(psi)	(MPa)
7/13/05	2.68	193.6	1.335	200.1	1.380
	3.29	196.1	1.352		
	2.84	210.7	1.453		
8/10/05	3.57	178.5	1.231	209.7	1.446
	3.77	237.1	1.634		
	3.05	213.6	1.473		
8/15/05	3.30	201.9	1.392	185.8	1.281
	3.61	180.0	1.241		
	3.73	175.6	1.211		
8/21/05	3.15	161.5	1.114	156.8	1.081
	4.10	155.6	1.073		
	3.20	153.3	1.057		
9/11/05	3.07	133.2	0.918	140.3	0.967
	2.79	146.3	1.009		
	3.28	141.5	0.975		
9/15/05	3.11	124.5	0.858	135.5	0.934
	3.36	135.8	0.936		
	2.50	146.3	1.009		
9/22/05	3.95	124.7	0.859	146.8	1.012
	3.66	134.4	0.927		
	3.25	181.4	1.251		
10/6/05	3.44	159.1	1.097	152.1	1.048
	3.59	151.2	1.042		
	3.62	145.9	1.006		
10/13/05	2.98	197.0	1.358	173.3	1.195
	3.36	147.8	1.019		
	3.50	175.0	1.207		
10/18/05	3.50	191.0	1.317	164.0	1.131
	3.66	155.2	1.070		
	3.47	145.9	1.006		

Table G4. Indirect tensile strength of Mix SMA.

Date	AV (%)	Indirect Tensile Strength (ITS)		ITS Average	
		(psi)	(MPa)	(psi)	(MPa)
10/4/05	3.47	118.4	0.816	134.4	0.927
	3.59	124.0	0.855		
	3.84	160.8	1.109		
10/13/05	3.22	141.8	0.978	144.4	0.996
	3.14	144.1	0.993		
	3.26	147.4	1.016		
10/31/05	3.56	129.5	0.893	118.4	0.816
	3.34	111.7	0.770		
	3.35	113.9	0.785		
11/4/05	4.33	109.4	0.755	131.4	0.906
	3.38	142.9	0.986		
	3.62	141.8	0.978		

Appendix H: Unconfined Compressive Strength of Asphalt Mixes

Table H1. Unconfined compressive strength of Mix 302.

Date	AV (%)	Unconfined Compressive Strength (UCS)		UCS Average	
		(psi)	(MPa)	(psi)	(MPa)
7/25/05	5.20	789.1	5.440	801.9	5.529
	5.60	852.7	5.879		
	4.20	763.9	5.267		
7/28/05	5.46	748.4	5.160	900.9	6.212
	3.04	1029.9	7.101		
	3.08	924.5	6.374		
8/12/05	3.73	1328.1	9.157	1366.0	9.418
	3.81	1285.3	8.862		
	3.20	1484.7	10.237		
8/16/05	4.50	1377.6	9.498	1354.6	9.340
	3.56	1390.3	9.586		
	4.09	1295.9	8.935		
8/23/05	3.11	784.1	5.406	761.0	5.247
	3.81	755.8	5.211		
	3.57	743.1	5.123		
8/28/05	4.35	850.2	5.862	958.2	6.607
	3.44	1061.4	7.318		
	4.31	963.1	6.640		
9/2/05	4.32	732.1	5.048	770.7	5.314
	4.28	756.2	5.214		
	3.95	823.7	5.679		
9/8/05	3.48	1214.2	8.371	1177.7	8.120
	4.01	1029.2	7.096		
	3.07	1289.9	8.893		
9/12/05	3.97	904.0	6.233	940.3	6.483
	4.15	983.2	6.779		
	4.01	933.7	6.438		
9/15/05	5.04	928.4	6.401	992.9	6.846
	5.00	1022.1	7.047		
	5.49	1028.1	7.089		
9/19/05	3.97	634.5	4.375	594.1	4.096
	3.93	551.4	3.802		
	4.59	596.3	4.111		
9/27/05	4.73	815.9	5.626	765.7	5.279
	3.59	711.2	4.904		
	4.93	770.0	5.309		

Table H1 Continues

Date	AV (%)	Unconfined Compressive Strength (UCS)		UCS Average	
		(psi)	(MPa)	(psi)	(MPa)
9/28/05	4.08	1017.9	7.018	1014.6	6.995
	4.33	1037.0	7.150		
	4.45	988.9	6.818		
9/30/05	3.96	607.3	4.187	745.9	5.143
	3.91	822.3	5.670		
	4.02	808.2	5.572		
10/9/05	3.21	1150.9	7.935	1010.0	6.964
	3.90	985.3	6.794		
	4.19	893.7	6.162		
10/16/05	4.01	937.2	6.462	967.7	6.672
	3.89	963.1	6.640		
	3.88	1002.7	6.913		
10/18/05	4.00	1091.4	7.525	1109.1	7.647
	3.75	1104.2	7.613		
	4.35	1131.8	7.803		
10/19/05	3.43	1261.9	8.701	1357.8	9.361
	3.43	1363.8	9.403		
	3.43	1447.6	9.981		
10/26/05	4.00	859.1	5.923	842.3	5.808
	3.35	744.8	5.136		
	3.67	923.1	6.365		
10/27/05	2.93	1144.9	7.893	1108.3	7.642
	3.91	1142.4	7.876		
	4.07	1037.7	7.155		

Table H2. Unconfined compressive strength of Mix 442.

Date	AV (%)	Unconfined Compressive Strength		UCS Average	
		(psi)	(MPa)	(psi)	(MPa)
9/20/05	3.55	842.5	5.809	809.3	5.580
	3.55	819.1	5.648		
	3.88	766.4	5.284		
10/11/05	4.12	1178.5	8.125	1073.6	7.403
	3.91	1006.9	6.942		
	3.94	1035.6	7.140		

Table H3. Unconfined compressive strength of Mix FRL.

Date	AV (%)	Unconfined Compressive Strength		UCS Average	
		(psi)	(MPa)	(psi)	(MPa)
7/13/05	2.60	723.3	4.987	658.2	4.538
	3.45	608.3	4.194		
	3.66	643.0	4.433		
8/10/05	2.70	1180.6	8.140	1227.9	8.466
	2.54	1199.3	8.269		
	3.20	1303.7	8.988		
8/15/05	3.01	1076.6	7.423	1061.3	7.317
	3.05	1005.9	6.935		
	3.05	1101.4	7.594		
8/21/05	3.85	842.5	5.809	905.1	6.240
	4.06	808.9	5.577		
	2.58	1063.9	7.335		
9/11/05	3.28	791.2	5.455	859.0	5.922
	3.20	852.0	5.874		
	2.79	933.7	6.438		
9/15/05	2.83	776.0	5.350	776.6	5.354
	2.70	832.6	5.740		
	3.28	721.1	4.972		
9/22/05	3.84	1066.3	7.352	1052.7	7.258
	3.75	1012.9	6.984		
	3.26	1078.7	7.437		
10/6/05	3.81	1263.0	8.708	1168.4	8.056
	3.36	1102.1	7.598		
	3.55	1140.3	7.862		
10/13/05	3.22	1038.0	7.157	1177.7	8.120
	2.89	1178.5	8.125		
	3.70	1316.7	9.079		

Table H4. Unconfined compressive strength of Mix SMA.

Date	AV (%)	Unconfined Compressive Strength		UCS Average	
		(psi)	(MPa)	(psi)	(MPa)
10/4/05	3.30	606.2	4.180	660.3	4.553
	3.34	612.6	4.224		
	4.04	762.2	5.255		
10/13/05	3.09	824.4	5.684	858.4	5.918
	3.01	865.8	5.970		
	3.42	884.9	6.101		
10/31/05	3.46	723.3	4.987	737.8	5.087
	3.40	786.6	5.423		
	3.35	703.5	4.850		
11/4/05	4.21	612.9	4.226	628.6	4.334
	3.51	628.1	4.331		
	3.59	644.8	4.445		

Appendix I: Implementation Plan

OHIO DEPARTMENT OF TRANSPORTATION OFFICE OF PAVEMENT ENGINEERING RESEARCH IMPLEMENTATION PLAN



Title: Determination of Mechanical Properties of Materials Used in WAY-30 Test Pavements

State Job Number: 437046

PID Number:

Research Agency: Ohio University

Researcher(s): Shad Sargand, Sang-Soo Kim

Technical Liaison(s): Roger Green

Research Manager: Monique Evans

Sponsor(s): ODOT

Study Start Date: January 1, 2004

Study Completion Date: February 15, 2009

Study Duration: 56 Months

Study Cost: \$106,882

Study Funding Type:

STATEMENT OF NEED:

Although long life pavements are clearly ideal, often times the pavements fail early. Currently, most highway agencies use empirical procedures to design pavements to last finite design lives, after which the pavements are intended to be failed. Premature failure inevitably results in unanticipated repair or reconstruction work, which causes traffic congestion, user delay, and increased overall pavement costs. For those reasons, many highway agencies attempted to design pavements that last longer. The Ohio Department of Transportation (ODOT), with joint efforts from pavement industries, constructed two test projects on the WAY-30 bypass of Wooster, Ohio for the evaluation of long life pavement design procedures as alternative pavement design methods. One project was constructed with a long lasting economical concrete pavement and the other with an asphalt pavement designed following perpetual pavement concept, which is rapidly gaining acceptance in the United States. The perpetual asphalt pavement concept uses mechanistic-empirical design procedure that requires accurate mechanical properties of materials, traffic, and environmental data as input to predict pavement responses and distresses. Using input data and pavement response models, the thickness of each pavement layer is determined to keep certain pavement responses at critical locations within limiting values for perpetual performance. Design of long-lived concrete pavement also requires accurate material properties.

RESEARCH OBJECTIVES:

- Determine the mechanical properties of the pavement materials used in WAY-30 test pavements during construction and in-service;
- Provide data to calibrate the long life pavement design procedures.

RESEARCH TASKS:

Task 1 – Development of Sampling and Testing Plan

Task 2 – Collection of Materials

Task 3 – Testing of Specimens

Task 4 – Write final Report

RESEARCH DELIVERABLES:

Final Report, Executive Summary, Data CDR

RESEARCH RECOMMENDATIONS:

None, as the project consists of reporting data for the WAY-30 test road. Data may be used for validation purposes as described under “expected benefits” below.

PROJECT PANEL COMMENTS:

IMPLEMENTATION STEPS & TIME FRAME:

The results and data from this study can be directly implemented by researchers validating or calibrating the long life pavement design procedures. In fact, some of the data have already been used in the ELS analysis in the previous report on WAY-30. [Sargand, Figueroa, and Romanello, 2008] Data obtained from this research project will be used as inputs for the elastic or viscoelastic models used in design of pavements to predict pavement responses. The predicted pavement responses may then be compared with the actual observed pavement response to validate the design. The ultimate result of this process will be revisions in specifications, standard drawings, and the Pavement Design and Rehabilitation Manual to incorporate the new materials and design procedures.

EXPECTED BENEFITS:

Results of this research project will provide data to be used for the validation and calibration of long lasting pavement design procedures. Long lasting asphalt and concrete pavements will reduce traffic congestion, user delays, and life-cycle costs. For given fixed financial resources, more highway system will be maintained with better quality.

The mechanical properties and other data obtained in this proposed research can also be used at two other current ODOT research projects; “Materials Properties for Implementations of Mechanistic/Empirical (ME) Pavement Design Procedures” [State Job No 14767(0)], and “Continued Monitoring of SHRP Pavement Instrumentation Including Soil Suction and Relationships with Resilient Modulus” [State Job No 14691(0)].

EXPECTED RISKS, OBSTACLES, & STRATEGIES TO OVERCOME THEM:

There are no immediate impediments to implementation.

OTHER ODOT OFFICES AFFECTED BY THE CHANGE:

PROGRESS REPORTING & TIME FRAME:

TECHNOLOGY TRANSFER METHODS TO BE USED:

IMPLEMENTATION COST & SOURCE OF FUNDING:

Approved By: (attached additional sheets if necessary)

Office Administrator(s):

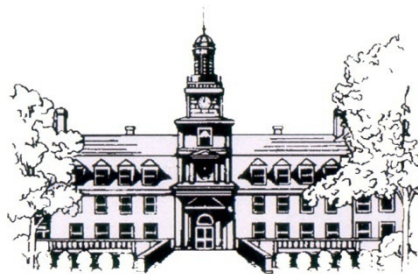
Signature: _____ Office: _____ Date: _____

Signature: _____ Office: _____ Date: _____

Division Deputy Director(s):

Signature: _____ Division: _____ Date: _____

Signature: _____ Division: _____ Date: _____



ORITE • 141 Stocker Center • Athens, Ohio 45701-2979 • 740-593-2476
Fax: 740-593-0625 orite@bobcat.ent.ohiou.edu <http://webce.ent.ohiou.edu//orite/>